ORIGINS OF COUNTRY ROCK-HOSTED NI-CU-PGE MASSIVE SULFIDES NEAR MAFIC-ULTRAMAFIC INTRUSIONS OF THE NORTH AMERICAN MIDCONTINENT RIFT SYSTEM AND THE STILLWATER COMPLEX

Joshua M. Smith

Submitted to the faculty of the University Graduate School

in partial fulfillment of the requirements for the degree

Doctor of Philosophy

in the Department of Earth and Atmospheric Sciences

Indiana University

November 2019

Accepted by the Graduate Faculty, Indiana University, in partial fulfillment of the requirements for the degree of Doctor of Philosophy

Doctoral Committee

_____
Edward M. Ripley, Ph.D.

_____
Chusi Li, Ph.D.

_____
James Brophy, Ph.D.

_____
Erika Elswick, Ph.D.

_____
Laura Wasylenki, Ph.D.

November 1st, 2019

This dissertation is dedicated to my wife, Courtney and my mother Mona, who have supported and encouraged me even when I wanted to give up. Thank you and I love you both.

Acknowledgments

Thank you to Dr. Ed Ripley, for offering me the opportunity to work on this great project and for immeasurable insight into the world of isotope geochemistry applied to mineral deposits. Additionally, thank you for reassuring me that persistence and patience pay off in the world of stable and radiogenic isotope analyses. Thank you both Dr. Ed Ripley and Dr. Chusi Li for helping me with various parts of the research, writing, and presentations over the past four years, and for helping me dramatically improve in all of those categories. Thank you to my committee members Dr. James Brophy, Dr. Erika Elswick, and Dr. Laura Wasylenki for providing helpful input at various stages of the process. Thank you to Benjamin Wernette for many discussions at Yogi's on various aspects of magmatic sulfide deposits and isotope geochemistry. I am grateful to Kennecott Exploration, Lundin Mining, and Teck Resources and all of the associated staff for allowing access to and sampling of drill core from the Tamarack, Eagle, and Mesaba deposits. Dr. Mike Zientek is gratefully thanked for providing a suite of samples from below the Stillwater Complex. Thank you to Benjamin Underwood in the SIRF lab at IU for vacuum line training, help with various analyses, and shared frustration while sitting at the multicollector. Thank you to Shui-jiong Wang and Hui Huang for training and assistance with Ni and Cu isotope preparation and analyses in the Metal Isotope Lab. Thank you to Mary Horan, Tim Mock, and Dr. Steve Shirey for assistance and training in the chemistry and mass spectrometer labs at the DTM. Extreme gratitude is also given to Dr. Craig Chesner, who taught the first geology class of my career and was the first to introduce me to economic geology in the Midcontinent Rift and elsewhere. I also appreciate recent friendships with and support from former students. I hope I have been able to provide encouragement to you, just as many of the above have to me. Most importantly, thank you to all of my friends and family who have supported me throughout my undergraduate and graduate career.

Joshua Smith

ORIGINS OF COUNTRY ROCK-HOSTED NI-CU-PGE MASSIVE SULFIDES NEAR MAFIC-ULTRAMAFIC INTRUSIONS OF THE NORTH AMERICAN MIDCONTINENT RIFT SYSTEM AND THE STILLWATER COMPLEX

Igneous rock-hosted sulfides in mafic-ultramafic intrusions produce most of the world's nickel and PGEs. These sulfides were produced by sulfide saturation in mafic-ultramafic magmas and accumulation of sulfide liquid in the magmatic systems. Some massive Ni-Cu-PGE sulfides also occur in local country rocks. Within the Midcontinent Rift System, sheet-style and conduit-style intrusions host disseminated to massive sulfides in igneous rocks. Country rock-hosted massive Ni-Cu-PGE sulfides are also found near at least three Midcontinent Rift-related intrusions; the Partridge River intrusion, the Tamarack Intrusive Complex, and the Eagle Intrusion. These massive sulfides have no known physical connections to igneous rocks, and consequently, their genesis remains controversial.

The Stillwater Complex in Montana also hosts disseminated to massive sulfides throughout the complex. Sulfide(-oxide) mineralization in the local country rocks also occurs below the Stillwater Complex as lenticular to laminated massive sulfide(-oxides) in the metamorphic aureole. Prevailing opinion is the sulfide(-oxides) are genetically related to igneous-hosted sulfides within the Stillwater Complex, but their genesis remains contentious.

Trace element and isotopic analyses of country rock-hosted massive sulfides near Eagle and Tamarack indicate minor crustal contamination of mafic-ultramafic magmas. Trace element and isotopic compositions of samples near the Partridge River intrusion require substantial crustal

contamination. Country rock-hosted sulfides near Tamarack were produced as immiscible sulfide liquids from the semi-massive sulfides from the underlying CGO unit were filter-pressed from the intrusion. Country rock-hosted massive sulfides at Eagle were produced via fractional crystallization of the massive sulfides in the igneous rocks. Massive sulfides below the Partridge River intrusion were produced when relatively low R-factor sulfide liquids leaked from the base of the intrusion.

Trace element and isotopic analyses of massive sulfide(-oxides) below the Stillwater Complex suggest the sulfide was deposited as sedimentary or seafloor hydrothermal sulfides before emplacement of the Stillwater Complex. Contact metamorphism dehydrated the pelitic country rocks and the Stillwater iron formation to produce anhydrous silicates, Fe-Ti oxides, and a metamorphic-hydrothermal fluid. Increased temperatures and circulating metamorphic fluid caused desulfidation and produced a sulfide composition more enriched in Fe-Ni-Cu and other metals, which cooled to produce hexagonal and monoclinic pyrrhotite with trace pentlandite, chalcopyrite, and cubanite.

_____
Edward M. Ripley, Ph.D.

_____
Chusi Li, Ph.D.

_____
James Brophy, Ph.D.

_____
Erika Elswick, Ph.D.

_____
Laura Wasylenki, Ph.D.

Table of Contents

List of Tables:

List of Figures:

Overview

Although advances in hydrometallurgical processing have made other Ni resources (Ni laterites) more viable, 60% of today's Ni (and nearly all PGEs and some Cu) is still recovered from sulfides in mafic and ultramafic rocks (Mudd, 2009; Mudd and Jowitt, 2014). As mining continues, the proportion of Ni, Cu, and PGEs remaining in igneous rock-hosted sulfides will continue to decline unless significant new discoveries are made.

Igneous rock-hosted sulfides are found as disseminated, semi-massive, and massive sulfides within mafic-ultramafic intrusions and are fundamentally related to mafic-ultramafic magmatism. Decades of combined field and laboratory studies on magmatic sulfide deposits have shown that the Ni-Cu-PGE concentrations of the sulfides can be explained by supersaturation of mafic-ultramafic magmas with respect to sulfide, sequestration of chalcophile elements (Ni-Cu-PGEs) by the sulfide (Mungall and Brenan, 2014), and fractional or equilibrium crystallization of the sulfide liquids (Li et al., 1994; Mungall, 2007). In many instances massive sulfides are found at the base of intrusions, such as those at the base of mafic sills from Noril'sk (Czamanske et al., 1995) or the base of bladed dikes, such as the Savannah Intrusion (Barnes et al., 2018). However, massive Ni-Cu-PGE sulfides are also found in many sedimentary and metasedimentary country rocks hosting the mafic-ultramafic intrusions. In some cases, there may be direct physical connections between massive sulfides in the country rocks and sulfides in the igneous rocks. In many cases, however, there is no documented connection between the country rock- and igneous rock-hosted sulfides.

One of the most well-known occurrences of Ni-Cu-PGE sulfides in sedimentary rocks are the sulfide-rich veins below the Sudbury Igneous Complex, which have been explained by both

leaking of fractionated sulfide liquids (Li et al., 1992; Lightfoot et al., 1992; Keays and Lightfoot, 2004; Lightfoot, 2007; Dare et al., 2014) and hydrothermal circulation (Hanley et al., 2005; Tuba et al., 2014). The footwall veins at Sudbury have a clear connection to the base of the Sudbury Complex, whereas at many localities, evidence of a physical connection between the massive sulfides and the ignoues rocks is lacking. In the Kharaelakh intrusion of the Noril'sk district, massive sulfides may be found in Devonian sedimentary rocks, up to 30 meters below the igneous sills (Czamankse et al., 1995). At the Savannah North Intrusion in Western Australia, intercepts of country rock-hosted massive sulfides are found in metamorphic rocks hundreds of meters below the intrusion, with grades of 1.68% Ni over 9.2 meters and 1.55% Ni over 10.8 meters, and the massive sulfide extends at least 0.5 km down dip (Panoramic Resource, LTD, 2017). Panoramic Resources has inferred that this is an extension of the mineralization from inside the Savannah North Intrusion, but, more importantly, the occurrence demonstrates that country rock-hosted Ni-Cu (-PGE) massive sulfides are potentially viable resources. The lack of direct evidence for physical connection between the sulfides and intrusions in many cases warrants investigation into the geologic and geochemical processes required to produce these deposits. Informed exploration models for these types of mineral occurrences will be contingent upon the ability to document where, why, and how country rock-hosted Ni-Cu-PGE massive sulfides may have formed. Discovery of these types of mineral occurrences may significantly prolong the lifetime of active mines or add to the resources of previously uneconomic prospects, but effective exploration will be hindered until genetic processes can be identified.

In the Midcontinent Rift System, country rock-hosted Ni-Cu (-PGE) massive sulfides, without clear connections to the igneous rocks, have been documented as satellites below and adjacent to

small “conduit-type” intrusions (Ripley, 2014), as well as below the larger “sheet-style” intrusions of the Duluth Complex (Ripley et al., 1999). The Eagle and Tamarack deposits of Michigan and Minnesota, respectively, are small, high-grade Ni-Cu-PGE mineral deposits associated with mafic-ultramafic intrusions that formed during early stages of mafic magmatism in the 1.1 Ga Midcontinent Rift System (Ding et al., 2012; Taranovic et al., 2014). Multiple generations and/or compositions of disseminated, semi-massive, and massive sulfides are found within the igneous rocks at both locations. The Duluth Complex, in Minnesota, is composed of many distinct intrusions found between the city of Duluth and the Canadian border. Igneous rock-hosted sulfides in the Partridge River Intrusion of the Duluth Complex are primarily Cu-rich, disseminated sulfides. All three of these systems (Eagle, Tamarack, Partridge River) also have spatially-associated massive Ni-Cu (-PGE) sulfides in the local Proterozoic country rocks, with no documented connection to the intrusions.

Sulfide minerals are found in most igneous rocks of the Stillwater Complex, although elevated concentrations of sulfide minerals are present in only a few localities: disseminated sulfides in rocks of the Basal Series, massive and net-textured sulfides in the lower part of the Ultramafic Series in the Iron Mountain area (known as the Camp deposit), disseminated sulfides in the J-M Reef within the Lower Banded Series, and in the much smaller PGE-enriched Picket Pin deposit in the Upper Banded Series. Massive sulfide lenses occur associated with the G chromitite in the Iron Mountain area. Ni-Cu-bearing massive sulfides (and oxides), with no physical connections to the igneous rocks, are also found in country rocks below the base of the Stillwater Complex in Montana. Massive sulfides(-oxides) below the Stillwater Complex are found predominantly in the hornfels, although some sulfide(-oxide) mineralization may also have been that which occurs in noritic sills beneath the Complex. A renewed interest in the

mineralization present in the Basal Series and within the metasedimentary hornfels is largely a function of the international need for Co, primarily for use as cathodes in batteries (Group Ten Metals https://grouptenmetals.com).

In order to better constrain the genesis of country rock-hosted massive sulfides near the Eagle and Tamarack deposits in Michigan and Minnesota; beneath the Partridge River Intrusion of the Duluth Complex in Minnesota; and below the Stillwater Complex in Montana, we initiated petrographic, isotopic, and major and trace element studies. We anticipate these results will help us answer questions such as "What are the source(s) of metals, S, and other components in the massive sulfides?"; "What pathways pathways and processes did those components undergo to arrive in the massive sulfides?"; and "When did the massive sulfides form and are they related to discrete magmatic, hydrothermal, or sedimentary events?". Results suggest that country rock-hosted massive sulfides at Eagle and Tamarack were derived from immiscible sulfide liquids that leaked from the associated intrusions. The massive sulfides from the Virginia Formation beneath the Partridge River Intrusion were also derived largely from magmatic sulfide liquids but must have experienced ongoing crustal assimilation subsequent to emplacement in the Virginia Formation, possibly due to devolatilization reactions that were occurring in the metamorphic aureole around the Partridge River intrusion. Massive sulfide(-oxide) mineralization below the Stillwater Complex is genetically unrelated to that which occurs in the igneous rocks of the Complex, and initially formed as marine, sedimentary sulfides or hydrothermal seafloor exhalations.

Chapter 1: Evidence of Igneous Controls on the Formation of Metasedimentary Rock-Hosted Massive Ni-Cu-PGE Sulfides Near Intrusions in the Midcontinent Rift

Introduction

A significant amount of Ni, Cu, and platinum group elements (PGEs) are mined from mafic-ultramafic intrusions and komatiites. Although advances in hydrometallurgical processing have made other Ni resources (Ni laterites) more viable, 60% of today's Ni (and nearly all PGEs) are still recovered from sulfides in mafic and ultramafic rocks (Mudd, 2009; Mudd and Jowitt, 2014). As mining continues, the proportion of Ni, Cu, and PGEs remaining in igneous rock-hosted sulfides will continue to decline unless significant new discoveries are made.

Igneous rock-hosted sulfides are found as disseminated, semi-massive, and massive sulfides within mafic-ultramafic intrusions and are fundamentally related to mafic-ultramafic magmatism. Decades of combined field and laboratory studies on magmatic sulfide deposits have shown that the Ni-Cu-PGE concentrations of the sulfides can be explained by supersaturation of mafic-ultramafic magmas with respect to sulfide, sequestration of chalcophile elements (Ni-Cu-PGEs) by the sulfide (Mungall and Brenan, 2014), and fractional or equilibrium crystallization of the sulfide liquids (Li et al., 1994; Mungall, 2007). In many instances massive sulfides are found at the base of intrusions, such as those at the base of mafic sills from Noril'sk (Czamanske et al., 1995) or the base of bladed dikes, such as the Savannah Intrusion (Barnes et al., 2018). However, massive Ni-Cu-PGE sulfides are also found in many sedimentary and metasedimentary country rocks hosting the mafic-ultramafic intrusions. In some cases, there may be direct physical connections between massive sulfides in the country rocks and sulfides in the igneous rocks. In many cases, however, there is no documented connection between the country rock- and igneous rock-hosted sulfides.

One of the most well-known occurrences of Ni-Cu-PGE sulfides in sedimentary rocks are the sulfide-rich veins below the Sudbury Igneous Complex, which have been explained by both leaking of fractionated sulfide liquids (Li et al., 1992; Lightfoot et al., 1992; Keays and Lightfoot, 2004; Lightfoot, 2007; Dare et al., 2014) and hydrothermal circulation (Hanley et al., 2005; Tuba et al., 2014). The footwall veins at Sudbury have a clear connection to the base of the Sudbury Complex, whereas at many localities, a connection is never seen. In the Kharaelakh intrusion of the Noril'sk district, massive sulfides may be found in Devonian sedimentary rocks, up to 30 meters below the igneous sills (Czamankse et al., 1995). At the Savannah North Intrusion in Western Australia, intercepts of country rock-hosted massive sulfides are found in metamorphic rocks hundreds of meters below the intrusion, with grades of 1.68% Ni over 9.2 meters and 1.55% Ni over 10.8 meters, and the massive sulfide extends at least 0.5 km down dip (Panoramic Resource, LTD, 2017). Panoramic Resources has inferred that this is an extension of the mineralization from inside the Savannah North Intrusion, but more importantly the occurrence demonstrates that country rock-hosted Ni-Cu (-PGE) massive sulfides are potentially viable resources. The lack of direct evidence for physical connection between the sulfides and intrusions in many cases warrants investigation into the geologic and geochemical processes required to produce these deposits. Informed exploration models for types of mineral occurrences will be contingent upon the ability to document where, why, and how country rock-hosted Ni-Cu-PGE massive sulfides may have formed. Discovery of these types of mineral occurrences may significantly prolong the lifetime of active mines or add to the resources of previously uneconomic prospects, but effective exploration will be hindered until genetic processes can be identified.

In the Midcontinent Rift System, country rock-hosted Ni-Cu (-PGE) massive sulfides, without clear connections to the igneous rocks, have been documented as satellites below and adjacent to small "conduit-type" intrusions (Ripley, 2014), as well as below the larger "sheet-style" intrusions of the Duluth Complex (Ripley et al., 1999). The Eagle and Tamarack deposits of Michigan and Minnesota, respectively, are small, high-grade Ni-Cu-PGE mineral deposits associated with mafic-ultramafic intrusions that formed during early stages of mafic magmatism in the 1.1 Ga Midcontinent Rift System (Ding et al., 2012; Taranovic et al., 2014). Multiple generations and/or compositions of disseminated, semi-massive, and massive sulfides are found within the igneous rocks at both locations. The Duluth Complex, in Minnesota, is composed of many distinct intrusions found between the city of Duluth and the Canadian border. Igneous rock-hosted sulfides in the Partridge River Intrusion of the Duluth Complex are primarily Cu-rich, disseminated sulfides. All three of these systems (Eagle, Tamarack, Partridge River) also have spatially associated massive Ni-Cu (-PGE) sulfides in the local Proterozoic country rocks, with no documented connection to the intrusions.

In order to better constrain the genesis of country rock-hosted massive sulfides beneath the Partridge River Intrusion of the Duluth Complex, and those located near the Eagle and Tamarack deposits, we initiated petrographic, isotopic, and major and trace element studies. We anticipate these results will help us answer questions such as "What are the source(s) of metals, S, and other components in the massive sulfides?"; "What pathways pathways and processes did those components undergo to arrive in the massive sulfides?"; and "When did the massive sulfides form and are they related to discrete magmatic, hydrothermal, or sedimentary events?". Results of petrography, trace element ratios, and S, Re-Os, and Pb isotopic measurements suggest that country rock-hosted massive sulfides at Eagle and Tamarack were derived from immiscible

sulfide liquids that leaked from the associated intrusions. The massive sulfides from the Virginia Formation beneath the Partridge River Intrusion were also derived largely from magmatic sulfide liquids but must have experienced ongoing crustal assimilation subsequent to emplacement in the Virginia Formation, possibly due to devolatilization reactions that were occurring in the metamorphic aureole around the Partridge River intrusion. Analyses of PGEs, in conjunction with geochemical models, confirm the igneous origin of the massive sulfides and provide further insight as to which generations of sulfide liquids escaped into the country rocks. At Eagle, sulfide liquids similar to the igneous-hosted massive sulfides escaped from the intrusions at various times in the crystallization history; at Tamarack, sulfide liquids evolved from the semi-massive sulfides, which are found in one intrusive type only, were expelled into the Thomson Formation; and at Partridge River, sulfide liquid similar to that which produced the lowest R-factor (mass ratio of silicate to sulfide magma) disseminated sulfides in the noritic and troctolitic sheets was emplaced into the Virginia Formation, where little to no fractionation of sulfide liquid appears to have occurred.

Regional Geology

The Midcontinent Rift System is a 1.1 Ga failed continental rift in the upper Midwest of the United States (Fig. 1). This area contains on the order of ~ 1 – 2 x 10^6 km^3 of mafic igneous rocks (Hutchinson et al., 1990; Merino et al., 2013). Rift-related volcanism includes voluminous tholeiitic flood basalt flows, minor picritic flows, and a few intermediate to felsic extrusions (Green, 1982, 2002). Genetically related intrusions are categorized into four groups: (1) Subvolcanic intrusive complexes (sheet-style); (2) Mafic dike and sill swarms; (3) Isolated alkalic and carbonatitic intrusions; and (4) Small dike-like mafic-ultramafic intrusions, (conduit-

style) (Wieblen, 1982; Miller and Nicholson, 2013). The sheet-style Partridge River intrusion within the Duluth Complex and conduit-style Tamarack Intrusive Complex are hosted in ~1.8 Ga shales and graywackes of the Animikie Basin, predominantly the Virginia and Thomson Formations, respectively (Hemming et al., 1995; Goldner, 2011). The Animikie Basin is temporally correlated with the Baraga Basin in the Upper Peninsula of Michigan. The Baraga Basin hosts the conduit-style Eagle intrusion in the ~1.8 Ga Michigamme Formation (Hemming et al., 1995; Ding et al., 2010).

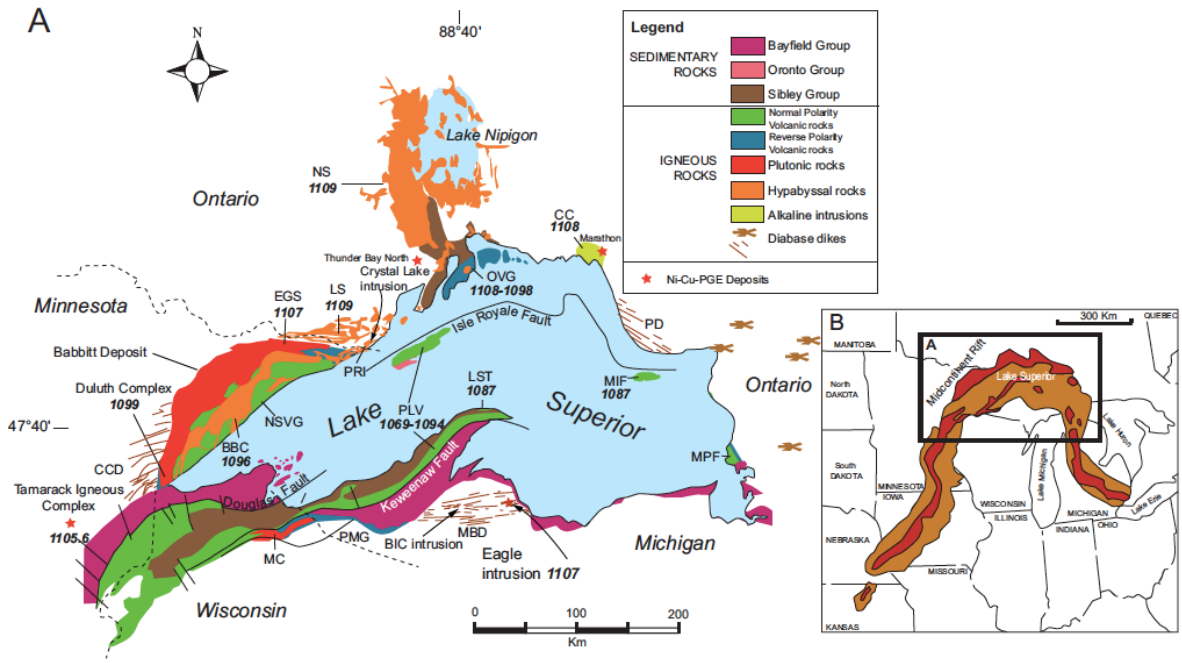

Figure 1: Generalized geology of the Lake Superior region with Midcontinent Rift-related intrusions, showing the location of the Tamarack Igneous Complex, the Eagle Intrusion, and the Duluth Complex relative to other Midcontinent Rift System intrusions (modified from Miller and Nicholson, 2013). Abbreviations: BBC = Beaver Bay Complex, CC = Coldwell Complex, CCD = Carlton Country dikes, EGS = Early Gabbro Series, LS = Logan Sills, LST = Lake Shore traps, MBD = Marquette=Baraga dikes, MC = Mellen Intrusive Complex, MIF = Michipicoten Island Formation, MPG = Mamainse Point Formation, NS = Nipigon Sills, NSVG = North Shore Volcanic Group, OVG = Osler Group, PD = Pukaskwa dikes, PLV = Portage Lake Volcanics, PMG = Powder Mill Group, PRI = Pigeon River intrusion. Previously published high-precision U-Pb dates are given in bold italics, in Ma.

During the early Paleoproterozoic the Animikie Basin was an unrestricted backarc basin, with predominantly turbidites and banded iron formations (Hemming et al., 1995; Van Wyck and Johnson, 1997; Ojakangas et al., 2001; Pufahl and Fralick, 2004; Schulz and Cannon, 2007; Poulton et al., 2010; Pufahl et al., 2010). Compression from the late Paleoproterozoic Penokean Orogeny caused the basin to become restricted from the ocean as it evolved into a foreland basin and accumulated turbidites and deltaic sediments (Poulton et al., 2010; Pufahl et al., 2010). The Baraga Basin to the east also became a restricted foreland basin during the Penokean Orogeny. Basinal restrictions promoted the accumulation of organic material, which in turn promoted bacterial reduction of seawater sulfate and the accumulation of carbonaceous, S-rich sedimentary rocks in the Virginia, Thomson, and Michigamme Formations (Poulton et al., 2010; Pufahl et al., 2010). Animikie and Baraga Group rock types include predominantly shales, argillites, and graywackes (Hemming et al., 1995), except where contact metamorphism of these rock types produced hornfels around rift-related intrusions.

Mesoproterozoic igneous activity related to the Midcontinent Rift began around 1115 Ma, as indicated by the presence of mafic-ultramafic intrusions in Ontario (Heaman et al., 2007). It is thought that uplift and subsequent erosion, brought on by an impinging mantle plume erased most evidence of correlative volcanic rocks (Campbell, 2001; Miller and Nicholson, 2013). From 1110 to 1105 Ma various ultramafic to felsic intrusions and lava flows were emplaced. Relatively uncontaminated picrites predominate earlier in this stage, and more felsic and contaminated compositions appear later. Early picritic lava flows, such as Groups 1 and 2 from the Mamainse Point Formation, are thought to be similar to parental magmas of some of the earliest intrusions in the rift, whereas Groups 3 – 5 from Mamainse Point are less primitive and temporally correlate with ferrogabbros and minor alkaline magmatism (Shirey et al., 1994;

Miller and Nicholson, 2013). A break in mafic magmatism occurred between 1105 to 1101 Ma (Miller and Vervoort, 1996). The remnants of this stage are mostly felsic clasts in the Copper Harbor Conglomerate of Michigan's upper peninsula (Davis and Paces, 1990). The clasts have been suggested to be the relics of eroded composite volcanoes (Miller and Nicholson, 2013). The main stage of igneous activity in the Midcontinent Rift occurred from 1101 to 1094 Ma, as volcanic and intrusive rocks filled the rift basin. Intrusive rocks are composed primarily of high aluminum olivine tholeiites, which correlate with tholeiitic rocks in the Portage Lake Volcanics (Paces and Bell, 1989). Most magmatic and volcanic activity ended by 1094 Ma, although irregular intermediate to felsic eruptions occurred as late as 1086 Ma (Miller and Nicholson, 2013). Final stages in rift activity were dominated by subsidence of the rift graben and deposition of fluvial and lacustrine sediments. Failure of the rift may have been due to reactivation of graben-bounding normal faults related to compression during the Grenville Orogeny, which produced both reverse and strike-slip motion in parts of the rift (Cannon, 1994).

Quantitative modeling by Moucha et al. (2013) has suggested that the vast volume of magma produced in the Midcontinent Rift is best explained by active rifting driven by a mantle plume, whereas others have argued that the ~ 30 million years of magmatism is far longer than the known range for other mantle plumes (Coffin and Eldholm, 1994; Ernst and Buchan, 2001). A more recent review by Stein et al. (2016) suggests that the Midcontinent Rift was between the endmembers of active and passive rifting and was produced by the convergence of a continental rift and a mantle plume. Although prevailing thought was that volcanic activity began to subside as extensional domains converted to compressional domains during the Grenville Orogeny (Cannon, 1994), more recent radiogenic isotope work has suggested that extension was terminated long before the onset of compression (Malone et al., 2016).

Geology of the Duluth Complex and the Tamarack and Eagle Deposits

The Duluth Complex is composed of several small tholeiitic intrusions, many of which have been previously described (*e.g.,* Weiblen and Morey, 1976; Ripley and Alawi, 1988; Ripley, 1990; Severson and Hauck, 1990; Miller and Ripley, 1996; Miller et al., 2002; Severson et al., 2002, and references therein). Two of the most prominent, the Partridge River and South Kawishiwi intrusions, are also host to potentially economic disseminated sulfide mineralization. The complex is broadly divided into four groupings based on mineralogy, texture, and igneous lithology. The main divisions are the early gabbro series, granophyres, the anorthosite series, and a troctolite series, although local variations in the series preclude complex-wide correlation. Cu-(PGE-Ni) deposits are usually found as disseminated sulfides at the base of troctolitic sheets emplaced at 1099 Ma (Paces and Miller, 1993). Currently, only the Partridge River and South Kawishiwi intrusions are known to host appreciable sulfide mineralization (Ripley, 2014). Some intrusions of the Duluth Complex are hosted in the 1.8 Ga Virginia Formation and within other members of the Animikie Group sedimentary rocks, including the Paleoproterozoic Biwabik Iron Formation (Ripley, 1990; Hemming et al., 1995). Animikie Group rocks near the Duluth Complex were originally composed of shales, argillites, and graywackes (Hemming et al., 1995), although contact metamorphism has produced extensive orthopyroxene-cordierite hornfels with subordinate quartz and biotite (Labotka et al., 1984). Other intrusions, primarily the South Kawishiwi intrusion, which hosts the Maturi and Spruce Road Ni-Cu deposits, are found in Archean granitoids (Severson, 1994; Lee and Ripley, 1996; Peterson, 2013).

The Eagle (1107 Ma) and Tamarack (1105 Ma) intrusions are vertical to sub-vertical dike-like intrusions hosted in predominantly Proterozoic sedimentary and metasedimentary country rocks of the Michigamme and Thomson formations, respectively (Ding et al., 2012; Taranovic et al.,

2016). The Michigamme Formation is part of the Baraga Group sedimentary rocks and is the time equivalent to the Virginia Formation. The Thomson Formation is also part of the Animikie Group and is a southward extension of the Virginia Formation (Hemming et al., 1995). Both Tamarack and Eagle were emplaced during early stages (~ 1110 – 1105 Ma) of rifting in the MRS and are associated with parental magmas with compositions similar to picritic basalts in the related volcanic sequence (Ding et al., 2010; Goldner, 2011; Taranovic et al., 2015). Eagle and Tamarack are hosted within the Marquette-Baraga (Ding et al., 2012) and Carlton County dike swarms (Taranovic et al., 2016), respectively. Igneous host rocks at Eagle include melatroctolites, olivine melagabbros, feldspathic pyroxenites, and feldspathic peridotites. All rock types host disseminated to semi-massive sulfide mineralization, whereas massive sulfides are generally restricted to the melatroctolites (Ding et al., 2012). Host rocks at Tamarack include peridotites, feldspathic peridotites, melatroctolites, and melagabbros. Two distinct intrusions are identified by olivine grain sizes. In the widest portions of the intrusion, the fine-grained olivine intrusion (FGO) overlies the coarse-grained olivine intrusion (CGO). Disseminated, semi-massive, and massive sulfides are found within the CGO, whereas the FGO contains disseminated and massive sulfides (Taranovic et al., 2015). The interface between the FGO and CGO is diffusive and is referred to as the "mixed zone," as it has textural features of both the FGO and CGO (Taranovic et al., 2015). The country rocks at both Eagle and Tamarack are composed primarily of weakly metamorphosed shales and graywackes. Adjacent to the intrusions the country rocks have been metamorphosed to biotite-cordierite hornfels (Ding et al., 2010; Taranovic et al., 2015).

Sampling and Analytical Procedures

Samples used in this study were taken from drillholes 48, 49, 138, 153, 158, 164A, 171, and 211, 213, 229 near Tamarack (Fig. 2); EAUG0069 and EAUG0070 at Eagle (Fig. 3); and MB07-04, MB07-13, MB07-14, MB08-25, MB08-28, MB08-36, and MB13086 below the Partridge River Intrusion in the Duluth Complex (Fig. 4). Table 1 provides latitude and longitudes of drillhole collars used in this study. Samples are primarily massive sulfides hosted in sedimentary and metasedimentary country rocks at each site. At Tamarack, the massive sulfides are hosted in a segment of the Thomson Formation that occupies a vertical gap between the CGO and the overlying FGO. Country rock-hosted massive sulfides at Eagle are found marginal to the contact between the igneous rocks and the Michigamme Formation and typically crosscut the intrusion. Below the Partridge River Intrusion, massive sulfides are found entirely within the Virginia Formation. Sulfur isotopes of the igneous-hosted sulfides at Tamarack, Eagle, and the Partridge River Intrusion have previously been described by Taranovic et al. (2018), Ding et al. (2012), Rao and Ripley (1983), Ripley and Al-Jassar (1987), and Arcuri et al. (1998), respectively, as part of studies aimed at understanding interactions between mafic intrusions and their host rocks. Fifty-four samples of country rock-hosted massive sulfides were studied petrographically in polished thin sections using transmitted and reflected light to document mineral assemblages and textures of the massive sulfides, host rocks, and contacts between the two.

Initial $\delta^{34}S$ analyses of massive sulfides were performed via a standard SO_2 combustion method (Studley et al., 2002) on 123 samples of country rock-hosted massive sulfides from Tamarack, Eagle, and Duluth. Standards used for SO_2 combustion analyses included international standards IAEA S-1($\delta^{34}S$ = -0.3 ‰) and S-2 ($\delta^{34}S$ = 21.7 ‰), as well as in-house standards ERE-Ag_2S ($\delta^{34}S$ = -4.7 ‰), EMR-Cp ($\delta^{34}S$ = 0.9 ‰), PQB2-barite ($\delta^{34}S$ = 40.85 ‰),

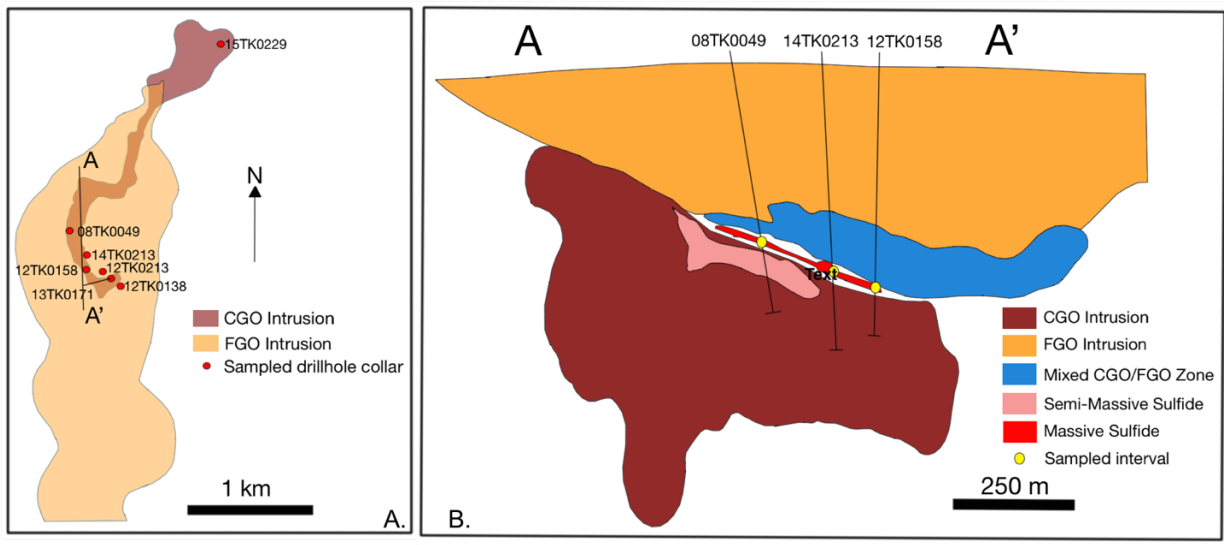

Figure 2: Map (A) and long-section (B) through the Tamarack Intrusive Complex, showing the simplified geology and drillholes sampled in this study. Map and section produced from 3D models provided courtesy of Talon Metals.

and PQM2-marcasite ($\delta^{34}S$ = -14.7 ‰); all values on the SO_2 scale. All analyses are reported relative to VCDT, and replicate analyses of in-house standards yield 2σ uncertainties of ± 0.2 ‰. A subset of 38 massive sulfide samples were analyzed for multiple S isotope compositions. Eight samples of igneous-hosted sulfide from Tamarack and 8 from Duluth were also analyzed for multiple S isotope compositions, in order to identify background S isotope compositions of the intrusions. Multiple S analyses of igneous-hosted sulfides from Eagle are available in Ding et al. (2012). Samples were initially microdrilled with a tungsten carbide drill bit to produce sulfide powders. Samples were boiled through a condenser with a mix of $CrCl_2$ and 12 M HCl, obtained by Zn-reduction of a HCl-$CrCl_3$ mixture (Acholla and Orr, 1993). The resulting H_2S gas was carried by a stream of N_2 into a trap of 0.1 M $AgNO_3$ to produce Ag_2S. Dried Ag_2S samples were placed in a Ni reaction vessel, evacuated to less than 10 millitorr, fluorinated with a mixture

of 80% He – 20% F_2, and heated to 400°C, for a minimum of 12 hours. The reaction produced SF_6 gas, which was cryogenically separated from the residual He and F_2 using liquid nitrogen.

Table 1: Collar locations of drillholes sampled for this study.

Location	Drillhole	Collar Latitude (North)	Collar Longitude (West)
Tamarack	08TK0049	46°40'19.4"	93°07'16.9"
Tamarack	12TK0138	46°40'5.0"	93°06'57.7"
Tamarack	12TK0153	46°40'8.9"	93°07'4.4"
Tamarack	12TK0158	46°40'9.3"	93°07'10.6"
Tamarack	13TK0171	46°40'7.1"	93°07'1.2"
Tamarack	14TK0213	46°40'13.1"	93°07'10.3"
Tamarack	15TK0229	46°41'7.8"	93°06'20.3"
Eagle	EAUG0069	46°44'54.8"	87°53'47.4"
Eagle	EAUG0070	46°44'54.8"	87°53'47.4"
Partridge River	MB 07-04	47°38'18.5"	92°15'40.0"
Partridge River	MB 07-13	47°38'16.6"	91°54'43.6"
Partridge River	MB 07-14	47°38'32.2"	91°55'5.4"
Partridge River	MB 08-25	47°38'30.8"	91°54'43.0"
Partridge River	MB 08-28	47°38'6.9"	91°55'23.0"
Partridge River	MB 08-36	47°38'17.4"	91°54'30.6"
Partridge River	MB13086	47°39'4.9"	91°53'27.7"

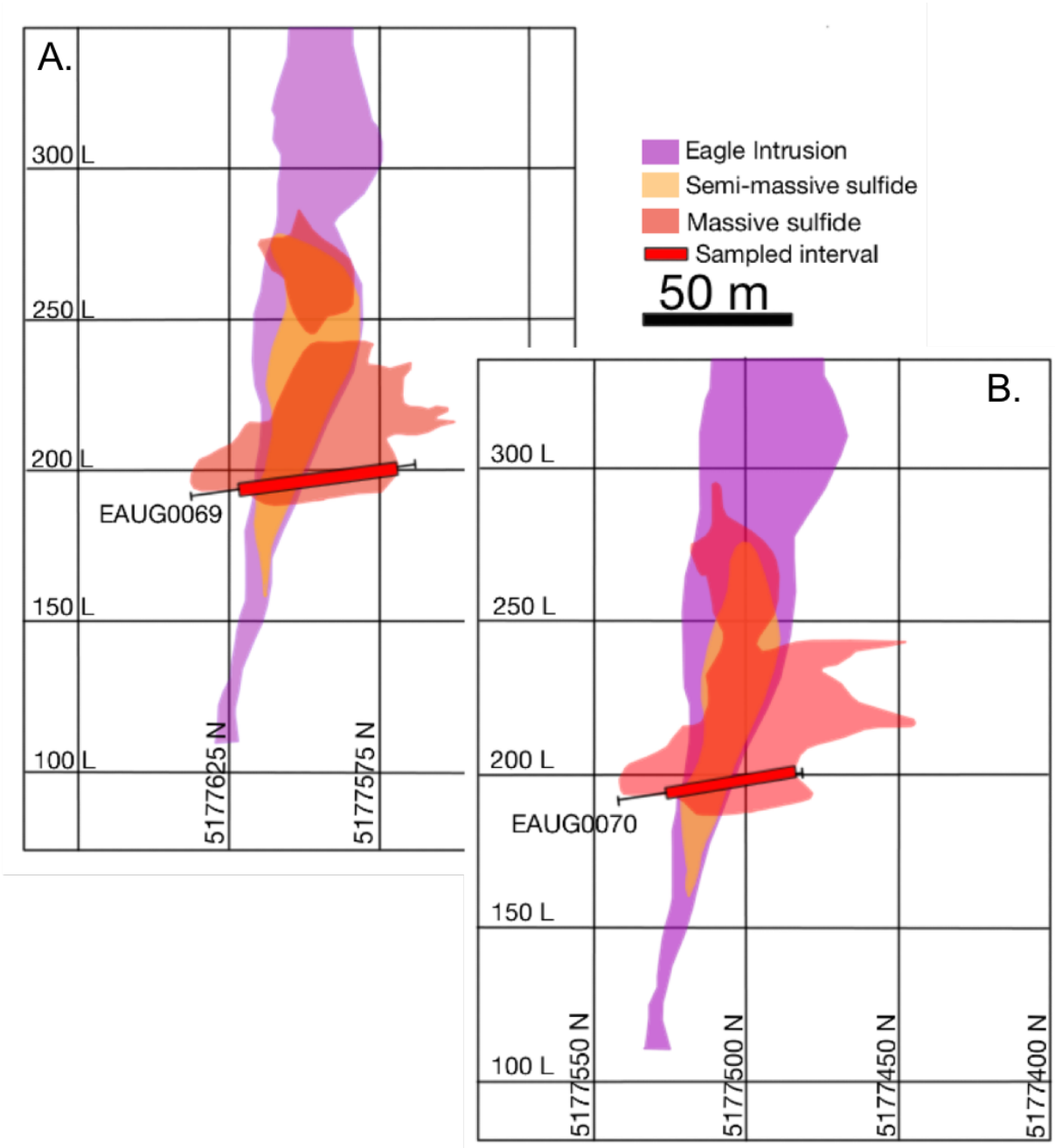

Figure 3: Cross-sections through the Eagle Intrusion, showing the intervals sampled from drillholes EAUG0069 (A) and EAUG0070 (B). Note that in the massive sulfides are hosted primarily outside the intrusion, but in some places, crosscuts the intrusion. Sections produced from 3D models provided courtesy of Lundin Mining.

A He carrier gas was then used to inject SF_6 into an HP gas chromatograph (GC) with a thermal conductivity detector. Purified SF_6 was then collected from the GC, frozen in a liquid nitrogen-cooled trap, and the He was pumped away. The sample gas was then allowed to flow, under vacuum, into a cold-finger and then the bellow of a ThermoFisher MAT 253 dual inlet isotope ratio-mass spectrometer (IR-MS). Both $\delta^{33}S$ and $\delta^{34}S$ were measured, and results are presented here in ‰ relative to the Vienna Canyon Diablo Troilite (VCDT). Calibration was performed using international standards IAEA S-1 ($\delta^{33}S$ = -0.05 ‰; $\delta^{34}S$ = -0.3 ‰) and IAEA S-2 ($\delta^{33}S$ = 11.64 ‰; $\delta^{34}S$ = 22.62 ‰; Ding et al., 2001; Mann et al., 2009). $\Delta^{33}S$ values were calculated following the method of Farquhar et al. (2010), where $\Delta^{33}S = \delta^{33}S - 1000 ((1 + \delta^{34}S/1000)^{\lambda} - 1)$. λ is the slope of the terrestrial reference line defined by mass dependent sulfur isotope fractionation with a slope of -0.515. Duplicate analyses of IAEA S-1 (n = 15) and our samples yielded 2 σ uncertainties of ± 0.2 ‰ for $\delta^{34}S$, ± 0.1 ‰ for $\delta^{33}S$, and ± 0.01 ‰ for $\Delta^{33}S$. Duplicate analyses of IAEA S-2 (n = 18) also yielded 2 σ uncertainties of ± 0.2 ‰ for $\delta^{34}S$ and ± 0.1 ‰ for $\delta^{33}S$; 2 σ uncertainties for $\Delta^{33}S$ was slightly larger at ± 0.03 ‰. Run statistics of all samples analyzed for $\delta^{34}S$ and $\delta^{33}S$ had 2σ uncertainties of better than 0.04 ‰. For the range of S isotope ratios reported in this study, the difference between delta values determined using the SF_6 and SO_2 methods is minor; conversion from one scale to the other can be made using the following expression: $\delta^{34}S\ (SF_6) = 1.0415 * \delta^{34}S\ (SO_2)$.

Twenty samples of country rock-hosted massive sulfides were analyzed for Re-Os isotopic compositions in the Department of Terrestrial Magnetism at the Carnegie Institution of Washington. Approximately 0.1 grams of sample was equilibrated in modified *aqua regia* with separate ^{185}Re and ^{190}Os spikes, using the Carius tube method described by Shirey and Walker (1995). Os was separated by CCl_4 solvent extraction and then distilled into HBr. The residual

aqua regia solution was put through anion exchange chromatography to recover the Re cut. The Os fraction in HBr was loaded onto a platinum filament and dried under a heat lamp. $Ba(OH)_2$ was added to the surface of the filament and dried again. Os was analyzed by negative thermal ionization mass spectrometry using a Thermo Finnigan Triton thermal ionization mass spectrometer in peak-hopping mode via a secondary electron multiplier. The purified Re fraction was diluted to 1.5 mL in 5% HNO_3, and $^{185}Re/^{187}Re$ were measured on a ThermoFisher iCAP-Qc RF quadrupole ICP-MS. Procedural blanks averaged 4.9 pg Re and 3.3 pg Os. Seven replicate measurements of the DTM J-M Os standard from July 2016 to May 2018 produced a $^{187}Os/^{188}Os$ ratio of 0.17388 ± 0.00038 (2-sigma of the population). Sample reproducibility of the $^{187}Os/^{188}Os$ was better than 0.01, based on numerous replicate analyses.

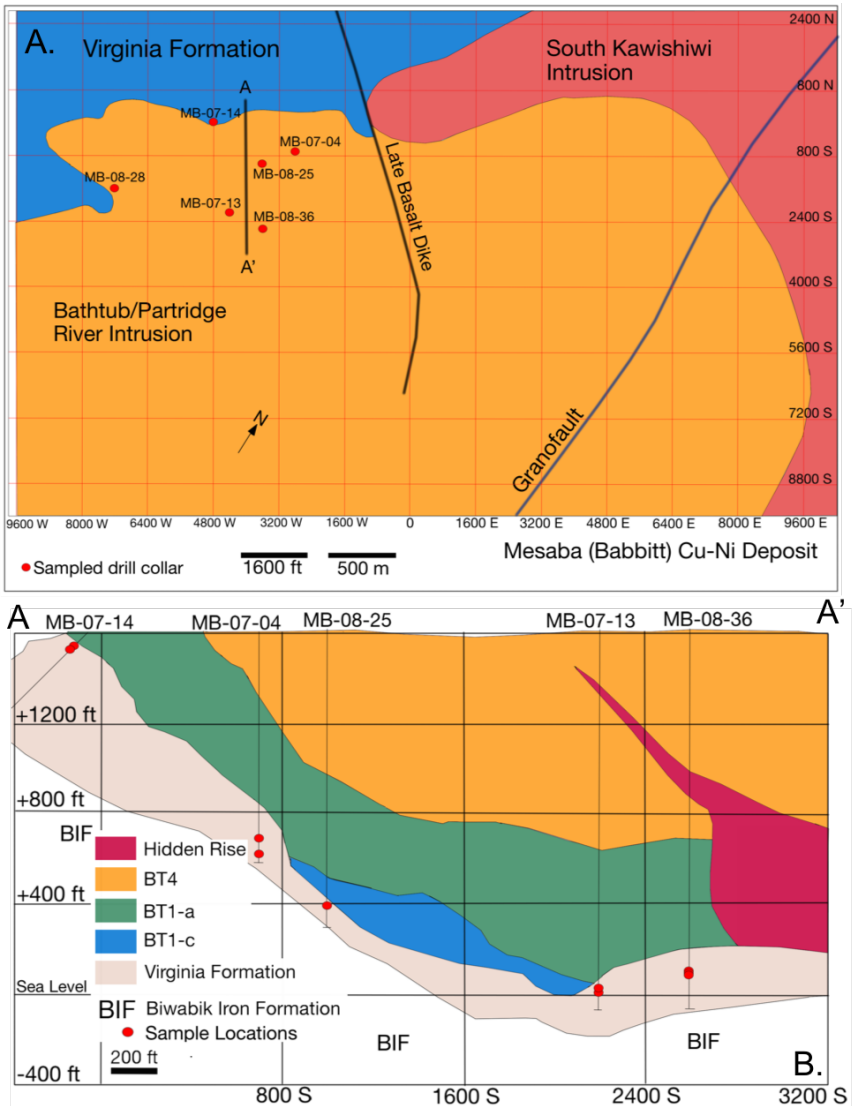

Figure 4: Map (A) and cross-sections (B) through the Mesaba Deposit, showing the simplified geology and drillholes sampled in this study. Map and cross-section modified from Severson and Hauck (2008).

Pb isotopic analyses were completed on 21 samples of massive sulfides. Pb analyses were performed in the Department of Terrestrial Magnetism at the Carnegie Institution of Washington. Crushed samples were digested in a mixture of concentrated HF and HNO_3. Samples were then dried, digested in HCl, and dried again before being taken up in HBr. The sample in HBr was put through anion exchange chromatography, and the Pb fraction was collected in HNO_3.

Samples were diluted with 5% HNO_3 and analyzed for $^{206}Pb/^{204}Pb$, $^{207}Pb/^{204}Pb$, and $^{208}Pb/^{204}Pb$ on a Nu-Plasma II multicollector ICP-MS. Standard-sample bracketing allowed isotopic ratios to be adjusted using a $^{205}Tl/^{203}Tl$ mass bias factor calculated from analyses of the NBS 981 standard. Thirteen replicate measurements of the NBS 981 standard, from July 2017 to May 2018 produced average $^{206}Pb/^{204}Pb$ of 16.94 ± 0.008,$^{207}Pb/^{204}Pb$ of 15.49 ± 0.01, and $^{208}Pb/^{204}Pb$ of 36.70 ± 0.03. Procedural blanks averaged 126 pg Pb, and analyzed sample solutions contained between 43 ppb and 7 ppm Pb.

Twenty-one samples were analyzed at the Université du Québec à Chicoutimi for Ni, Cu, Co, S, PGEs, and Au concentrations. Ni, Cu, and Co were determined by atomic absorption spectroscopy. Sulfur concentrations were measured on a Horiba elemental analyzer. Detection limits were 0.16 % S, 0.001 % Ni and Cu, and 3 ppm Co. PGEs and Au were measured by inductively coupled plasma mass spectrometry, following NiS preconcentration and *aqua regia* digestion. Analytical uncertainties of all PGEs and Au are better than ±5 %, and detection limits are 0.065 ppb Os, 0.025 ppb Ir, 0.12 ppb Ru, 0.082 ppb Rh, 0.084 ppb Pt, 0.471 ppb Pd, and 0.484 ppb Au. Further details of the analytical method are available in Savard et al. (2010). Se was analyzed by ICP-MS in the Metal Isotope Lab at Indiana University, Bloomington. Detection limits were < 1 ppb, and analytical uncertainties, based on duplicate sample analyses, were within 5 % relative.

Results

Mineralogy and textures

At Tamarack and Eagle, massive sulfides in country rocks are primarily composed of pyrrhotite, pentlandite, and chalcopyrite (Fig. 5A). Pyrrhotite is predominantly “massive,”

homogenous grains, or less commonly occurs as hexagonal/monoclinic pyrrhotite intergrowths. Pentlandite occur as distinct grains or exsolution lamellae in pyrrhotite. Trace to minor amounts of magnetite are present in most samples, but typically less than ~2 % by volume of the massive sulfides (Fig. 5B). Massive sulfide-country rock contacts display lobate and cuspate pods of sulfide embaying the country rocks (Fig. 5C), and commonly show a gradational boundary of pure massive sulfide, inter-mixed sulfide and silicate, and silicate country rocks (Fig. 5D). This texture is most similar to the "emulsion texture" of sulfides in a melt infiltration front as discussed in Barnes et al. (2018). In many samples, an 1- to 2-cm selvage in the silicates surrounds the massive sulfides. The selvage consists primarily of biotite and cordierite, whereas the country rocks outside of this selvage are composed of muscovite/illite, quartz, and chlorite. In many cases, massive sulfides are observed cross-cutting biotite (Fig. 5E) and cordierite grains. Some samples also display cumulate-like textures, with cumulus pyrrhotite surrounded by intercumulus nets of chalcopyrite-pentlandite (Fig. 5F).

At Partridge River the country rock-hosted massive sulfides are also primarily composed of pyrrhotite, pentlandite, and chalcopyrite. Intergrown hexagonal/monoclinic pyrrhotite is more abundant compared to samples from Eagle and Tamarack (Fig. 5G). Minor cubanite and magnetite, as well as trace bornite are also present. Sulfide-silicate contacts are similar to those at Tamarack and Eagle, showing diffusive boundaries with emulsion textures, with the exception that country rocks are composed of cordierite and orthopyroxene and only minor biotite (Fig. 5H).

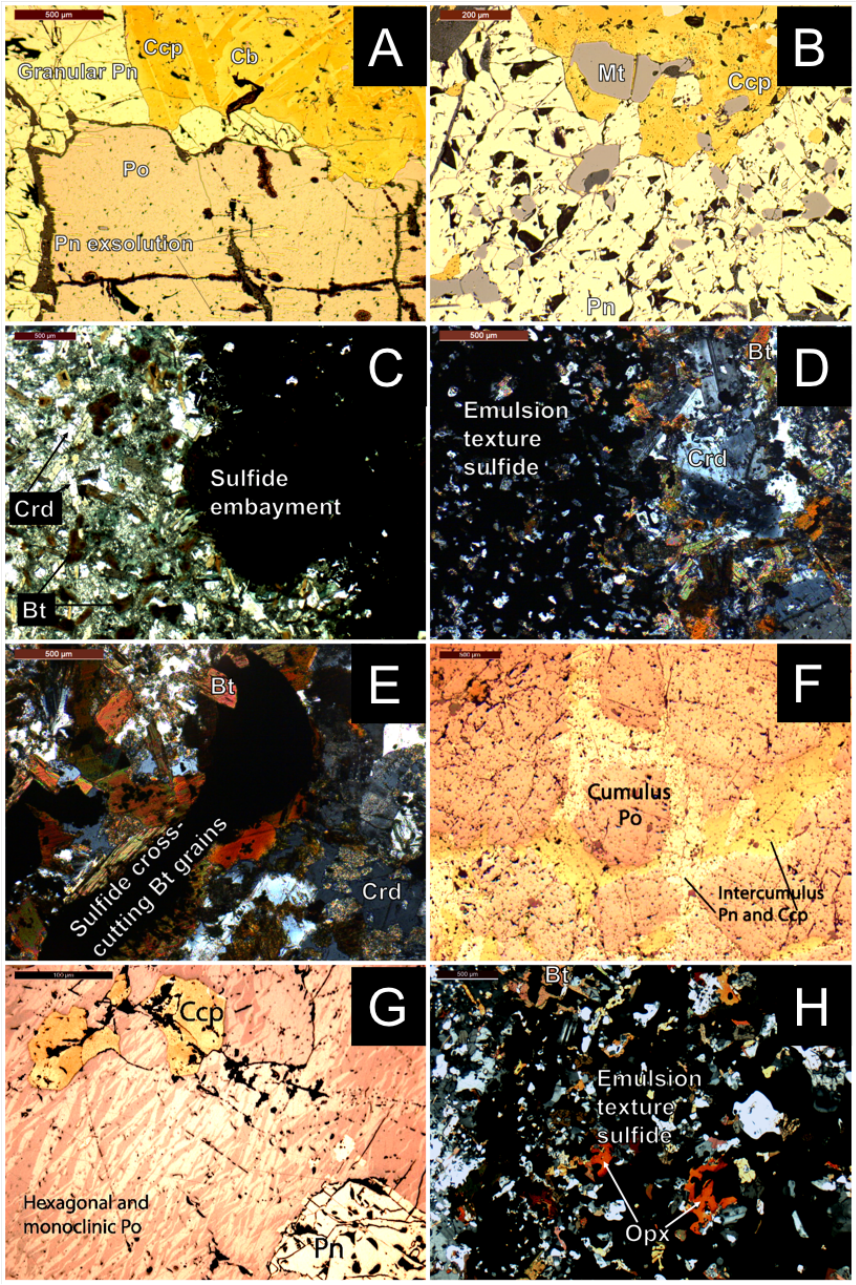

Figure 5: Photomicrographs of minerals and textures found in country rock-hosted massive sulfides near the Tamarack, Eagle, and Partridge River intrusions. A. Typical sulfide assemblage of massive sulfides from Tamarack, Eagle, and Partridge River (Po = pyrrhotite; Pn = pentlandite; Ccp = chalcopyrite; Cb = cubanite). B. Magnetite (Mt)-bearing massive sulfides from Eagle. C. Cuspate massive sulfide embayment in cordierite-biotite country rocks from Tamarack. D. Emulsion texture sulfide-silicate contacts from Tamarack. E. Massive sulfide embayment crosscutting multiple biotite grains at Tamarack. F. Cumulus pyrrhotite with intercumulus pentlandite and chalcopyrite at Eagle. G. Intergrown hexagonal and monoclinic pyrrhotite near the Partridge River intrusion. H. Emulsion texture sulfide-silicate contacts from Partridge River.

Co/Ni ratios

Co/Ni ratios are of particular interest in the discrimination of hydrothermal versus non-hydrothermal sulfide deposits (Bajwah et al., 1987). Co/Ni ratios of samples used in this study can be found in Table 2. Country rock-hosted massive sulfides at Tamarack have Co/Ni ratios of 0.016 to 0.022. Co/Ni ratios of massive sulfides at Eagle range from 0.024 to 0.033. Samples below the Partridge River intrusion have Co/Ni ratios of 0.077 to 0.22.

S/Se ratios

S/Se ratios are commonly used to identify the source of sulfur in magmatic sulfide deposits (Queffurus and Barnes, 2015; Smith et al., 2016). Sedimentary rocks are generally depleted in selenium due to the enhanced solubility of S over Se in sedimentary environments (Ewers, 1977), and thus elevated S/Se ratios are indicative of country rock assimilation during magmatic sulfide genesis (Ripley, 1990b; Thériault and Barnes, 1998). S/Se ratios of samples from this study can be found in Table 2. Samples from Tamarack have S/Se ratios from 1,302 to 2,688. At Eagle, massive sulfides in the country rocks have S/Se ratios from 3,196 to 4,925. Samples from below the Partridge River intrusion have S/Se ratios from 3,294 to 10,079. A summary diagram of Co/Ni and S/Se ratios from samples used in this study can be found in Figure 6.

Sample	Location	S (%)	Ni (%)	Cu (%)	Os (ppb)	Ir (ppb)	Ru (ppb)	Rh (ppb)	Pt (ppb)	Pd (ppb)	Au (ppb)	Co (ppm)	As (ppm)	Sb (ppm)	Se (ppm)	Te (ppm)	Co/Ni	S/Se
49-398.68	Tamarack	32.68	18.91	6.69	9.99	15.05	3.53	27.34	488.76	884.80	31.99	3418.26	27.48	5.18	250.94	34.25	0.018	1302
49-404.81	Tamarack	34.10	19.89	2.52	6.96	12.20	2.91	16.73	433.41	1052.10	19.34	3380.65	14.89	2.13	261.63	14.40	0.017	1303
49-405.78	Tamarack	33.10	16.61	4.88	0.78	5.55	0.17	13.09	468.09	876.71	520.09	2884.05	8.68	1.87	235.08	11.09	0.017	1408
49-406.61	Tamarack	32.34	6.97	2.24	4.50	8.57	1.18	16.29	439.93	493.87	17.73	1132.15	13.38	0.68	153.55	8.52	0.016	2106
213-455.19	Tamarack	35.15	8.06	2.05	80.34	163.42	34.70	128.95	31.48	1011.41	93.56	1662.77	22.91	1.10	163.95	25.30	0.021	2144
213-459.55	Tamarack	35.34	2.88	0.09	99.60	166.00	48.75	131.83	19.48	132.87	5.44	491.45	18.15	0.53	145.00	5.97	0.017	2437
213-460.49	Tamarack	34.07	11.78	2.84	105.38	159.24	57.46	115.56	1370.56	1816.56	77.78	2573.98	11.86	1.14	126.76	-	0.022	2688
213-461.19	Tamarack	34.81	10.10	2.23	55.56	121.54	25.47	107.60	4.11	894.30	8.61	2111.57	10.02	3.29	177.82	-	0.021	1958
69-26.26	Eagle	29.25	4.99	6.95	40.98	47.70	37.11	23.11	3163.53	1798.03	494.45	1213.86	1.33	3.18	86.31	-	0.024	3388
70-37	Eagle	34.52	5.72	4.91	115.84	118.91	120.02	51.77	1846.84	3468.26	449.71	1408.62	6.22	0.83	101.59	24.01	0.025	3398
69-38	Eagle	34.52	5.91	4.40	245.11	250.81	266.87	89.38	1499.79	604.41	350.95	1470.16	3.27	0.39	79.84	4.34	0.025	4324
70-43.59	Eagle	35.20	8.83	4.80	222.20	224.90	212.92	89.40	988.42	527.21	191.93	2276.10	2.26	0.18	102.26	5.83	0.026	3443
69-55.75	Eagle	36.03	12.13	5.41	572.30	615.78	546.98	211.39	903.71	586.18	296.86	3753.98	2.33	0.10	112.74	4.91	0.031	3196
70-58.36	Eagle	36.13	5.91	2.23	737.95	795.20	725.35	259.21	965.39	191.11	37.38	1634.43	1.62	0.39	73.35	3.60	0.028	4925
69-71.8	Eagle	37.15	8.40	2.62	859.52	874.99	899.73	253.60	1794.58	953.98	182.50	2779.30	1.86	0.04	90.33	7.93	0.033	4113
07-04-925.9	Partridge River	35.21	1.12	1.42	12.39	7.80	31.91	19.96	0.23	17.85	18.14	1377.93	65.45	0.80	34.94	-	0.123	10079
07-04-994.3	Partridge River	26.62	1.34	4.75	9.97	8.66	32.24	17.34	0.69	94.22	20.71	1188.61	31.15	2.22	35.23	-	0.089	7555
08-28-1045.2	Partridge River	31.30	0.59	2.56	5.60	8.93	26.10	21.77	0.11	3.65	1.85	707.75	57.41	1.72	40.38	-	0.121	7752
08-36-1549.6	Partridge River	34.76	0.18	20.84	1.60	6.36	6.44	11.72	21.90	89.93	3.23	395.92	51.36	3.85	66.72	-	0.220	5210
08-36-1552	Partridge River	34.33	0.15	31.03	0.50	2.57	3.04	5.00	5.02	20.66	1.02	117.95	274.58	1.66	104.22	-	0.077	3294
07-13-1605.1	Partridge River	34.23	0.49	1.84	1.45	11.34	8.15	26.83	0.14	22.39	3.32	529.34	1.98	0.08	46.73	-	0.107	7326

Table 2: Major and trace element concentrations and trace element ratios of country rock-hosted massive sulfides near Tamarack, Eagle, and the Partridge River intrusions.

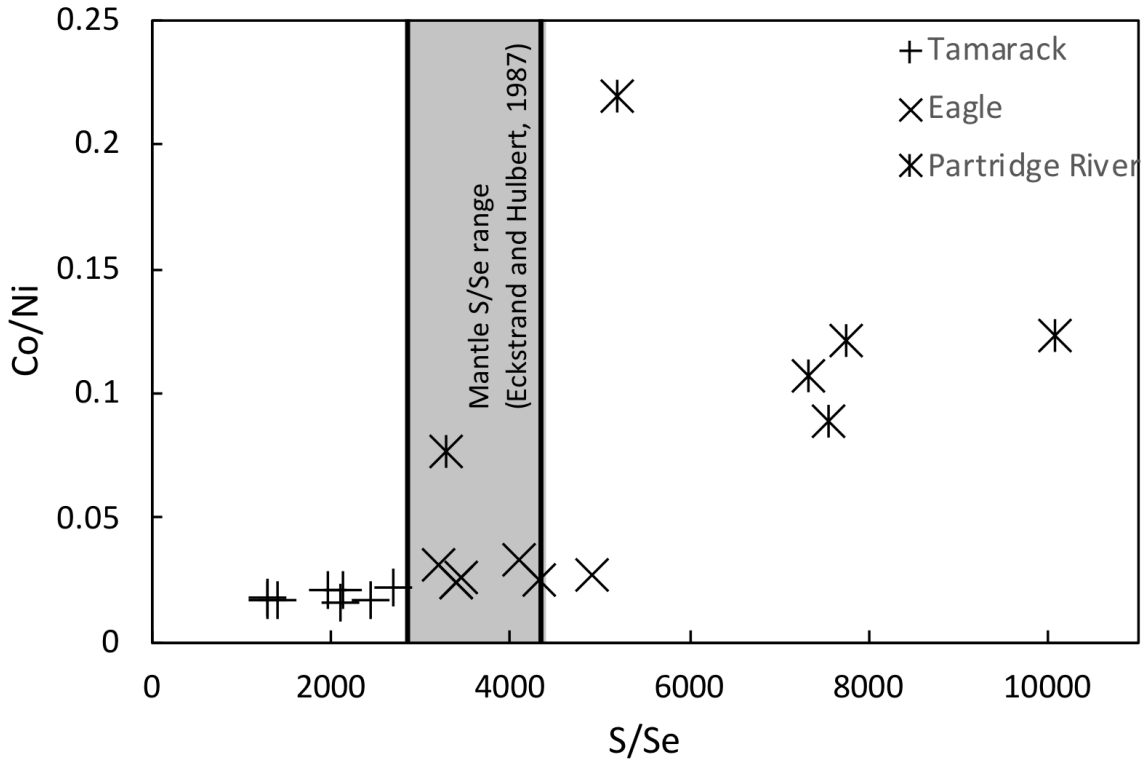

Figure 6: Co/Ni vs S/Se ratios of country rock-hosted massive sulfides near the Tamarack, Eagle, and Partridge River intrusions.

Ni-Cu-PGE concentrations in sulfide

Major and trace element concentrations of country rock-hosted massive sulfides near Tamarack, Eagle, and Partridge River are listed in Table 2, and metal tenors (concentration in 100 % sulfide) are listed in Table 3. Massive sulfides have whole rock Ni/Cu ratios ranging from 2.8 to 31.3 at Tamarack and 0.7 to 3.2 at Eagle. Taranovic et al. (2016) report whole rock Ni/Cu of 0.6 to 3.6 for disseminated sulfides, 1.6 to 3.2 for the semi-massive sulfides, and 1.4 to 5.6 for the massive sulfides of the Tamarack deposit. Ding et al. (2012) report whole rock Ni/Cu ratios of 1.3 to 2.5 for the disseminated sulfides, 0.5 to 5.1 for the semi-massive sulfides, and 1.3

to 6.8 for the massive sulfides of the Eagle deposit. Minor Cu-rich veins in the country rocks have Ni/Cu ratios of 0.1 to 1.3. Ni/Cu ratios are significantly lower in massive sulfides below the Partridge River intrusion and range from 0.005 to 0.8. Theriault et al. (1997) and Ripley (1990a) report whole rock Ni/Cu ratios of 0.2 to 0.6 and 0.003 to 1.7, respectively for the disseminated sulfides of the Duluth Complex.

On Ni/Cu vs. Pd/Ir discrimination diagrams (Fig. 7A), samples from Tamarack plot within and near the field of high MgO basalt-related Ni-Cu-PGE sulfide deposits, similar to samples of igneous-hosted sulfides. Massive sulfides in the country rocks, however, tend be slightly more Ni-rich with higher Ni/Cu ratios. Country rock-hosted massive sulfides from the Eagle deposit also plot within or near the field for high MgO basalt-related Ni-Cu-PGE sulfide deposits (Fig. 7B) and plot very near the igneous-hosted sulfides, especially the igneous rock-hosted massive sulfides. Most massive sulfide samples from below the Partridge River intrusion plot slightly outside the field of flood basalt-related Ni-Cu-PGE sulfide deposits (Fig. 7C) and near many of the disseminated sulfides from the base of troctolitic sheets in the Partridge River intrusion (Ripley, 1990a). Disseminated sulfides from norites and troctolites studied by Theriault et al. (1997) are consistently more enriched in Pd (+Pt), based on their high Pd/Ir ratios.

Individual IPGE (Os, Ir, Ru, Rh) show good positive correlations between them for all three localities, although the correlations are slightly better at Tamarack and Eagle than at Partridge River. No PGEs have a significant correlation with S, as S concentrations range from 27 to 37 wt. % S. With the exception of Ru, massive sulfide samples from Tamarack and Eagle are more enriched in all PGEs than those from Partridge River.

Sample	Location	Ni (%)	Cu (%)	Os (ppb)	Ir (ppb)	Ru (ppb)	Rh (ppb)	Pt (ppb)	Pd (ppb)	Au (ppb)	Co (ppm)	As (ppm)	Sb (ppm)	Se (ppm)	Te (ppm)
49-398.68	Tamarack	20.17	7.13	10.65	16.04	3.77	29.15	521.17	943.47	34.11	3644.92	29.30	5.52	267.58	36.52
49-404.81	Tamarack	20.63	2.62	7.43	13.01	3.10	17.84	462.14	1121.86	20.62	3604.82	15.88	2.27	278.98	15.36
49-405.78	Tamarack	17.83	5.24	0.83	5.92	0.18	13.96	499.12	934.85	554.58	3075.29	9.25	2.00	250.66	11.83
49-406.61	Tamarack	8.12	2.61	4.80	9.14	1.26	17.37	469.10	526.62	18.91	1207.22	14.27	0.72	163.73	9.09
213-455.19	Tamarack	8.63	2.19	85.67	174.25	37.00	137.50	33.57	1078.48	99.77	1773.03	24.43	1.18	174.82	26.98
213-459.55	Tamarack	3.18	0.10	106.20	177.01	51.99	140.57	20.77	141.68	5.80	524.04	19.35	0.57	154.62	6.36
213-460.49	Tamarack	12.72	3.06	112.37	169.80	61.27	123.23	1461.44	1937.01	82.93	2744.66	12.65	1.22	135.17	-
213-461.19	Tamarack	10.81	2.39	59.24	129.60	27.16	114.74	4.38	953.61	9.18	2251.58	10.69	3.51	189.61	-
69-26.26	Eagle	6.35	8.83	43.69	50.87	39.57	24.65	3373.30	1917.26	527.24	1294.35	1.42	3.39	92.04	-
70-37	Eagle	6.24	5.36	123.52	126.80	127.98	55.20	1969.30	3698.24	479.53	1502.02	6.63	0.88	108.33	25.60
69-38	Eagle	6.45	4.81	261.36	267.45	284.56	95.30	1599.24	644.48	374.22	1567.64	3.49	0.41	85.13	4.62
70-43.59	Eagle	9.32	5.06	236.93	239.82	227.03	95.33	1053.96	562.17	204.65	2427.03	2.41	0.19	109.04	6.21
69-55.75	Eagle	12.30	5.49	610.24	656.61	583.25	225.41	963.64	625.05	316.54	4002.90	2.48	0.10	120.21	5.24
70-58.36	Eagle	6.23	2.35	786.88	847.92	773.45	276.40	1029.41	203.78	39.85	1742.81	1.73	0.41	78.22	3.84
69-71.8	Eagle	8.50	2.65	916.52	933.01	959.39	270.41	1913.57	1017.24	194.61	2963.60	1.98	0.05	96.32	8.45
07-04-925.9	Partridge River	1.25	1.57	13.21	8.32	34.03	21.29	0.25	19.03	19.35	1469.30	69.79	0.86	37.26	-
07-04-994.3	Partridge River	1.93	6.83	10.63	9.24	34.38	18.48	0.73	100.47	22.08	1267.42	33.22	2.36	37.57	-
08-28-1045.2	Partridge River	0.73	3.19	5.97	9.52	27.83	23.22	0.11	3.89	1.97	754.68	61.22	1.83	43.05	-
08-36-1549.6	Partridge River	0.19	21.93	1.70	6.79	6.87	12.49	23.35	95.89	3.45	422.18	54.77	4.10	71.14	-
08-36-1552	Partridge River	0.16	31.86	0.53	2.74	3.24	5.33	5.35	22.03	1.08	125.77	292.79	1.77	111.13	-
07-13-1605.1	Partridge River	0.57	2.11	1.55	12.09	8.69	28.61	0.15	23.88	3.54	564.44	2.11	0.08	49.82	-

Table 3: Major and trace element concentrations in 100 % sulfide for country rock-hosted massive sulfides near Tamarack, Eagle, and the Partridge River intrusions. Concentrations in 100 % sulfide were calculated using the equation of Barnes and Lightfoot, 2005.

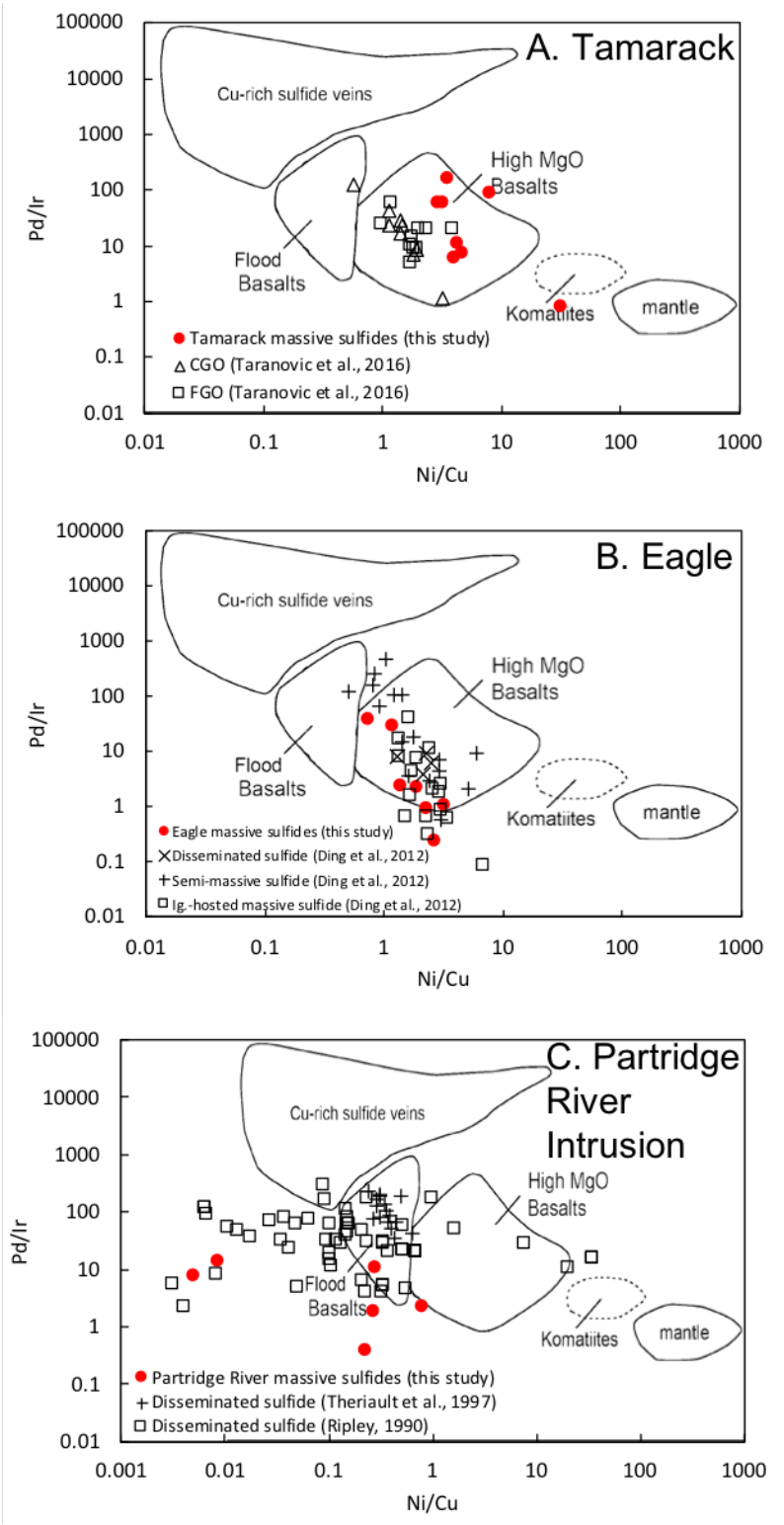

Figure 7: Pd/Ir vs. Ni/Cu discrimination diagrams for country rock-hosted massive sulfides near the Tamarack, Eagle, and Partridge River intrusions.

Mantle normalized PGE patterns for Eagle and Tamarack samples are shown in Fig. 8A-B and Fig. 9A-B recalculated to 100 % sulfide using the equation of Barnes and Lightfoot (2005). Country rock-hosted massive sulfides from Eagle are IPGE-enriched (Os, Ir, Ru, Rh), relative to the lower semi-massive and disseminated sulfides in the igneous rocks, and have similar trends to the igneous rock-hosted IPGE-rich and "unfractionated" massive sulfides (Ding et al., 2012). In most instances the samples are enriched in IPGEs compared to disseminated or semi-massive sulfides by 1 to 2 orders of magnitude. Two samples of country rock-hosted massive sulfides are more similar to PPGE-enriched massive sulfides in the igneous rocks, although this also makes them qualitatively similar to the disseminated sulfides and semi-massive sulfides (Ding et al., 2012).

Country rock-hosted massive sulfides from Tamarack are all characterized by highly erratic (not smooth) mantle-normalized PGE profiles. There are, however, two distinct groupings. Group I samples are IPGE-enriched and are broadly similar to semi-massive sulfides from the CGO, which also display highly erratic PGE trends and have similar Cu enrichments. Three of the four samples also display Pt depletions, like many of the CGO semi-massive sulfides. Group II are PPGE-enriched and have no Pt depletion and are broadly similar to massive sulfides reported by Taranovic et al. (2016). Among both groups, seven of the eight samples of country rock-hosted massive sulfides also have Au depletions. PGE trends of disseminated sulfides from the CGO and FGO, however, are more PGE-rich (in 100 % sulfide) than country rock-hosted massive sulfides. Disseminated sulfides from both the CGO and FGO intrusions are also slightly more Cu-enriched compared to many of the country rock-hosted massive sulfides.

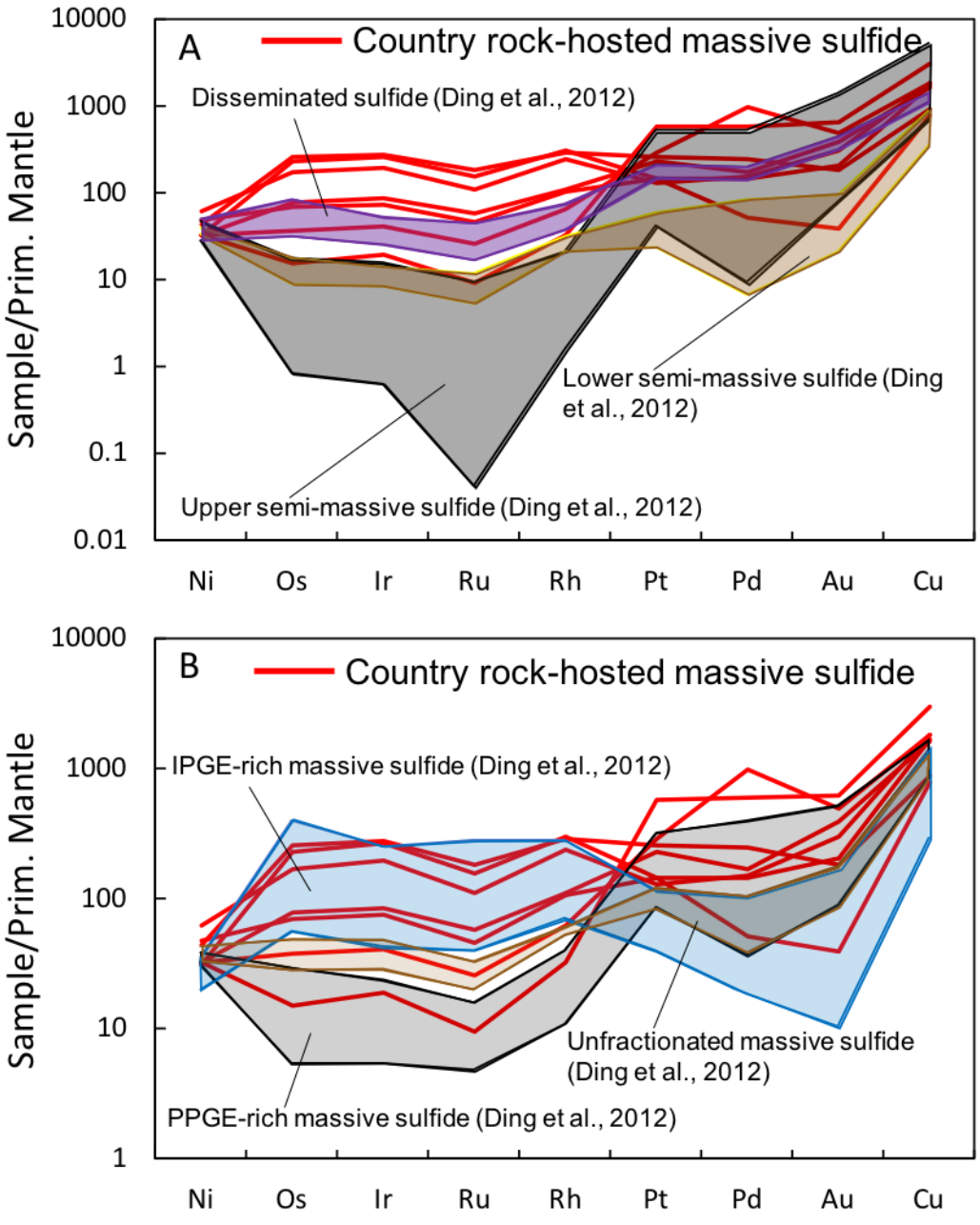

Figure 8: Mantle normalized PGE patterns for country rock-hosted massive sulfides near the Eagle intrusion, shown in comparison to igneous-hosted disseminated and semi-massive sulfides (A) and igneous-hosted massive sulfides (B) from Eagle.

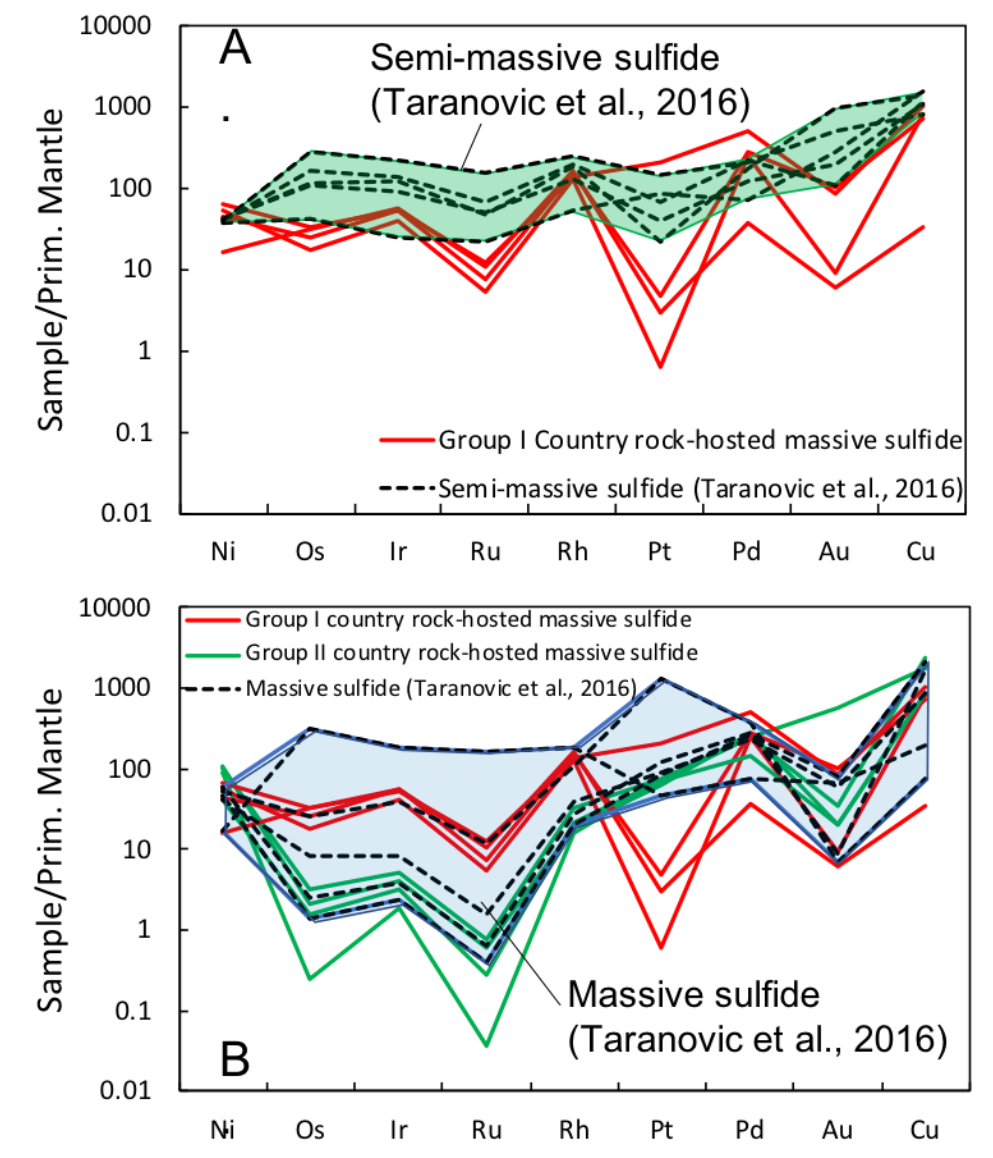

Figure 9: Mantle normalized PGE patterns of country rock-hosted massive sulfides near the Tamarack intrusive complex, shown in relation to mantle normalized patterns for igneous-hosted semi-massive sulfides (A) and other related massive sulfides (B).

Massive sulfides below the Partridge River Intrusion (Fig. 10A–C) are characterized by sloping mantle-normalized PGE profiles, which have high Ni, decrease at Os, and begin to rise through Ir, Ru, and Rh. Pt, Pd, and Au depart from the rising trend, with exceptionally large negative Pt anomalies (2 to 3 orders of magnitude compared to surrounding Rh and Pd). The

rising trend again becomes apparent for Cu, which is generally enriched 2 to 3 orders of magnitude relative to adjacent Au. Mantle-normalized PGE patterns of the massive sulfides from this study are nearly identical to massive sulfides located at the contact between the Partridge River intrusion and the underlying Virginia Formation reported by Ripley (1990a), although samples from this study are more depleted in Pt in most cases. Mantle-normalized PGE trends of troctolite-hosted disseminated sulfides reported in Theriault et al. (1997) and Ripley (1990a) generally increase from Ni to Cu. Samples from this study overlap the range of trends for troctolites reported in Theriault et al. (1997) in terms of Ni, Os, Ir, Ru, and Rh, as well as Cu. Samples from this study are substantially depleted in Pt, Pd, and Au compared to the Theriault et al. (1997) samples. The most PGE-poor troctolite-hosted disseminated sulfides from Ripley (1990a) overlap well with our data with the exception of Pt and Os.

S Isotopes

Results of S isotope measurements of country rock-hosted massive sulfides at Tamarack, Eagle, and the Partridge River Intrusion are listed in Table 4 and multiple S data are shown in Figure 11. S isotope analyses (SO_2 method) from the massive sulfides at Tamarack have a $\delta^{34}S$ range from 0.3 to 3.5 ‰ (1.0 to 3.8 ‰ for SF_6 method), with an average of 1.5 ‰. $\Delta^{33}S$ (SF_6 method) values at Tamarack cluster between -0.01 and 0.04 ‰. SO_2 analyses of samples from Eagle have $\delta^{34}S$ from 3.0 to 3.9 ‰ (2.9 to 3.9 ‰ for SF_6 method), with average $\delta^{34}S$ of 3.4 ‰. $\Delta^{33}S$ values range from -0.02 to 0.05 ‰. A single replicable sample from Eagle had a $\delta^{34}S$ of 8.5 ‰. SO_2 analyses of samples below the Partridge River Intrusion have $\delta^{34}S$ between 9.9 and 19.3 ‰ (10.4 to 13.7 ‰ for SF_6 method) and average 13.4 ‰, with $\Delta^{33}S$ values from -0.03 to 0.02 ‰. Multiple S isotope compositions of igneous rock-hosted sulfides from Tamarack are listed in

Table 5. Tamarack igneous-hosted sulfides have $\delta^{34}S$ from 1.5 to 3.0 ‰ (SF_6 method) and $\Delta^{33}S$ from 0.01 to 0.03 ‰.

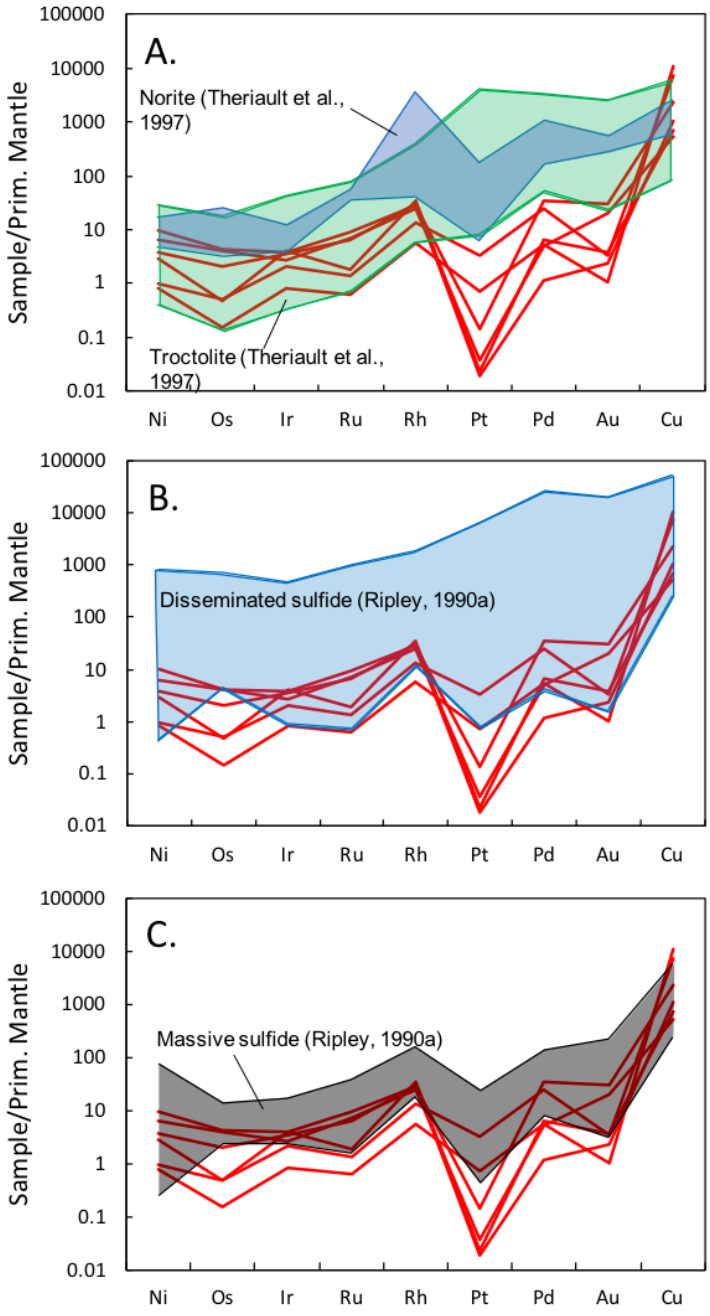

Figure 10: Mantle normalized PGE trends for country rock-hosted massive sulfides below the Partridge River intrusion and associated igneous-hosted disseminated sulfides (A, B) and previously analyzed massive sulfides (C).

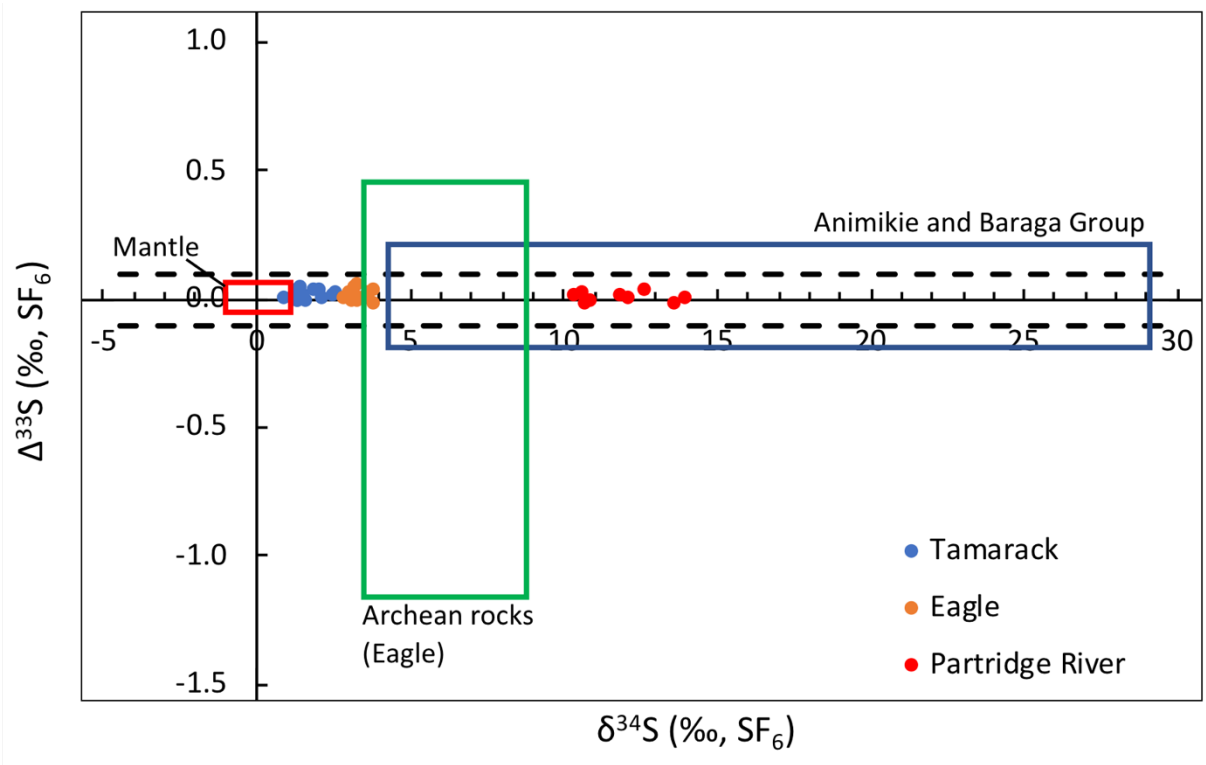

Figure 11: $\delta^{34}S$ and $\Delta^{33}S$ values of country rock-hosted massive sulfides near the Tamarack Intrusive Complex, the Eagle deposit, and beneath the Partridge River Intrusion.in relation to $\delta^{34}S$ and $\Delta^{33}S$ ranges for mantle (red box) (Ripley et al., 2017), Proterozoic rocks of the Animikie (Ripley, 1981; Ripley and Al-Jassar, 1987) and Baraga Group sediments (blue box) (Ding et al., 2012), and Archean rocks near the Eagle deposit (green box) (Ding et al., 2012). Brackets for typical "non-anomalous" $\Delta^{33}S$ values are shown from -0.1 to +0.1 ‰.

Table 4: S isotope measurements of country rock-hosted massive sulfides from Tamarack, Eagle, and below the Partridge River Intrusion. Note that *PR* refers to massive sulfides from the Virginia Formation below the Partridge River Intrusion.

Sample Name	Location	$\delta^{34}S$ [1]	$\delta^{33}S$ [2]	$\delta^{34}S$ [2]	$\Delta^{33}S$ [2,3]
229-694.47	Tamarack	1.9			
229-700.53	Tamarack	1.8			
229-702.81	Tamarack	1.6	2.0	3.8	0.00
138-502.23	Tamarack	1.3	0.8	1.5	0.04
138-518.17	Tamarack	1.1			
49-396.99	Tamarack	0.3			
49-397.44	Tamarack	1.1	0.5	1.0	0.00
49-398.34	Tamarack	1.5			
49-398.68	Tamarack	1.4			
49-399.56	Tamarack	1.3			
49-400.5	Tamarack	1.2	0.8	1.4	0.03
49-401.18	Tamarack	1.5			
49-401.58	Tamarack	1.7			
49-402.83	Tamarack	1.2			
49-403.56	Tamarack	1.4			
49-404.81	Tamarack	1.2			
49-405.26	Tamarack	1.5			
49-405.78	Tamarack	1.6			
49-406.61	Tamarack	1.5	0.9	1.5	0.11
49-407.88	Tamarack	1.2			
213-434.44	Tamarack	3.5	1.9	3.6	0.00
213-434.74	Tamarack	3.1			
213-435.81	Tamarack	1.6			
213-436.71	Tamarack	1.3			
213-437.96	Tamarack	1.7			
213-438.52	Tamarack	1.4			
213-439.61	Tamarack	1.2			
213-440.19	Tamarack	1.8			
213-441.05	Tamarack	2.2	1.4	2.6	0.02
213-442.22	Tamarack	1.1			
213-455.19	Tamarack	1.3			
213-458.38	Tamarack	1.6	1.1	2.1	0.03
213-459.55	Tamarack	1.4			
213-460.49	Tamarack	1.3			
213-461.19	Tamarack	1.6			
213-461.78	Tamarack	1.6			
213-464	Tamarack	1.7	1.0	2.0	0.03
213-464.57	Tamarack	1.5			
158-483.53	Tamarack	1.7			
158-484.89	Tamarack	1.4			
158-485.29	Tamarack	1.5			
158-486.39	Tamarack	1.5			
158-487.38	Tamarack	1.4	0.7	1.3	0.00
158-487.75	Tamarack	1.4			
158-488.23	Tamarack	1.4			
158-490.1	Tamarack	1.7			
158-490.75	Tamarack	1.5	0.8	1.6	0.01
158-491.46	Tamarack	1.8			
158-492.78	Tamarack	1.5			
158-493.53	Tamarack	1.2	0.9	1.7	-0.01
158-494.79	Tamarack	1.3			
158-494.94	Tamarack	1.5			
158-495.57	Tamarack	1.8			
153-555.65	Tamarack	1.6			
153-556.74	Tamarack	1.3			
153-557.95	Tamarack	1.8			
153-560.35	Tamarack	1.4			
153-561.32	Tamarack	1.2			
153-561.49	Tamarack	1.2			
153-562.51	Tamarack	1.5			
153-563.87	Tamarack	1.2			
153-564.9	Tamarack	1.3			
153-565.85	Tamarack	1.3			
153-566.6	Tamarack	1.4	0.8	1.5	-0.01
153-567.12	Tamarack	1.7			
153-567.62	Tamarack	1.5			
153-568.07	Tamarack	1.3			
153-572.77	Tamarack	1.2			
153-573.23	Tamarack	1.3			
153-573.84	Tamarack	0.9			
153-574.2	Tamarack	1.3			
153-574.8	Tamarack	1.4	0.7	1.1	0.12
153-575.86	Tamarack	1.2			
171-575.38	Tamarack	1.4	0.8	1.4	0.03
171-579.91	Tamarack	1.8	1.1	2.2	0.00
69-20.23	Eagle	3.5	1.5	2.9	0.00
69-23.19	Eagle	3.8	2.0	3.9	-0.02
69-26.26	Eagle	3.1	1.7	3.2	0.01
69-29.27	Eagle	3.8			
69-32.28	Eagle	3.9			
69-35.08	Eagle	3.9			
69-38	Eagle	3.6	1.9	3.7	0.01
69-40.97	Eagle	3.2			
69-46.7	Eagle	3.5			
69-48.89	Eagle	3.9			
69-49.6	Eagle	3.7			
69-52.56	Eagle	3.9			
69-55.75	Eagle	3.0	1.6	3.1	-0.01
69-58.79	Eagle	3.1			
69-63.01	Eagle	3.2			
69-65.7	Eagle	3.1			
69-69.95	Eagle	3.1			
69-71.80	Eagle	3.2	1.8	3.5	-0.01
70-17.22	Eagle	3.4	3.3	6.5	-0.02
70-17.82	Eagle	8.5			
70-25.87	Eagle	3.4	1.6	3.0	0.09
70-31.88	Eagle	3.6	2.0	3.9	0.03
70-34.4	Eagle	3.1			
70-37.72	Eagle	3.1	1.7	3.3	0.03
70-40.65	Eagle	3.3			
70-43.59	Eagle	3.5	1.8	3.4	0.05
70-49.27	Eagle	3.4			
70-49.46	Eagle	3.0			
70-52.51	Eagle	3.2			
70-55.48	Eagle	3.2			
70-58.36	Eagle	3.4	1.9	3.7	0.02
70-60.66	Eagle	3.0	1.7	3.4	-0.01
MB07-04-925.9	PR	13.1	7.0	13.7	-0.03
MB07-04-994.3	PR	13.2	7.2	14.1	-0.01
MB07-13-1605.1	PR	10.5	5.5	10.8	-0.02
MB07-13-1614.3	PR	12.0	6.2	12.1	0.00
MB07-14-79.8	PR	15.9			
MB07-14-101	PR	17.9			
MB08-25-1255.2	PR	12.1	6.6	12.7	0.02
MB08-28-1045.2	PR	11.6	6.1	12.0	0.00
MB08-36-1549.6	PR	10.2	5.5	10.7	0.01
MB08-36-1552	PR	10.5	5.4	10.4	0.01
MB08-36-1556.7	PR	9.9	5.6	10.9	-0.01
MB13086-467.1	PR	10.5			
MB13086-468.55	PR	14.0			
MB13086-476.9	PR	15.4			
MB13086-487.1	PR	17.4			
MB13086-517.1	PR	19.3			

1: SO_2 method

2: SF_6 method

3: $\Delta^{33}S = \delta^{33}S - 1000*((1+\delta^{34}S/1000)^{0.515}-1)$

Table 5: S isotope measurements of igneous-hosted sulfides from Tamarack.

Sample	Drillhole	Sulfide type	Unit	$\delta^{34}S$ [1]	$\delta^{33}S$ [2]	$\delta^{34}S$ [2]	$\Delta^{33}S$ [2,3]
58-479.5	08TK0058	Disseminated	CGO	1	1	2	0.01
67-399.4	08TK0067	Disseminated	CGO	1.2	0.8	1.5	0.01
58-467.48	08TK0058	Semi-massive	CGO	1.1	0.9	1.8	0.02
58-487.48	08TK0058	Semi-massive	CGO	1.2	0.9	1.7	0.01
58-529.8	08TK0058	Semi-massive	CGO	1.4	0.9	1.8	0.02
67-455.5	08TK0067	Semi-massive	CGO	1.1	0.8	1.5	0.01
67-460.2	08TK0067	Semi-massive	CGO	1.9	0.9	1.6	0.02
67-466.7	08TK0067	Semi-massive	CGO	1.7	0.9	1.7	0.02

1: SO_2 method
2: SF_6 method
3: $\Delta^{33}S = \delta^{33}S - 1000*((1 + \delta^{34}S/1000)^{0.515}-1)$

Re-Os Isotopes

Re and Os concentrations and isotopic ratios for 20 massive sulfides in country rocks at Tamarack, Eagle, and Partridge River are reported in Table 6. At Tamarack, Re concentrations vary from 38 to 123 ppb, and Os concentrations range from 2 to 114 ppb. $^{187}Re/^{188}Os$ ratios range from 4.69 to 114.16, and $^{187}Os/^{188}Os$ ratios range from 0.2265 to 2.254. Calculated γOs, or the percent deviation from a primate upper mantle reservoir, from the massive sulfides range from +14 to +30 (1100 Ma, primitive mantle). Massive sulfides in sedimentary rocks near Eagle have Re concentrations from 71 to 315 ppb. Os concentrations are between 48 and 969 ppb Os. $^{187}Re/^{188}Os$ ratios extend from 1.46 to 7.16, and $^{187}Os/^{188}Os$ range from 0.1736 to 0.2944, with calculated γOs (1100 Ma) between 21 and 33. Massive sulfides in metasedimentary rocks below the Partridge River Intrusion have between 40 and 300 ppb Re and between 1.3 and 14.7 ppb Os. $^{187}Re/^{188}Os$ ratios range from 75 to 631, and $^{187}Os/^{188}Os$ ratios extend from 3.04 to 13.4. Calculated γOs (1100 Ma) range from 793 to 1341.

Table 6: Re-Os isotope analyses of country rock-hosted massive sulfides from Tamarack, Eagle, and beneath the Partridge River Intrusion. Note that *PR* refers to massive sulfides from the Virginia Formation below the Partridge River Intrusion.

Sample	Location	Re (ppb)	2σ	Os (ppb)	2σ	$^{187}Re/^{188}Os$	2σ	$^{187}Os/^{188}Os$	2σ	γOs (1100 Ma)
49-398.68	Tamarack	100.1	0.042	13.01	0.019	40.82	0.061	0.9032	0.0004	22
49-404.81	Tamarack	60.93	0.037	9.313	0.016	34.23	0.063	0.7849	0.0003	25
49-405.78	Tamarack	37.64	0.040	2.030	0.016	114.2	0.93	2.2544	0.001	18
49-406.61	Tamarack	51.19	0.041	5.081	0.017	55.22	0.19	1.1794	0.0006	30
213-459.55	Tamarack	123.5	0.048	108.0	0.038	5.594	0.0029	0.2434	0.0001	15
213-460.49	Tamarack	109.5	0.048	113.9	0.038	4.691	0.0026	0.2265	0.00008	15
213-461.19	Tamarack	85.63	0.049	54.00	0.028	7.797	0.0060	0.2826	0.00008	14
70-37	Eagle	108.1	0.044	128.0	0.039	4.128	0.0021	0.2353	0.00009	31
69-38	Eagle	156.5	0.049	283.6	0.068	2.686	0.0011	0.2051	0.00007	28
70-43.59	Eagle	180.2	0.048	269.0	0.065	3.266	0.0012	0.2169	0.00006	29
69-55.75	Eagle	275.7	0.049	649.7	0.131	2.061	0.00055	0.1866	0.00004	22
70-58.36	Eagle	315.0	0.049	844.9	0.164	1.809	0.00045	0.1800	0.0001	21
69-71.8	Eagle	292.5	0.048	969.2	0.185	1.463	0.00037	0.1736	0.00004	21
69-26.26	Eagle	70.87	0.049	48.73	0.028	7.162	0.0064	0.2944	0.0001	33
07-04-925.9	PR	262.5	0.046	14.74	0.020	121.8	0.17	3.3369	0.003	793
07-04-994.3	PR	284.4	0.047	13.73	0.020	153.8	0.23	4.2695	0.01	1074
08-28-1045.2	PR	299.4	0.049	12.23	0.021	195.5	0.33	5.1658	0.002	1176
08-36-1549.6	PR	40.30	0.048	3.593	0.020	74.61	0.42	3.0450	0.001	1270
08-36-1552	PR	64.28	0.047	1.337	0.019	631.2	9.0	13.3501	0.009	1279
07-13-1605.1	PR	165.7	0.049	5.684	0.020	257.5	0.91	6.5137	0.003	1341

Pb Isotopes

Results of Pb isotopic measurements from country rock-hosted massive sulfides at Tamarack, Eagle, and below the Partridge River Intrusion are listed in Table 7. Samples from Tamarack have $^{207}Pb/^{204}Pb$ ratios, from 15.51 to 15.54. $^{206}Pb/^{204}Pb$ range from 16.78 to 17.10. At Eagle, the $^{207}Pb/^{204}Pb$ range from 15.69 to 15.71, and $^{206}Pb/^{204}Pb$ ratios extend from 17.38 to 17.58. Massive sulfides from the Virginia Formation have $^{207}Pb/^{204}Pb$ between 15.54 and 15.73, while $^{206}Pb/^{204}Pb$ range from 18.37 to 19.18. Regression ages are not reported, as samples plot along mixing lines rather than isochrons.

Table 7: Pb isotope measurements of country rock-hosted massive sulfides from Tamarack, Eagle, and beneath the Partridge River Intrusion. Note that *PR* refers to massive sulfides from the Virginia Formation below the Partridge River Intrusion.

Sample	Location	$^{206}Pb/^{204}Pb$	2σ	$^{207}Pb/^{204}Pb$	2σ	$^{208}Pb/^{204}Pb$	2σ
49-398.68	Tamarack	16.870	0.0009	15.512	0.0009	37.063	0.002
49-404.81	Tamarack	16.807	0.0006	15.508	0.0006	37.037	0.001
49-405.78	Tamarack	16.782	0.0007	15.506	0.0007	37.024	0.002
49-406.61	Tamarack	16.778	0.0005	15.506	0.0005	37.023	0.001
213-455.19	Tamarack	17.102	0.0006	15.538	0.0006	36.874	0.002
213-459.55	Tamarack	17.00	0.002	15.528	0.002	36.838	0.007
213-460.49	Tamarack	17.027	0.0006	15.531	0.0006	36.880	0.001
213-461.19	Tamarack	16.952	0.0006	15.517	0.0006	36.779	0.002
70-37	Eagle	17.384	0.0009	15.702	0.0008	36.535	0.002
69-38	Eagle	17.435	0.0009	15.707	0.0006	36.553	0.002
70-43.59	Eagle	17.419	0.0007	15.706	0.0006	36.535	0.002
69-55.75	Eagle	17.394	0.0005	15.700	0.0005	36.543	0.001
70-58.36	Eagle	17.576	0.0006	15.693	0.0007	36.634	0.002
69-71.8	Eagle	17.505	0.0008	15.696	0.0008	36.580	0.002
69-26.26	Eagle	17.395	0.0010	15.698	0.0007	36.534	0.002
07-04-925.9	PR	18.56	0.002	15.646	0.002	36.803	0.004
07-04-994.3	PR	18.368	0.0008	15.633	0.0008	37.181	0.002
08-28-1045.2	PR	19.18	0.002	15.733	0.001	37.173	0.003
08-36-1549.6	PR	18.53	0.002	15.615	0.002	37.581	0.004
08-36-1552	PR	17.60	0.004	15.542	0.004	36.877	0.009
07-13-1605.1	PR	18.95	0.002	15.652	0.001	37.688	0.004

Discussion

Co/Ni ratios

Co/Ni ratios are routinely used to determine the origin of sulfides in sedimentary rocks, especially where hydrothermal mineralization may be suspected. Data compilations in Bajwah et al. (1987) indicate nearly all hydrothermal sulfides (typically pyrite) have Co/Ni > 2, whereas sedimentary sulfides have Co/Ni in the range 0.01 to 2 (Gregory et al., 2015). Co/Ni ratios of magmatic Ni-Cu-PGE sulfides are variable but are generally between 0.01 and 0.5 (Fig. 12), overlapping much of the expected range for sedimentary sulfides. The low Co/Ni ratios of the

Tamarack, Eagle, and Partridge River samples from this study are inconsistent with a hydrothermal origin. Furthermore, the relatively low S/Se ratios and lack of low-temperature sulfides such as pyrite exclude their origin as metal-rich sedimentary sulfides (Eckstrand and Hulbert, 1987; Queffurus and Barnes, 2015; Smith et al., 2016). Instead, the low Co/Ni ratios of the massive sulfides reported here (0.016 to 0.22) are consistent with derivation as crystallizing magmatic sulfide liquids, as discussed further below.

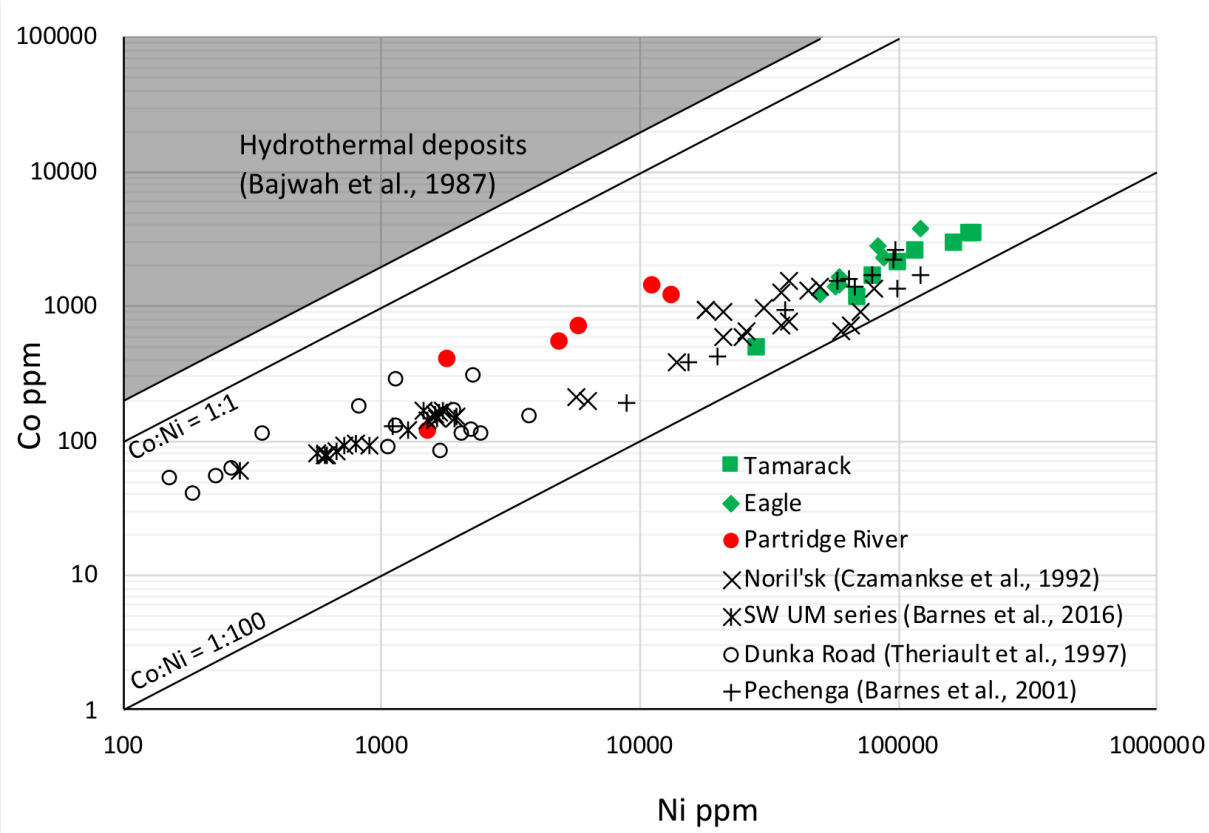

Figure 12: Co vs Ni concentrations of country rock-hosted massive sulfides from Tamarack, Eagle, and Partridge River, in comparison to igneous-hosted sulfides from Noril'sk, the ultramafic series of the Stillwater Complex, the Dunka Road deposit, and Pechenga, in addition to a field for hydrothermal mineral deposits.

S/Se ratios

Mantle S/Se ratios are well-constrained between 2,850 and 4,350 (Eckstrand and Hulbert, 1987), and magmatic Ni-Cu-PGE deposits with little evidence of crustal contamination commonly have mantle-like S/Se ratios (Smith et al., 2016). S/Se ratios can be reduced by high ratios of silicate magma to sulfide magma, otherwise known as the R-factor (Queffurus and Barnes, 2015), magmatic exchange processes (Kerr and Leitch, 2005), re-melting of the mantle (Hattori et al., 2002), and postmagmatic hydrothermal alteration (Queffurus and Barnes, 2015). Conversely, S/Se ratios may be elevated by prior sulfide saturation (Barnes et al., 2009) or crustal contamination (Ripley, 1990b; Theriault and Barnes, 1998). For example, crustal rocks can have S/Se as high as 100,000 (Yamamoto, 1976), and magmatic Ni-Cu-PGE sulfides with substantial crustal contamination commonly have elevated S/Se ratios if the contaminants were Se-poor and the magmatic sulfides experienced little post-magmatic alteration.

No Se data have been published for igneous rock-hosted sulfides from Tamarack or Eagle. For comparison, S/Se ratios, in addition to PGE (Pt+Pd) enrichments for other Ni-rich magmatic sulfides are shown in Fig. 13A and B. Ni-rich igneous rock-hosted sulfides at Voisey's Bay have S/Se ratios between 3,663 and 7,142 (Ripley et al., 2002) and are quite similar to S/Se at Eagle. Picrite associated mineralization at Pechenga has S/Se ratios of 3,308 to 5,108 (Barnes et al., 2001), which overlaps both the mantle S/Se range and the range for country rock-hosted massive sulfides from Eagle. Sulfides from mineralized sills at Noril'sk have S/Se ratios of 1,010 to 7,692 (Czamanske et al., 1992), overlapping those we report for Tamarack and Eagle massive sulfides. Theriault et al. (1996) showed that the highest S/Se ratios from the Dunka Road deposit were observed in mineralized norites (4,098 - 7,634); troctolites had lower S/Se ratios (3,185 - 4,587), consistent with the range of mantle values; and the two most PGE-enriched samples had

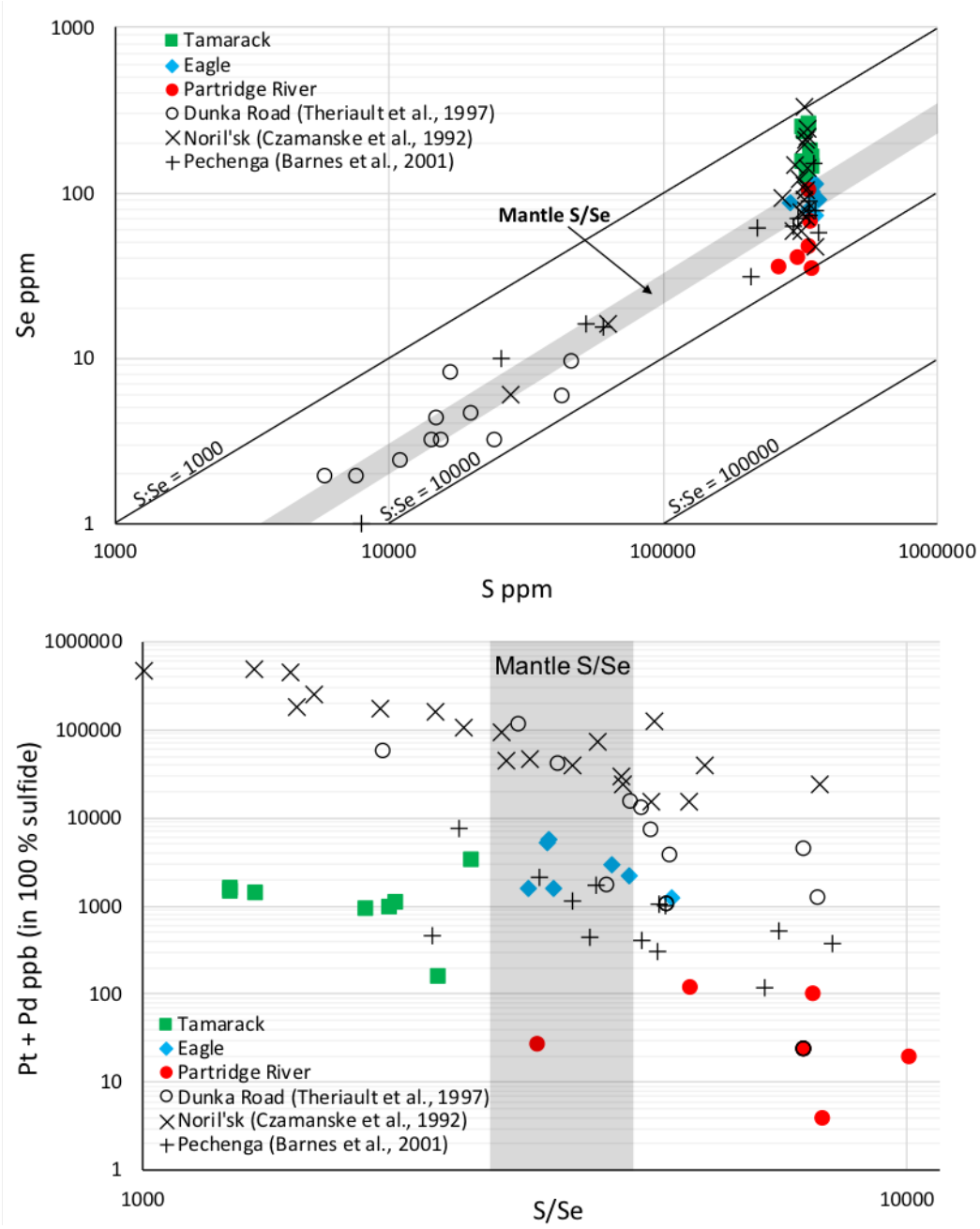

Figure 13: A. S vs. Se and B. Pt+Pd (in 100% sulfide) vs S/Se ratio for country rock-hosted massive sulfides near the Tamarack, Eagle, and Partridge River intrusions. Data for Dunka Road, Noril'sk, and Pechenga are shown for comparison, in addition to the mantle S/Se range (Eckstrand and Hulbert, 1987).

the lowest S/Se ratios (2,061 and 3,125). S/Se ratios of the un-metamorphosed Virginia Formation range from 2,000 to 66,667 (Ripley, 1990b), with an average of 8,118 and 10,264 at the Dunka Road and Babbitt deposits, respectively. A single analysis of the bedded pyrrhotite unit of the Virginia Formation has a S/Se ratio of 29,000 (Thériault and Barnes, 1998). S/Se ratios of country rock-hosted massive sulfides beneath the Partridge River Intrusion are in the same range as the mineralized norites at the Dunka Road deposit, although one of our samples has a ratio of 10,079 and is consistent with higher degrees of bulk contamination than sulfides in the intrusions. A similar relationship is noted in the Re-Os, Pb, and S isotope systematics presented below. Moreover, country rock-hosted massive sulfides from Tamarack, Eagle, and Partridge River all have S/Se ratios consistent with those expected and measured in corresponding igneous rock-hosted sulfides. The relatively narrow and lower ranges of S/Se in the massive sulfides compared to the Virginia Formation suggests the massive sulfides are not related to Proterozoic sedimentation. Instead, they appear to reflect contamination of primary mantle melts by high S/Se sedimentary rocks.

S Isotope Systematics

Previous radiogenic and stable isotopic studies of igneous rock-hosted sulfides from the Duluth Complex, Tamarack, and Eagle have firmly supported the view that crustal contamination was involved in, and necessary for, the genesis of magmatic sulfides. $\delta^{34}S$ measurements from Ripley (1980) and Ripley and Al-Jassar (1987) demonstrated that contamination of mafic magmas of the Partridge River Intrusion by S-bearing sediments of the Virginia Formation produced elevated S isotopic values of sulfide minerals hosted by the igneous rocks. Oxygen isotope exchange zones between igneous rocks in the Dunka Road and

Babbitt deposits and Virginia Formation xenoliths, as well as the presence of pyrrhotite (rather than pyrite) in the Virginia formation, indicate the importance of desulfidation of sedimentary pyrite and other devolatilization reactions for derivation of external S and O (Ripley and Al-Jassar, 1987). Additionally, Ripley et al. (1999) have illustrated that Os, Pb, and Nd isotopic ratios from the troctolites, plagioclase separates, and massive sulfides of the Duluth Complex were produced by mixing of mantle-derived magmas with rocks of the Virginia Formation (1 – 5 % bulk mixing). $\delta^{34}S$ values of igneous rock-hosted sulfides in the Duluth Complex range from 7 to 14 ‰ (Ripley, 1980; Ripley and Al-Jassar, 1987), which is slightly lower than the range reported here for country rock-hosted massive sulfides (~10 – 19 ‰).

The median $\delta^{34}S$ value of the country rock-hosted massive sulfides below the Partridge River Intrusion is clearly higher than that of the igneous-hosted sulfides (Fig. 14A). The differences in $\delta^{34}S$ values cannot be explained by high-temperature equilibrium fractionation of S isotopes associated with igneous processes, as $\Delta^{34}S$ between sulfide species are only on the order of 0.1 at 1,000 °C (Li and Liu, 2006). An alternative explanation for the disparity between the $\delta^{34}S$ ranges could be that while both country rock-hosted massive sulfides and igneous-hosted sulfides at Partridge River represent a mixture of mantle- and crustally-derived S, higher $\delta^{34}S$ values in the country rock-hosted massive sulfides record greater degrees of crustal contamination than the igneous rock-hosted sulfides. Another alternative explanation is that massive sulfides were originally sedimentary sulfides, based on the overlap of $\delta^{34}S$ compositions between the massive sulfides and disseminated/laminated sedimentary sulfides from the Virginia formation/Animikie Group (Fig. 14A). However, sedimentary sulfides in the Virginia formation are composed primarily of pyrrhotite, whereas the massive sulfides have substantial amounts of chalcopyrite-

cubanite and can contain up to 30 wt. % Cu. This translates to an enrichment factor of more than 1,700 compared to other typical Paleoproterozoic sedimentary sulfides (Gregory et al., 2015).

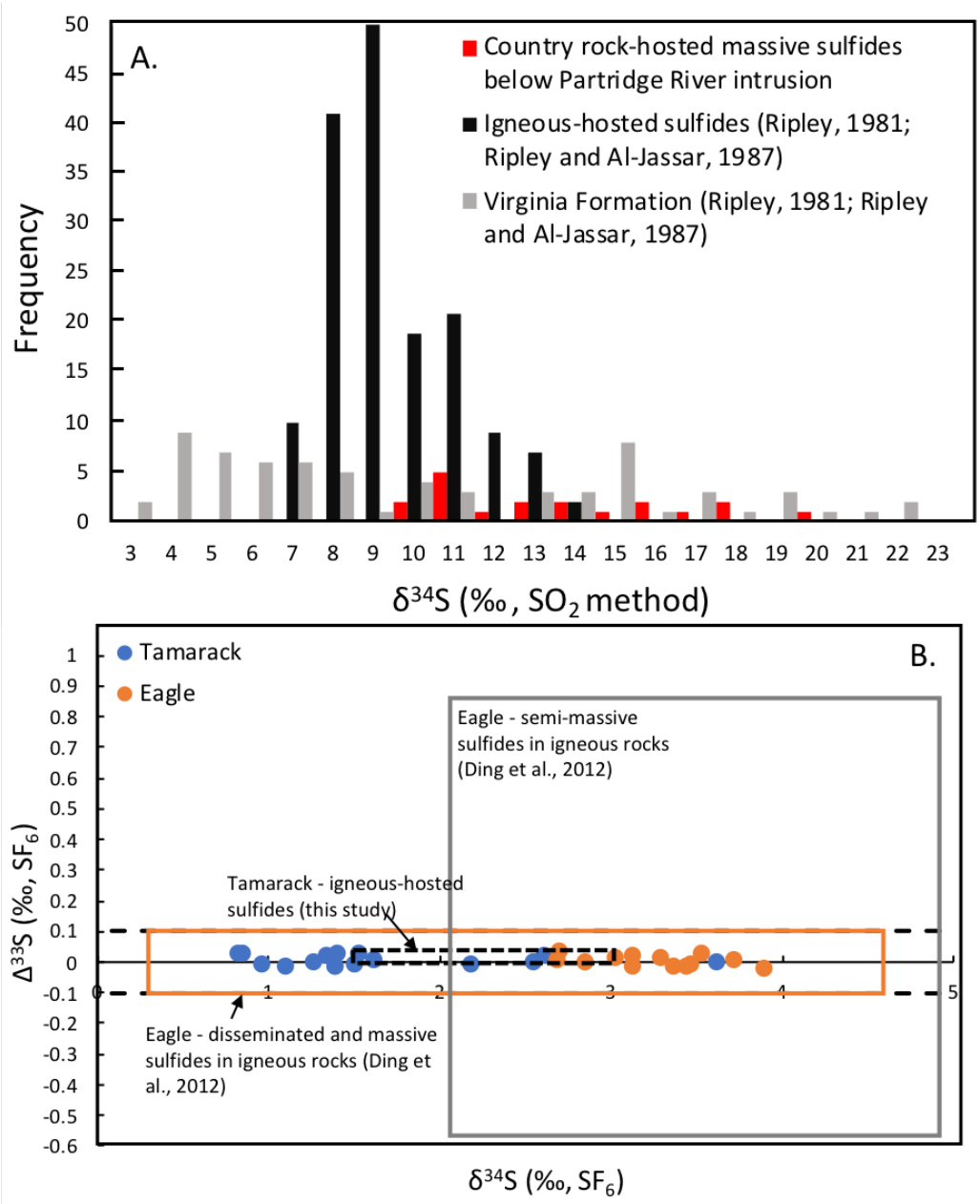

Figure 14: A. Histogram of $\delta^{34}S$ values for country rock-hosted massive sulfides beneath the Partridge River Intrusion, in comparison to $\delta^{34}S$ and ranges for igneous rock-hosted sulfides and the Virginia Formation. B. $\delta^{34}S$ and $\Delta^{33}S$ values of country rock-hosted massive sulfides from the Tamarack Intrusive Complex and the Eagle deposit in relation to $\delta^{34}S$ and $\Delta^{33}S$ ranges for igneous-hosted mineralization at both locations.

Ding et al. (2012) reported $\delta^{34}S$, $\delta^{33}S$, and $\Delta^{33}S$ for igneous-hosted sulfides and Archean and Proterozoic sedimentary rocks at the Eagle deposit. Igneous rock-hosted sulfides had $\delta^{34}S$ values from 0.1 to 4.1 ‰. $\Delta^{33}S$ values range from -0.09 to 0.09 ‰ in the disseminated and massive sulfides and from -0.8 to 0.8 ‰ in the semi-massive sulfides. Archean sedimentary and metamorphic rocks had $\delta^{34}S$ values of 3.9 to 7.4 ‰ with a single value at -3.4 ‰. $\Delta^{33}S$ range from -1.16 to 0.45 ‰. Proterozoic rocks have $\delta^{34}S$ values between 4.7 and 28.5 and $\Delta^{33}S$ values from -0.19 to 0.2 ‰. Ding et al. (2012) suggested that the relatively low $\delta^{34}S$ and anomalous $\Delta^{33}S$ reflect bulk or selective contamination between a mantle-derived magmatic component and local Archean and Proterozoic sedimentary rocks. Statistical *t*-tests suggest that $\delta^{34}S$ values of country rock-hosted massive sulfides at Eagle are statistically identical to $\delta^{34}S$ values measured in the igneous rock-hosted massive and semi-massive sulfides. The *t*-tests of $\Delta^{33}S$, however, show the country rock-hosted massive sulfides are statistically identical to the massive and disseminated sulfides from within the intrusion (see Fig. 14B). In conjunction, the two suggest that the S isotope ratios of massive sulfides in the country rocks are statistically identical to those of massive sulfides in the igneous rocks.

Taranovic et al. (2018) reported SO_2 $\delta^{34}S$ analyses of disseminated, semi-massive, and massive sulfides within the Tamarack Intrusive Complex, in addition to analyses of the local country rocks, the Thomson formation. Igneous-hosted sulfides had $\delta^{34}S$ values from -0.2 to 2.8 ‰, whereas local sedimentary rocks had $\delta^{34}S$ values from 1.6 to 9.4 ‰. Taranovic et al. (2018) attributed the low $\delta^{34}S$ values in the igneous-hosted sulfides to a combination of both low degrees of crustal contamination and conduit exchange reactions between sulfides and fresh, incoming magmas. T-tests and analysis of variance indicate that S isotopic compositions of country rock-hosted massive sulfides are statistically identical to S isotopic compositions of

disseminated sulfides from the CGO intrusion, referred to as CGO_2, which are classified as sulfides with high Pt-Pd tenors (up to 2 ppm Pt and 0.4 ppm Pd in 100 % sulfide; Taranovic et al., 2018). Multiple S isotope analyses also show that neither the country rock- or igneous rock-hosted sulfides have substantial evidence of anomalous $\Delta^{33}S$ values (Fig. 14B).

Re-Os Isotope Systematics

Previous Re-Os analyses of igneous hosted sulfides from the Eagle intrusion (Ding et al., 2012), Tamarack Intrusive Complex (Taranovic, 2014), and the Partridge River Intrusion (Ripley et al., 1999) were interpreted to be the result of mixing between mantle-derived melts and Proterozoic country rocks. Elevated γOs (1100) of samples from the Partridge River Intrusion indicated that there was significant Os addition from crustal sources, likely the Virginia Formation, which has γOs (1100) of ~ 150 to 4600 (Ripley et al., 1999; Ripley et al., 2001). Ripley et al. (1999) determined that ~1 – 3 % bulk contamination by the Virginia Formation could have produced the observed Re-Os compositions of the massive sulfides. For selective assimilation models, this translates to > 35% crustally-derived Os.

Our analyses of country rock-hosted massive sulfides in the Virginia Formation have γOs from +793 to +1340 (Fig. 15) and are broadly similar to γOs for country rock-hosted massive sulfides (+453 +1114) reported by Ripley et al. (1999). Two analyses of disseminated sulfide-bearing troctolites have lower γOs (-26 and +533) than most of the massive sulfides and are consistent with lower degrees of contamination, regardless of bulk or selective assimilation models.

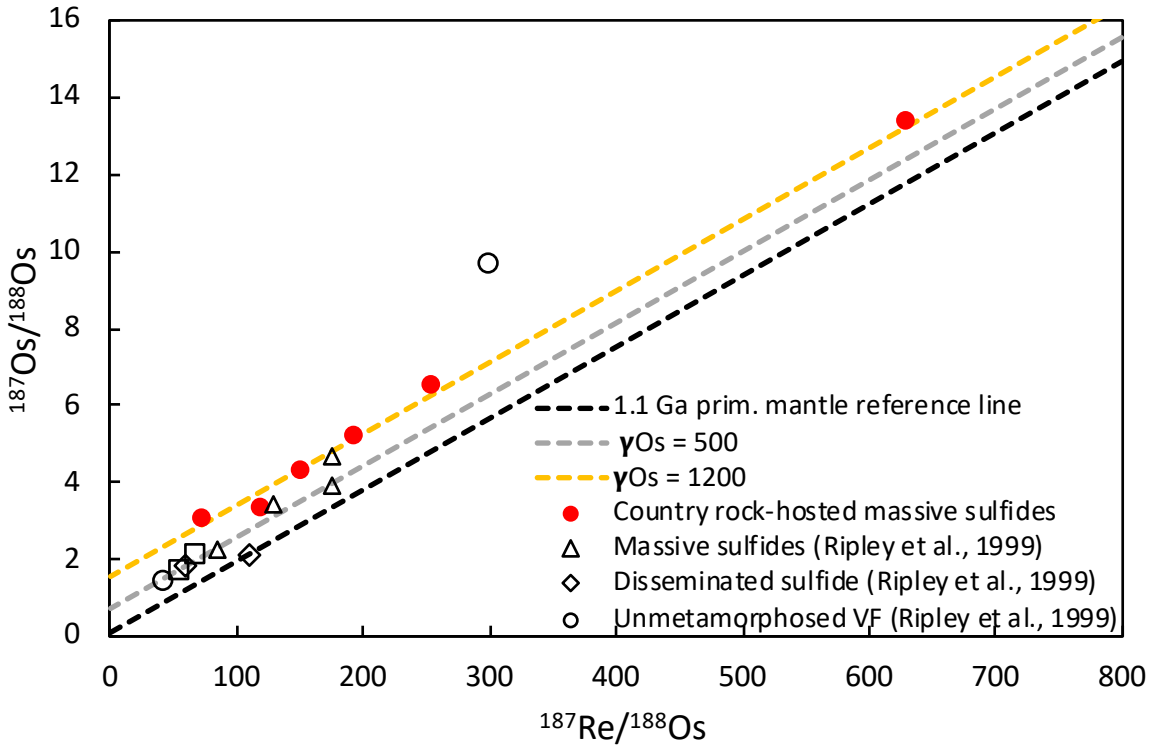

Figure 15: Re-Os systematics of country rock-hosted massive sulfide and igneous rock-hosted disseminated sulfides from the Partridge River Intrusion and selected analyses of the Virginia Formation. A 1.1 Ga primitive mantle reference line (γOs = 0), and two parallel radiogenic reference lines (γOs = 500 and 1200) are also shown. Average γOs for new data is ~ +1154.

Ding et al. (2012) performed Re-Os analyses of igneous rock-hosted sulfides from the Eagle intrusion, in addition to sedimentary sulfides from the Michigamme Formation. They concluded that γOs of the igneous rock-hosted sulfides ranged from +21 to +51 and could have been produced by as little as 2% bulk contamination by the Michigamme Formation, or only ~ 6% crustally-derived Os for selective assimilation. Similarly, Taranovic et al. (2018) determined that igneous rock-hosted sulfides from the Tamarack Intrusive Complex with γOs from +10 to +98 could have been produced by low degrees of bulk (< 1%) or selective (<< 1%) contamination by the Proterozoic Thomson Formation. Ding et al. (2012a, b) and Taranovic et

al. (2016, 2018) also emphasized the possibility of conduit exchange processes, which may have acted to subdue the expected isotopic signatures of crustal contamination in conduit-type intrusions.

Country rock-hosted massive sulfides near the Tamarack and Eagle intrusions are characterized by γOs values that are identical to those of igneous rock-hosted sulfides, as shown in Figures 16 and 17, respectively. This interpretation is also supported by *t*-tests and analysis of variance. In both cases the country rock-hosted massive sulfides are interpreted to represent leaked magmatic sulfide liquid, which initially formed due to low degrees of bulk or selective contamination, or conduit exchange processes between primary mantle melts and Proterozoic country rocks, as suggested by Ding et al. (2012) and Taranovic et al. (2018). The relatively low number of samples used for Re-Os analyses in this study, as well as that of Ding et al. (2012) and Taranovic et al. (2018), make it difficult to assess whether one type of igneous rock-hosted sulfide is more similar than another to the massive sulfides in the country rocks, based on Re-Os isotopic ratios alone.

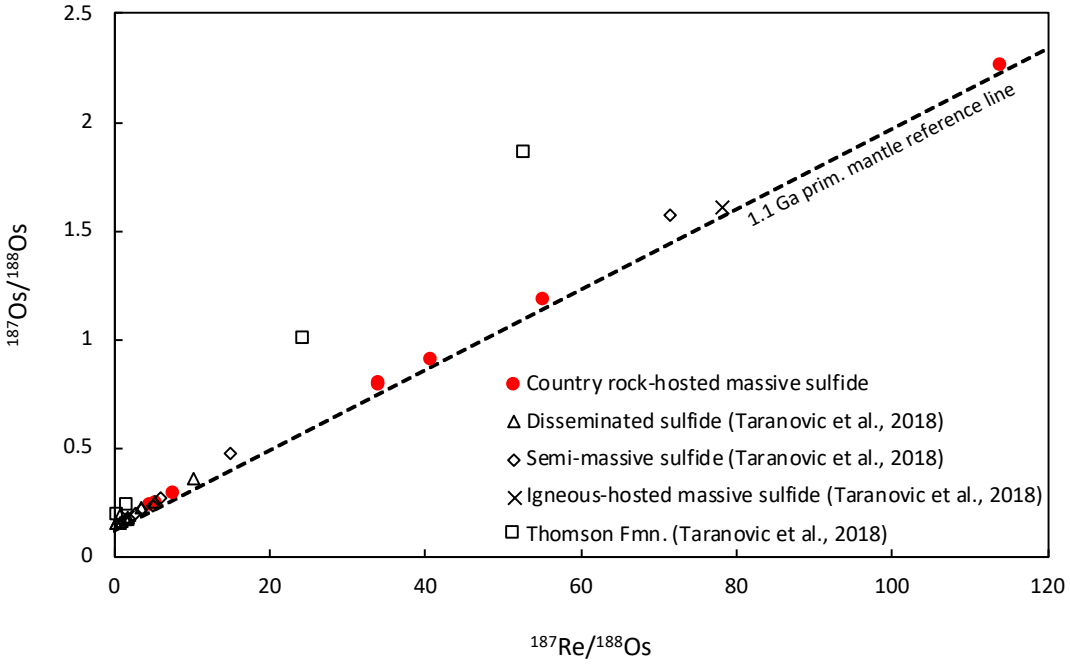

Figure 16: Re-Os systematics of country rock-hosted massive sulfide and igneous-hosted sulfides from the Tamarack Intrusive Complex, as well as sedimentary rocks of the Proterozoic Thomson Formation. A 1.1 Ga primitive mantle reference line ($\gamma Os = 0$) is also shown. Average γOs for new data is ~ +20.

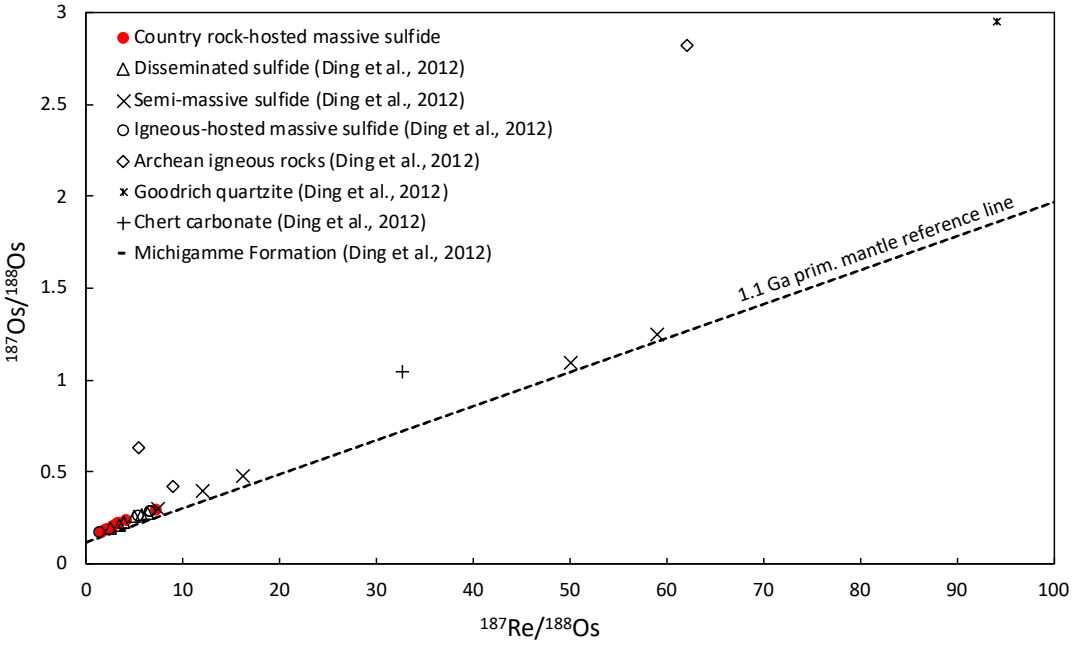

Figure 17: Re-Os systematics of country rock-hosted massive sulfide and igneous-hosted sulfides from the Eagle intrusion in addition to Proterozoic and Archean country rocks. A 1.1 Ga primitive mantle reference line ($\gamma Os = 0$) is also shown. Average γOs for new data is ~ +26**.**

Pb Isotope Systematics

Ripley et al. (1999) clearly illustrated that Pb isotope data of disseminated and massive sulfides from the Babbitt area of the Partridge River Intrusion could have been produced by mixing of mantle- and crustally-derived Pb components. Massive sulfides were characterized by a higher degree of contamination than that indicated by the disseminated sulfides. Their data define a 1.1 Ga mixing line in $^{207}Pb/^{204}Pb$ vs. $^{206}Pb/^{204}Pb$ space, with mantle endmember growth from initial Pb compositions defined by primordial Pb and single stage $\mu = 8$. The upper mixing endmember was defined by analyses of the Virginia Formation and a second stage $\mu = 25$. Calculations from Ripley et al. (1999) showed that Pb isotopic compositions in the igneous rock-hosted sulfides could have been obtained by 1-5% bulk contamination of a mantle-derived melt by the Virginia Formation.

To date, no Pb isotopic analyses are available for small, conduit type intrusions in the MRS, such as Tamarack or Eagle, and statistical comparisons cannot be used in such cases. However, Pb isotopic analyses of group 1 and 2 lavas from the Mamainse Point Formation (Shirey et al., 1994) are virtually identical to our Pb isotope analyses of country rock-hosted massive sulfides from Eagle, and the lavas are compositionally similar to the Eagle parental magmas (picrites). Analyses from Tamarack are less radiogenic than those from Eagle, as well as the group 1 and 2 Mamainse Point samples (Shirey et al., 1994). Re-Os, Sm-Nd, and multiple S analyses from Eagle (Ding et al., 2012), have shown there are signals of both Proterozoic and Archean sedimentary components within the igneous rock-hosted sulfides, whereas mineralization at Tamarack and the Duluth Complex have, to this point, only shown signals of Proterozoic sedimentary components. Positive γOs and negative εNd values in the igneous rock-hosted sulfides at all locations are consistent with small amounts of crustal contamination by local

Proterozoic rocks, or isotopic exchange between contaminated igneous sulfides and fresh, mantle derived magmas. At Eagle there are anomalous $\Delta^{33}S$ values in the semi-massive sulfides, indicating input from Archean sedimentary sources and the involvement of multiple generations of sulfide mineralization (Ding et al., 2012). Due to the crustal contamination involved in the production of magmatic sulfides at Tamarack and Eagle, Pb isotope compositions of the associated country rock-hosted massive sulfides should plot along mixing lines between mantle and crustal reservoirs if they are leaked igneous sulfides.

Pb isotopic data from the massive sulfides in this study are presented in Figs. 18 and 19, along with two separate models which may explain their distribution. In Fig. 18, the data are presented along with single-stage, mantle growth curves at μ = 8, 8.23, and 8.48, projected to the 1.1 Ga geochron. These μ values are consistent with Shirey et al. (1994) who suggest that Midcontinent Rift mantle plume sources ranged from $\mu \approx 8$ to 8.4. A growth curve for Animikie and Baraga Group sediments (Virginia, Thomson, Michigamme) is shown with an upper estimate of the second stage μ of 53 and derivation from mantle-like material at 1.8 Ga. This model is based on analyses from Ripley et al. (1999) and Hemming et al. (1995). It should be noted that the lower estimate for the second stage growth of the Virginia formation has a μ = 12 (Hemming et al., 1995). This μ value is too low to produce any of the measured sulfide compositions reported in this work by crustal contamination, and subsequently, only the upper estimate for the Virginia Formation is included in Fig. 18. In Fig. 19, data from Tamarack and Eagle are presented with a single mantle growth curve (μ = 8) projected to the 1.1 Ga geochron, as well as estimated endmember compositions of Archean crust from the Michipicoten greenstone belt (Shirey et al., 1994).

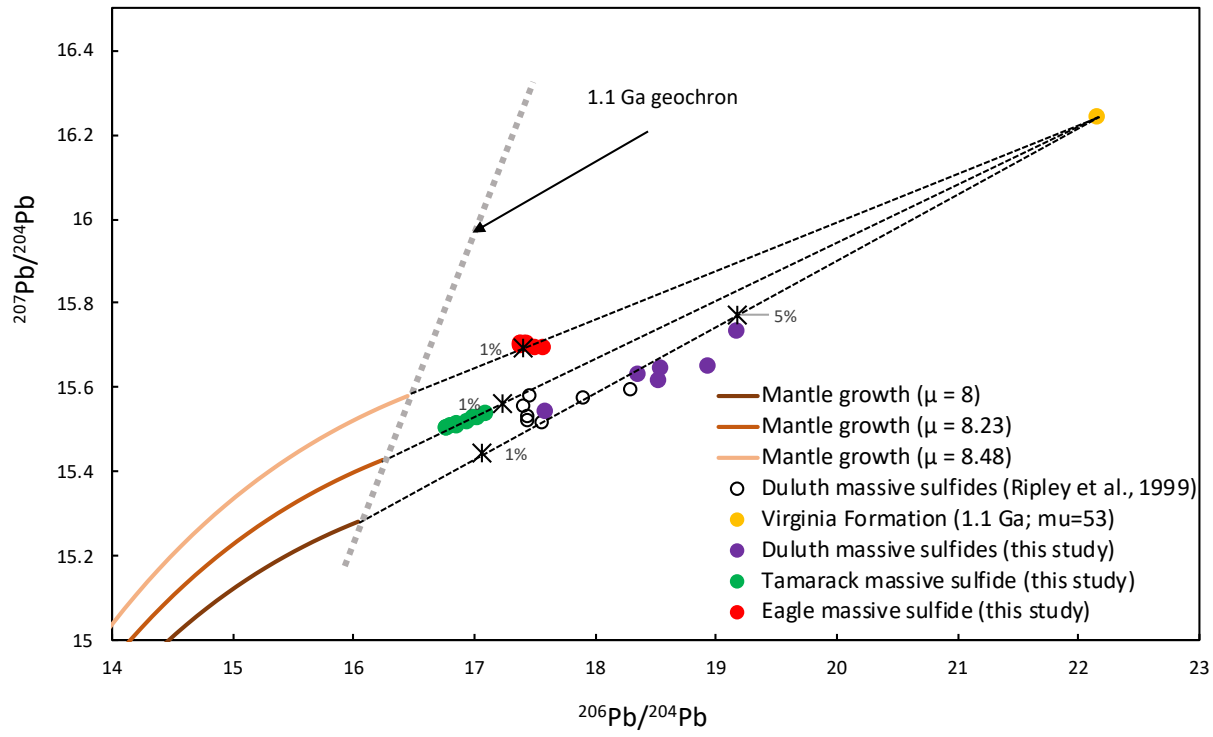

Figure 18: Pb isotope data from Tamarack, Eagle, and below the Partridge River Intrusion shown relative to single-stage mantle growth models with μ = 8, μ = 8.23, and μ = 8.48 and an endmember for Animikie Group sediments at 1.1 Ga. Ticks are shown for 1% bulk contamination at Tamarack, Eagle, and Duluth, and a tick for 5% contamination is also shown for samples near Partridge River. Endmember mantle melts were taken to have 1 ppm Pb and Virginia Formation was taken to have 20 ppm Pb.

Clearly, none of the sample compositions presented here may be explained simply by formation of immiscible sulfides from uncontaminated mantle magmas, as uncontaminated mantle sulfides formed at 1.1 Ga would plot along the 1.1 Ga geochron at $\mu \approx 8 - 8.4$, assuming little U is partitioned into the sulfides as indicated from known partition coefficients (Bea et al., 1994; Wheeler et al., 2006). Because our analyses were performed on massive sulfides (with effectively no U decay to Pb), the observed ratios required the input of radiogenic Pb produced by a second stage process (to allow U decay prior to mixing/crustal contamination) in order to

have produced the measured radiogenic compositions. At Eagle and Tamarack, the massive sulfide data may be explained by contamination from either Archean or Proterozoic crust, whereas massive sulfides beneath the Partridge River Intrusion must have been contaminated by Proterozoic crustal rocks.

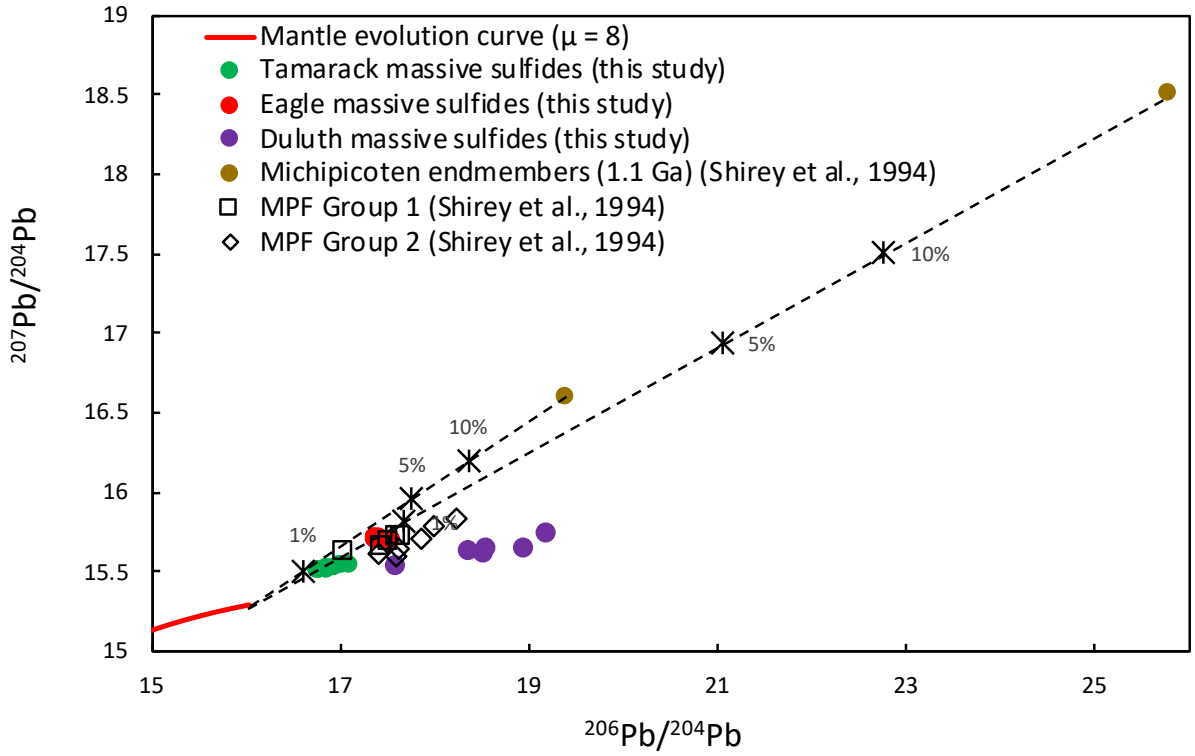

Figure 19: Pb isotope data from Tamarack and Eagle shown relative to a single-stage mantle growth with μ = 8 and endmembers for crust in the Michipicoten greenstone belt at 1.1 Ga. Ticks are shown for 1%, 5%, and 10% bulk contamination for both the upper and lower endmember estimates for rocks of the Michipicoten greenstone belt (Shirey et al., 1994). Endmember mantle melts were taken to have 1 ppm Pb, and Michipicoten greenstone belt rocks were taken to have 20 ppm Pb.

Figure 18 illustrates that massive sulfides in the country rocks below the Partridge River Intrusion and at Tamarack and Eagle may have formed from primary mafic melts that were

contaminated by Proterozoic Animikie and Baraga Group sediments at 1.1 Ga. This would require mantle heterogeneities between all three locations, as mixing lines for all three project to different initial $^{207}Pb/^{204}Pb$ and $^{206}Pb/^{204}Pb$ values. Such heterogeneities have been documented in the Mamainse Point Formation, with first stage $\mu \approx 8 – 8.4$ (Shirey et al., 1994). Isotopic mantle heterogeneities in the MRS are not unreasonable and have also been proposed as a potential source of disparity in Cu isotope measurements between sheet- and conduit-style intrusions (Ripley et al., 2015).

Calculation of mantle-country rock mixing processes at 1.1 Ga are shown in Figures 18 and 19. For the Proterozoic model, mixing calculations for massive sulfides beneath the Partridge River Intrusion based on mantle values of $\mu = 8$ and 1 ppm Pb, with sediments with a $\mu = 53$ and 20 ppm Pb indicate the Pb isotopic values of the country rock-hosted massive sulfides could have been attained by up to 5% bulk contamination. Similar mixing calculations for the massive sulfides at Tamarack show that with a mantle $\mu = 8.23$, measured Pb isotopic values can be explained by slightly less than 1% bulk contamination from the Animikie Group. Eagle values, with mantle $\mu = 8.48$, can also be explained by slightly more than 1% bulk contamination by Baraga Group sediments. Although the above calculations use a second stage μ value of 53, it should be noted the minimum required second stage μ value for the Virginia Formation would have needed to be at least ~ 31 to produce any of the isotopic values in the massive sulfides by 2-component mixing.

Massive sulfides beneath the Partridge River Intrusion cannot be explained by contamination from Archean crust, as the slope of the data is much shallower than mixing lines between mantle and Archean endmembers (Fig. 19). At Tamarack and Eagle, however, the massive sulfides may have been produced by contamination from Archean rocks. Such a model was proposed for the

Mamainse Point Formation, which Shirey et al. (1994) suggested being contaminated by highly radiogenic rocks of the 2.88 Ga Michipicoten greenstone belt. In that area, however, country rocks are predominantly Archean, with virtually no Proterozoic crustal material. Shirey et al. (1994) estimated the Pb isotope values of Archean rocks in the Mamainse Point area from Pb isotope analyses of crust in the Michipicoten belt (Turek et al., 1992). Their estimate places endmember Pb isotope ratios between 19.4 and 25.8 ($^{206}Pb/^{204}Pb$) and 16.6 and 18.5 ($^{207}Pb/^{204}Pb$). Calculations using a mantle with μ = 8 and 1 ppm Pb, mixed with the Archean endmembers (variable μ, 20 ppm Pb) suggest that the measured Pb isotopic ratios at Tamarack and Eagle can be explained by 0.5 to 5 % bulk contamination from Archean crust like that found in the Michipicoten greenstone belt.

Ni-Cu-PGE concentrations

Sulfides hosted in country rocks at Eagle, Tamarack, and below the Partridge River Intrusion show both compositional similarities to, and differences from the sulfide mineralization hosted in the igneous rocks of each occurrence. Isotopic and trace element data strongly suggest that the country rock-hosted massive sulfides originated as part of the magmatic system. We propose that any compositional differences between the sulfide in the igneous rocks and those in the country rocks may be a result of fractionation of a sulfide liquid within the country rock host. Models were developed to evaluate how observed variations in Ni-Cu-PGE distribution in the country rock-hosted massive sulfides may result from fractional crystallization of a sulfide liquid initially derived from within the spatially associated magma. Fractional crystallization of sulfide liquids begins with monosulfide solid solution (MSS), and the remaining liquid becomes enriched in Cu and PPGEs (Pt, Pd, Rh, and Au) (Li and Naldrett, 1994; Ebel and Naldrett, 1997).

A relatively simple ordinary differential equation, like that of Cox et al. (1979), can be applied to any sulfide liquid in order to assess the effects of fractional crystallization on Cu, PGE, and Au contents of both the coexisting monosulfide solid solution (MSS) and the sulfide liquid.

$$C_{MSS} = C^{L.}_{initial} * F^{(D_L^{MSS} - 1)}$$

C_{MSS} is the calculated concentration of any metal in the crystallized MSS; $C^{L.}_{initial}$ is the concentration of the metal in the initial sulfide liquid; F is the fraction of the original liquid remaining; and D_L^{MSS} is the partition coefficient for the metal into MSS vs the sulfide liquid. Partition coefficients are large for MSS-compatible components (for the IPGEs Os, Ir, and Ru, D_L^{MSS} ~ 1 – 10; Mungall et al., 2005) and small for incompatible components (for Cu, Au, and PPGEs, D_L^{MSS} < 1; Mungall et al., 2005).

At Eagle the lack of $\Delta^{33}S$ anomalies in the country rock-hosted massive sulfides suggest that the sulfide liquid which crystallized in the country rocks was not derived from the sulfide liquid which produced the upper semi-massive mineralization in the igneous rocks. Ding et al. (2012) determined that the unfractionated massive sulfides at Eagle were produced from a parental magma with ~ 4 ppb Pt, 2.5 ppb Pd, and 0.5 ppb Ir. Utilizing a graphical representation like that of Li and Naldrett (1994), country rock-hosted massive sulfides from Eagle consistently show slightly higher Pt and Pd concentrations than do the massive sulfides from Ding et al. (2012), and many samples plot along the upper line corresponding to the sulfide liquid composition (Fig. 20A–C). Because our samples plot at variable fractions of liquid remaining, we suggest that massive sulfides must have been expelled into the country rocks at various stages during sulfide fractionation, and not as a solitary event. Furthermore, country rock-hosted massive sulfides were derived from the same parental sulfide liquids that formed the igneous-hosted massive sulfides.

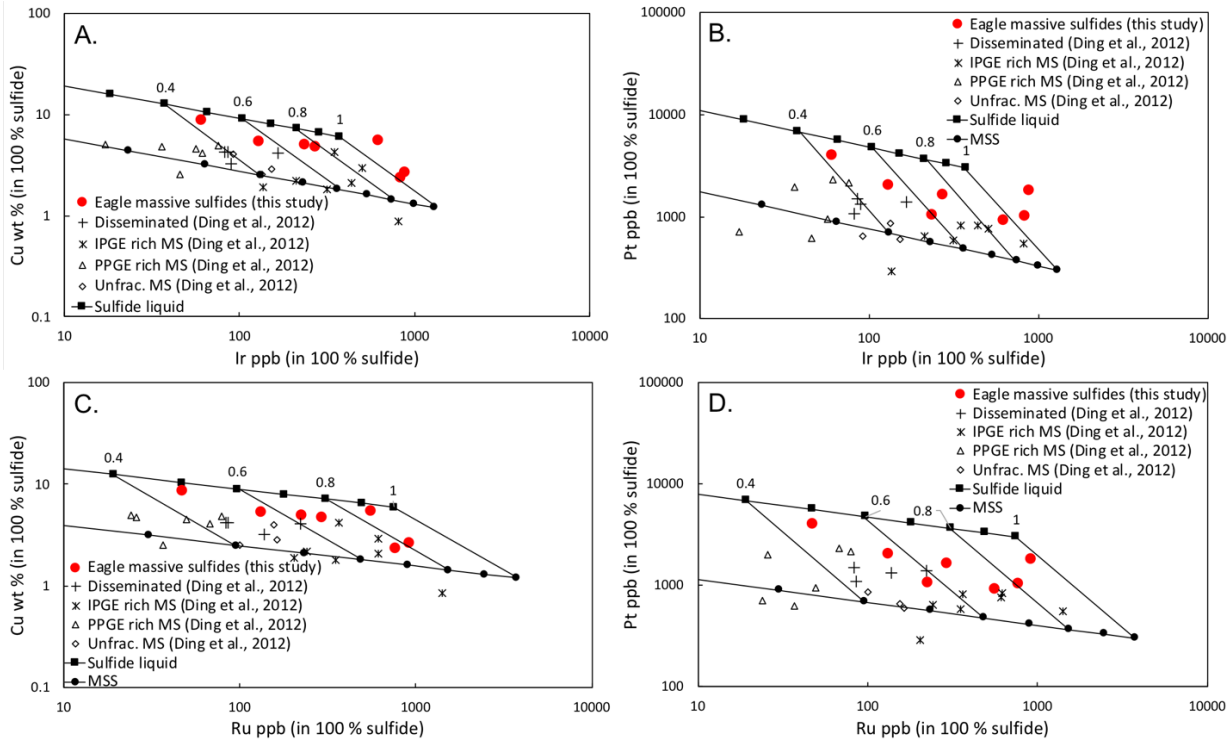

Figure 20: Fractional crystallization models of monosulfide solid solution from parental sulfide liquids at Eagle.

Taranovic et al. (2016) interpreted the positive Pt-Pd vs. Ir correlations in the disseminated sulfides at Tamarack to be the result of variable R-factors and an initial silicate magma with 2 ppb Pt, 1.8 ppb Pd, and 0.2 ppb Ir, which are within estimates of mantle melts from Barnes and Lightfoot (2005). Modeling from Taranovic et al. (2016) illustrated that a sulfide liquid formed at R-factors of ~ 500 to 1,500 would then be able to produce the PGE compositions in the semi-massive sulfides from the CGO by MSS fractional crystallization. Disseminated sulfides in the CGO and FGO correspond to R-factors up to 5,000 and are distinct from the sulfide liquids that produced the semi-massive sulfides.

Here we present MSS fractionation models of sulfide liquids formed at R-factors of 600 (Fig. 21A and B). Cu and Pd vs. Ir diagrams suggest sulfide liquids that fractionated to produce the

semi-massive sulfides could also have produced the country rock-hosted massive sulfides by further MSS fractional crystallization, due to the concomitant increases of incompatible elements (Cu and Pd) and decrease of the compatible element (Ir) observed in the massive sulfides. The semi-massive sulfides represent the least evolved sulfide liquids; the Group I massive sulfides (IPGE-enriched) represent minor degrees of MSS fractional crystallization; and Group II massive sulfides represent the most fractionated sulfide liquids. In other words, both the massive sulfides in the country rocks and the semi-massive sulfides from the CGO were produced by fractionation of the same sulfide parental magma. The Group I and Group II massive sulfides are all from drillholes 14TK0213 and 08TK0049, respectively and are from the same massive sulfide occurrence. The massive sulfide body plunges ~ 20 to 25° to the south-southeast, with the Group I massive sulfides (less fractionated) laying down-plunge of the Group II massive sulfides (more fractionated), suggesting the massive sulfide liquids fractionally crystallized from the bottom upwards. The initial sulfide liquids were likely filter-pressed from the semi-massive sulfides in the underlying CGO.

It is difficult to reconcile the Pt depletions in the Group I massive sulfides with the otherwise well-behaved PGE systematics. Taranovic et al. (2016) noted a massive sulfide sample from drillhole 08TK0058 with a positive Pt (but not Pd) anomaly and suggested this may be due to postmagmatic hydrothermal redistribution; This massive sulfide intercept from hole 08TK0058 lies between those from 14TK0213 and 08TK0049, and thus the massive sulfide body has samples with both negative and positive Pt anomalies, as well as no anomaly. This suggests that the anomalies are not related to the initial melt composition or mantle source compositions. Because Pt and Pd will behave similarly during MSS fractional crystallization, this process also cannot cause the decoupling between Pt and Pd. Early crystallization of Pt minerals, such as Pt

sulfides or alloys (Skinner et al., 1976) will produce positive Pt anomalies in the earliest-formed products. The later products will then be depleted in Pt, giving those sulfides negative Pt anomalies. This implies that the least fractionated sulfide liquids (in terms of MSS) will be IPGE-enriched and have positive Pt anomalies and that the most fractionated sulfide liquids will be IPGE-depleted and have negative Pt anomalies. Instead, three of the four IPGE-enriched massive sulfides we report here have negative Pt anomalies, whereas the IPGE-depleted samples have no Pt anomaly. We suggest then that early crystallization of Pt-bearing phases has had little influence on the Pt anomalies. The Pt anomalies may be related to post-magmatic hydrothermal alteration, wherein some samples have experienced Pt loss and others have experienced Pt gain. A similar phenomenon has been observed in sulfides of the J-M reef of the Stillwater Complex, which appears to have been caused by local redistribution at the hand-sample scale due to hydrothermal alteration (Wernette, 2017). However, low-temperature Fe-Ni-Cu sulfide assemblages (i.e.: pyrite, millerite) are rare at Tamarack. Typically, low temperature alteration of primary magmatic sulfides will increase Pd concentrations in all but the most altered sulfides (Holwell et al., 2017). However, Pt is also less soluble than Pd in most hydrothermal fluids (Mountain and Wood, 1988; Barnes and Liu, 2012), and any Pt loss should hypothetically result in more pronounced Pd loss. The possibility also remains that unexpectedly high and low Pt concentrations, in conjunction with otherwise well-behaved PGE concentrations, is consistent with a nugget effect. It has been well-documented that Pt in many magmatic sulfide systems occurs chiefly as discrete grains of platinum group minerals (PGMs), whereas Pd occurs in both PGMs and pentlandite solid solution (Genkin and Evstigneeva, 1986; Godel and Barnes, 2008; Huminicki et al., 2008; Prichard et al., 2013). Taranovic et al. (2016) confirmed the presence of trace PGMs in semi-massive sulfides from the CGO, which are not accounted for in modeling

MSS fractional crystallization. Pt-enriched samples could then be explained by a nugget effect, whereas Pt-depleted samples could be explained by a "reverse" nugget effect, due to the absence of PGM grains.

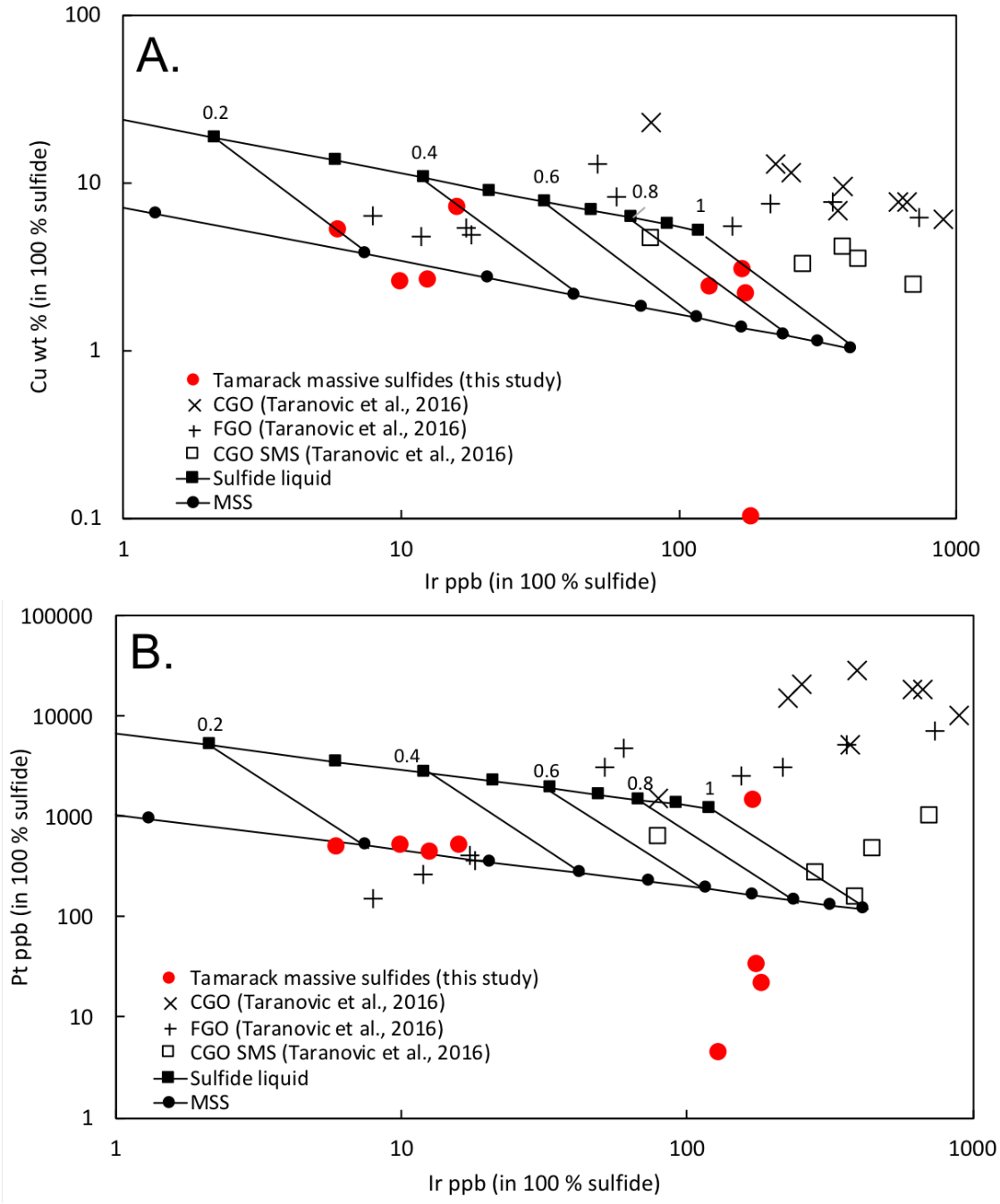

Figure 21: Fractional crystallization models of monosulfide solid solution from parental sulfide liquids at Tamarack.

Ripley (1990a) interpreted the strong correlations and spatial distributions of Ir, Ru, Os, and Rh in the basal troctolites of the Partridge River intrusion to be the result of primary magmatic processes. Strong correlations between Ir, Ru, Os, and Rh from massive sulfides (data from this study and Ripley, 1990a) are also interpreted to result from magmatic processes. Conversely, high-grade Pt-Pd-Au zones are thought to be the result of post-magmatic hydrothermal alteration, as suggested by the presence of lower temperature sulfide phases and local Pt-Pd-Au depletions and enrichments (Ripley, 1990a). Theriault et al. (1997) investigated PGE contents of mineralized norites, troctolites, and PGE-enriched horizons from the Dunka Road deposit and concluded that all three formed from similar parental magmas but formed at variable R-factors (50 – 11,000) and degrees of crustal contamination.

Here we present PGE data for country rock-hosted massive sulfides below the Partridge River intrusion, which plot at the bottom end of the trend produced by the combination of data from Ripley (1990a) and Theriault et al. (1997), being extremely depleted in all PGEs (Fig. 22A–D). A parental silicate magma with 0.05 ppb Os, 0.05 ppb Ir, and 0.15 ppb Ru, and 2 ppb Pt and Pd will produce sulfide liquid concentrations like the disseminated sulfides from Dunka Road at R-factors of ~20 to 10,000 (Fig. 22A–D), which are similar to R-factor calculations from Theriault et al. (1997). Disseminated sulfide data from Ripley (1990a) correspond to R-factors of ~ 50 to 10,000, with one sample corresponding to an R-factor of nearly 35,000. Ripley (1990a) noted a strong decoupling of Pt, Pd, and Au from Ir, Ru, Os, and Rh, which is also apparent in the country rock-hosted massive sulfides. Ripley (1990a) attributed the IPGE-PPGE decoupling to hydrothermal processes.

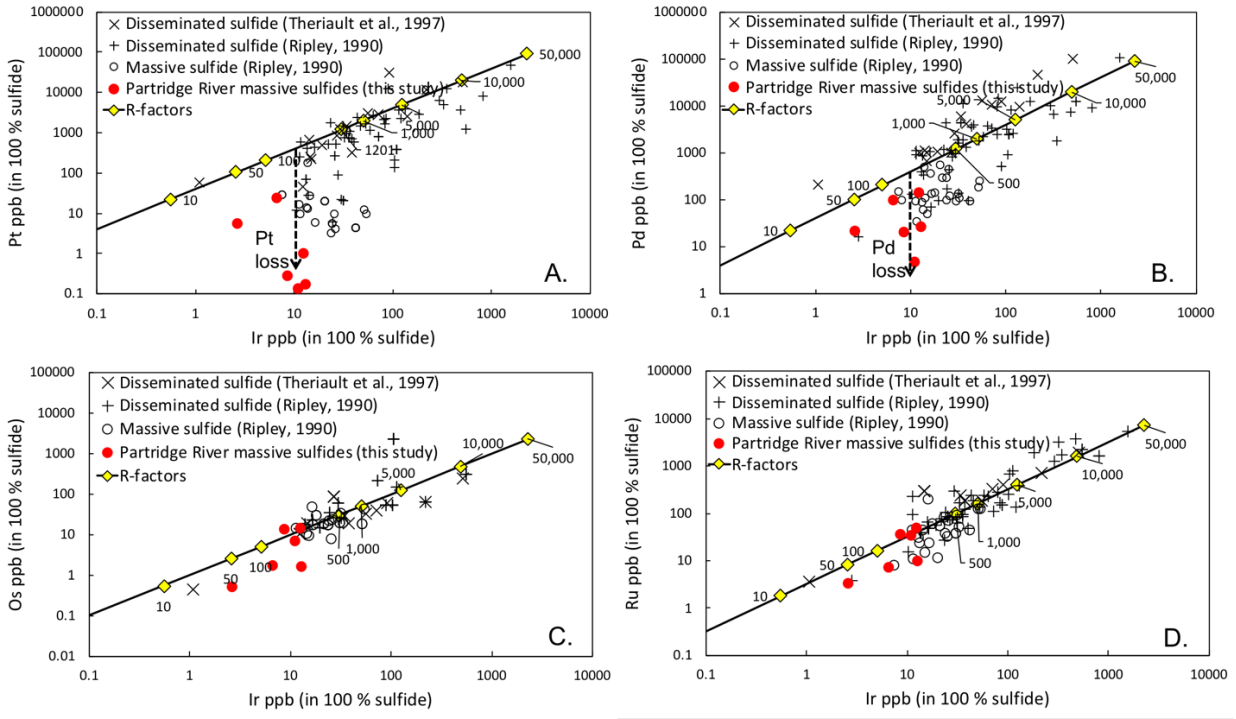

Figure 22: Modeling of variable R-factors during sulfide liquid segregation at the Partridge River intrusion.

The extreme negative Pt anomalies compared to Pd (Fig. 10A–C) cannot be explained by MSS fractionation, as the $D^{MSS}_{Sulf.Liq.}$ for Pt and Pd are virtually identical (Li et al., 1996; Mungall et al., 2005). Additionally, mass-balance calculations of the initial silicate magma, suggest that the Pt concentration of the initial silicate liquid would have to have been an order of magnitude less than Pd in order to produce the observed disparity in Pt and Pd concentrations in the country rock-hosted massive sulfides (data from here and Ripley, 1990a). This would be uncommon, as analyses of basalts and mantle melting models suggest Pt and Pd concentrations are typically on the same order of magnitude, and in many cases, Pt is more concentrated than Pd in mantle melts (Barnes and Lightfoot, 2005). Additionally, the presence of sulfides with negative Pt anomalies and without any anomalies suggests the variation in the variation in the Pt concentrations are

unrelated to variations in the source. Because both MSS fractional crystallization and source variability (Pt-Pd disparity in the initial silicate melt) fail to explain the disparity in Pt and Pd concentrations and decoupling of IPGEs and PPGEs in the country rock-hosted massive sulfides, we suspect postmagmatic hydrothermal remobilization, as in Ripley (1990a). Massive sulfides are thought to have leaked into the Virginia Formation after they initially formed as magmatic sulfide liquids produced by R-factors of ~ 40 to 250 (Fig. 22C–D), which are consistent with the low end of R-factors suggested by Theriault et al. (1997). These relatively low R-factors would have been sufficient to produce the IPGE compositions of the country rock-hosted massive sulfides, provided the PPGE decoupling and extreme Pt loss were the result of postmagmatic hydrothermal redistribution.

Conclusions

Mineral assemblages and textures of country rock-hosted massive sulfides near Tamarack, Eagle, and the Partridge River intrusion are similar to those of typical magmatic sulfides, supporting a magmatic origin for the country rock-hosted massive sulfides. Co/Ni ratios of country rock-hosted massive sulfides located adjacent to the Tamarack Igneous Complex, and the Eagle and Partridge River intrusions are all less than 2, which is the typical minimum Co/Ni of hydrothermal sulfides. Co/Ni ratios of country rock-hosted massive sulfides at Tamarack and Eagle are similar to those from Noril'sk, Pechenga, and other known magmatic sulfides. S/Se ratios of country rock-hosted massive sulfides at Tamarack and Eagle are similar to mantle S/Se ranges and have S/Se ratios that overlap those reported for igneous-hosted sulfides at Noril'sk and Pechenga, again consistent with origins as magmatic sulfide liquids. S/Se of samples beneath the Partridge River intrusion have similar S/Se ratios as those from mineralized norites

and are consistent with derivation from magmatic sulfide liquids. S/Se ratios of country rock-hosted massive sulfides from all three locations, especially those from Tamarack and Eagle, are lower than S/Se of sulfidic sediments in the Virginia Formation, excluding an origin as metal-rich sedimentary sulfides.

S, Re-Os, and Pb isotope data indicate that mixing of mantle and crustally-derived components was required for the genesis of country rock-hosted massive sulfides at Tamarack, Eagle, and beneath the Partridge River intrusion. $\delta^{34}S$ values of the massive sulfides below the Partridge River intrusion are higher than those from igneous rock-hosted sulfides, and are consistent with higher degrees of contamination, but are also still within the range identified for Animikie Group sedimentary rocks. Pb and Re-Os isotopes of massive sulfides in the Virginia Formation are slightly more radiogenic than igneous rock-hosted sulfides (Ripley et al., 1999), again suggesting slightly higher proportions of a radiogenic crustal component in the massive sulfides relative to that indicated for the igneous rock-hosted sulfides. Our interpretation is that massive sulfides continued to incorporate S from the Virginia Formation well after emplacement in the country rocks, most likely by continued desulfidation of pyrite to pyrrhotite during contact metamorphism, as suggested by Ripley (1981), and Ripley and Al-Jassar (1987)

At Tamarack and Eagle, $\delta^{34}S$ and γOs values of country rock-hosted massive sulfides are identical to previously reported values for igneous rock-hosted sulfides. The $\delta^{34}S$ values of country rock-hosted massive sulfides near Tamarack and Eagle are only slightly higher than the range for mantle $\delta^{34}S$ values, but they are consistent with minor amounts of bulk or selective mixing between mantle and crustal S reservoirs, or mixing followed by isotopic exchange (Ripley and Li, 2003; Ding et al., 2012; Taranovic et al., 2015). Pb isotope data for country rock-hosted massive sulfides from Tamarack and Eagle may be explained by mixing of a

homogenous mantle component with Archean rocks at 1.1 Ga, or by mixing of heterogeneous mantle sources with Animikie and Baraga Group sediments at 1.1 Ga. S, Pb, and Os isotope measurements all corroborate slightly higher bulk mixing proportions at Eagle than at Tamarack. These stable and radiogenic isotope characteristics are all consistent with magmatic sulfides derived from mantle-derived, crustally-contaminated silicate melts. The preferred model is that heterogenous mantle melts were contaminated by Proterozoic rocks, based on the lack of anomalous $\Delta^{33}S$ signatures in the country rock-hosted massive sulfides from the MRS. Ding et al. (2012) identified semi-massive sulfides at Eagle with highly anomalous $\Delta^{33}S$, but that generation of sulfide liquid appears to be unrelated to formation of massive sulfides in the Michigamme Formation.

MSS fractional crystallization models have helped to distinguish which generations of sulfide liquids have leaked into the country rocks near Tamarack, Eagle, and the Partridge River intrusion. At Tamarack, the country rock-hosted massive sulfides were produced by MSS fractionation of sulfide liquids like those from the semi-massive sulfides in the CGO unit. The massive sulfides are found in the Thomson formation, between the underlying CGO and the overlying FGO, suggesting the massive sulfides were emplaced by filter-pressing of residual sulfide liquids from the semi-massive sulfides in the CGO. Near Eagle, the country rock-hosted massive sulfides and the igneous rock-hosted disseminated and massive sulfides were derived from a common parental sulfide liquid at an R-factor of ~ 600 via MSS fractional crystallization. The wide range of sulfide compositions observed here suggests that sulfide liquids must have been expelled from the intrusion at various times during their crystallization history, and sulfide leaking did not occur as a solitary event. Country rock-hosted massive sulfides below the Partridge River intrusion were derived from basaltic liquids characterized by relatively low R-

factors (~40 to 250), similar to disseminated sulfides from noritic sheets in the Partridge River intrusion. After emplacement in the country rocks the sulfides likely underwent near-equilibrium crystallization to maintain the observed IPGE and Cu concentrations.

Chapter 2: Non-magmatic Origins of Country Rock-Hosted Massive Sulfide(-Oxides) Beneath the Stillwater Complex, Montana

Introduction

Nearly 60 % of the world's Ni is mined from mafic-ultramafic intrusions and komatiites (Mudd, 2010; Mudd, 2012; Mudd and Jowitt, 2014). These deposits are products of Ni-Cu-PGE-rich immiscible sulfide liquids that have separated from parental silicate melts. Massive sulfide ore bodies occur within the igneous rocks in many deposits (e.g., Sudbury, Noril'sk, Voisey's Bay, Kambalda, Raglan, Eagle, Nebo-Babel, Kabanga to name a few). However, massive sulfides are also found in surrounding sedimentary or metasedimentary rocks at many of these deposits. In the case of the world-famous Sudbury deposits, sulfide-rich veins are found in country rocks beneath the intrusion. Origins related to draining of fractionated sulfide melts from the overlying intrusion, or the involvement of hydrothermal fluids, have been proposed (e.g., Li et al., 1992; Keays and Lightfoot, 2004; Hanley et al., 2005; Mungall, 2007; Lightfoot, 2007; Dare et al., 2014; Tuba et al., 2014). Sulfide liquid penetration into the country rocks has been proposed at the Reid Brook Zone of the Voisey's Bay deposit by Lightfoot (2007) to explain country rock-hosted massive sulfides. Maier and Barnes (2010) document massive sulfides in the sedimentary rocks at Kabanga and suggest that they are also the result of sulfide liquid percolation from the intrusion, or solid-state remobilization of ductile sulfides during faulting events. Massive sulfide mineralization is also found in country rocks related to conduit-type Ni-Cu-PGE mineralization at the Eagle and Tamarack deposits (Ding et al., 2012; Taranovic et al., 2015); an origin related to the emplacement of immiscible sulfide liquid that formed in the igneous environment in a manner analogous to that at Voisey's Bay has been proposed (e.g., Smith et al., in press); these deposits are the subject of forthcoming publications.

In some localities, however, massive sulfide mineralization in country rocks may show no documented physical connection with the sulfides in the igneous rocks. Massive sulfides may occur 30 m below igneous-rock hosted sulfide mineralization in the Kharaelakh intrusion in the Noril'sk district (e.g., Kunilov, 1994; Distler and Kunilov, 1994; Czamanske et al., 1995; Malitch and Latypov, 2011), with no unequivocal evidence for a physical connection to the sulfides hosted in igneous rocks. Massive sulfide layers and lenses, commonly with substantial oxide components, are also found in country rocks beneath the Stillwater Complex of Montana. The Stillwater Complex is well-known for the existence of the PGE-rich J-M Reef, but early exploration in the Complex focused on Ni-Cu-bearing sulfide mineralization found near the basal contact. Most previous studies focused on the Ni-Cu-PGE sulfide mineralization within the igneous rocks. Due to fewer studies, the origin of the sulfide-oxide mineralization in the metasedimentary country rocks of the complex is still uncertain.

Recent multiple S isotopic analyses reported by Ripley et al. (2017) show that massive and disseminated sulfides in the hornfels and the Basal Series sulfides display anomalous S isotope fractionation when compared to the average terrestrial fractionation curve (generally referred to as mass-independent fractionation, or MIF). The occurrence of anomalously fractionated S in the Archean is proposed to be a function of SO_2 photolysis in a reduced atmosphere largely devoid of ozone (e.g., Farquhar and Wing, 2003). Although debate continues as to the exact origins and implications of mass-independent S fractionation (Ohmoto et al., 2006; Claire et al., 2014), natural samples with such anomalous S isotope compositions are found primarily in Archean sedimentary rocks, or rocks that have been contaminated by Archean sediments (Farquhar and Wing, 2003; Penniston-Dorland et al., 2008; Farquhar et al., 2010). Anomalous multiple S isotope values in igneous rocks of the Basal Series reflect assimilation of S with a MIF signature

contained in country rocks. However, the massive sulfides(-oxides) in the hornfels may originate from three possible mechanisms. One is that they reflect the draining of magmatic sulfide-oxide liquid characterized by anomalous S isotope ratios. The second is that they represent sulfides and oxides that formed in the sedimentary environment, with sulfide originating from the reduction of seawater sulfate moderated by bacterial activity. A third possibility is the massive sulfides (-oxides) formed near the seafloor from hydrothermal fluids that either originated from seawater that contained S with MIF signals, or from fluids that leached S with MIF signals from sedimentary country rocks. These sulfides could also have then served as crustal contaminants, which are thought to have altered the stable and radiogenic isotopic characteristics of the Basal and Ultramafic Series (Lambert et al., 1989; Zientek and Ripley, 1990; Lambert et al., 1994; Horan et al., 2001; Ripley et al., 2017). In order to evaluate these possible alternatives, we have undertaken petrographic and geochemical investigations of massive sulfide(-oxides) found in the pelitic rocks in the Mountain View area below the Stillwater Complex, with a conclusion that the massive sulfide-oxide mineralization is genetically unrelated to that which occurs in the igneous rocks of the Complex, and initially formed as marine, sedimentary sulfides or hydrothermal seafloor exhalations.

Regional Geology

The Stillwater Complex is a 2.7 Ga layered mafic-ultramafic intrusion in south-central Montana. The exposed sequence is more than 6 km thick and 45 km long and is found along the Beartooth Front, in Archean metasedimentary rocks of the Wyoming craton (Fig. 23). The Complex, along with exposed contact metamorphic rocks, dip steeply to the north-northeast as a result of regional Laramide thrust faulting. To the northwest, the basal contact is an intrusive

contact with the underlying hornfels, and to the southeast the Complex is in fault contact with a younger quartz monzonite. The true dimensions of the entire Stillwater Complex are unknown, due to both erosion of overlying material and deep burial of the unexposed portions of the Complex.

A series of major crust-forming events are documented in this area starting at ~3.0 Ga, mostly as felsic intrusions. Igneous activity ultimately culminated in the intrusion of the Stillwater Complex and a series of related mafic sills and dikes at ~ 2.7 Ga (Wooden and Mueller, 1989; Premo et al., 1990). Mafic dikes continued to be emplaced into the Proterozoic (Baadsgaard and Mueller, 1973). When the Wyoming craton was completely assembled around 1.7 Ga, low grade regional metamorphism drove circulation of hydrothermal fluids (Giletti, 1966; Page, 1977). Uplift and erosion of the Stillwater block began during the late Proterozoic. Unconformable marine sedimentation overlying the Complex is recorded from the early Paleozoic to late Mesozoic, and includes a well-documented series of sandstones, shales, and carbonate units that are now exposed along the Beartooth Front. Laramide tectonics resulted in tilting a portion of the Stillwater Complex and surrounding rocks to the northeast (Jones et al., 1960; Page, 1977; Geraghty, 2013; Thacker et al., 2016;). Erosion exposed the nearly vertically dipping section to produce the present-day configuration.

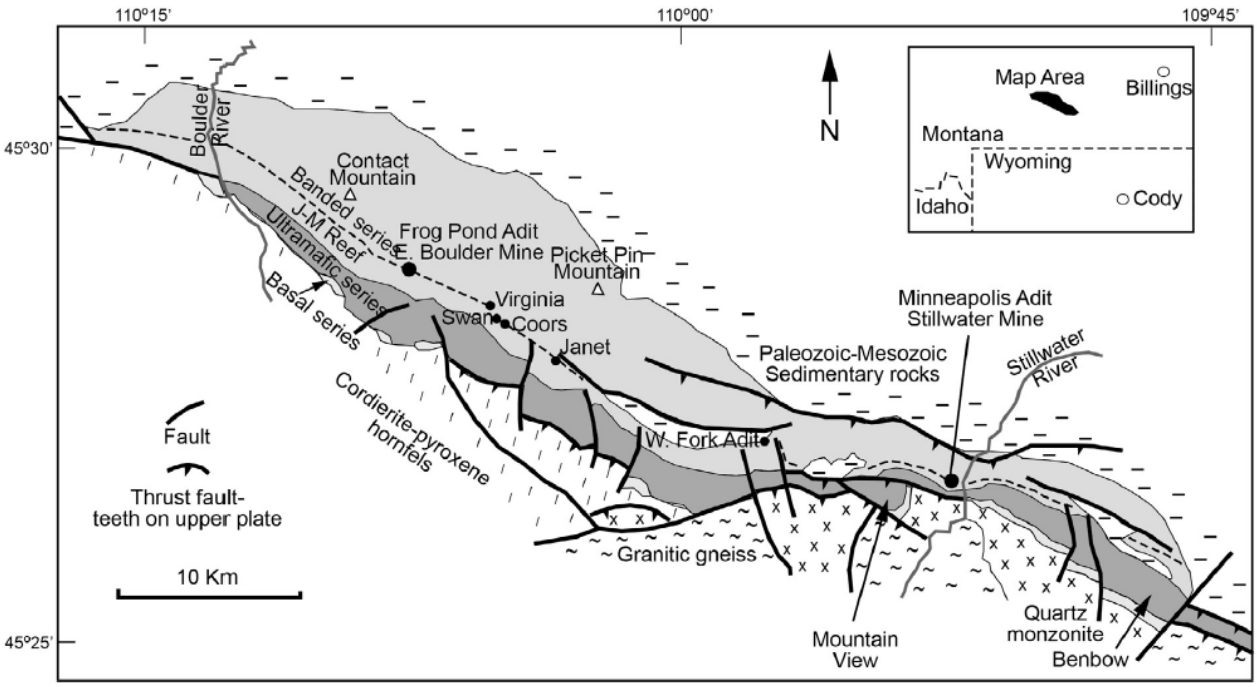

Figure 23: Geologic map of the Stillwater Complex (modified from Lambert et al. 1994 and McCallum et al. 1999). Samples were collected from a series of drill holes in the Mountain View area.

Background and Previous Studies of the Stillwater Complex and Associated Country Rocks

Rock types, metamorphism, and geochronology

The igneous stratigraphy in the Complex has been reviewed by several researchers, and petrologic studies of the Complex have been ongoing for the past ~ 70 years (see Boudreau, 2016 for a recent review). The Complex has been divided into a Basal Series, an Ultramafic Series, and Lower, Middle, and Upper Banded Series (Fig. 23, e.g. Jackson, 1961; Page, 1979; McCallum et al., 1980; Segerstrom and Carlson, 1982; Todd et al., 1982; Raedeke and McCallum, 1984; Zientek et al., 1985). The well-known PGE-rich J-M Reef is contained in the Lower Banded Series, and exceptional stratigraphic details of the rock types in and around the

Reef have been published by many researchers (e.g. McCallum et al., 1980; Bow et al., 1982; Todd et al., 1982; Irvine et al., 1983; Zientek et al., 1985; Raedeke and Vian, 1986; Barnes and Naldrett, 1986; Corson et al., 2002). High precision U-Pb zircon-baddeleyite dating of the Reef by Wall and Scoates (2016) and Wall et al. (2018) indicate an age of 2709.11±0.56 Ma for that portion of the Complex. Earlier U-Pb age determinations by Nunes and Tilton (1971) provided an age of 2750 Ma for the Basal Series, and a gabbro analyzed by DePaolo and Wasserburg (1979) produced a Sm-Nd isochron age of 2701±8 Ma. Nunes (1981) determined a U-Pb age of 2713±3 Ma for rocks of the Basal Series. Premo et al. (1990) found a U-Pb age of 2705±4Ma for the sills and dikes below the Complex. Zircon U-Pb dates from tonalitic gneiss in the area range from 2800 to 2900 Ma (Mueller et al., 2008).

Country rocks located at the base of the Complex include contact metamorphosed hornfels, quartzite, and iron formation. The proximal hornfels is composed of cordierite and orthopyroxene, or quartz and pyroxenes;the distal hornfels is composed of cordierite and cummingtonite (Barker, 1975; Vaniman et al., 1980; Page and Zientek, 1985; Geissman and Mogk, 1986; Zientek and Ripley, 1990; Labotka and Kath, 2001; Thomson, 2008). Protoliths of the hornfels are thought to be predominantly marine shales and graywackes. Labotka and Kath (2001) and Labotka et al. (1982) reported that in the Boulder River area temperatures in the cordierite-orthopyroxene hornfels reached at least 600 °C, up to a maximum of 825 °C, likely facilitated by pre-Stillwater regional metamorphism in the range of 450 to 625 °C. Thomson (2008) studied contact metamorphic rocks from the Mountain View – Mouat Mine area. Unlike Labotka and Kath (2001), she found evidence for partial melting of the hornfels, with back reaction between crystallizing melt and restite in the form of skeletal intergrowths of biotite and quartz. Average temperature and pressure conditions of hornfels and melt genesis were estimated

by these authors to be 786 ° C and 3.7 kb. The presence of pigeonite in iron formation near the contact (Lindsley, 1980; Vaniman et al., 1980; Labotka, 1985) also suggests that temperatures > 825 ° C were attained near the contact. Barker (1975), Vaniman et al. (1980), Page and Zientek (1985), and Thomson (2008) noted the relatively high Ni contents of the hornfels (see below). Barker (1975) and Vaniman et al. (1980) suggested that Ni, as well as Cu and Cr, were introduced into the pelitic rocks from the Stillwater Complex. Page and Zientek (1985) and Thomson (2008) suggested that mafic and ultramafic rocks with relatively high Ni contents were present in the source region of the sedimentary rocks.

A depositional age of the protoliths to the hornfels has not been determined, but the rocks contain 3.14 Ga detrital zircons (Nunes and Tilton, 1971) and have been intruded by quartz monzonite dated at 2.7 Ga (Nunes and Tilton, 1971). Therefore, the depositional age is constrained to be between ~ 2.8 and 3.1 Ga. More recent analyses from Zientek (person. commun.) confirms the presence of 2.8 to 3.1 Ga detrital zircons in the hornfels from the Mountain View area. Nunes and Tilton (1971) suggested, based on U-Pb analyses of detrital zircons from the hornfels, that the U-Pb system was not rehomogenized during emplacement of the Stillwater Complex. Mueller and Wooden (1976) performed Rb-Sr analyses on hornfels samples and determined an isochron age of 2,750 ± 45 Ma, and an initial $^{87}Sr/^{86}Sr$ of 0.705. Other Rb-Sr analyses by Powell et al. (1969) produced an isochron age of 2,730 ± 30 Ma with an initial $^{87}Sr/^{86}Sr$ of 0.705. They suggested this is either a depositional age or the result of isotopic rehomogenization during contact metamorphism. Thomson (2008) suggested the Rb-Sr data of Powell et al. (1969) were due to isotopic rehomogenization, although she also suggested that the calculated age may be that of contact metamorphism related to the Stillwater Complex or that of earlier regional metamorphism. Pb-Pb analyses of the hornfels plot along a 2.8 Ga reference

isochron produced from a two-stage crustal Pb model (Wooden et al., 1991). Massive sulfide(-oxides) used for this study are hosted primarily in the cordierite-orthopyroxene hornfels. Zientek and Ripley (1990) reported that sulfide assemblages in the cordierite-orthopyroxene hornfels consist of pyrrhotite, pentlandite, and chalcopyrite, but at greater distance from the intrusion pyrite is present along with chalcopyrite.

Sulfide Mineralization in the Stillwater Complex

Sulfide minerals are found in most rocks of the Stillwater Complex, although typical modes are less than 0.01 volume percent (Page, 1971). Recent work by Aird et al. (2016) on trace sulfide assemblages in the Complex has shown that variable proportions of pyrrhotite, chalcopyrite, and pentlandite are present throughout the stratigraphy of the Complex. Elevated concentrations of sulfide minerals are present in only a few localities: disseminated sulfides in rocks of the Basal Series, massive and net-textured sulfides in the lower part of the Ultramafic Series in the Iron Mountain area (known as the Camp deposit), disseminated sulfides in the J-M Reef within the Lower Banded Series, and in the much smaller PGE-enriched Picket Pin deposit in the Upper Banded Series. Massive sulfide lenses occur associated with the G chromitite in the Iron Mountain area. The J-M Reef contains between 0.5 and 3 volume percent sulfides; sulfide abundance is less in the Picket Pin deposit. Disseminated sulfides are present throughout the Basal Series, but sulfide abundance is greater in the lower noritic rocks of the Basal Series (Page et al., 1985; Zientek et al., 1985). Sulfur isotope analyses by Zientek and Ripley (1990) and Ripley et al. (2017) indicate that a large component of the sulfur present in Basal Series rocks has been derived from sulfide in the underlying metasedimentary rocks. In contrast, sulfur isotope ratios of the J-M Reef are consistent with the premise that most of the S in the Reef is of mantle derivation (Zientek and Ripley, 1990; Ripley et al., 2017).

Interest in the Ni-Cu potential of sulfide mineralization near the base of the Stillwater Complex began in 1883 when sulfide-rich rocks were found in the Mountain View, Benbow, and Initial Creek areas (Page et al., 1985). The Verdigris Creek-Mouat nickel mine operated for a short time in the early 1900's. The massive sulfide occurrences at the mine appear to be largely those found in the hornfels, although some sulfide mineralization may also have been that which occurs in noritic sills beneath the Complex. Drilling for Ni-Cu resources by a variety of companies continued sporadically until at least 1983. A renewed interest in the mineralization present in the Basal Series and within the metasedimentary hornfels is largely a function of the international need for Co used primarily as cathodes in batteries (Group Ten Metals https://grouptenmetals.com).

Although some economic interest has always remained in the hornfels-hosted sulfides, relatively little detailed geochemical work has been published. Page (1979) described massive sulfides in the hornfels and found hexagonal and monoclinic pyrrhotite, pentlandite, and chalcopyrite, which was in some cases altered to bravoite, violarite, mackinawite, marcasite, pyrite, cuprite, and native Cu. Page (1979) also noted an oxide portion which was composed of magnetite with ilmenite exsolution, as well as minor chromite and goethite. He suggested that silicate magma, along with sulfide-oxide liquids that formed early in the crystallization history of the basal series were injected into the metasedimentary rocks as dikes and lenses.

Zientek (1985) came to a similar conclusion regarding the origin of the hornfels-hosted sulfide-rich mineralization. The S isotope study of Zientek and Ripley (1990) reveals that S isotopic ratios in the Basal Series and the cordierite-orthopyroxene hornfels are similar to those of sulfides in the iron formation. They suggested that S from the iron formation was assimilated by magmas and therefore massive sulfides in the hornfels were consistent with either leaking

downward from magmas of the Basal Series, or with emplacement related to intrusion of the norite sills and dikes.

Sampling and Analytical Procedures

Samples used in this study were taken primarily from drillcores 368-313, 370-316, 373-322, 384-326, and M-17, which intersected massive sulfide-oxide layers or lenses hosted in the cordierite-orthopyroxene hornfels and quartz-orthopyroxene hornfels below the Stillwater Complex (Fig. 24). All drill collars were located at ~ 45°23'19" N and 109°54'0.7". Nineteen samples were studied petrographically in polished thin sections using transmitted and reflected light to document the mineral assemblages and textures of the massive sulfides-oxides and host rocks, with emphasis on their interface. Mineral compositions were determined using a CAMECA SX50 electron microprobe at Indiana University.

Nine massive sulfide-oxide samples from below the Stillwater Complex were analyzed for S-Ni-Cu-Co-Au-PGE at the Université du Québec á Chicoutimi. Ni, Cu, and Co were determined by atomic absorption spectroscopy. S was analyzed using a Horiba elemental analyzer. PGEs and Au were preconcentrated by NiS fire assay, digested in a modified aqua regia mixture, diluted, and analyzed using a ICP-MS instrument. The analytical uncertainties are estimated to be better than 10 % based on the results for the standards LK-NIP-1 and KPT-1 (Savard et al., 2010). The detection limits for PGE and Au are 0.065 ppb Os, 0.025 ppb Ir, 0.12 ppb Ru, 0.082 ppb Rh, 0.084 ppb Pt, 0.471 ppb Pd, and 0.484 ppb Au. Detection limits of other major and trace elements are 0.16 % S, 0.001 % Ni and Cu, and 3 ppm Co (Savard et al., 2010).

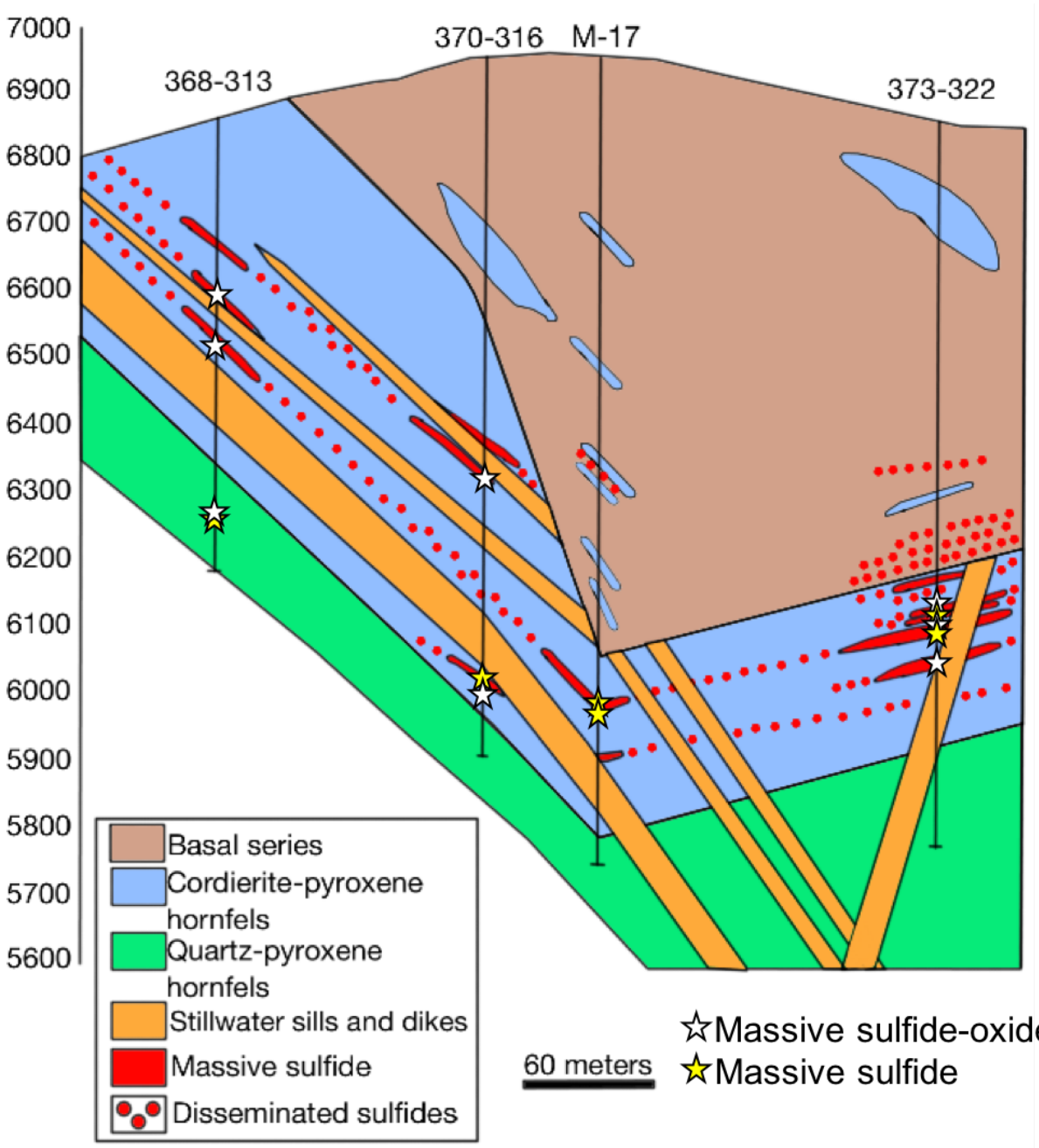

Figure 24: Cross-section through the Mouat area of the Stillwater Complex. Samples of country rock-hosted massive sulfides (gold stars) and massive sulfide-oxides (white stars) were taken primarily from the cordierite-pyroxene hornfels, with a few from the quartz pyroxene hornfels. Geology based on core logging from Roger Cooper.

The full method, including all standards, can be found in Savard et al. (2010). As, Se, and Te were analyzed using an Agilent 7700 series quadrupole ICP-MS instrument in the Metal Isotope

Lab at Indiana University, Bloomington. A series of diluted, multi-element ICP standards, from 1 to 500 ppb were used to calibrate the mass spectrometer. The analytical reproducibility is estimated to be ± 5 %, based on duplicate analyses.

Eight samples were also analyzed for Re-Os isotopic compositions in the Department of Terrestrial Magnetism at the Carnegie Institution of Washington. Approximately 0.1 grams of sample powder was equilibrated in modified aqua regia with separate ^{185}Re and ^{190}Os spikes, using the Carius tube method described by Shirey and Walker (1995). Os was separated by CCl_4 solvent extraction and then distilled into HBr. The residual aqua regia solution was put through anion exchange chromatography to recover the Re. The Os fraction in HBr was loaded onto a platinum filament and dried under a heat lamp. $Ba(OH)_2$ was added to the surface of the filament and again dried. Os was analyzed by negative thermal ionization mass spectrometry using a Thermo Finnigan Triton instrument, in peak-hopping mode via a secondary electron multiplier. The Re fraction was diluted in 5% HNO_3 and $^{185}Re/^{187}Re$ were measured on a ThermoFisher iCap-Qc RF quadrupole ICP-MS. Procedural blanks averaged 4.9 pg Re and 3.3 pg Os. Seven replicate measurements of the DTM J-M Os standard within a 20-month period produced a $^{187}Os/^{188}Os$ ratio of 0.17388 ± 0.00038 (2-sigma of the population).

Pb isotopic analyses were performed on eleven samples of massive sulfides. Pb analyses were also performed in the DTM at the Carnegie Institution of Washington. Crushed samples were digested in a mixture of concentrated HF and HNO_3. Samples were then dried, digested in HCl, and dried again before being taken up in HBr. The Pb in HBr was put through anion exchange chromatography and collected in dilute HNO_3. Samples were diluted with 5% HNO_3 and analyzed for $^{206}Pb/^{204}Pb$, $^{207}Pb/^{204}Pb$, and $^{208}Pb/^{204}Pb$, using a Nu-Plasma II multicollector ICP-MS instrument. Standard-sample bracketing allowed isotopic ratios to be adjusted using a

$^{205}Tl/^{203}Tl$ mass bias factor calculated from analyses of the NBS 981 standard. Thirteen replicate measurements of the NBS 981 standard produced average $^{206}Pb/^{204}Pb$ of 16.94 ± 0.008, $^{207}Pb/^{204}Pb$ of 15.49 ± 0.01, and $^{208}Pb/^{204}Pb$ of 36.70 ± 0.03. Procedural blanks averaged 126 pg Pb, and analyzed solutions contained between 7 and 70 ppb Pb.

Six magnetite separates from the massive sulfides-oxides beneath the Stillwater Complex and for comparative purposes five magnetites from the massive sulfide ore body of the Voisey's Bay deposit were analyzed for oxygen isotopic compositions. Four samples of magnetite and two samples of quartz from the Stillwater Iron Formation were also analyzed for O isotope compositions. Magnetite was microdrilled from hand samples and magnetically separated from associated sulfides and silicates. Samples were prepared using a standard BrF_5 vacuum line. Samples weighing 2 to 6 mg were placed in Ni reaction vessels and heated overnight with excess BrF_5 at 500 °C (Clayton and Mayeda, 1963). Liberated oxygen was passed over a heated graphite disk and converted to CO_2. Results are reported in standard delta notation relative to VSMOW with multiplication by 1000 to yield values in ‰. Samples and standards were analyzed on a MAT 253 isotope ratio mass spectrometer in dual inlet mode with 2σ of ± 0.04 ‰ or better and standard reproducibility of ± 0.3 ‰ for Kanaga pyroxene.

Results

Sulfide Mineralogy and Textures

Massive sulfide- and oxide-rich mineralization associated wth the hornfels beneath the Stillwater Complex (Fig. 25 A-C) occurs as layers and lenses ranging from 1 cm up to 2 m in thickness. Mineral assemblages are composed of variable proportions of pyrrhotite (23 – 94 volume %), magnetite and ilmenite (< 1 – 37 %), chalcopyrite (< 1 – 43 %), and pentlandite (< 1

– 6 %). Samples with less than 10 % oxides in the opaque fraction are classified as "massive sulfides", and samples are labeled as "massive sulfides-oxides" if they contain greater than 10 % oxide in the opaque fraction. A full list of modal compositions and sample classifications can be found in Table 8. Anhedral hexagonal pyrrhotite commonly contains exsolved monoclinic pyrrhotite (Fig. 26A). Some pyrrhotite grains have pentlandite exsolution lamellae (Fig. 26B). Magnetite and ilmenite occur as euhedral to anhedral intergrowths; magnetite commonly contains exsolved ilmenite (Fig. 26C). Minor intergrown pentlandite and chalcopyrite are found interstitially to pyrrhotite grains (Fig. 26D) and, locally, cubanite is exsolved from chalcopyrite. Graphite needles and coatings can also be found in thin section (less than 1 %) and on drill core fracture surfaces.

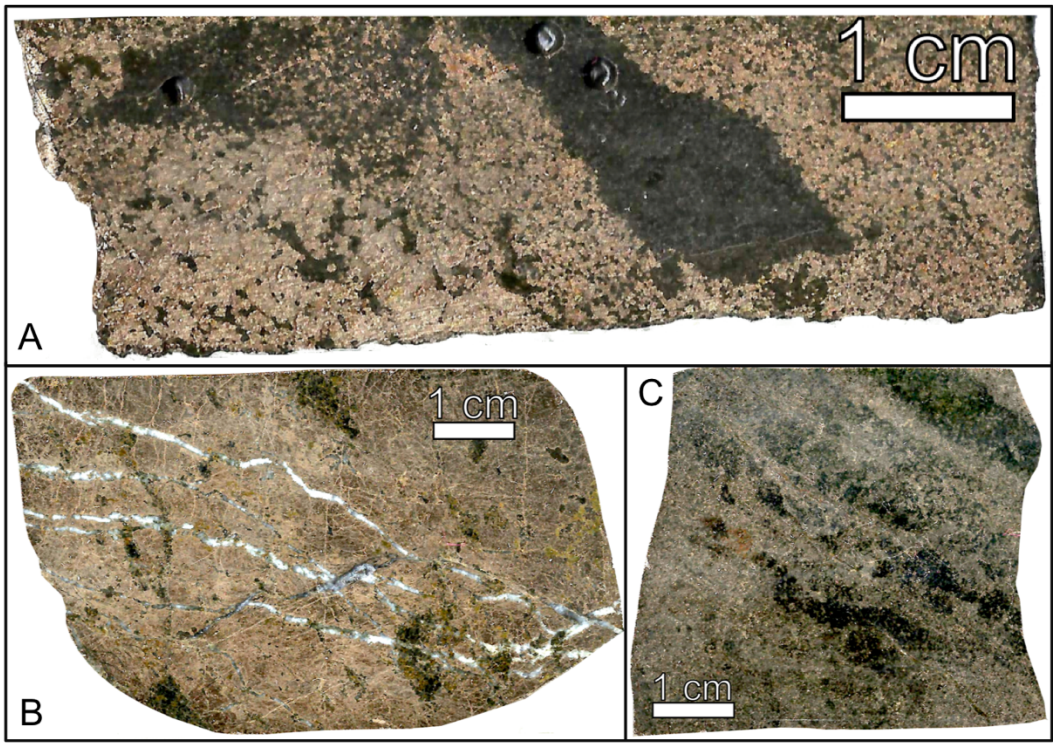

Figure 25: Hand sample photos of country rock-hosted massive sulfide(-oxide) (A), massive sulfide with cross-cutting serpentine-carbonate veinlets (B), and layered massive sulfide(-oxide) (C) below the Stillwater Complex.

Table 8: Modal mineralogy of massive sulfides and massive sulfide-oxides beneath the Stillwater Complex, normalized to 100 % opaque minerals.

Sample	Classification	Po	Mt/Ilm	Ccp	Pn
M17-979.5	Massive sulfide	89	4	< 1	7
M17-985	Massive sulfide	96	4	< 1	< 1
M17-1048	Massive sulfide	35	< 1	65	< 1
M17-1049.5	Massive sulfide	85	4	8	4
368-313-275.5	Massive sulfide-oxide	33	31	36	< 1
368-313-276	Massive sulfide-oxide	53	19	28	< 1
368-313-338	Massive sulfide-oxide	85	11	4	< 1
368-313-574.5	Massive sulfide-oxide	71	29	< 1	< 1
370-316-576	Massive sulfide	93	< 1	7	< 1
370-316-622.5	Massive sulfide-oxide	68	31	1	< 1
370-316-908.2	Massive sulfide	81	< 1	19	< 1
370-316-918	Massive sulfide-oxide	84	16	< 1	< 1
373-322-726.5	Massive sulfide-oxide	63	37	< 1	< 1
373-322-738	Massive sulfide	94	6	< 1	< 1
373-322-756	Massive sulfide	83	3	14	< 1
373-322-804	Massive sulfide-oxide	76	21	3	< 1
373-322-809	Massive sulfide	88	6	6	< 1
373-322-868	Massive sulfide-oxide	79	21	< 1	< 1
384-326-1455	Massive sulfide-oxide	56	24	20	< 1

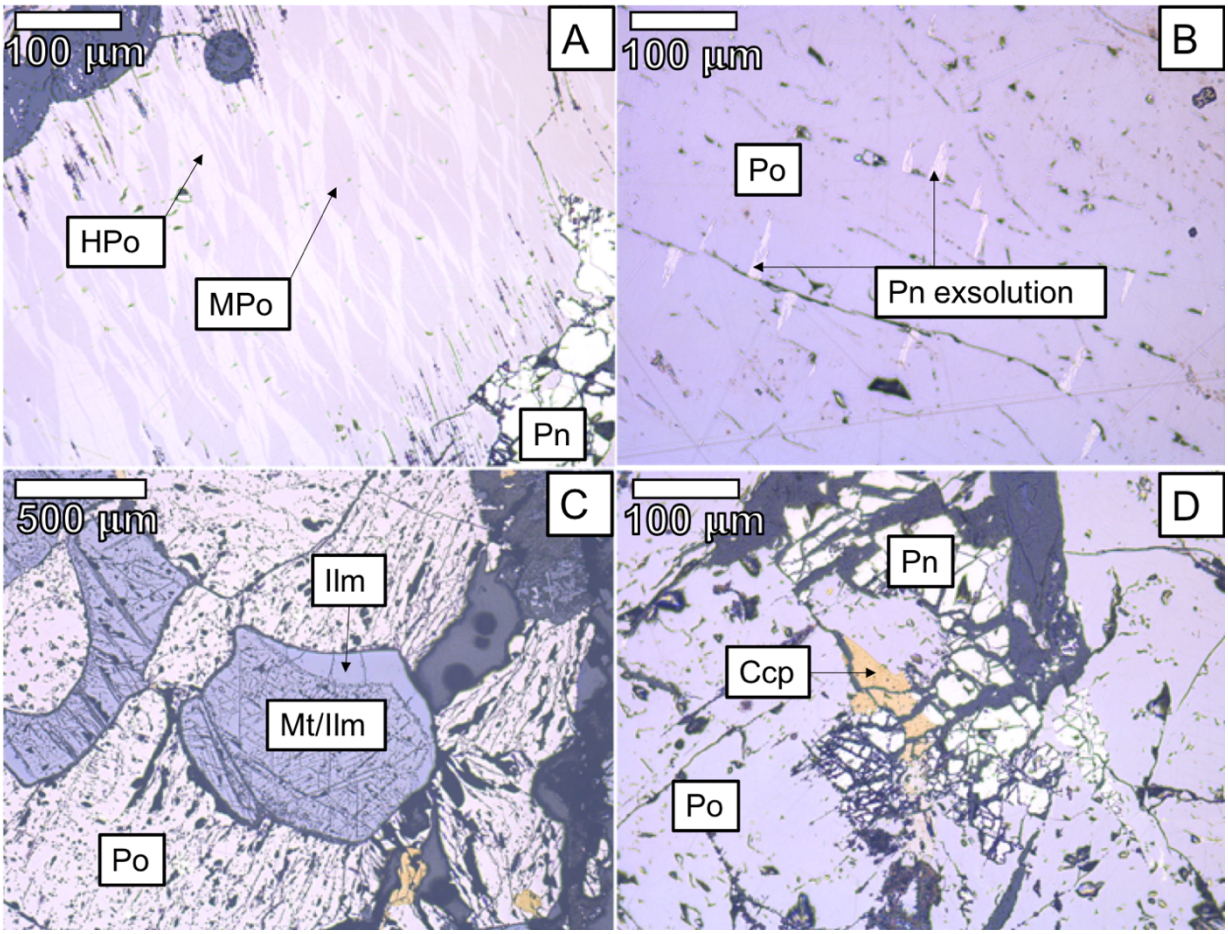

Figure 26: Photomicrographs of country rock-hosted massive sulfides below the Stillwater Complex and associated rocks of the cordierite-orthopyroxene hornfels. A. Intergrown hexagonal (HPo) and monoclinic pyrrhotite (MPo) and pentlandite (Pn) B. Pentlandite exsolution in pyrrhotite. C. Intergrown chromite (Cr) and magnetite (Mt) with ilmenite exsolution (ılm). D. Intergrown pentlandite and chalcopyrite (Ccp).

Cordierite-orthopyroxene hornfels may be interlayered with the massive sulfides (-oxides) and fragments, or inclusions, of hornfels may occur within the sulfides. Importantly, many of the hornfels are described as 'hornfels breccia'; the fragmentation may have occurred prior to or during emplacement of the Stillwater Complex. This also indicates that any preexisting sulfide layers, lenses, and other modes of occurrence, may have been disrupted as well, and may now be found surrounding fragments of hornfels. The silicate fraction may be altered to tremolite-

actinolite, and serpentine-carbonate veinlets (< ~ 200 μm thickness) are observed cross-cutting the sulfides, oxides, and silicates. In one sample the silicate fraction is composed of ferrohypersthene and fayalite, and the opaque fraction is predominantly pyrrhotite and magnetite (~ 20 volume %), with minor chalcopyrite and hercynite.

Samples of the non-brecciated cordierite-orthopyroxene and cordierite-biotite hornfels that occur between the massive sulfide (-oxide) layers were also examined. Both types of hornfels have disseminated pyrrhotite (< 2%) and ilmenite (< 2 %) with trace amounts of chalcopyrite and magnetite (< 0.5 %), in agreement with the observations of Singha (2011).

Trace Element Concentrations

Major and trace element concentrations of massive sulfide-oxides beneath the Stillwater Complex, along with selected elemental ratios, are shown in Table 9. In the Mountain View area, Ni and Cu show no positive correlation in the country rock-hosted massive sulfides-oxides. In addition, Ni, Cu, PGEs, and Au do not co-vary with S content. Cu/Ni ratios in the massive sulfides range from 0.025 to 0.952. For comparison, Godel and Barnes (2008) reported Cu/Ni ratios for the JM Reef (0.51 to 0.8), along with values from the hanging wall (0.008 to 0.125), and footwall (0.028 to 0.67) of the JM Reef. Cu/Ni ratios of sulfides from the Ultramafic Series are between 0.001 and 0.18 (Barnes et al., 2016).

Individual IPGEs (Ir, Os, Ru) are well correlated with each other (R^2>0.96). There is no positive correlation between IPGEs and PPGEs (Pt, Pd, Rh). In the hornfels-hosted massive sulfide samples Pd contents range from 50 to 150 ppb, whereas Pt concentrations are 2 orders of magnitude lower, between 0.24 to 3 ppb.

Table 9: Major and trace element compositions and ratios of samples from this study.

Sample	Mineralization type	S (%)	Ni (%)	Cu (%)	Os (ppb)	Ir (ppb)	Ru (ppb)	Rh (ppb)	Pt (ppb)	Pd (ppb)	Au (ppb)	Co (ppm)
368-313-275.5	Massive sulfide-oxide	25.60	0.79	0.23	0.66	0.07	0.27	0.41	0.89	100.90	35.84	418.81
368-313-276	Massive sulfide-oxide	26.03	1.24	1.16	0.56	0.13	0.13	0.37	3.02	109.10	155.68	663.30
368-313-574.5	Massive sulfide-oxide	29.92	1.32	0.03	3.83	4.22	11.39	9.63	0.72	150.51	34.57	936.63
373-322-726.5	Massive sulfide-oxide	32.47	1.77	0.07	3.31	3.78	6.96	7.87	0.24	32.03	16.08	1296.70
373-322-804	Massive sulfide-oxide	29.12	2.06	0.09	0.61	1.63	2.54	5.26	1.12	56.31	23.79	1536.73
373-322-809	Massive sulfide	26.11	0.89	0.58	0.56	0.87	0.59	19.19	0.91	89.72	27.25	704.17
373-322-868	Massive sulfide-oxide	34.83	1.28	0.03	1.53	1.96	2.76	4.18	0.52	103.87	11.92	927.11
M17-979.5	Massive sulfide	37.18	2.09	0.04	0.86	1.73	1.82	8.84	0.93	740.10	29.49	1214.28
M17-1049.5	Massive sulfide	32.56	1.43	1.36	6.42	6.30	15.07	4.54	0.35	29.50	14.49	1018.10

Sample	Mineralization type	As (ppm)	Sb (ppm)	Se (ppm)	Te (ppm)	Co/Ni	S/Se	As/Au	Sb/Au	Cu/Ni	As/Ni	Te/Au
368-313-275.5	Massive sulfide-oxide	60.18	0.19	53.48	4.35	0.053	4788	1679.0	5.4	0.296	0.008	121.2
368-313-276	Massive sulfide-oxide	59.67	1.53	44.10	-	0.054	5901	383.3	9.8	0.938	0.005	-
368-313-574.5	Massive sulfide-oxide	15.98	0.11	38.25	6.65	0.071	7820	462.0	3.3	0.025	0.001	192.3
373-322-726.5	Massive sulfide-oxide	9.46	0.09	56.54	11.44	0.073	5743	587.9	5.3	0.041	0.001	711.4
373-322-804	Massive sulfide-oxide	2.39	0.12	50.93	4.66	0.074	5718	100.6	5.2	0.045	0.000	195.7
373-322-809	Massive sulfide	36.20	2.61	34.03	-	0.079	7673	1328.7	95.6	0.655	0.004	-
373-322-868	Massive sulfide-oxide	8.01	2.15	36.29	-	0.073	9598	672.2	179.9	0.023	0.001	-
M17-979.5	Massive sulfide	7.22	0.06	41.76	10.82	0.058	8903	244.9	1.9	0.017	0.000	367.0
M17-1049.5	Massive sulfide	36.93	BDL	44.60	2.93	0.071	7301	2548.1	-	0.952	0.003	202.1

Primitive mantle-normalized patterns of Ni, Cu, Au and PGE tenors (whole-rock concentration normalized to 100% sulfide) in the massive sulfides-oxides beneath the Stillwater Complex are illustrated in Fig. 27. The oxide-rich and oxide-poor massive sulfides beneath the Stillwater Complex have similar patterns and are grouped together in the presentation below. These samples are all depleted in PGEs plus Au as compared to Ni and Cu, showing downward

concave patterns. They also show significant negative Pt anomalies (~2 – 3 orders of magnitude below the primitive mantle-normalized ratios for Pt), which are not present in the samples from the Banded Series (Fig. 27A, Godel and Barnes, 2008), Ultramafic Series (Fig. 27B, Barnes et al., 2016) and the Basal Series of the Stillwater Complex (Fig. 27C, data from the USGS National Geochemical Database). Furthermore, the PGEs+Au tenors of the country rock-hosted massive sulfides-oxides are significantly lower than those of the igneous rocks of the Stillwater Complex (Fig. 27A-C). The hornfels of the complex from previous studies (data from the USGS National Geochemical Database) have higher PGE tenors and less degrees of negative Pt anomaly than the country-hosted massive sulfide(-oxides) analyzed in this study (Fig. 27D).

Co and Ni concentrations in the country rock-hosted massive sulfides-oxides are from 0.04 to 0.15 wt % and from 0.8 to 2.1, respectively. They show a positive correlation, with R^2 of 0.83. Higher Ni contents in some cordierite-rich hornfels were previously documented in a USGS Ni-Cu assessment of the Mountain View area (Attanasi and Bawiec, 1987). Co/Ni and S/Se ratios of country rock-hosted massive sulfides-oxides range from 0.053 to 0.079 and from 4,788 to 9,598, respectively (Fig. 28). For comparison, Co/Ni ratios of the JM Reef and Ultramafic Series of the Stillwater Complex range from 0.01 to 0.75 and 0.096 to 0.21, respectively; the S/Se ratios range from 1,673 to 2,259 and 646 to 3,866, respectively (Godel and Barnes, 2008; Barnes et al., 2016). Thus, the sedimentary rock-hosted massive sulfides have similar Co/Ni ratios but much higher S/Se ratios than the igneous rock-hosted sulfides. Other trace element concentrations (As, Se, Te) and trace element ratios (Cu/Ni, Te/Au, and As/Au) can also be found in Table 8. Cu/Ni ratios of country rock-hosted massive sulfides range from 0.017 to 0.952. The Te/Au and As/Au ratios range from 121 to 711 and from 245 to 2,548, respectively.

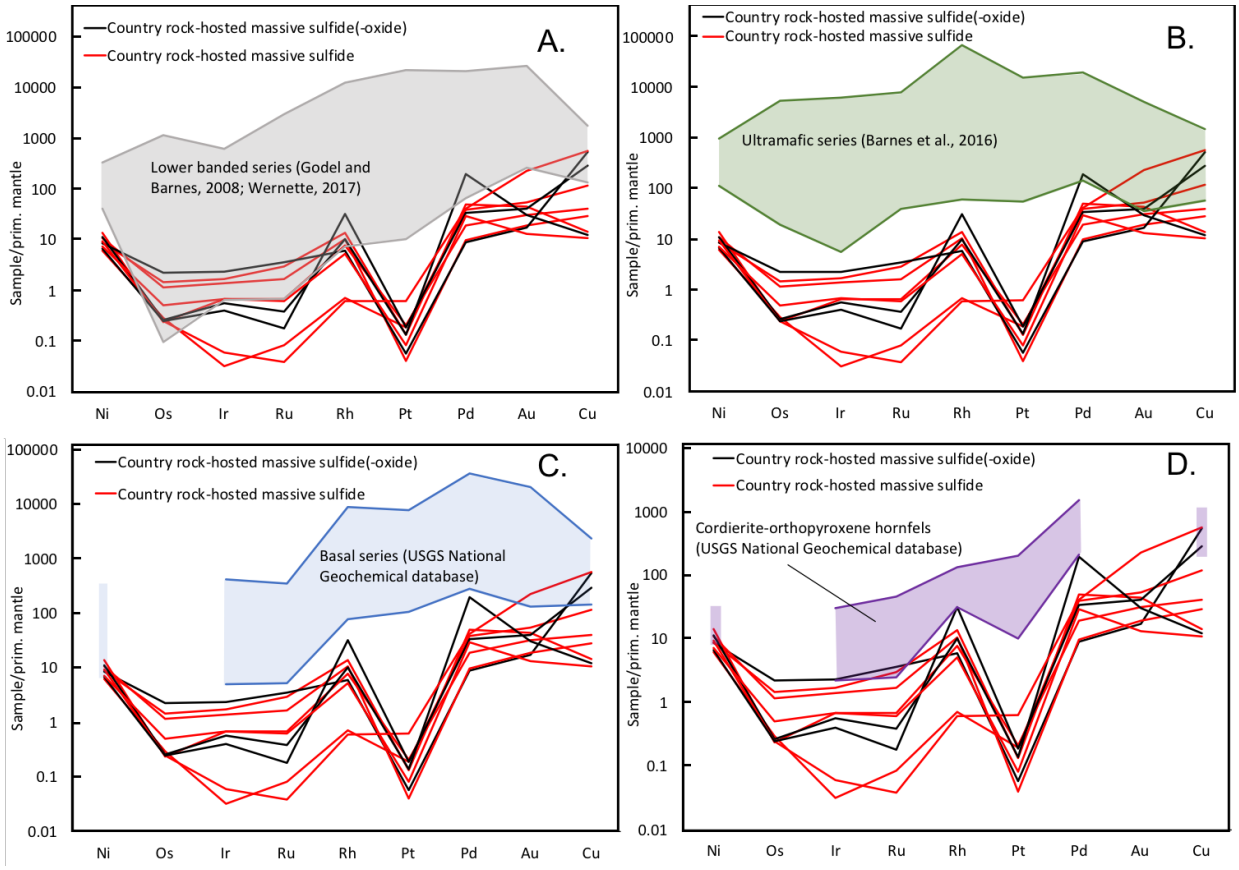

Figure 27: Primitive mantle-normalized PGE plots of massive sulfide data from this study (red) compared to PGE data from the banded series (A), the ultramafic series (B), and the basal series (C), and disseminated sulfides in the hornfels (D). All samples have been normalized to 100 % sulfide using the equation of Barnes and Lightfoot (2005).

Re-Os Isotopes

Re and Os concentrations and isotopic ratios for 8 samples of massive sulfide and massive sulfides-oxides beneath the Stillwater Complex are reported in Table 10. Re concentrations vary considerably from 1.6 to 164 ppb, whereas Os concentrations are more restricted, ranging from 0.16 to 12 ppb. $^{187}Re/^{188}Os$ ratios range from 40.3 to 508. $^{187}Os/^{188}Os$ ratios range from 1.94 to 23.7 and plot parallel to, although slightly above, a 2.709 Ga primitive mantle reference line. Calculated γOs (% deviation from chondrite at 2709 Ma, using parameters from Shirey and

Walker, 1998) from the massive sulfides-oxides range from -29 to +234, with an average γOs of +105. The samples are all characterized by extremely high Re/Os ratios from 6.8 to 25.9. Regression of the Re-Os isotopic data using the online IsoplotR software (Vermeesch, 2018) produces an isochron age of 2721 ± 13 Ma, which is within error of the whole-rock Rb-Sr age for the hornfels at 2730 Ma (± 30 Ma; Powell et al., 1969). Initial $^{187}Os/^{188}Os$ of the regression is 0.169, which translates to a γOs (2721) of +56.

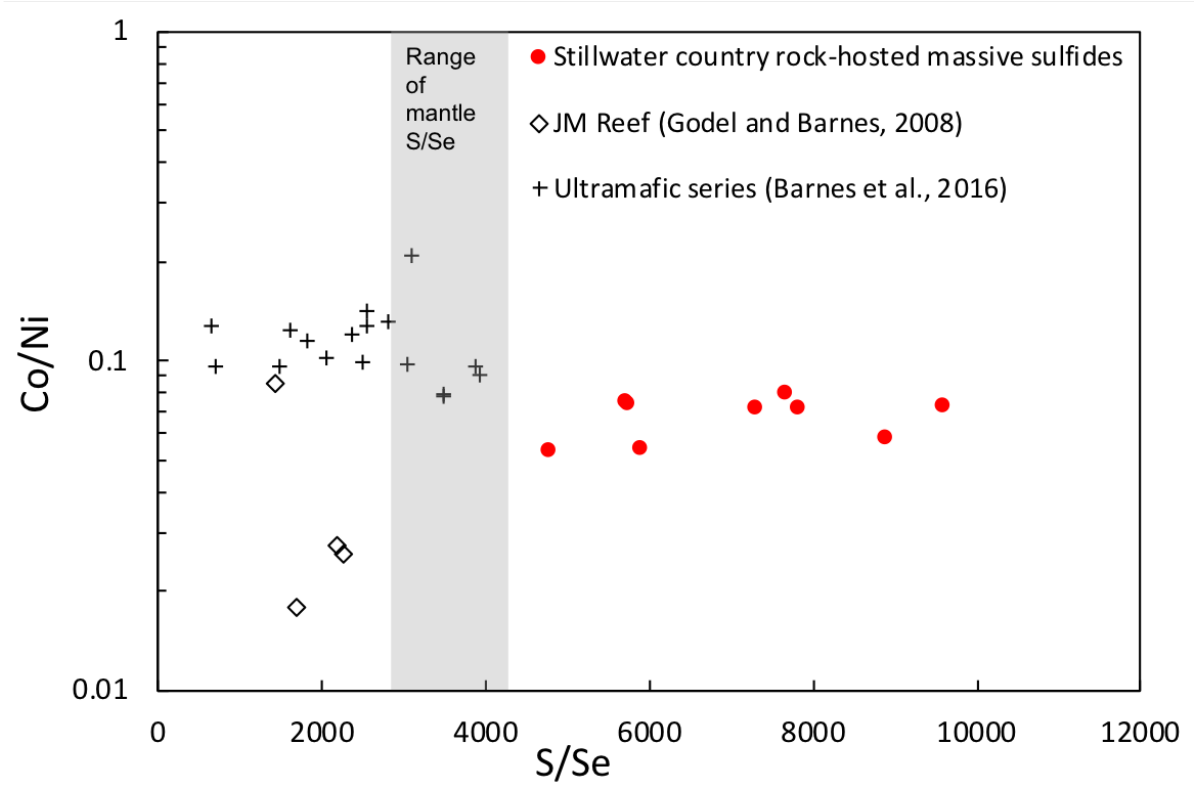

Figure 28: Ni/Co vs S/Se ratios for JM Reef, Ultramafic series, and country rock-hosted massive sulfide(-oxides). Range of mantle S/Se ratios taken from Eckstrand and Hulbert (1987).

Pb Isotopes

Results of Pb isotopic measurements of massive sulfides-oxides beneath the Stillwater Complex are listed in Table 11. Samples have $^{207}Pb/^{204}Pb$ ratios from 15.13 to 15.55. $^{206}Pb/^{204}Pb$ are more variable and range from 14.76 to 16.67 and cluster along a shallow linear trend in $^{207}Pb/^{204}Pb$ – $^{206}Pb/^{204}Pb$ space. The range of our data are similar to that for metamorphosed iron formation below the Stillwater Complex reported in Wooden et al. (1991), which have $^{207}Pb/^{204}Pb$ ratios from 15.03 to 15.49 and $^{206}Pb/^{204}Pb$ ratios from 15.03 to 17.19. Analyses of silicates from the hornfels have $^{207}Pb/^{204}Pb$ ratios from 15.6 to 17.26 and $^{206}Pb/^{204}Pb$ ratios from 16.38 to 25.18 (Wooden et al., 1981).

Table 10: Re and Os concentrations and isotopic ratios for samples from this study. γOs is calculated as percent deviation from chondrite at 2.709 Ga.

Sample	type	Re (ppb)	2σ	Os (ppb)	2σ	$^{187}Re/^{188}Os$	2σ	$^{187}Os/^{188}Os$	2σ	γOs (2.709 Ga)
368-313-275.5	Massive sulfide-oxide	1.661	0.05	0.1664	0.02	68.63	7.95	3.339	0.003	56
368-313-276	Massive sulfide-oxide	1.567	0.05	0.2320	0.02	40.29	3.35	1.937	0.001	-30
368-313-574.5	Massive sulfide-oxide	77.00	0.05	5.855	0.02	103.3	0.36	4.964	0.001	76
373-322-726.5	Massive sulfide-oxide	110.7	0.05	6.688	0.02	156.8	0.47	7.534	0.003	169
373-322-804	Massive sulfide-oxide	42.50	0.05	1.947	0.02	295.6	2.96	14.01	0.01	231
373-322-809	Massive sulfide	34.66	0.05	1.339	0.02	508.1	7.39	23.70	0.02	119
373-322-868	Massive sulfide-oxide	79.24	0.05	4.057	0.02	219.4	1.03	10.33	0.01	86
M17-1049.5	Massive sulfide	164.2	0.05	11.74	0.02	115.0	0.20	5.547	0.002	116

O Isotopes

Results of O isotopic analyses of magnetite from the massive sulfides-oxides are listed in Table 12. Samples have $\delta^{18}O$ values from 5.1 to 6.7 ‰. Samples of the Stillwater Iron Formation with granular magnetite (up to 5 mm in diameter) and intergranular pyrrhotite have $\delta^{18}O$ value of 5.3 to 6.3 ‰. For samples 355-3-484.3 and 355-3-516.3 from the iron formation, coexisting quartz had $\delta^{18}O$ values of 12.2 and 11.8, respectively. In order to compare the Stillwater magnetite data with known magmatic magnetite associated with mafic rock-hosted massive sulfide mineralization, we also performed five analyses of sulfide-hosted magnetite from the Voisey's Bay deposit in Labrador, Canada. The magnetite samples from Voisey's Bay range from 2.3 to 3.7 ‰.

Table 11: Pb isotopic ratios for samples from this study.

Sample	Sample type	$^{206}Pb/^{204}Pb$	2σ	$^{207}Pb/^{204}Pb$	2σ	$^{208}Pb/^{204}Pb$	2σ
368-313-275.5	Massive sulfide-oxide	16.29	0.004	15.55	0.003	35.02	0.008
368-313-276	Massive sulfide-oxide	16.26	0.003	15.52	0.003	36.58	0.008
368-313-574.5	Massive sulfide-oxide	14.89	0.003	15.20	0.003	34.44	0.007
370-316-622.5	Massive sulfide-oxide	15.91	0.001	15.38	0.002	35.52	0.006
373-322-726.5	Massive sulfide-oxide	16.55	0.007	15.40	0.005	35.96	0.01
373-322-804	Massive sulfide-oxide	16.09	0.01	15.41	0.005	36.27	0.005
373-322-809	Massive sulfide	15.47	0.004	15.33	0.004	35.8	0.01
373-322-868	Massive sulfide-oxide	16.11	0.006	15.38	0.006	35.0	0.01
384-326-1455	Massive sulfide-oxide	14.76	0.006	15.13	0.006	34.44	0.02
M17-979.5	Massive sulfide	16.33	0.003	15.39	0.002	34.95	0.005
M17-1049.5	Massive sulfide	14.86	0.002	15.18	0.002	34.54	0.006

Discussion

Effects of silicate-sulfide-oxide reactions

The observed mineral assemblage of cordierite, hypersthene, magnetite/ilmenite ± quartz ± plagioclase ± K-feldspar is consistent with the result of prograde metamorphism of Archean pelitic sedimentary rocks during intrusion of the Stillwater Complex (Barker, 1975; Labotka and Kath, 2001; Thomson, 2008). Barker (1975) suggested prograde metamorphic reactions in the greywacke and shale protoliths may have been:

$$2K_{1.9}(Mg_{2.1}\,Fe_{2.6})(Al_{0.4}Ti_{0.5})(Si_{5.4}Al_{2.6})O_{20}\,(OH)_4 + 2.1SiO_2 + 3.8H^+_{aq} =$$

(Bt) (Qtz)

$$1.5Al_3(Mg_{1.2}Fe_{0.8})(Si_5Al_1)O_{18} + 2.7(Mg_{0.9}Fe_{1.1})Si_2O_6 + FeTiO_3 + 3.8K^+ + 5.9H_2O \qquad (1)$$

(Crd) (Hyp) (Ilm)

This reaction would have produced a metamorphic fluid in the contact aureole around the intrusion. Sample DC-8 reported by Zientek and Ripley (1990) and Thomson (2008) appears to be a low-grade equivalent of the cordierite-orthopyroxene-bearing hornfels where pyrite is present rather than pyrrhotite. The presence of pyrite suggests that pyrrhotite in the hornfels may have been produced by a reaction similar to that given by Ripley (1981);

$$FeS_2 + 2H_2O + 2C = FeS + H_2S + CO_2 + CH_4 \qquad (2)$$

(Py) (Po)

Ripley (1981) proposed that this reaction occurred in pyrite- and organic carbon-rich Proterozoic sedimentary rocks of the bedded pyrrhotite unit from the Virginia Formation around the Duluth Complex to produce pyrrhotite and H_2S-bearing fluids. The probable conversion of pyrite to pyrrhotite in the contact aureole of the Stillwater Complex strongly suggests that the disseminated pyrrhotite found in the hornfels is not a product of leaked magmatic immiscible sulfide liquid, or hydrothermal fluids. The disseminated ilmenite that occurs in the hornfels is thought to represent the metamorphism of detrital Fe-Ti oxides. We also suggest that desulfidation reactions similar to that of reaction 2 drove the bulk sulfide compositions to higher Ni and Cu compositions, leading to the production of minor Ni-Cu sulfide phases. This is consistent with experimental phase relations in the Fe-Ni-S and Fe-Cu-S systems. Sulfides can display primary depositional features up to middle to upper greenschist facies metamorphism (McClay and Ellis, 1984), but the pyroxene hornfels facies metamorphism experienced by the massive sulfide-oxides below the Stillwater Complex appears to have destroyed any primary depositional features. The bedded pyrrhotite unit below the Duluth Complex, which also reached pyroxene hornfels facies metamorphism, commonly shows disrupted sulfide laminations as a result of metamorphism (Fig. 29). For comparison, an image of massive sulfide(-oxide) below the Stillwater Complex is also included, with what appears to be disrupted sulfide layers.

Sample 368-313-276 contains fayalite, ferrohypersthene, pyrrhotite, and magnetite, with trace chalcopyrite, hercynite, and ilmenite. Vaniman et al. (1980) reported a nearly identical mineral assemblage in fayalite-ferrohypersthene-bearing varieties of the Stillwater iron formation, with the principal difference being the presence of pyrite in the sulfide fraction. They suggest the presence of quartz-free and olivine-free varieties of the Stillwater Iron Formation was the result of an external fO_2 buffer imposed by igneous rock-derived fluids. However, Frost (1982) argued

that quartz-free iron formation simply represents a Si-poor protolith. Bonnichsen (1975) and French (1968) suggest fayalite and ferrohypersthene assemblages found in the Biwabik Iron Formation in Minnesota were the result of progressive contact metamorphism during intrusion of the Duluth Complex and thermal breakdown of lower temperature greenalite-minnesotaite assemblages. The fayalite-ferrohypersthene-bearing sample indicates the presences of ferruginous sediments and iron formation in close spatial proximity to the sulfide-oxide layers.

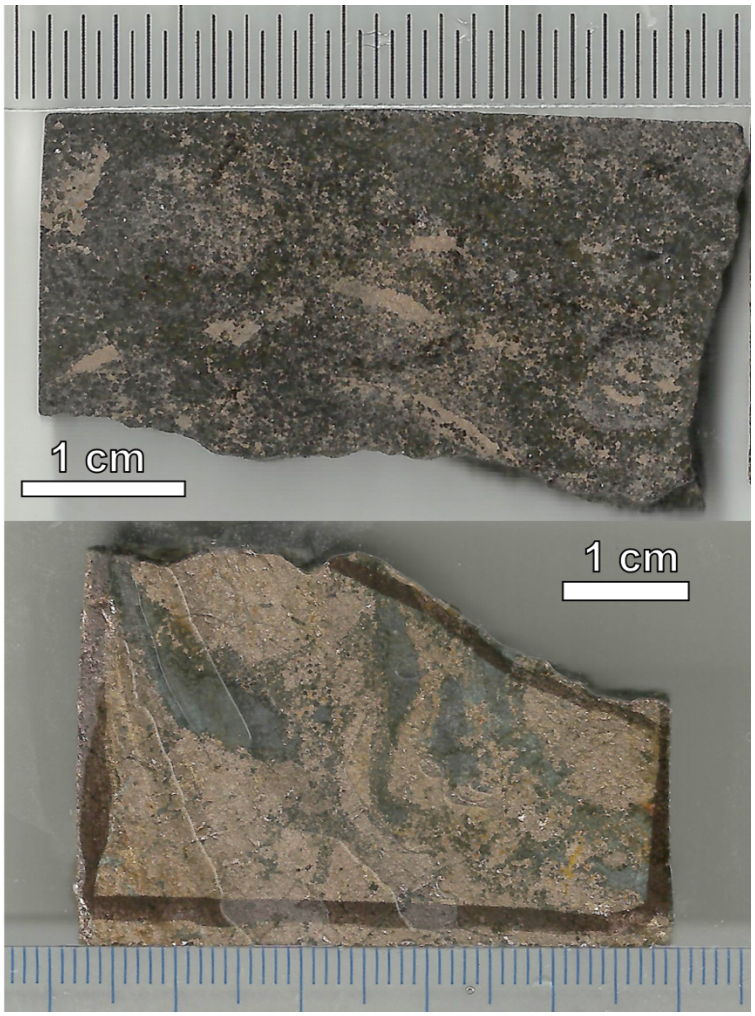

Figure 29: Comparison of disrupted bedded pyrrhotite unit below the Duluth Complex (top) and disrupted massive sulfide(-oxide) below the Stillwater Complex.

The spatial association between sulfides and oxides, as well as the sheer abundance of oxide cannot be dismissed. Experimental cotectic sulfide-oxide magmas can contain up to 25 to 30 wt. % magnetite, or up to ~ 23 to 28 volume % magnetite (Naldrett, 1969; Fonseca et al., 2008), assuming a simple Fe-S-O system. Many natural systems, however, usually contain far less magnetite than this, commonly as a result of O diffusion from the sulfide into the silicate (Naldrett, 1969; Naldrett et al., 2000; Fonseca et al., 2008; Dare et al., 2012). The 21 to 37 volume % magnetite we report for the massive sulfide-oxides correspond to ~ 23 to 40 wt. % magnetite in a FeS-Fe_3O_4 mixture. This is clearly too much magnetite to be the result of magmatic processes. We believe that these relationships argue against a magmatic origin for the massive sulfide-oxide layers.

Causes of contrasting element compositions between country rock-hosted and igneous-hosted sulfides

The mantle-normalized patterns of PGE tenors clearly show the differences between the country rock-hosted massive sulfides-oxides and the igneous-hosted sulfides of the Stillwater Complex (see Fig. 27A – 27C). Leaking of unfractionated igneous sulfide liquid cannot account for the extreme PGE depletions observed in the former, as the leaked sulfide liquids should have identical PGE tenors to the igneous-hosted sulfides. In addition, the very low Cu concentrations, pyrrhotite-rich assemblages, and high oxide components in most of the country rock-hosted massive sulfide-oxides precludes an origin from fractionated sulfide liquid.

Table 12: Oxygen isotope compositions of magnetite from selected samples from this study.

	Sample ID	Sample type	$\delta^{18}O$ (‰) magnetite	2σ	$\delta^{18}O$ (‰) quartz	2σ	Δ (Quartz-Magnetite)
below Stillwater Complex	373-322-726.5	Massive sulfide-oxide	6.1	0.03	-	-	-
	373-322-804	Massive sulfide-oxide	5.8	0.04	-	-	-
	373-322-809.5	Massive sulfide	6.7	0.02	-	-	-
	384-326-1455	Massive sulfide-oxide	6.6	0.02	-	-	-
	387-339-53.5	Massive sulfide-oxide	5.1	0.01	-	-	-
	370-316-918	Massive sulfide-oxide	6.7	0.02	-	-	-
	CC-2-1112.5	Iron formation	5.5	0.03	-	-	-
	355-3-484.3	Iron formation	6.3	0.03	12.2	0.03	5.9
	355-3-516.3	Iron formation	6.0	0.04	11.8	0.04	5.8
	355-3-493.9	Iron formation	5.3	0.02	-	-	-
Voisey's Bay - Ovoid	VB-1	Magnetite-bearing massive sulfide	3.5	0.01	-	-	-
	VB-2	Magnetite-bearing massive sulfide	3.7	0.01	-	-	-
	VB-3	Magnetite-bearing massive sulfide	2.3	0.03	-	-	-
	VB-4	Magnetite-bearing massive sulfide	3.4	0.01	-	-	-
	VB-5	Magnetite-bearing massive sulfide	3.7	0.03	-	-	-

S/Se, and to a lesser extent Co/Ni, ratios have been applied to a wide variety of mineral deposits to determine the source of these elements, and to track processes such as hydrothermal redistribution and crustal contamination. The mantle and unaltered mantle-derived rocks generally have S/Se ratios in the range of 2,850 – 4,350 (Eckstrand and Hulbert, 1987; McDonough and Sun, 1995; Hattori et al., 2002; and Lorand et al., 2003) depending on factors such as variations in R-factors (silicate/sulfide ratios), compatibility of Se over S during mantle melting events, exchange and dissolution processes, and sulfide liquid fractionation (Queffurus and Barnes, 2015; Smith et al., 2016). Yamamoto (1976) determined that crustal rocks have S/Se ratios <100,000. Smith et al. (2016) demonstrated that hydrothermal disturbance of

primary mantle-derived sulfides will tend to decrease S/Se ratios due to the enhanced solubility of S compared to Se in hydrothermal fluids. Additionally, these authors showed that elevated S/Se may be used to assess crustal contamination, especially when used in conjunction with more robust S isotope measurements.

As PGE concentrations ruled out the possibility of leaked magmatic sulfide liquids from the Stillwater Complex, the high S/Se ratios reported here for the country rock-hosted massive sulfides-oxides is consistent with a sedimentary origin. The very low S/Se ratios reported for the J-M Reef (Godel and Barnes, 2008) and the Ultramafic series (Barnes et al., 2016), as shown in Figure 28, are consistent with post-magmatic S-loss, possibly due to hydrothermal alteration. The aforementioned hydrothermal alteration features found in the country rock-hosted massive sulfides-oxides, which commonly contain serpentine carbonate veins and secondary tremolite-actinolite patches, imply the observed S/Se ratios may also be lower than the original ratios and should be taken as minimum values. Regardless of any post-depositional S loss, the high S/Se ratios of the hornfels-hosted sulfides-oxides are still consistent with a sedimentary origin.

Co/Ni ratios are routinely used to determine the origin of sulfides in sedimentary rocks. Data compilations in Bajwah et al. (1987) indicate hydrothermal pyrites have Co/Ni > 2, whereas sedimentary pyrite are in the range 0.01 to 2 (Gregory et al., 2015). Co/Ni ratios of the massive sulfides-oxides in this study are consistent with a sedimentary, as opposed to hydrothermal origin. However, Co/Ni ratios of magmatic sulfides are highly variable due to the selective partitioning of Ni into olivine, as well as pentlandite crystallization, and may overlap the range for sedimentary sulfides. Additionally, Gregory et al. (2015) found Paleo- and Neoarchean sedimentary pyrites have average Ni concentrations of ~2,700 and 620 ppm, respectively, with some pyrite containing nearly 1 wt. % Ni. Such high Ni concentrations are attributed to

increased weathering of mafic-ultramafic rocks during the Archean, as are elevated Co concentrations (up to 4000 ppm) in Archean sedimentary pyrites (Large et al., 2014; Gregory et al., 2015). An interpretation of this type is consistent with the premise that high-Ni rocks were present in the source areas for the sediments that produced the protoliths of the hornfels (Page and Zientek, 1985; Thomson, 2008). Gregory et al. (2015) noted other characteristic trace element ratios for sedimentary pyrite, including Cu/Ni (0.01 – 2), Te/Au (1 – 1000), and As/Au (>200). Data from massive sulfide(-oxides) below the Stillwater Complex are in agreement with these ratios.

Re-Os isotope tracer

Re-Os data from the country rock-hosted massive sulfides(-oxides) and the igneous rocks of the Stillwater Complex are compared in Fig. 30. No Re-Os analyses of other rocks within the contact metamorphic aureole were included in previous Re-Os isotope studies, with the exception of one iron formation sample (Horan et al., 2001). Lambert et al. (1989) and Lambert et al. (1994) reported $^{187}Re/^{188}Os$ between 0.321 and 2.15 for the Banded Series ($12 \leq \gamma Os$ (2.709 Ga, chond.) ≤ 34), 0.0116 and 102.3 for the Ultramafic Series ($-2 \leq \gamma Os \leq 34$), and a single value of 112 in the Basal Series ($\gamma Os = 136$). Horan et al. (2001) reported $^{187}Re/^{188}Os$ between 0.003 and 1.744 ($2 \leq \gamma Os \leq 17$) for peridotites from the Ultramafic Series and $^{187}Re/^{188}Os$ from 53.1 to 139 ($-690 \leq \gamma Os \leq 12000$) for the crosscutting sills and dikes. A single analysis of iron formation below the Complex had $^{187}Re/^{188}Os = 402$ and $\gamma Os = -9800$, indicating open system behavior sometime after 2.7 Ga (Horan et al., 2001), possibly due to hydrothermal alteration.

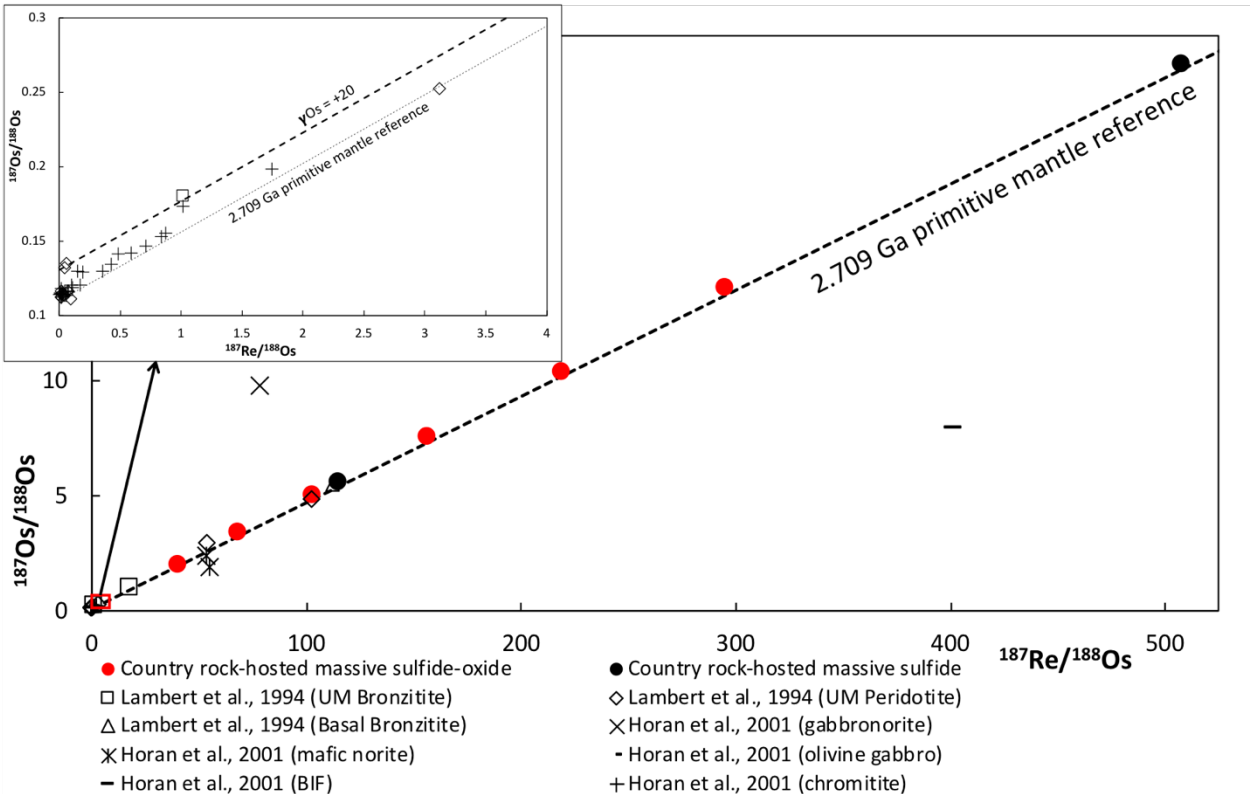

Figure 30: Plot of Re-Os isotopic compositions for country rock-hosted massive sulfides and sulfide-oxides with igneous rocks from the Stillwater Complex for comparison.

Marcantonio et al. (1993) reported Re-Os compositions from chromitites in the Ultramafic Series using the older $^{187}Os/^{186}Os$ vs $^{187}Re/^{186}Os$ notation. They found that in all the chromitites, which exception of the G chromitite, $^{187}Os/^{186}Os$ are essentially mantle-like, with low $^{187}Re/^{186}Os$. They suggested magmas that produced the Stillwater chromitites experienced little to no crustal contamination. Variations in the G chromitite were attributed to later hydrothermal disturbance and molybdenite precipitation.

Country rock-hosted massive sulfides-oxides in the hornfels have much higher $^{187}Re/^{188}Os$ than any samples of igneous-hosted sulfides from the Complex. Lambert et al. (1994) and Horan et al. (2001) suggested the relatively low $^{187}Re/^{188}Os$ and γOs from the igneous-hosted sulfides reflect magma mixing and/or crustal contamination of mafic magmas by Archean marine

sediments (Lambert et al., 1994; Horan et al., 2001), although the source of these sediments was never confirmed by Re-Os analyses.

Re-Os systematics have also been successfully applied to geochronology of carbonaceous sedimentary rocks with synsedimentary and diagenetic sulfides. High $^{187}Re/^{188}Os$ ratios are characteristic of Proterozoic and younger carbonaceous, sulfidic sediments, such as the Virginia Formation in Minnesota ($43 \leq {}^{187}Re/^{188}Os \leq 837$; Ripley et al., 2001), the Niutitang Formation in China ($673 \leq {}^{187}Re/^{188}Os \leq 813$; Mao et al., 2002), the Aralka Formation in Australia ($252 \leq {}^{187}Re/^{188}Os \leq 447$; Kendall et al., 2006), and the Exshaw Formation in Alberta ($189 \leq {}^{187}Re/^{188}Os \leq 392$; Selby and Creaser, 2005), in addition to many others. Re-Os analyses of carbonaceous and S-bearing metapelites in the Archean Joy Lake sequence in Minnesota (Yang et al., 2009) have also produced exceptionally high $^{187}Re/^{188}Os$ ratios (> 500), suggesting this characteristic feature also extends to Archean sedimentary rocks.

Re and Os are both soluble in oxidized fluids, but Re is consistently more mobile than Os (Pierson-Wickmann et al., 2002; Jaffe et al., 2002). Relatively anoxic, Archean oceans then would likely have been dominated by mafic, mantle-derived sources, with expected near-mantle-like $^{187}Os/^{188}Os_i$ and high $^{187}Re/^{188}Os$. Archean sedimentary sulfides would also then be expected to show these characteristics. Yang et al. (2009) have shown that slates from drillhole 26503 of the ~2.7 Ga Joy Lake sequence have extremely high $^{187}Re/^{188}Os$ ratios (>500) and slightly suprachondritic $^{187}Os/^{188}Os_i$ (0.16; γOs (2695 Ma) = +38.), which are consistent with this premise for Archean sedimentary sulfides.

Ripley et al. (2001) showed that the sulfide and organic fractions host nearly all the Re and Os in the Virginia Formation in Minnesota, which plots along a 1.85 Ga chondritic reference line. They suggest this may have been due to seawater leaching Re and Os from mafic rocks in the

backarc Animikie Basin characterized by mantle-like $^{187}Os/^{188}Os_i$. Again, preferential leaching of Re over Os could have produced the simultaneously high $^{187}Re/^{188}Os$ ratios and near-chondritic $^{187}Os/^{188}Os_i$ in those samples.

Because the country rock-hosted massive sulfides-oxides have both higher γOs and $^{187}Re/^{188}Os$ than igneous-hosted sulfides from the Stillwater Complex, it is impossible for the igneous-hosted sulfides to have produced Os isotopic compositions like those in the country rock-hosted massive sulfides simply by leaking of sulfide liquid or leaking combined with sulfide liquid fractionation. Instead, the high $^{187}Re/^{188}Os$ and slightly radiogenic $^{187}Os/^{188}Os_i$ of the sulfides are consistent with Archean sedimentary sulfides, followed by rehomogenization of the Re-Os systematics at 2.7 Ga by contact metamorphism associated with intrusion of the Stillwater Complex. Experimental (Brenan et al., 2000) and case studies (Lambert et al., 2000) of the Re-Os system has suggested that in as little as 0.5 million years, the Re-Os system can be re-homogenized to new $^{187}Os/^{188}Os_i$ at 500°C. Labotka (1985) estimated maximum temperatures for the Stillwater contact metamorphic aureole at 825°C, which are clearly sufficient to overcome the closure temperature of the Re-Os system.

To have a slightly higher than mantle-like $^{187}Os/^{188}Os_i$ after metamorphism at ~2.7 Ga, a mantle-like sulfide protolith must have previously undergone radioactive decay. Rocks with high $^{187}Re/^{188}Os$ ratios (like the massive sulfides) will produce extremely high $^{187}Os/^{188}Os$ ratios as a result of prolonged decay. When the Os composition is able to homogenize, the resulting $^{187}Os/^{188}Os_i$ will be more radiogenic than the mantle, provided Re originally concentrated in the sulfide. The longer that the first stage of Re decay proceeded, the higher the $^{187}Os/^{188}Os_i$ will be for the second stage of Re decay.

Although some basalts (notably OIBs), when contaminated by crustal material with high Re/Os ratios, can have high $^{187}Re/^{188}Os$ (up to 5,000) (Shirey and Walker, 1998), there is no geologic or geochemical evidence to suggest the Stillwater Complex was emplaced in an OIB environment. In most cases, however, mantle sources and uncontaminated, mantle-derived rocks will have both low $^{187}Re/^{188}Os$ and near-chondritic $^{187}Os/^{188}Os_i$ ($\gamma Os < +20$) (Shirey and Walker 1998), unlike the massive sulfides (-oxides) reported here.

Pb isotope tracer

Pb isotope data for the country rock-hosted massive sulfides-oxides are shown in Fig. 31, along with analyses of rocks from the Stillwater Complex and the contact metamorphic aureole. Pb isotopic analyses of both the igneous rocks in the Complex (Manhes et al., 1980; McCallum et al., 1999) and contact metamorphic rocks beneath the Complex (Wooden et al., 1991) have very similar ranges of Pb isotope ratios. Previous interpretations have used a variety of Pb growth models to explain measured isotopic trends.

Manhes et al. (1980) regressed Pb data of igneous silicates from the Stillwater Complex and observed that the initial Pb isotopic composition plotted at the intersection of a 2.7 Ga reference isochron with a single-stage Pb growth curve with μ ($^{238}U/^{204}Pb$) = 8.53. Using the corresponding initial $^{206}Pb/^{204}Pb$, calculated second stage μ values for samples from Manhes et al. (1980) range from ~4 to 12.5, with a single value near 40, and may represent analyses of extremely U-rich phases. McCallum et al. (1999) leached and analyzed sulfides from the Stillwater Complex and found they plot along a 1.7 Ga mixing line, between a sulfide Pb component at 2.7 Ga and a crustal Pb component at 1.7 Ga. All data were interpreted relative to the two-stage Stacey and Kramers (1975) model for average continental crust, and they

concluded that because the sulfide samples with the most radiogenic Pb compositions were also the samples with the most abundant secondary hydrous alteration, the 1.7 Ga mixing was related to hydrothermal circulation due to regional metamorphism during the final assembly of the Wyoming craton. Wooden et al. (1991) analyzed hornfels, as well as metamorphosed iron formation, below the Stillwater Complex and determined that the Pb isotopic compositions of the metamorphic rocks could also be explained by a two-stage Pb growth curve, similar to a Stacey-Kramers type model.

In Figure 31 we show Pb data relative to both the single stage mantle Pb growth curve of Manhes et al. 1980 and a two-stage growth curve for crustal rocks. Data for the hornfels and igneous silicates plot near a 2.7 Ga reference isochron with variable μ values, whereas igneous-hosted sulfides plot along a 1.7 Ga mixing line between mantle sulfide Pb at 2.7 Ga and crustal Pb at 1.7 Ga. Notably, the country rock-hosted massive sulfides (-oxides) reported here also plot along a 2.7 Ga reference isochron, at significantly lower μ values (1.3 to 4.6) than the silicate hornfels reported in Wooden et al. (1991) (μ = 4.2 to 21.1). Wooden et al. (1991) also reported analyses of metamorphosed iron formation below the Stillwater Complex, which also have lower μ values, similar to the country rock-hosted massive sulfides (-oxides). This is consistent with available partitioning data (Bea et al., 1994; Wheeler et al., 2006) that shows U will partition into silicates to produce higher $^{238}U/^{204}Pb$ ratios, whereas Pb will partition into sulfide to produce lower $^{238}U/^{204}Pb$.

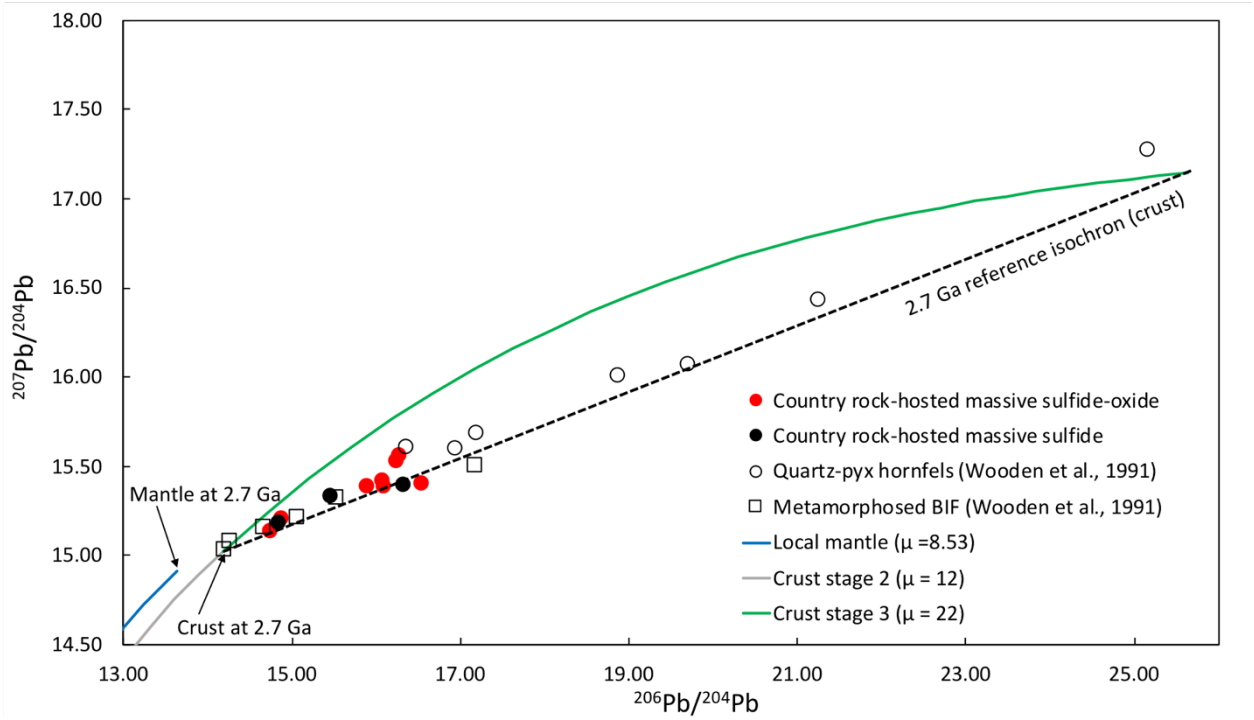

Figure 31: $^{207}Pb/^{204}Pb$ vs $^{206}Pb/^{204}Pb$ variations for Stillwater igneous silicates (Manhes et al. 1980), igneous-hosted sulfides (McCallum et al. 1999), hornfels silicates (Wooden et al. 1991), and massive sulfides in the hornfels (this study). Samples are shown in relation to a single-stage (mantle) growth curve evolving to 2.7 Ga (μ = 8.53) and a two-stage growth curve for local country rocks. The two-stage model evolves from 4.558 Ga to 3.7 Ga with μ_1 = 7.2 and from 3.7 Ga to 2.7 Ga with μ_2=12.

O isotope tracer

Dunn (1986) performed oxygen isotope analyses of plagioclase, orthopyroxene, and whole rocks from the Ultramafic and Banded Series. The Ultramafic Series had average $\delta^{18}O$ of 6.1 ‰ in plagioclase, 6.0 ‰ in orthopyroxene, and 6.4 ‰ in the whole rock. The Banded Series had average $\delta^{18}O$ of 6.5 ‰ in plagioclase, 5.9 ‰ in orthopyroxene, and 6.3 ‰ in the whole rock. Average $\delta^{18}O$ of the parental melt was calculated to be 5.9 ‰ and is extremely homogeneous from the base of the Ultramafic Series through the Upper Banded Series.

In terms of $\delta^{18}O$, magnetite crystallized from mafic melts are consistently lighter than the associated plagioclase, pyroxenes, and whole rocks. Lee and Ripley (1996) showed that the average $\delta^{18}O$ of the South Kawishwi intrusion from the Duluth Complex in Minnesota was around 6.3 ‰, whereas magnetite reached as low as 2.3 ‰ (Ripley et al., 2008). Empirical equations of melt-oxide fractionations were determined from the Kiglapait Intrusion (Kalamarides, 1986), and $\Delta^{18}O_{(melt\text{-}oxide)}$ ranged from +3.1 to +1.7 ‰ (indicating an isotopically heavier melt phase) over the temperature range of 900 to 1200 °C. Calculation of $\Delta^{18}O_{(melt\text{-}oxide)}$ from Zheng and Zhao (2003) are quite similar and range from +2.3 to +1.5 ‰ over the range of 900 to 1200 °C. Additionally, our analyses of massive sulfide-hosted magnetite from Voisey's Bay have $\delta^{18}O$ values of 2.3 to 3.7 ‰. Ripley et al., (2000) demonstrated that most of the troctolites and gabbros from Voisey's Bay range from 5.5 to 6.7 ‰. This corresponds to median $\Delta_{(melt\text{-}oxide)}$ of ~ 2.7 ‰ and demonstrates that magmatic magnetite will be lighter than the silicate melt from which it was derived, even where it has become entrained in sulfide melts. Assuming an average $\delta^{18}O$ of 5.9 ‰ for the Stillwater Complex (Dunn, 1986), associated magmatic magnetite should have $\delta^{18}O$ of approximately 3.2 ‰. In contrast, the heavier $\delta^{18}O$ of 5.1 to 6.7 ‰ in the massive sulfide-oxides could not have been produced from a silicate magma with $\delta^{18}O$ of 5.9 ‰, such as Stillwater, precluding an igneous origin for magnetite in the massive sulfide-oxides. Instead, the oxygen isotope data are similar to the samples of iron formation below the Stillwater Complex, which have values of 5.3 to 6.3 ‰. Analyses of quartz-magnetite pairs from samples 355-3-484.3 and 355-3-516.3 have $\Delta^{18}O_{(quartz\text{-}magnetite)}$ of 5.9 and 5.8 ‰, respectively. These fractionation factors correspond to temperatures of 746°C and 755°C, respectively (Clayton and Kieffer, 1991).

Possibility of massive sulfides-oxides as contaminants of the Stillwater magma

Horan et al. (2001) previously predicted there should be country rocks near the Stillwater Complex which are moderately radiogenic in terms of Os, with $^{187}Os/^{188}Os_i < \sim 1$, if Os isotopic compositions of the Stillwater peridotites were produced via crustal contamination. Massive sulfides analyzed in this study have average $^{187}Os/^{188}Os_i$ of 0.17 and are clearly more radiogenic than a chondritic source at 2.709 Ga ($^{187}Os/^{188}Os_i = 0.1085$). If the country rock-hosted massive sulfides analyzed in this study are a match for potential crustal contaminants (in regard to their isotopic compositions) for the Stillwater Complex, then they are consistent with having formed prior to the emplacement of the Stillwater Complex, possibly by sedimentary origins. Results of mixing models of hypothetical source magmas and the massive sulfides-oxides from the hornfels are presented in Figure 32. The mantle melt endmember is assumed to have γOs (2709 Ma) = 1.6 (primitive upper mantle; Shirey and Walker, 1998) and a range of common Os concentrations (0.01 – 0.5 ppb; based on modeling from Barnes and Lightfoot, 2005). The massive sulfide endmember was taken to have γOs (2709) = 105 (average of our dataset) and common Os = 0.2 ppb (average massive sulfide concentration is ~ 2 ppb common Os, and assuming 10 percent sulfide due to silicate dilution).

For primary mantle melt endmembers with 0.1 ppb common Os or less (< 10 % mantle partial melt; Barnes and Lightfoot, 2005), most of the reported Os isotopic compositions (first three quartiles) from Lambert et al. (1994) and Horan et al. (2001) can be produced by 0.5 to 4% bulk mixing with the country rock-hosted massive sulfides-oxides from the hornfels. For a primary mantle melt with 0.5 ppb common Os (~25% partial mantle melting, Barnes and Lightfoot, 2005), 16% or less bulk contamination can explain the first three quartiles of published Os compositions from the Stillwater Complex. If selective contamination (partial melting,

metamorphic fluids, etc.), rather than bulk contamination, is considered, calculations suggest only about 2 to 8 % of the Os would have been crustally-derived.

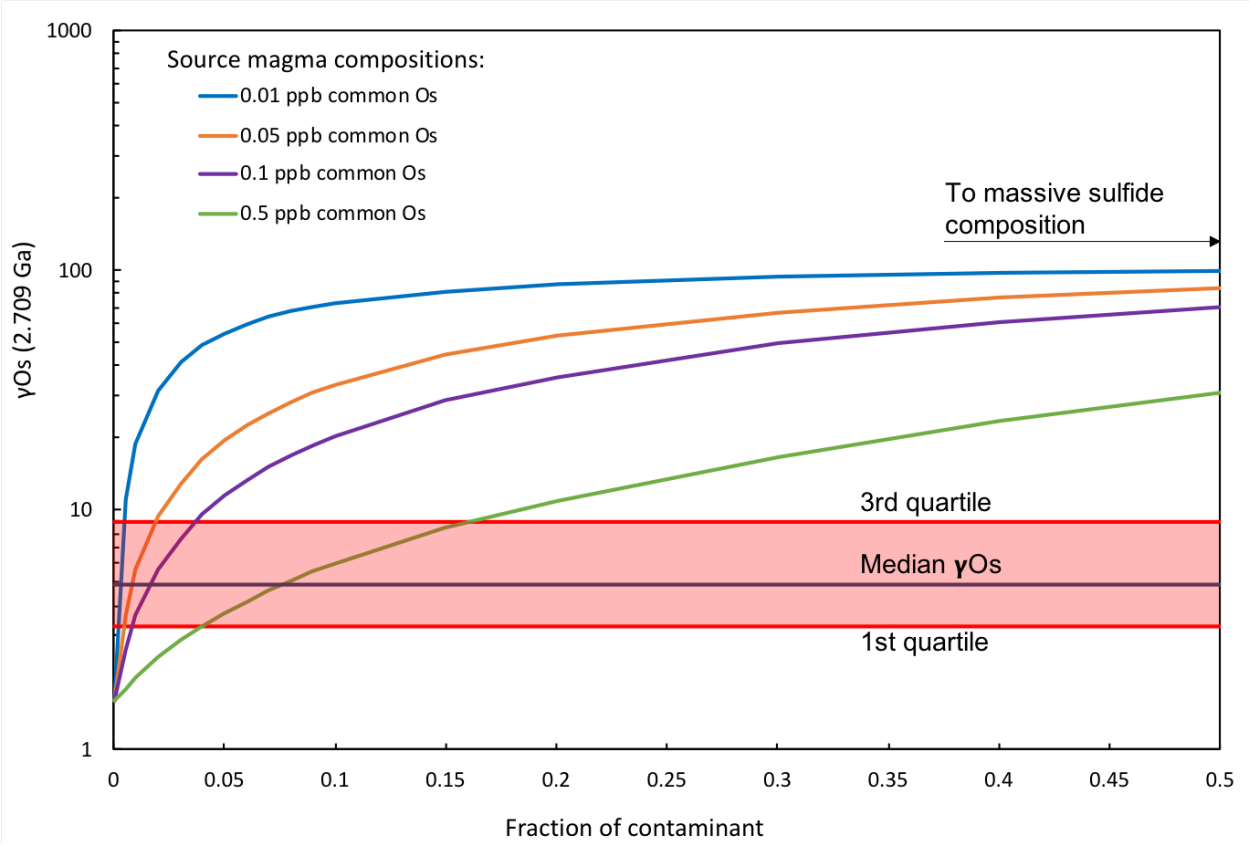

Figure 32: Various mixing models for potential Stillwater parent magmas with country rock-hosted massive sulfides from this study. γOs (2709 Ma) of the mixed magmas are shown as solid curves. Median Stillwater γOs = 4.9 and is shown bracketed by bounds of the first and third quartiles of the γOs from Horan et al. (2001) and Lambert et al. (1994).

It is possible to estimate mixing proportions for the igneous-hosted sulfides using refined Pb growth curves presented previously. Similar to the Re-Os mixing calculations, if Pb isotopic compositions of the Stillwater Complex can be explained by mixing between a mantle source and the country rock-hosted massive sulfides-oxides, then the massive sulfides-oxides may have

served as contaminants to the Complex. Because igneous-hosted sulfides appear to plot along a mixing line due to low-T hydrothermal alteration in the Proterozoic (McCallum et al., 1999), we assume the least radiogenic sulfide represents sulfide that was undisturbed at 1.7 Ga, retaining its composition from 2.7 Ga. The least radiogenic sulfide plots on the mixing line in Figure 33, between "mantle at 2.7 Ga" and "crust at 2.7 Ga," and represents from 5 to 10% bulk mixing, which is only slightly higher than previous Pb isotopic measurements of the hornfels and Stillwater cumulates, which were interpreted to reflect 3 to 7 % bulk contamination of the Stillwater magma(s) (Wooden et al., 1991). If selective assimilation models are considered, our mixing models suggest ~ 60 to 75% of Pb being of crustal derivation. Regardless of the mixing mechanism, these calculations show the country rock-hosted massive sulfides were appropriate contaminants to the Complex and may have predated igneous activity. This is also consistent with contamination of the Basal Series by massive sulfide-bearing sedimentary rocks, as strongly indicated by MIF fractionation observed in the Basal Series (Ripley et al., 2017).

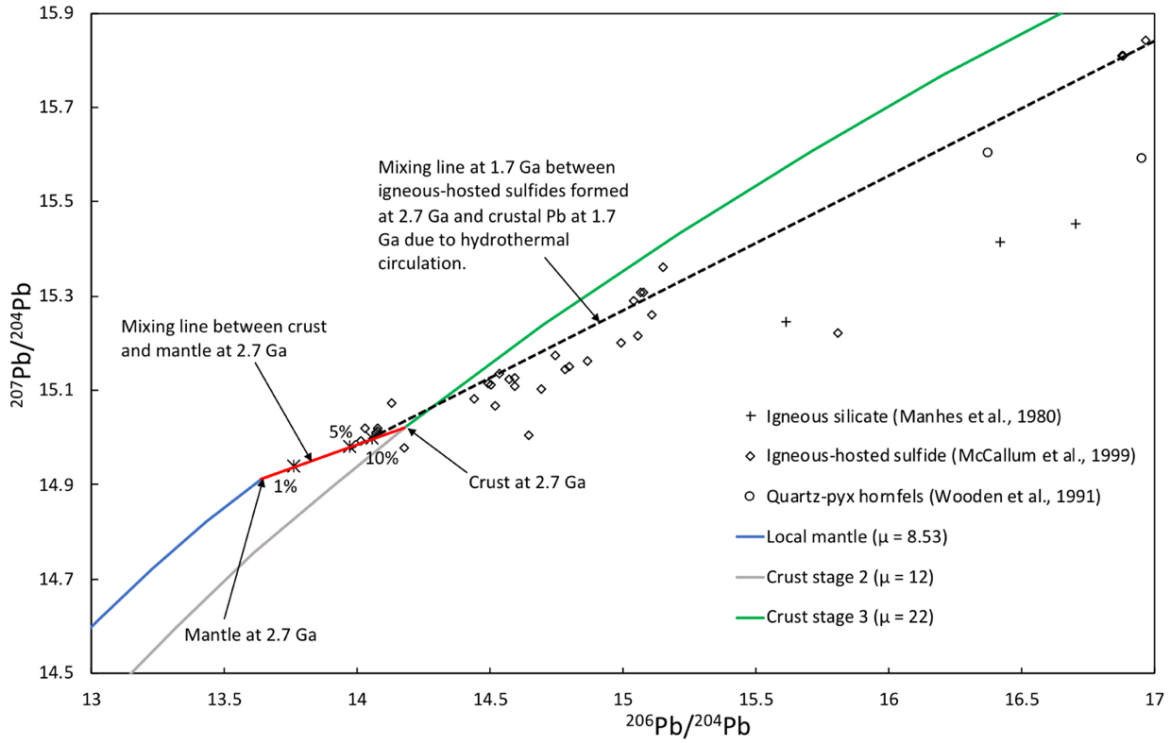

Figure 33: Pb-Pb mixing model for igneous-hosted sulfides in the Stillwater Complex, using refined parameters for mantle and crustal growth curves based on data from McCallum et al. (1999); Manhes et al. (1980); Mueller and Wooden (1988); Wooden et al. (1991); and data from this study. Crust is assumed to have 30 ppm Pb and mantle melt is assumed to have 1 ppm Pb (Wooden et al. 1991). Tick marks are shown on the red mixing line for 1%, 5%, and 10% bulk mixing between mantle and crust at 2.7 Ga. See text for other details.

Summary and Conclusions

Multiple S isotope analyses from Ripley et al. (2017) suggested three possible mechanisms for massive sulfide-oxide deposition: 1) leaking of magmatic sulfide liquid from the basal or ultramafic series (with or without sulfide liquid fractionation), 2) deposition of Archean sedimentary sulfides, or 3) deposition of seafloor hydrothermal exhalations. PGE trends in all of the country rock-hosted massive sulfide(-oxides) are depleted in PGEs relative to Ni and Cu and depleted by 1 to 3 orders of magnitude relative to the primitive mantle reference, whereas igneous-hosted sulfides are either more enriched in PGEs or near the same concentration as the

primitive mantle reference. Leaking (or combined leaking and fractionation) of sulfide liquid into the country rocks cannot account for these differences. These characteristics suggest the country rock-hosted massive sulfide-oxides are not related to igneous-hosted sulfides. Additionally, high S/Se ratios, in conjunction with non-zero $\Delta^{33}S$ compositions (Ripley et al., 2017), suggest the sulfides are more similar to Archean sedimentary sulfides (Fig. 34). Other trace element ratios (Co/Ni, Cu/Ni, Te/Au, and As/Au) are consistent with those measured in known sedimentary sulfides.

Re-Os isotopic compositions of the country rock-hosted massive sulfide-oxides show extremely high present day $^{187}Re/^{188}Os$ and elevated γOs values compared to the Basal, Ultramafic, and Banded series. These features are consistent with sedimentary sulfide accumulation and Archean seawater leaching of near-chondritic Re and Os sources. Elevated γOs values are the result of Re decay from deposition until intrusion of the Stillwater magmas. Contact metamorphism homogenized the Os isotopic ratios of the massive sulfides-oxides, with production of a slightly higher initial Os isotopic composition. Additionally, mixing calculations suggest that the massive sulfides-oxides may have been entrained in the intruding magmas, possibly inducing sulfide saturation.

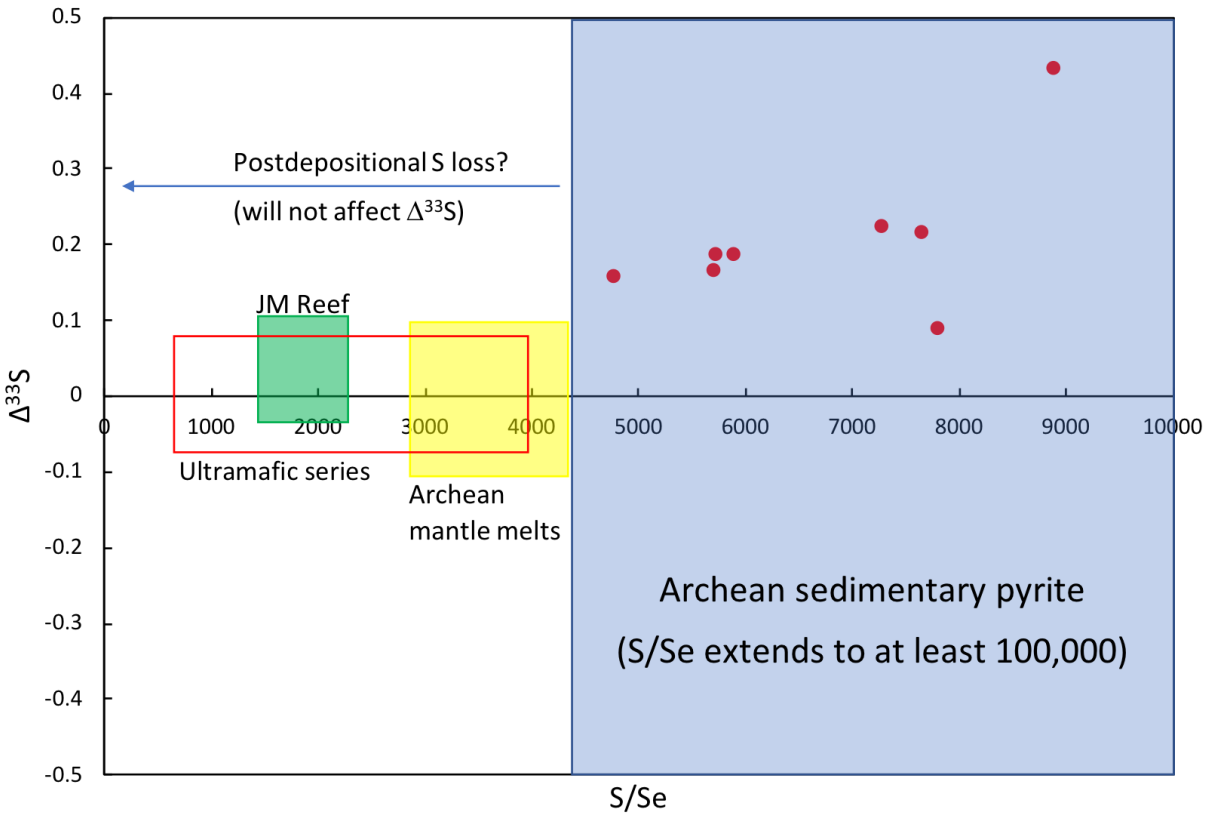

Figure 34: $\Delta^{33}S$ vs S/Se for country rock-hosted massive sulfides near the Stillwater Complex (red filled circles). S/Se ratios are those reported in this paper, and corresponding $\Delta^{33}S$ values were reported in Ripley et al. (2017). Fields are included for the JM Reef, Ultramafic series, Archean mantle melts, and Archean sedimentary pyrite (fields compiled from Godel and Barnes 2008; Gregory et al. 2015; Barnes et al. 2016; Smith et al. 2016; Ripley et al. 2017).

Pb isotopic results are also indicative of a non-magmatic origin for the massive sulfides-oxides. Samples from this study plot at the less radiogenic end of a 2.7 Ga $^{207}Pb/^{204}Pb$-$^{206}Pb/^{204}Pb$ isochron for local country rocks, whereas sulfides from the intrusion plot along a 1.7 Ga mixing line between the magma at 2.7 Ga and crust at 1.7 Ga. Minor deviation of the massive sulfide(-oxide) samples from the 2.7 Ga isochron is likely related to hydrothermal disturbance at 1.7 Ga. Any radiogenic Pb in the sulfide-oxide samples is suggested to be in microinclusions in the sulfide, or in the oxide fraction, as U partitions weakly into sulfide (Wheeler et al., 2006). Previous Pb isotope analyses of the hornfels silicates plot on the more

radiogenic end of the 2.7 Ga isochron (Wooden et al., 1991) due to U partitioning into silicates. Pb isotope mixing calculations also suggest the massive sulfides were contaminants to the Stillwater magmas. Although contamination of Stillwater magmas by radiogenic country rocks was previously suggested from Sm-Nd, Pb, and Re-Os analyses of the magmas (Wooden et al., 1991; Lambert et al., 1989; Lambert et al., 1994; Horan et al., 2001), these appropriate contaminants previously remained elusive.

O isotope analyses of magnetite from massive sulfide-oxides are similar to analyses of the Stillwater iron formation analyzed in this study. The presence of fayalite-ferrohypersthene in at least one massive sulfide-oxide sample also suggests the massive sulfide-oxides may be related to hydrothermal seafloor exhalations, which are thought to be responsible for deposition of iron formations (Bekker et al., 2010), especially Archean iron formations. More importantly, a magma with $\delta^{18}O$ of 5.9 ‰, such as Stillwater, could not have produced magmatic magnetite with $\delta^{18}O$ of 5.1 to 6.7 ‰.

Maximum metamorphic temperature estimates (825 ° C; Labotka, 1985) suggest that it was impossible for the sedimentary-hosted massive sulfides-oxides from Stillwater to have melted, but contact metamorphism was more than capable of producing S-rich metamorphic fluids by dehydration reactions or thermally converting pyrite to pyrrhotite plus a S-rich volatile phase. McClay and Ellis (1984) found that pyrites from a variety of mining districts may display relict depositional features up to greenschist facies conditions. At higher temperatures, however, recrystallization and pyrrhotite formation appeared to destroy any primary textural features, as well as evidence of deformation. Similarly, any sulfide textures indicative of a sedimentary origin in the country rock-hosted massive sulfides beneath the Stillwater Complex, such as framboids, patches and laminations of microcrystalline euhedra, and rounded and elongate

nodules (Large et al., 2014) have likely been destroyed by pyroxene hornfels facies metamorphic temperatures and deformation associated with emplacement of the Stillwater Complex.

Experimental phase diagrams of the low temperature portions of the Fe-Ni-S, and Fe-Cu-S systems (Kullerud et al., 1969; Cabri et al., 1976; Naldrett, 2004) indicate that the assemblage hexagonal-monoclinic pyrrhotite, chalcopyrite, pentlandite, and cubanite are stable during subsolidus cooling of sulfides, and the assemblage is compositionally controlled. This suggests that the assemblage, however, is not restricted to magmatic sulfide liquids, but may result from subsolidus cooling of any sulfide with appropriate temperatures and compositions, such as Ni-Cu bearing pyrite. Desulfidation of Ni-Cu-bearing sedimentary pyrite in the presence of metamorphic fluids driven off during prograde metamorphism can (based on experimental phase diagrams), produce coexisting hexagonal and monoclinic pyrrhotite, pentlandite, and chalcopyrite, and is consistent with the overwhelming pyrrhotite abundance compared to only minor chalcopyrite and pentlandite.

This model does require some amount of Ni to be contained in solid solution within the sedimentary pyrite (see phase diagram in Fig. 35). Even a small amount of Ni in pyrite during desulfidation would be sufficient to drive the composition further away from the Fe-S binary, where hexagonal and monoclinic pyrrhotite are located. At higher temperatures, after desulfidation, the Ni would be contained in an MSS-like composition, but upon cooling, pentlandite would exsolve from pyrrhotite in the three-phase field of hexagonal pyrrhotite, monoclinic pyrrhotite, and pentlandite.

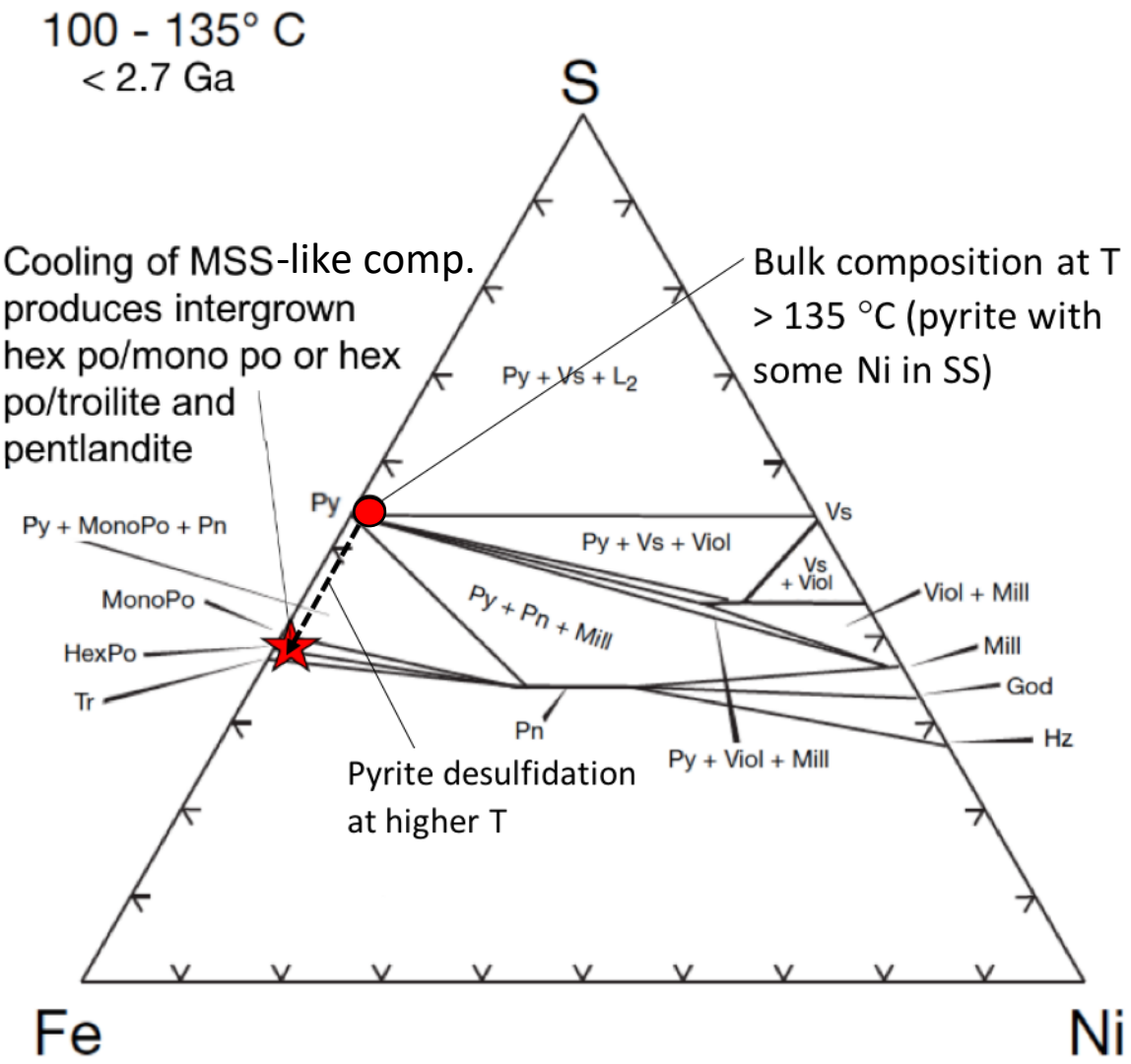

Figure 35: Low temperature phase relationships in the Fe-Ni-S system as applied to the country rock-hosted massive sulfides below the Stillwater complex. Desulfidation of Ni-bearing pyrite (red circle) at higher temperature causes the composition to shift to more Fe- and slightly more Ni-rich compositions (red star). Cooling of the massive sulfides at this new composition is dominated by hexagonal and monoclinic pyrrhotite (or hexagonal pyrrhotite and troilite) and produces minor pentlandite upon cooling. Phase diagram modified from Kullerud et al. (1969) and Barnes and Lightfoot (2005).

Calculations of pyrite desulfidation reactions that produce pyrrhotite show that a bulk concentration of up to 1.4 wt % Ni (assuming 1 wt % or 10,000 ppm Ni in Archean pyrite) can be produced. The relatively high Ni concentrations observed in the country rock-hosted massive

sulfides (up to 2.7 Wt % Ni in 100 % sulfide) would require initial sedimentary pyrite concentrations of ~ 2 wt. % Ni (Fig. 36). Sedimentary pyrite is rarely characterized by Ni concentrations this high. However, significant Ni has also been documented in the organic fraction of many black shales. Lewan and Maynard (1982) reported Ni concentrations of bitumen in excess of 1,000 ppm. Our documentation of graphite in some samples also suggests some of the Ni now contained in sulfide may have come from organic matter.

We believe that available evidence indicates that the sulfide mineralization in the contact aureole of the Stillwater Complex formed as part of the sedimentary sequence. The sulfide assemblages with low magnetite percentage represent sedimentary pyrite that formed as a result of bacterial sulfate reduction in a marine environment, with minor detrital oxide input. The oxide-rich assemblages may represent deposition of exhalative iron mineralization, whereas the sulfides may have formed in anoxic environments on the seafloor. Alternatively, the massive sulfide-oxide assemblages may represent deposition from Fe-rich exhalative solutions near the seafloor. In this respect they bear similarity to sulfide-bearing exhalative iron formations, consistent with the presence of ferrohypersthene and fayalite in some samples. Additionally, metamorphism may have driven production of Fe-oxides from Fe-rich silicates. Metamorphism and deformation related to emplacement of the Stillwater Complex may have led to disruption and potential mixing of the distinct assemblages.

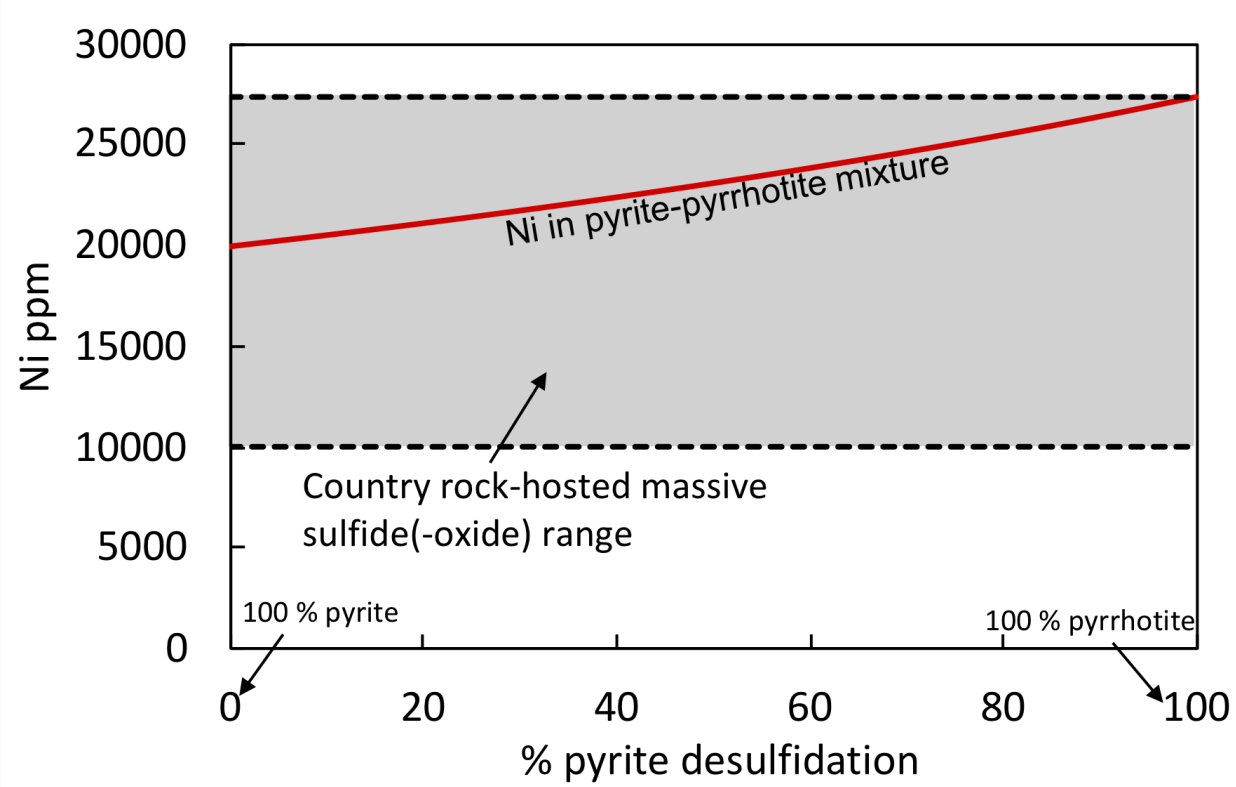

Figure 36: Calculation of pyrite desulfidation to produce pyrrhotite. The red curve tracks progressive desulfidation in the bulk sulfide mixture, from pure pyrite at 0 % to pure pyrrhotite at 100 % desulfidation. Starting Ni is assumed to be contained in sulfide phases only, although some Ni is likely to be in oxide or organic fractions. To produce pyrrhotite with roughly 2.7 wt % Ni, the initial pyrite must have initially contained nearly 2 wt % Ni.

Chapter 3: Ni and Cu Isotope Variations of Country Rock-Hosted Massive Sulfides from the Midcontinent Rift and below the Stillwater Complex, Montana

Introduction

Cu isotope studies of magmatic Ni-Cu-PGE deposits have been focused on conduit- and sheet-style intrusions of the North American Midcontinent Rift System (MRS) (Ripley et al., 2015; Asp, 2016), the Noril'sk district in Russia (Malitch et al., 2014), and the Tulaergen deposit in China (Zhao et al., 2017). Despite interesting results and applications to exploration, this initial work has yet to determine the underlying reasons for variable Cu isotope signatures and trends in magmatic Ni-Cu-PGE sulfide deposits. Assessment of this variability may help to resolve the importance of externally-derived metals on the overall metal budget of mineralized intrusions.

Ripley et al. (2015) present an intriguing problem regarding the disparity of Cu isotope analyses of magmatic sulfide deposits in conduit- and sheet-style intrusions of the Midcontinent Rift System (Fig. 37). Conduit-style intrusions have δ^{65}Cu values from 0.5 to 2.0 ‰, whereas sheet-style intrusions like the Partridge River Intrusion of the Duluth Complex have δ^{65}Cu values from -0.5 to 0.5 ‰. There are a number of other key differences between the conduit- and sheet-style intrusions. Conduit-style intrusions have roughly dike-like geometries (Ripley, 2014); are associated with picritic parental magmas; host disseminated, semi-massive, and massive sulfides; have Cu/Ni ratios ≤ 1 (Ripley, 2014); and display subdued evidence of crustal contamination in terms of stable and radiogenic isotopes (Ding et al., 2012b; Taranovic et al., 2018). Sheet-style mineralization includes layers of predominantly troctolitic rocks, typically found at the base of intrusions from the Duluth Complex, such as the Partridge River and South Kawishiwi Intrusions (Ripley, 2014). They are associated with more evolved, high-aluminum olivine tholeiite

(HAOT) parental magmas; have disseminated sulfides with Cu/Ni ratios ≥ 3 (Taib, 2001); and display obvious evidence of crustal contamination (Ripley, 1981; Ripley and Al-Jassar, 1987; Ripley et al., 1999). Ripley et al. (2015) suggest multiple potential mechanisms for the Cu isotope disparity between conduit- and sheet-style intrusions, including crustal contamination, mantle heterogeneities, Cu isotopic fractionation during mantle melting, or Cu fractionation associated with sulfide liquid fractional crystallization. Relatively few Cu or Ni isotope analyses are available for other large mafic-ultramafic intrusions. For this reason, the systematics of Cu and Ni isotope fractionation in mafic magmatic systems are poorly understood, including the potential importance of externally-derived metals.

Massive sulfides in sedimentary and metasedimentary country rocks below the Duluth Complex (MN), Tamarack Intrusive Complex (MN), the Eagle Intrusion (MI), and the Stillwater Complex (MT) have recently been studied using a variety of stable and radiogenic isotope systematics and trace element geochemistry. Those results confirm that massive sulfides in country rocks near the conduit-style Eagle and Tamarack intrusions formed from sulfide liquid that leaked from the intrusions into the surrounding country rocks. Below the sheet-style Partridge River Intrusion of the Duluth Complex massive sulfides in the local sedimentary rocks formed from sulfide liquid that also originated from the intrusion. Sulfide liquids in the heated country rocks continued to incorporate additional country rock S relative to the sulfides in the Partridge River Intrusion. This produced slightly different isotopic compositions of the country rock-hosted massive sulfides relative to those found in igneous rocks of the intrusion. Massive sulfides beneath the Stillwater Complex formed as Archean metal-rich sedimentary (or seafloor hydrothermal) sulfides and were later metamorphosed during emplacement of the Complex. These results from previous mineralogic and isotopic studies of the country rock-hosted massive

sulfides near the Eagle, Partridge River, and Tamarack intrusions and the Stillwater Complex provide a sound framework for investigation of the Cu and Ni isotope systematics of the occurrences.

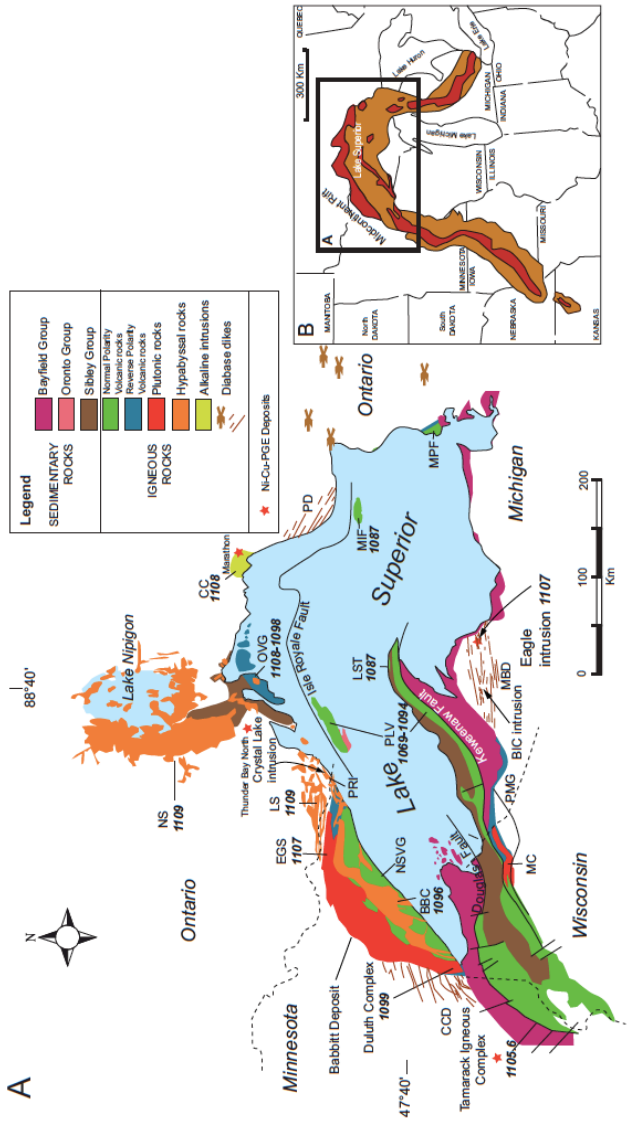

Figure 37: Generalized geology of the Lake Superior region with Midcontinent Rift-related intrusions, showing the location of the Tamarack Igneous Complex, the Eagle Intrusion, and the Duluth Complex relative to other MRS intrusions (modified from Miller and Nicholson, 2013). Abbreviations: BBC = Beaver Bay Complex, CC = Coldwell Complex, CCD = Carlton Country dikes, EGS = Early Gabbro Series, LS = Logan Sills, LST = Lake Shore traps, MBD = Marquette-Baraga dikes, MC = Mellen Intrusive Complex, MIF = Michipicoten Island Formation, MPG = Mamainse Point Formation, NS = Nipigon Sills, NSVG = North Shore Volcanic Group, OVG = Osler Group, PD = Pukaskwa dikes, PLV = Portage Lake Volcanics, PMG = Powder Mill Group, PRI = Pigeon River intrusion. Previously published high-precision U-Pb dates are given in bold italics, in Ma.

A question left unresolved by that previous work is what is the importance of externally-derived metals in mineralized intrusions in the Midcontinent Rift and the Stillwater Complex. Additionally, are the observed Cu isotope variations simply a result of equilibrium fractionations? Are there variable magma sources or contaminants to intrusions imparting distinct Cu isotope signatures? Do fractionations arise from fractionation of sulfide and silicate magmas? How do reservoir effects (amount of silicate vs. sulfide magma) control δ^{65}Cu values? Relatively little literature exists for Ni isotopes in ore deposits and available analyses are restricted to komatiite-hosted Ni-sulfide deposits (Gall et al., 2013) and the Partridge River intrusion of the Duluth Complex (Asp, 2016). However, application of Ni isotopes, in conjunction with Cu isotopes, may help resolve some of the above questions. To explain the Cu isotope disparity and to determine metal sources and high-temperature fractionation mechanisms, we have measured Cu and Ni isotope ratios from a suite of carefully selected Ni-Cu-PGE massive sulfides that occur in sedimentary country rocks near three intrusions of the Midcontinent Rift System and below the Stillwater Complex in Montana.

To explain the Cu isotope disparity between sheet- and conduit-style intrusions of the MRS and to constrain relevant fractionation mechanisms of Cu and Ni isotopes in magmatic sulfide deposits, we measured Cu and Ni isotope ratios from a suite of carefully selected Ni-Cu-PGE massive sulfides that occur in sedimentary country rocks near the conduit-style Eagle and Tamarack intrusions and the sheet-style Partridge River Intrusion within the MRS. Analyses were also performed on massive sulfide-oxides below the Stillwater Complex to assess the source of metals in those sulfides and operative processes in their formation. Our analytical results are compared to available Cu and Ni isotope data for magmatic sulfides and sedimentary rocks. We have modeled the effects of variable silicate:sulfide ratios, or R-factors (mass ratio of

silicate magma to sulfide magma), contamination, and olivine fractional crystallization on the Ni isotope composition of the sulfides. We ultimately arrive at a conclusion that near-zero and slightly negative Ni isotope compositions of leaked magmatic sulfide liquids near Tamarack and Eagle can be explained by minor degrees of crustal contamination of a mantle-derived melt at variable R-factors. Massive sulfides from below the Partridge River intrusion that originated from the overlying magma have low δ^{60}Ni ratios and require significantly more contamination from ^{60}Ni-depleted sedimentary sulfides, similar to those measured in some of the local sedimentary rocks. Cu isotopic ratios of country rock-hosted massive sulfides near Eagle and Tamarack are lower than those reported by Ripley et al. (2015) and are mostly around 0 ‰, similar to those expected for melts derived from unaltered mantle. Cu isotope ratios of samples from beneath the Partridge River intrusion are similar to those of igneous-hosted sulfides from Ripley et al. (2015) and Asp (2016), supporting their origin from a magmatic sulfide liquid. The lower δ^{65}Cu compositions in the massive sulfides below the Partridge River intrusion cannot be explained by contamination from ^{65}Cu-rich sediments in the Virginia and Thomson Formations, unless a substantially light reservoir has yet to be discovered in the local Proterozoic rocks. Cu and Ni isotope measurements of country rock-hosted massive sulfides below the Stillwater Complex are negative and are within the range of available analyses for most igneous-hosted sulfides and Archean sedimentary sulfides.

Geologic Setting

The Duluth Complex is composed of multiple intrusions that occur in the ~ 1.1 Ga Midcontinent Rift (Severson and Hauck, 1990; Severson, 1994). The Partridge River intrusion is a 1099 Ma (Paces and Miller, 1993) mafic intrusion containing disseminated sulfides in

troctolitic and noritic sheets near the base of the intrusion (Severson and Hauck, 1990). Country rocks to the Partridge River intrusion are predominantly metapelites of the 1.8 Ga Virginia Formation and the Biwabik Iron Formation, both of which are truncated by the base of the intrusion (Severson and Hauck, 1990). Disseminated sulfide minerals within the Partridge River intrusion are principally pyrrhotite, chalcopyrite, cubanite, and pentlandite, in addition to minor amounts of other Cu-Fe sulfides (Severson and Hauck, 1990) and platinum group minerals (PGMs; Ripley, 1990). Extensive crustal contamination of the magmas from the Partridge River intrusion has been illustrated using S (Ripley, 1981; Ripley and Al-Jassar, 1987), O (Ripley and Al-Jassar, 1987), Re-Os, and Pb isotopes (Ripley et al., 1999). Below the Partridge River Intrusion, massive sulfides are found entirely within the Virginia Formation.

The Eagle Ni-Cu deposit is hosted within a mafic-ultramafic intrusion spatially associated with the Marquette-Baraga dike swarm. The dike-like geometry of the intrusion (referred to as conduit-style) is in contrast to the sheet-like occurrences in the Partridge River intrusion. The Eagle intrusion is hosted in metapelitic rocks of the 1.8 Ga Michigamme Formation. Disseminated, semi-massive, and massive sulfides are found within olivine-rich rocks in the intrusion, including feldspathic peridotite, melatroctolite, and melagabbro. The massive sulfides are primarily pyrrhotite, pentlandite, chalcopyrite, and cubanite, with minor magnetite (Ding et al., 2010, 2012a,b). Country rock-hosted massive sulfides at Eagle are found marginal to the contact between the igneous rocks and the Michigamme Formation and typically crosscut the intrusion. The Tamarack Intrusive Complex is another olivine-rich conduit-style deposit associated with a local dike swarm, the Carlton County dikes. The main igneous bodies at Tamarack are the fine-grained olivine-bearing intrusion (FGO) and the coarse-grained olivine-bearing intrusion (CGO). The Eagle and Tamarack deposits are associated with early stages of

Rift development and were emplaced at 1107 and 1105.6 Ma, respectively (Ding et al., 2010; Goldner, 2011). At Tamarack, the massive sulfides are hosted in a segment of the Thomson Formation that occupies a vertical gap between the CGO intrusion and the overlying FGO intrusion.

The 2.7 Ga Stillwater Complex (Nunes and Tilton, 1971; DePaolo and Wasserburg, 1979; Nunes, 1981; Premo et al., 1990) is a classic layered mafic-ultramafic intrusion in south-central Montana, most noted for the Pd-Pt-rich JM Reef. A slice of the Stillwater Complex has been exposed along the Beartooth uplift by Laramide tectonics (Fig. 38). The Complex is commonly divided into the Basal Series, Ultramafic Series, and the Banded Series. The Basal Series is further divided into the Basal Norite and Basal Bronzite Cumulate (Page, 1977). The Ultramafic Series is divided into Peridotite and Bronzitite units (Jackson, 1961; Raedeke and McCallum, 1984; Cooper, 1997). The Banded Series is divided into the Lower, Middle, and Upper Banded Series. The JM Reef is found in the Lower Banded Series, at the reoccurrence of cumulus olivine (Corson et al., 2002). Other notable mineral occurrences include the Picket Pin PGE deposit, which is found near the boundary between the Middle and Upper Banded Series (Boudreau and McCallum, 1986); a number of chromitite seams from the Ultramafic Series (Page and Jackson, 1967; Campbell and Murck, 1993; Spandler et al., 2005); and disseminated to massive Ni-Cu sulfide mineralization primarily in the Basal Norite (Page, 1979). Below the Stillwater Complex, massive sulfide(-oxides) are found within the cordierite-orthopyroxene hornfels, as well as the Stillwater Iron Formation.

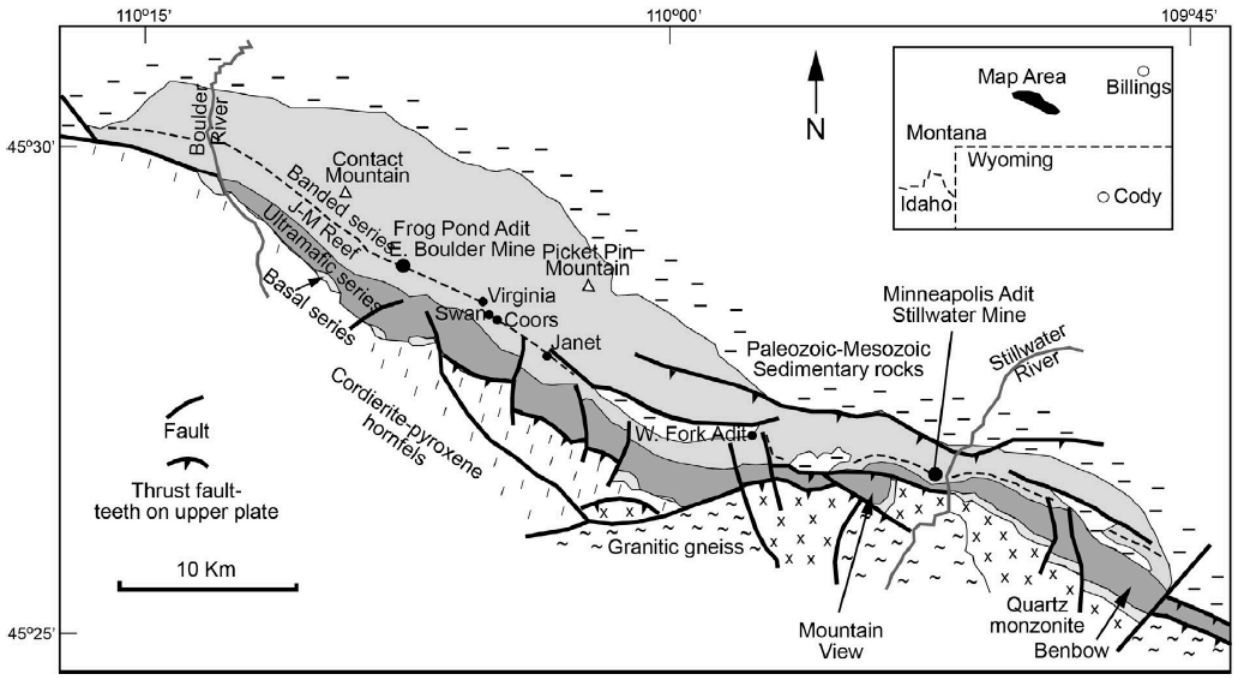

Figure 38: Generalized geologic map of the Stillwater Complex, MT (modified from Lambert et al., 1994 and McCallum et al., 1999). Samples were taken from drillholes primarily in the Mountain View area. Samples from the JM Reef were collected from the East Boulder Mine.

Sampling and Analytical Methods

Samples of country rock hosted massive sulfides used in this study were taken from drillholes 08TK0049 and 14TK0213 at Tamarack (Fig. 39); EAUG0069 and EAUG0070 near Eagle (Fig. 40); MB07-04, MB07-13, MB08-28, and MB08-36 below the Partridge River intrusion at the Mesaba deposit (Fig. 41); and 368-313, 373-322, and M17 at the Stillwater Complex (Fig. 42). All analyses of country rock-hosted massive sulfides were performed on whole-rock sulfide powders obtained by crushing in an alumina shatterbox. A sample of the Biwabik Iron Formation was taken from the Peter Mitchell Mine in Minnesota. Three samples of sedimentary pyrite from the Thomson Formation were taken from drillhole 10TK0112 on the Tamarack property. A sample of S-rich Virginia Formation was taken from hole B1-135 below the Partridge River intrusion at the Mesaba (or Babbitt) deposit, and a sample of the bedded

pyrrhotite unit in the Virginia Formation was also taken from below the Partridge River intrusion at the Dunka Pit. Three samples of the JM Reef were taken from the 6450 level of the East Boulder Mine in the Stillwater Complex. All analyses of disseminated sulfides in igneous and sedimentary rocks were performed on sulfide separates that were microdrilled from hand samples. Table 13 lists collar coordinates or mine locations for all samples used in this study.

Table 13: Location of drill core and mine samples used in this study.

Drillhole/Sample Number	Location	Collar Latitude (North)	Collar Longitude (West)
08TK0049	Tamarack	46°40'19.4"	93°07'16.9"
14TK0213	Tamarack	46°40'13.1"	93°07'10.3"
EAUG0069	Eagle	46°44'54.8"	87°53'47.4"
EAUG0070	Eagle	46°44'54.8"	87°53'47.4"
MB 07-04	Partridge River	47°38'18.5"	92°15'40.0"
MB 07-13	Partridge River	47°38'16.6"	91°54'43.6"
MB 08-28	Partridge River	47°38'6.9"	91°55'23.0"
MB 08-36	Partridge River	47°38'17.4"	91°54'30.6"
368-313	Stillwater	45°23'19.0"	109°54'0.7"
373-322	Stillwater	45°23'19.0"	109°54'0.7"
M17	Stillwater	45°23'19.0"	109°54'0.7"
PMM-BIF	Peter Mitchell Mine - Biwabik Iron Fmn.	47°39'44"	91°56'30"
BDD-Po	Dunka Pit - Bedded Pyrrhotite Unit	47°42'20"	91°51'4"
B1-135	Babbit Deposit - Virginia Fmn.	47°38'28"	91°52'59"
10TK0112	Tamarack - Thomson Fmn.	46°39'27.8"	93°07'04.7"
EB-2	JM Reef - face sample	East Boulder Mine, 1E 6450 Level	
EB-5	JM Reef - face sample	East Boulder Mine, 1E 6450 Level	
EB-6	JM Reef - face sample	East Boulder Mine, 43W 6450 Level	

Twenty-one Cu isotope measurements were performed at Indiana University, Bloomington and are listed in Table 14. Approximately 5 – 10 mg of sample were digested in a mixture of concentrated and distilled HNO_3, HCl, and HF at 160°C for 48 hours. Samples were dried down and taken back up in ~5 mL of 7 M HCl. A small aliquot of this solution (~ 0.1 mL) was put through anion exchange chromatography, using 2 mL of AG MP-1M resin in Bio-Rad polypropylene columns. The column procedure was identical to that described in Ripley et al. (2015). The collected Cu fractions were dried down and refluxed with distilled, concentrated HNO_3, and the final Cu fractions were dissolved in 0.32 M HNO_3 before analysis. All sample

and beaker weights were recorded before and after digestions and column chemistry. Gravimetric yields of all sample aliquots that were put through column chemistry were checked using an Agilent 7700 quadrupole ICP-MS, and samples were only run for isotopic analyses if they yielded 95 to 105 % of the original Cu, so that on-column fractionation was not manifest in the final analyses, within current analytical capabilities. Analytical uncertainties from the ICP-MS are estimated to be ± 5 %, based on duplicate sample analyses. Isotopic analyses were performed on a Nu-Plasma II MC-ICP-MS for $\delta^{65}Cu$, using a standard-sample-standard bracketing technique. Samples and standards were run in wet plasma mode at ~200 ppb Cu. The international Cu standard NIST SRM-976 served as the isotopic standard, and the rock standard SU-1 was also monitored in each batch. Cu isotopic ratios are reported in standard δ notation, relative to NIST SRM-976, and were calculated using the standard equation:

$$\delta^{65}Cu = (((^{65}Cu/^{63}Cu)_{sample} / (^{65}Cu/^{63}Cu)_{SRM\text{-}976})\text{-}1)$$

Delta values are reported in (‰) after multiplication by 1000. Replicate analyses of the SU-1 standard gave a value of -0.11 ± 0.14 ‰, which are within error of the value of -0.018 ± 0.08 ‰ from Chapman et al. (2006) and -0.09 ± 0.09 ‰ from Ripley et al. (2015).

Thirty-nine samples were also analyzed for Ni isotopic compositions at IU Bloomington and are listed in Table 15. Approximately 1 - 3 mg of sample were digested in a mixture of concentrated HNO_3, HCl, and HF at 160°C for 48 hours. Before ion exchange chromatography, Ni concentrations of the prepared solutions were determined using the Agilent 7700 quadrupole ICP-MS. An aliquot of sample solution was taken, with approximately 1 µg Ni, and mixed with a ^{61}Ni-^{62}Ni double-spike solution, in the proportions 640 ng spike Ni: 360 ng sample Ni, based

on recommendations from Rudge et al. (2009). Samples were dried down and redissolved to ensure standard-spike equilibration. Samples were then put through column chemistry to remove Fe and other impurities via cation exchange chromatography. The procedure was performed with Bio-Rad 200 – 400 mesh AG50W-X8 resin, in a mixture of 20 % 10 M distilled HCl and 80% HPLC-grade acetone. The samples were eluted using 6 M HCl and were subsequently dried down and refluxed with concentrated HNO_3 to depolymerize and oxidize any organic residue from resin. Samples were then dried down and redissolved in 0.32 M HNO_3. Samples were diluted to ~ 200 ppb Ni and were introduced into a Cetac Aridus II desolvating nebulizer, and nickel isotopic ratios were determined on a Nu Plasma II MC-ICP-MS. The international Ni standard, NIST-986, served as the isotopic standard and standard-sample-sample-standard bracketing was utilized to account for instrumental mass bias. The rock standard Nod-A-1 and the internal standard NiAA were monitered during each analytical session. Ni isotopic ratios are reported in standard δ notation, relative to NIST SRM-986, and were calculated using the following equation:

$$\delta^{60}Ni = (((^{60}Ni/^{58}Ni)_{sample} / (^{60}Ni/^{58}Ni)_{SRM\text{-}986})\text{-}1)$$

Delta values are reported in (‰) after multiplication by 1000. Replicate analyses of the Nod-A-1 and NiAA standards produced values of 1.13 ± 0.15 ‰ (n =16) and -0.16 ± 0.08 ‰ (n = 18), respectively, and are within error of results from Gueguen et al. (2013) and Spivak-Birndorf et al. (2018).

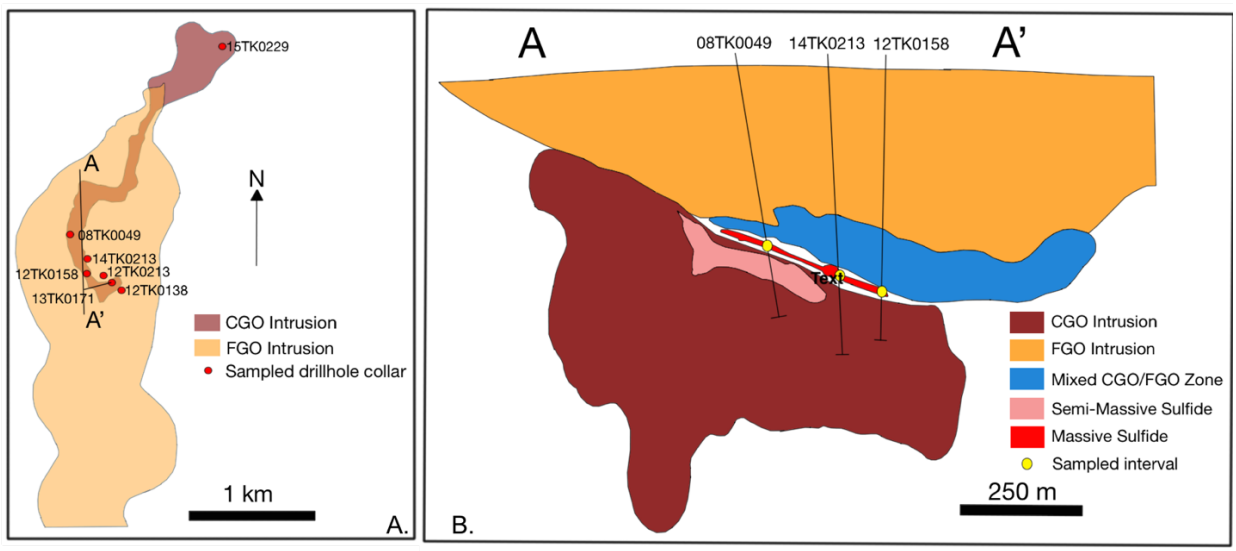

Figure 39: Map (A) and long-section (B) through the Tamarack Intrusive Complex, showing the simplified geology and drillholes sampled in this study. Map and section produced from 3D models provided courtesy of Talon Metals. No vertical exaggeration.

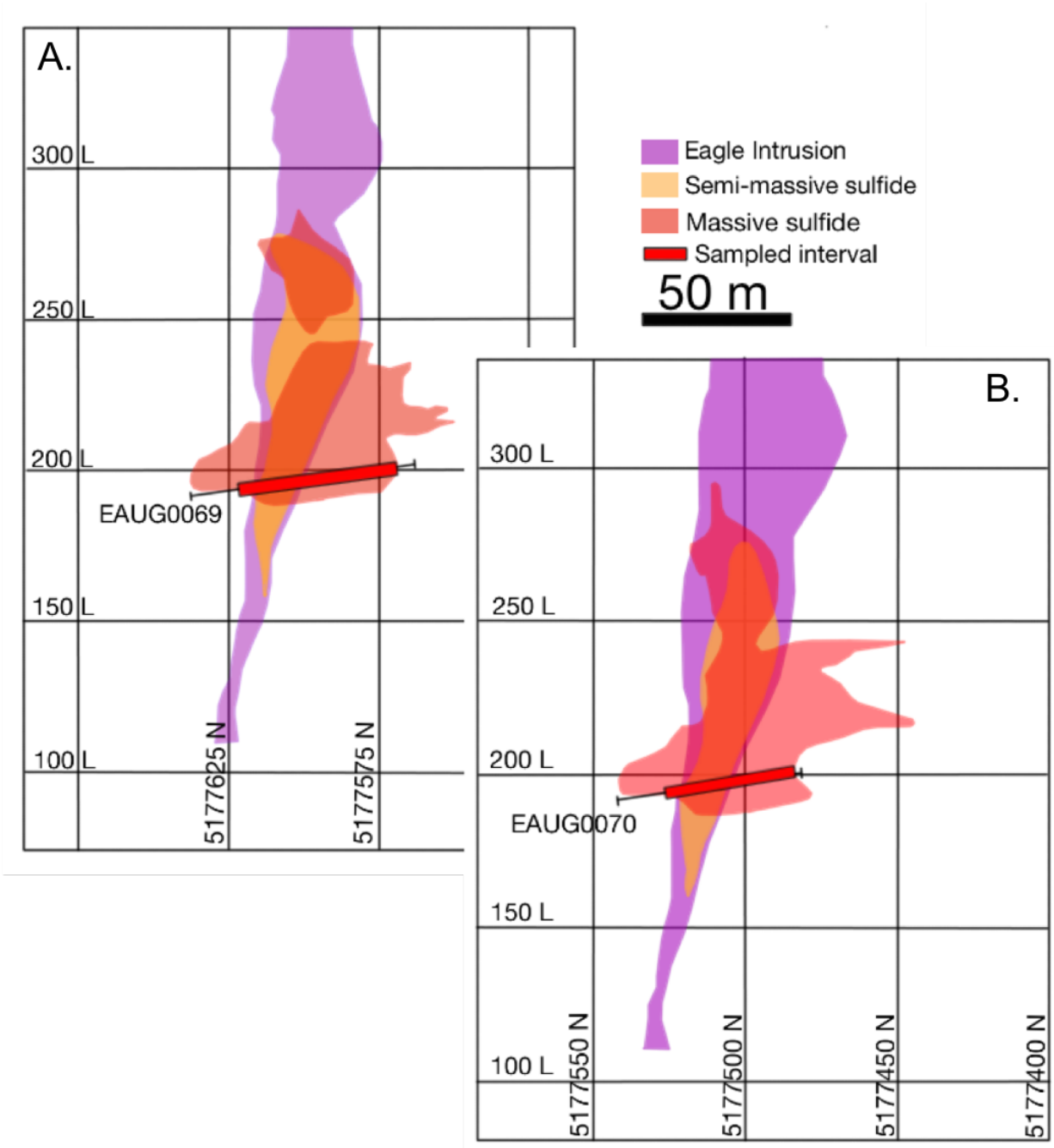

Figure 40: Cross-sections through the Eagle Intrusion, showing the intervals sampled from drillholes EAUG0069 (A) and EAUG0070 (B). Note that in the massive sulfides are hosted primarily outside the intrusion, but in some places, crosscuts the intrusion. Sections produced from 3D models provided courtesy of Lundin Mining. No vertical exaggeration.

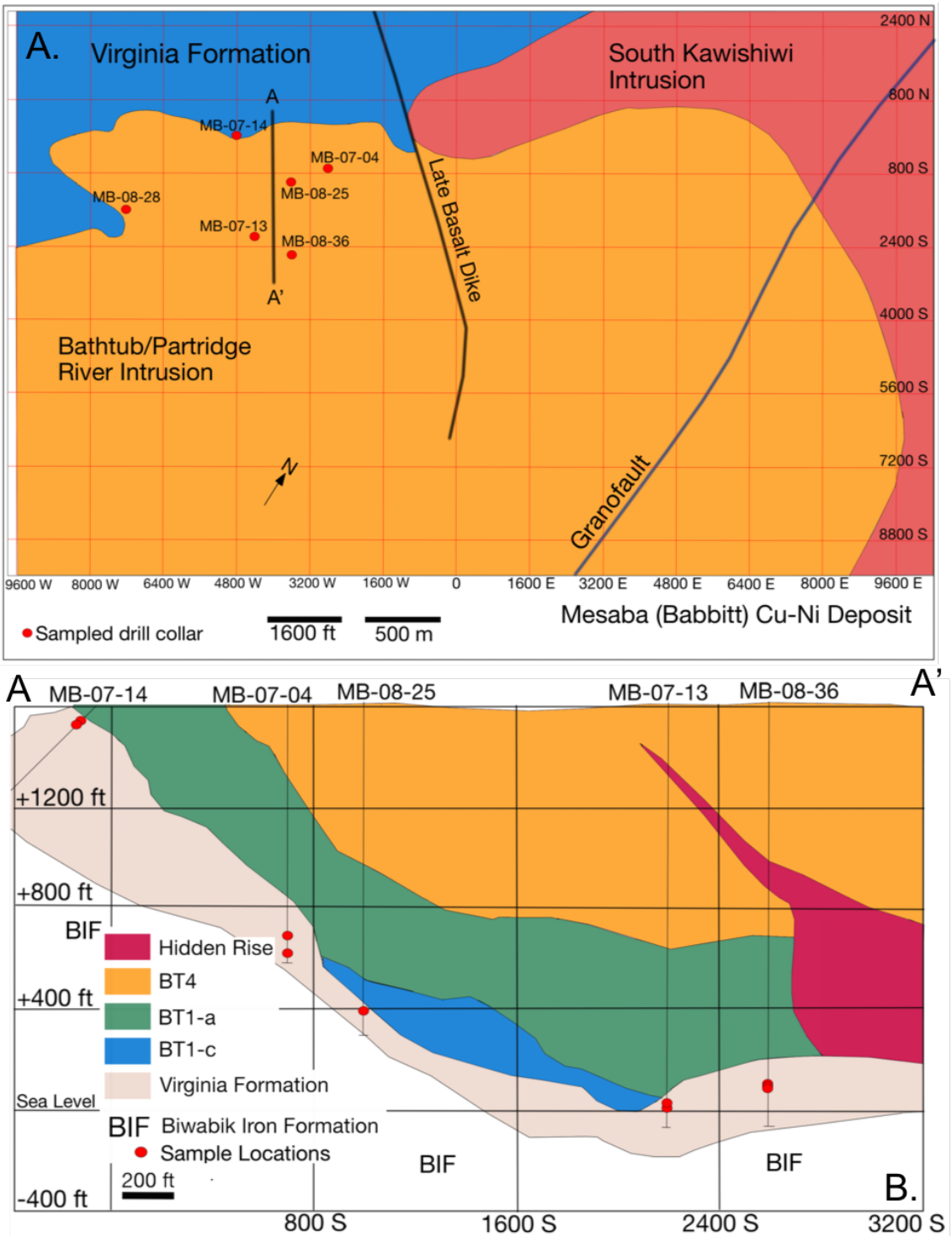

Figure 41: Map (A) and cross-sections (B) through the Mesaba Deposit, showing the simplified geology and drillholes sampled in this study. Maps and cross-sections modified from Severson and Hauck (2008). No vertical exaggeration.

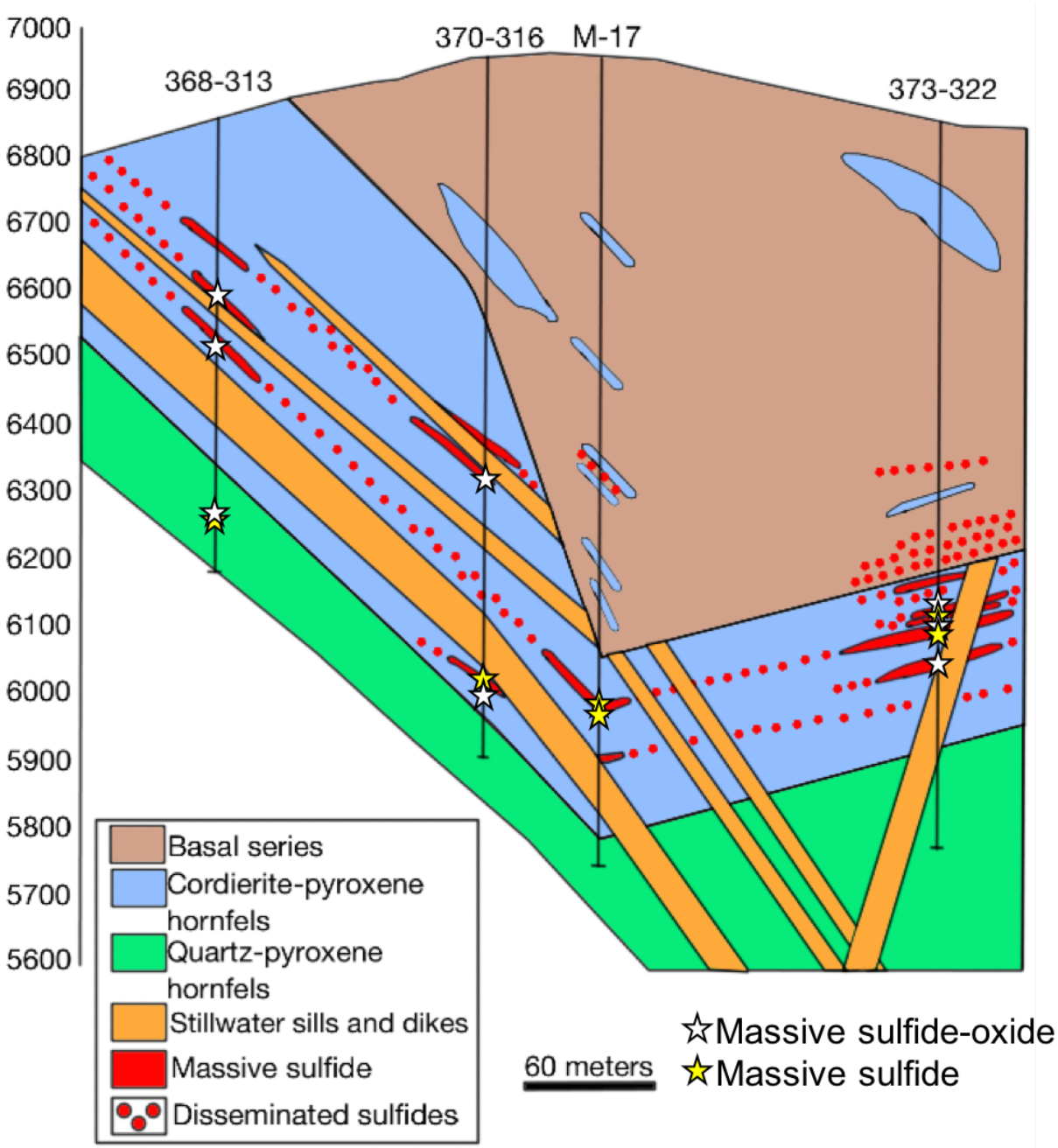

Figure 42: Cross-section through the Mouat area of the Stillwater Complex. Samples of country rock-hosted massive sulfides (gold stars) and massive sulfide-oxides (white stars) were taken primarily from the cordierite-pyroxene hornfels, with a few from the quartz pyroxene hornfels. Geology based on core logging from Roger Cooper. No vertical exaggeration.

Results

Cu isotopes

Results of copper isotope measurements of sulfide minerals from country rock-hosted massive sulfides are given in Table 14 and are shown graphically in Figure 43. Cu in the sulfides is contributed primarily by chalcopyrite and lesser cubanite. Trace amounts of bornite are present in some samples below the Partridge River Intrusion. δ^{65}Cu values of samples near Tamarack range from -0.39 to 1.06 ‰. Massive sulfides near the Eagle intrusion have δ^{65}Cu values from -0.43 to 0.15 ‰. Massive sulfides below the Partridge River Intrusion can be classified as Cu-rich and Cu-poor samples. Cu-poor samples have < 20 % Cu and have δ^{65}Cu values from -1.14 to -0.01 ‰. Cu-rich samples have > 20 % Cu and have δ^{65}Cu values of 0.25 and 0.09‰. Samples of massive sulfide(-oxides) from below the Stillwater Complex have δ^{65}Cu values from -0.74 to -0.16 ‰.

Ni isotopes

Results of nickel isotope measurements of country rock-hosted massive sulfides, igneous-hosted sulfides, and laminated sedimentary sulfides are reported in Table 15 and displayed in Figure 44. Ni is found primarily in granular pentlandite and minor pentlandite exsolution in pyrrhotite. Massive sulfides near the Tamarack intrusive complex have δ^{60}Ni values from -0.4 to 0.17 ‰. Samples near Eagle have δ^{60}Ni values of -0.45 to -0.29 ‰. Cu-poor massive sulfides below the Partridge River Intrusion have δ^{60}Ni values between -0.77 and -0.52 ‰. Cu-rich samples have δ^{60}Ni values of 1.64 and 3.01 ‰. Thomson Formation samples from near the Tamarack intrusive complex have disseminated sulfides (~ 1 – 2 volume % sulfide) with δ^{60}Ni values from -3.12 to -0.83 ‰. A sample of disseminated sulfide from the Virginia Formation

(Fig. 45A) has a δ^{60}Ni value of 1.71 ‰. A sample of the Bedded Pyrrhotite Unit (also from the Virginia Fm.) with layered sedimentary sulfides (Fig. 45B) has ~ 10 volume % sulfide and a δ^{60}Ni value of -1.55 ‰. A sample of the Biwabik Iron Formation has a δ^{60}Ni values of 0.35 ‰. Samples of country rock-hosted massive sulfides from below the Stillwater Complex have δ^{60}Ni from -0.45 to -0.21 ‰. Sulfides from the JM reef of the Stillwater Complex have δ^{60}Ni values from 0.25 to 0.64 ‰.

Table 14: Cu concentrations and isotopic composition of country rock-hosted massive sulfides near the Tamarack, Eagle, and Partridge River Intrusions, and the Stillwater Complex.

Sample	Location	Cu (wt.%)	δ^{65}Cu (‰)	2σ
49-398.68	Tamarack	6.69	0.18	0.14
49-404.81	Tamarack	2.52	0.28	0.14
49-405.78	Tamarack	4.88	-0.39	0.14
49-406.61	Tamarack	2.24	0.11	0.14
213-455.19	Tamarack	2.05	0.67	0.14
213-460.49	Tamarack	2.84	0.04	0.14
213-461.19	Tamarack	2.23	1.06	0.14
69-38.00	Eagle	4.40	0.04	0.14
70-43.59	Eagle	4.80	-0.09	0.14
69-55.75	Eagle	5.41	-0.43	0.14
70-58.36	Eagle	2.23	-0.29	0.14
69-71.8	Eagle	2.62	-0.21	0.14
69-26.26	Eagle	6.95	0.15	0.14
M17-1049.5	Stillwater	1.36	-0.16	0.14
368-313-276	Stillwater	1.16	-0.22	0.14
373-322-809	Stillwater	0.58	-0.74	0.14
07-04-994.3	Partridge River	4.75	-1.14	0.14
08-28-1045.2	Partridge River	2.56	-0.01	0.14
08-36-1549.6	Partridge River	20.84	0.09	0.14
08-36-1552	Partridge River	31.03	0.25	0.21
07-13-1605.1	Partridge River	1.84	-1.02	0.14

Table 15: Ni concentrations and isotopic composition of country rock-hosted massive sulfides and sedimentary sulfides near the Tamarack, Eagle, and Partridge River Intrusions, and country rock-hosted massive sulfides and the JM Reef from the Stillwater Complex.

Sample	Location	Type	Ni (wt. %)	δ^{60}Ni (‰)	2σ
49-398.68	Tamarack	massive sulfide	18.91	-0.13	0.15
49-404.81	Tamarack	massive sulfide	19.89	-0.40	0.15
49-405.78	Tamarack	massive sulfide	16.61	-0.35	0.15
49-406.61	Tamarack	massive sulfide	6.97	-0.38	0.15
213-455.19	Tamarack	massive sulfide	8.06	0.17	0.15
213-459.55	Tamarack	massive sulfide	2.88	-0.10	0.26
213-460.49	Tamarack	massive sulfide	11.78	0.07	0.15
213-461.19	Tamarack	massive sulfide	10.10	-0.19	0.15
368-313-275.5	Stillwater	massive sulfide	0.79	-0.32	0.15
368-313-574.5	Stillwater	massive sulfide	1.32	-0.43	0.15
373-322-726.5	Stillwater	massive sulfide	1.77	-0.45	0.15
373-322-804	Stillwater	massive sulfide	2.06	-0.33	0.15
M17-979.5	Stillwater	massive sulfide	2.09	-0.25	0.15
M17-1049.5	Stillwater	massive sulfide	1.43	-0.34	0.15
368-313-276	Stillwater	massive sulfide	1.24	-0.25	0.15
373-322-809	Stillwater	massive sulfide	0.89	-0.21	0.15
373-322-868	Stillwater	massive sulfide	1.28	-0.35	0.15
69-26.26	Eagle	massive sulfide	4.99	-0.35	0.15
70-37	Eagle	massive sulfide	5.72	-0.29	0.15
69-38	Eagle	massive sulfide	5.91	-0.32	0.15
70-43.59	Eagle	massive sulfide	8.83	-0.37	0.15
69-55.75	Eagle	massive sulfide	12.13	-0.40	0.15
70-58.36	Eagle	massive sulfide	5.91	-0.44	0.15
69-71.8	Eagle	massive sulfide	8.40	-0.45	0.15
07-04-925.9	Partridge River Intrusion	massive sulfide	1.12	-0.52	0.15
07-04-994.3	Partridge River Intrusion	massive sulfide	1.34	-0.57	0.15
08-28-1045.2	Partridge River Intrusion	massive sulfide	0.59	-0.69	0.15
08-36-1549.6	Partridge River Intrusion	massive sulfide	0.18	3.01	0.15
08-36-1552	Partridge River Intrusion	massive sulfide	0.15	1.64	0.15
07-13-1605.1	Partridge River Intrusion	massive sulfide	0.49	-0.77	0.15
PMM-BIF	Below Partridge River Int.	Biwabik Iron Fmn	0.25	0.35	0.15
BDD-Po	Below Partridge River Int.	Bedded Pyrrhotite Unit	0.44	-1.55	0.15
135-1492	Below Partridge River Int.	Virginia Formation	1.22	1.71	0.15
112-178.53	Near Tamarack	Thomson Fmn.	1.17	-3.12	0.15
112-192.35	Near Tamarack	Thomson Fmn.	0.02	-0.83	0.15
112-191.3	Near Tamarack	Thomson Fmn.	0.04	-0.93	0.15
EB-2	Stillwater Complex	JM Reef	15.52	0.64	0.15
EB-5	Stillwater Complex	JM Reef	7.03	0.25	0.15
EB-6	Stillwater Complex	JM Reef	27.07	0.60	0.15

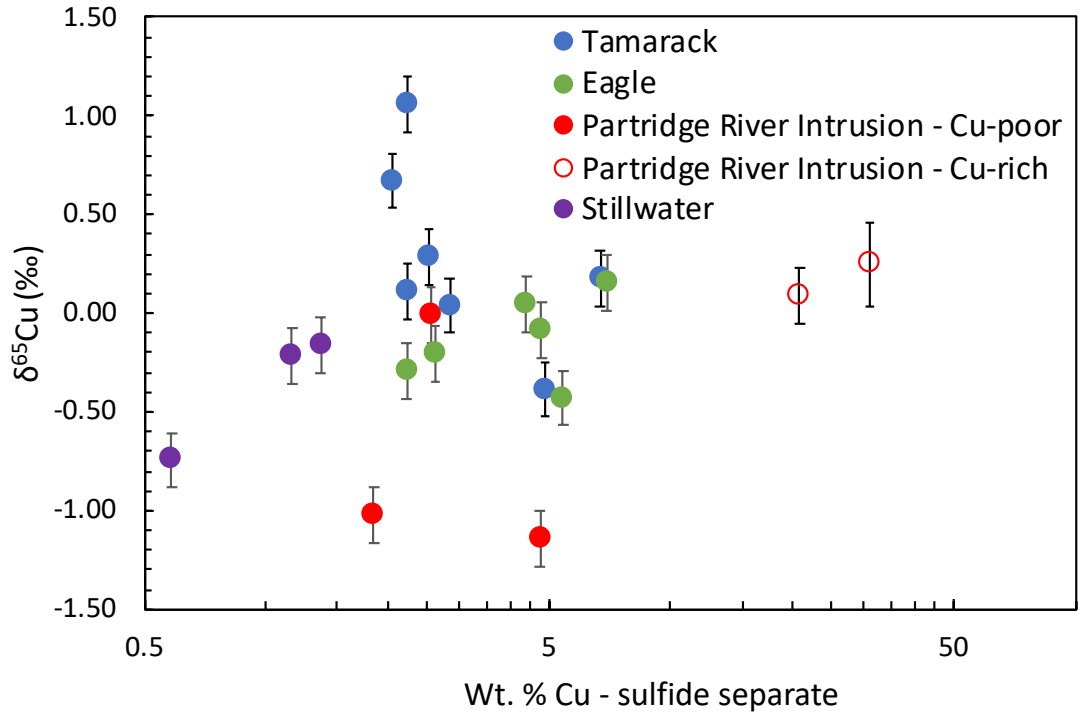

Figure 43: Plot of δ^{65}Cu values vs Cu concentration for samples of country rock-hosted massive sulfides used in this study. Error bars are shown at the 2σ level.

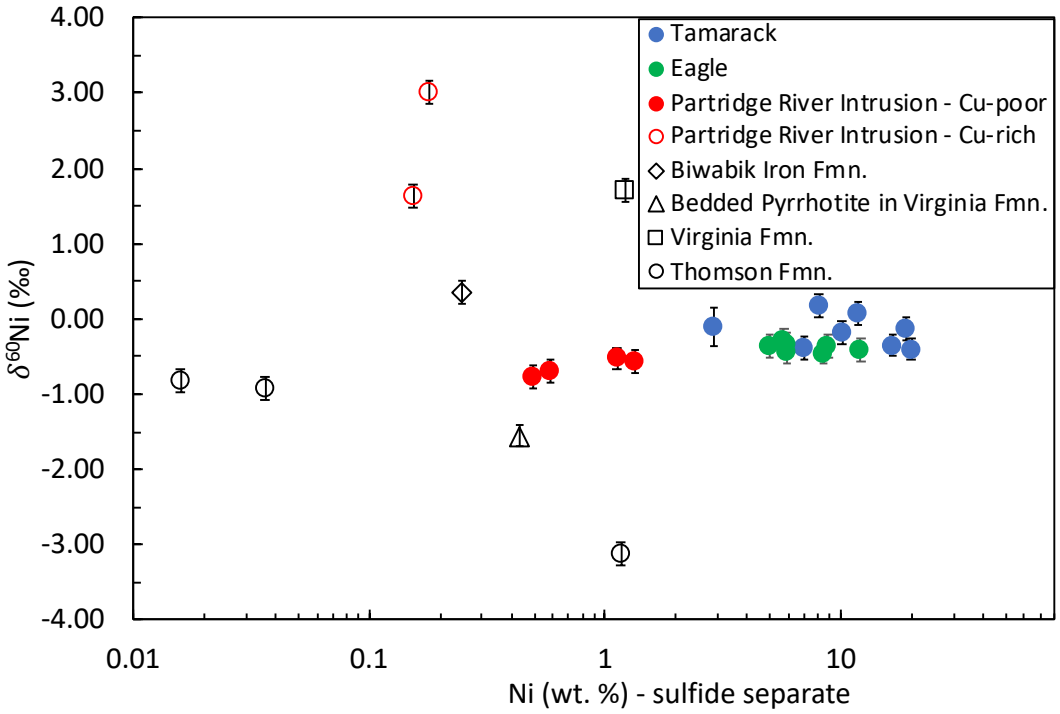

Figure 44: Plot of δ^{60}Ni values vs Ni concentration for samples of country rock-hosted massive sulfides near Midcontinent Rift intrusions used in this study. Error bars are shown at the 2σ level.

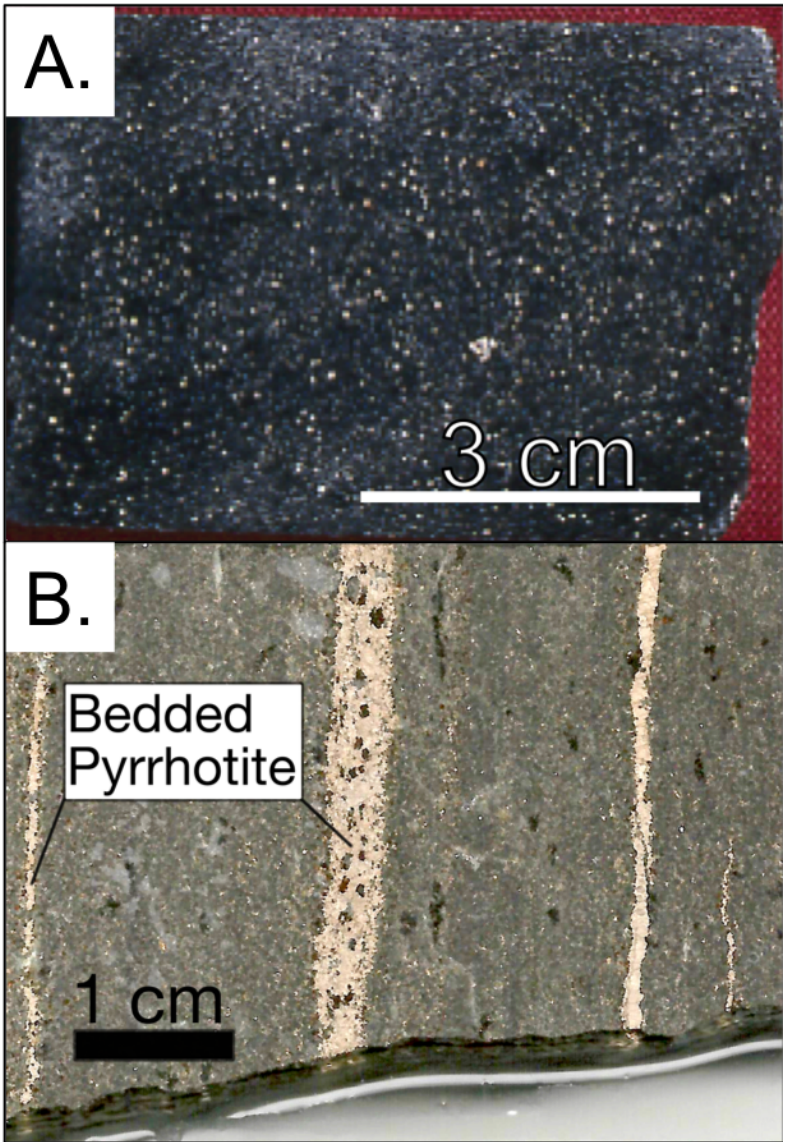

Figure 45: Hand sample scans of sedimentary sulfides in the Thomson Formation (A), Virginia Formation (B), and the Bedded Pyrrhotite Unit of the Virginia Formation (C).

Review of Cu and Ni Isotopic Systematics

Cu isotopes in igneous and sedimentary rocks and associated mineral deposits

Analyses of komatiites, basalts, and orogenic lherzolites have shown that the mantle $\delta^{65}Cu$ ranges from -0.03 to 0.17 ‰ (Ben Othman et al., 2006; Savage et al., 2015; Liu et al., 2015). Zhao et al. (2017) reported sulfide $\delta^{65}Cu$ values of -2 to 0.2 ‰ for magmatic sulfides from the

Tulaergen Ni-Cu deposit. Malitch et al. (2014) discovered that economic intrusions from the Noril'sk District have strong negative correlations between Cu and S isotope systematics, whereas sub-economic and uneconomic intrusions have an apparent decoupling of Cu and S isotope systematics. They reported δ^{65}Cu values from -2.3 to 1.0 ‰, demonstrating a wide range of values for magmatic sulfides in the district (Malitch et al., 2014). From the Midcontinent Rift system, δ^{65}Cu values of igneous rock-hosted sulfides at Tamarack and Eagle range from 0.99 to 1.84 ‰ and 0.69 to 1.32 ‰, respectively (Ripley et al., 2015). Asp (2016) reported two samples of igneous rock-hosted sulfides at Eagle with δ^{65}Cu values of -0.16 and 1.36 ‰. δ^{65}Cu values of disseminated sulfides from the Partridge River intrusion range from -0.85 to 0.36 ‰ (Ripley et al., 2015; Asp, 2016) and those from the nearby South Kawishiwi intrusion have δ^{65}Cu values from -0.36 to 0.42 ‰ (Ripley et al., 2015). Larson et al. (2003) report a δ^{65}Cu value of -1.06 ‰ for one sample at the base of the Stillwater Complex, but they note the sample has undergone post-magmatic hydrothermal alteration. Malitch et al. (2014) report a δ^{65}Cu value of -0.1 ‰ for a sample in the JM Reef.

Studies of lower-temperature, hydrothermal ore deposits and supergene environments have demonstrated a substantial redox-dependent fractionation (Rouxel et al., 2004; Mathur et al., 2005; Mason et al., 2005; Mathur et al., 2009; Sherman et al., 2013). Hypogene mineralization in porphyry Cu, skarn, and epithermal Au-Ag systems mostly range from -1 to 1 ‰ (Mathur et al., 2009; Saunders et al., 2016; Wang et al., 2017), which is broadly coincident with the mantle range. In comparison, supergene mineralization can have δ^{65}Cu values from ~ -17 to +10 ‰ (Mathur et al., 2009).

Oceanic sediments have δ^{65}Cu values from 0.41 to 0.95 ‰ (Dekov et al., 2013). Manganese nodules have an average δ^{65}Cu value of 0.31 ± 0.23 ‰ (Albaréde, 2004). Ripley et al. (2015)

reported $\delta^{65}Cu$ values from -0.33 to 3.12 ‰ for samples of the Virginia and Thomson Formations in the Paleoproterozoic Animikie Basin. Nearly all existing Cu isotope data from sedimentary environments have $\delta^{65}Cu$ values > 0 ‰, with the exception of late Archean sulfide-bearing black shales, which have $\delta^{65}Cu$ values as low as -0.55 ‰ (Chi Fru et al., 2016). Present-day seawater has $\delta^{65}Cu$ values from 0.8 to 1.5 ‰ (Vance et al., 2008; Takano et al., 2013; Thompson et al., 2013).

Experimental studies of Cu isotope fractionation

Low-temperature experimental results of Cu^{2+} adsorption onto Fe-oxyhydroxides have shown the minerals are consistently enriched in ^{65}Cu relative to the solution (Balistrieri et al., 2008; Pokrovsky et al., 2008). Presently, there are only limited high-temperature Cu isotope data for experimental silicate-sulfide-alloy systems (Williams and Archer, 2011; Savage et al., 2015). Williams and Archer (2011) showed that metal-sulfide systems that underwent fractional crystallization have lighter $\delta^{65}Cu$ values in the sulfides and heavier $\delta^{65}Cu$ values in the metal. They attributed this difference to preferential diffusion of ^{63}Cu from the metal into the sulfide. Continued crystallization causes the sulfides to become more similar to the $\delta^{65}Cu$ value in the metal phase. Savage et al. (2015) documented $\Delta^{65}Cu_{silicate\text{-}metal}$ of -0.1 to -0.2 ‰.

Potential Cu fractionation mechanisms

Previous studies have considered various possible mechanisms of Cu isotope fractionation in magmatic systems. The incompatible nature of Cu in silicates suggests little in the way of silicate-sulfide fractionation. At the Tulaergen deposit, Zhao et al. (2017) discovered earlier-formed sulfides had lower $\delta^{65}Cu$ values than later-formed sulfides. They proposed that an

increase in Fe^{+3}/Fe^{+2} ratios caused by crystallization of Fe^{+2} -bearing silicate minerals drove oxidation of Cu^{+} to Cu^{+2} during reduction of Fe^{+3}. Redox-driven Cu isotope fractionation was proposed to have occurred after magmas had already attained sulfide saturation and sulfide liquids had segregated.

At Noril'sk, Malitch et al. (2014) suggested the ranges of $\delta^{65}Cu$ values are a primary feature of the ores but also could not rule out the possibility of sedimentary rock-derived Cu, especially for the Kharaelakh intrusion. Ripley et al. (2015) speculated that the difference in Cu isotope ratios between sheet- and conduit-style intrusions in the Midcontinent Rift may be the result of one or more of the following processes: 1) Assimilation of Cu-bearing, sulfidic sediments from the Animikie Basin, 2) Heterogeneous $\delta^{65}Cu$ compositions in the mantle, 3) Isotopic fractionation during variable degrees of mantle partial melting, or 4) Cu isotope fractionation accompanying fractional crystallization of monosulfide solid solution (MSS).

Ripley et al. (2015) demonstrated that assimilation of Cu-bearing sedimentary rocks could explain the differences in Cu isotopic compositions only if the mantle were characterized by low ($\leq$ -0.25 ‰) $\delta^{65}Cu$ values. This value is much lower than the recent mantle estimate from Savage et al. (2015) and Liu et al. (2015). Additionally, the $\delta^{65}Cu$ values from the Partridge River and South Kawishiwi intrusions are the same, despite the fact that the South Kawishiwi intrusion is hosted by Archean granitoids, whereas the Partridge River intrusion is hosted by pelitic, sulfide-rich sedimentary rocks and the Biwabik Iron Formation.

The possibility of $\delta^{65}Cu$ heterogeneities in the Proterozoic mantle beneath the Midcontinent Rift remains poorly constrained. It is clear that the mantle was heterogeneous in terms of Pb isotopes during emplacement of Midcontinent Rift magmas (Shirey et al., 1994; Smith et al., in press), and other isotopic heterogeneities may be expected.

Variable degrees of mantle partial melting may potentially produce variable Cu isotope compositions, assuming Cu is held entirely in sulfides in the mantle (Huang et al., 2017). Naldrett (2011) showed that all of the Cu in the mantle will be extracted when the mantle attains ~ 12 % partial melting. This implies that melts produced by more than ~12 % partial melting will have diluted Cu concentration, but their Cu isotopic compositions should be identical to the initial mantle. At lower degrees of partial melting, before all of the Cu is extracted as sulfide, there is potential for fractionation between Cu_{melt} and $Cu_{residual}$. Huang et al. (2017) have shown the $\Delta^{65}Cu_{residue\text{-}melt}$ may be as high as 0.3 ‰ for low degree partial melts. It remains unclear whether HAOTs in the MRS were produced by fractional crystallization of picritic magmas or low degrees of partial melting (Ripley, 2014; Ripley et al., 2015).

The remaining possibility, that Cu isotopic fractionation accompanied MSS fractional crystallization, suggests that as sulfide liquids fractionally crystallized, the incorporation of minor Cu in MSS produced substantial fractionations between the MSS and residual liquid (Ripley et al., 2015). Williams and Archer (2011) have shown that fractional crystallization of metallic melts has affected the Cu isotopic composition of a variety of iron meteorites, but it is unknown whether MSS fractional crystallization will produce appreciable Cu isotope fractionation, and experimental work is needed to determine whether any fractionations exist. However, the geologic implication of this mechanism is that the Cu isotope disparity between conduit- and sheet-style intrusions is a function of the stage of sulfide liquid fractional crystallization recorded in the sulfides. For example, high Cu/Ni ratios from the Partridge River Intrusion may be the result of high degrees of sulfide liquid fractionation retaining Cu in the liquid. Hypothetically, if MSS is enriched in ^{65}Cu relative to the sulfide liquid, then we expect the sulfide liquid would have lower $\delta^{65}Cu$ values than typical mantle-derived sulfides. While it

has been shown that many of the Cu- and PPGE-rich sulfides at Eagle and Tamarack were produced by MSS fractional crystallization (Ding et al., 2012a; Taranovic et al., 2016), the sulfides from the Partridge River intrusion appear to be produced by extremely variable R-factors (ratios of silicate magma to sulfide magma), instead of fractional crystallization (Thériault et al., 1997; Smith et al., in press).

Ni isotopes in igneous and sedimentary rocks and associated mineral deposits

The mantle δ^{60}Ni composition has been relatively well-documented to be 0.23 ± 0.06 ‰ (Gall et al., 2017). Komatiite-hosted Fe-Ni-Cu sulfides from the Yilgarn Craton in Australia and the Abitibi Belt in Canada have distinctly different δ^{60}Ni values between -1.04 and -0.1 ‰ (Gueguen et al., 2013). Systematic study of δ^{60}Ni from magmatic Ni-Cu-PGE deposits is limited to igneous-hosted sulfides from the Partridge River intrusion (Asp, 2016), and no analyses are available for the Tamarack or Eagle deposits or any of the rocks from the Stillwater Complex. Results from Asp (2016) show that igneous-hosted sulfides from Partridge River have δ^{60}Ni values from -0.97 to 0.22 ‰.

Ferromanganese crusts have average δ^{60}Ni values of 1.9 ‰ (Gall et al., 2013), and organic-rich Paleozoic and Mesozoic sedimentary rocks range from 0.2 to 2.5 ‰ (Porter et al., 2014). Sulfidic sediments from the Black Sea are routinely in the range of 0.3 to 0.6 ‰, indicating a $\Delta^{60}Ni_{solution\text{-}sulfide}$ of ~ 0.7 ‰ (Vance et al., 2016). Vance et al. (2016) report δ^{60}Ni values as low as 0.14 ‰ for sedimentary sulfides in the Black Sea, but highly negative δ^{60}Ni values have yet to be found in sedimentary rocks. Cameron and Vance (2014) found that fluvial systems have average weighted δ^{60}Ni values of 0.8 ‰, which is significant, as nearly all crustal rocks have δ^{60}Ni values between -0.1 and 0.2 ‰ (Cameron et al., 2009; Gueguen et al., 2013; Gall et al.,

2017). Ocean water is even heavier than fluvial inputs and has an average $\delta^{60}Ni$ value of 1.44 ± 0.15 ‰ (Cameron and Vance, 2014).

Experimental studies of Ni isotope fractionation

Wang and Wasylenki (2017) performed experiments of ferrihydrite precipitation to approximate deposition of banded iron formations and found aqueous solutions are routinely heavier than the precipitated solids ($\Delta^{60}Ni_{solution\text{-}solid}$ = 0.08 to 0.5 ‰), except in low-pH experiments. They also demonstrated that transformation of ferrihydrite to hematite showed little fractionation compared to current analytical uncertainties.

Little experimental data exists on Ni isotope fractionation at elevated temperatures. Lazar et al. (2012) performed experiments on Ni-bearing metal-talc systems and found that the metal was consistently enriched in ^{60}Ni compared to talc.

Potential Ni Fractionation Mechanisms

In the Black Sea, waters range from 1.0 to 1.3 ‰, whereas sulfides commonly range from 0.3 to 0.6 ‰, indicating a $\Delta^{60}Ni_{solution\text{-}sulfide}$ of ~ 0.7 ‰ (Vance et al., 2016) during deposition of euxinic sediments.

Asp (2016) demonstrated a substantial $\Delta^{60}Ni_{silicate\text{-}sulfide}$ of around 0.5 ‰, which is in agreement with other low- and high-temperature studies in which the light isotope is preferentially incorporated into the sulfide phases (Gueguen et al., 2013; Vance et al., 2016). Asp (2016) attributed the 1.19 ‰ spread in igneous-hosted sulfide $\delta^{60}Ni$ values from the Partridge River intrusion solely to primary fractionation between igneous silicates and sulfide. However, Asp (2016) did not measure $\delta^{60}Ni$ variations in the sedimentary country rocks, and

therefore was not able to assess the potential for Ni contribution from the sedimentary or metasedimentary rocks.

Gall et al. (2017) suggested δ^{60}Ni variations in ultramafic rocks are a function of modal mineralogy of the rocks, as well as the modal mineralogy of the mantle from which it was extracted, based on the occurrence of isotopically light olivine and orthopyroxene versus isotopically heavy garnet and clinopyroxene.

Discussion

Cu isotopes of massive sulfides and other samples from the Midcontinent Rift System

Country rock-hosted massive sulfides near Tamarack and Eagle have consistently lower δ^{65}Cu values than their respective igneous rock-hosted sulfides reported by Ripley et al. (2015), although it should be noted that most of the Eagle analyses from Ripley et al. (2015) were from semi-massive sulfides, which have shown to be the result of a distinct pulse of mineralization and are genetically unrelated to the igneous rock-hosted disseminated and massive sulfides (Ding et al., 2012b), as well as the country rock-hosted massive sulfides (Smith et al., in press). Asp (2016) reported one sample of igneous rock-hosted sulfide from Eagle with a low δ^{65}Cu value of -0.16 ‰, which is more similar to what is observed in our samples from Eagle analyzed in this study. All but two of the Tamarack samples reported by Ripley et al. (2015) are from igneous-hosted disseminated sulfides. Smith et al. (in press) have suggested that the country rock-hosted massive sulfides at Tamarack were produced by fractional crystallization of the semi-massive sulfides. Therefore, the previously reported results from Eagle and Tamarack may not be appropriate for comparison to the country rock-hosted massive sulfides, as many of them represent distinct generations of sulfide liquids. Instead, the Eagle and Tamarack analyses

reported here are more similar to near-zero "mantle" values from Ben Othman et al. (2006), Savage et al. (2015), and Liu et al. (2015). Ripley et al. (2015) reported a substantial disparity in Cu isotopic compositions between the isotopically light intrusions of the Duluth Complex compared to the heavy Tamarack and Eagle samples. Although the disparity does not appear to be as substantial, our samples from Duluth extend to much lighter δ^{65}Cu compositions than samples from Eagle and Tamarack.

The mantle-like (near 0 ‰) Cu isotope compositions of many of the Eagle and Tamarack samples require little to no assimilation of local sedimentary rocks (Fig. 46). This is consistent with low degrees of crustal contamination (or conduit exchange processes) indicated by S, Os, and Pb isotopic results from Eagle and Tamarack (Ding et al., 2012b; Taranovic et al., 2018; Smith et al., in press). The value of 1.06 ‰ reported for sample 213-461.19 from Tamarack could easily be produced by mixing of mantle derived melts with isotopically heavy Cu from the Thomson Formation, which has δ^{65}Cu values up to 3.12 ‰ (Ripley et al., 2015). The range of δ^{65}Cu values reported here for massive sulfides below the Partridge River intrusion are within the range of values for igneous rock-hosted sulfides reported by Ripley et al. (2015) and Asp (2016). In light of the now better-constrained mantle values (Savage et al., 2015; Liu et al., 2015), the compositions of the Partridge River samples cannot be explained by mixing between near-zero mantle values and local sedimentary rocks, such as the Virginia and Thomson Formations (Fig. 46), unless a reservoir of isotopically light Cu in the country rocks has yet to be discovered (i.e.: the bedded pyrrhotite unit or Biwabik Iron Formation). It should be noted that the Bedded Pyrrhotite Unit has up to 0.5 wt % Cu in some samples (Samalens et al., 2017a,b). If characterized by substantially negative δ^{65}Cu values, much of the Cu in the Partridge River intrusion could have been derived from the Bedded Pyrrhotite Unit. However, this mechanism

remains purely speculative until appropriate analyses have been undertaken. Because HAOTs related to the Partridge River intrusion are consistent with lower degrees of partial mantle melting, and ^{65}Cu is generally depleted in those melts (Huang et al., 2017), the lower $\delta^{65}Cu$ values from the Partridge River and South Kawishiwi intrusions and country rock-hosted massive sulfides may have been partly produced by low degrees of mantle partial melting and retention of ^{65}Cu in the mantle residue.

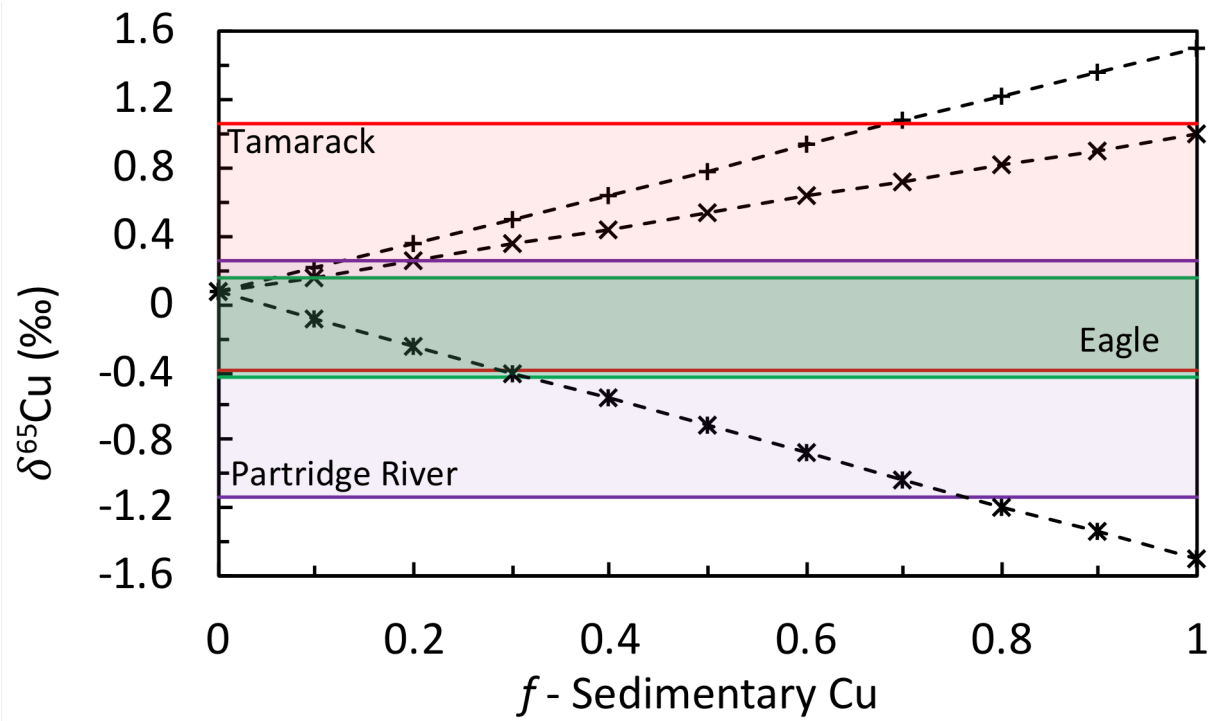

Figure 46: Mixing diagram showing the Cu isotope values of various mixtures of mantle-derived magmas with a mantle $\delta^{65}Cu$ values of 0.07 ‰ and sedimentary Cu with $\delta^{65}Cu$ values of -1.5, 1, and 1.5 ‰. The magmas and contaminants were assumed to have the same Cu concentrations for simplification. Most values measured at Tamarack (red shaded box) and Eagle (green shaded box) can be explained by addition of Cu from isotopically heavy sources, such as the Virginia and Thomson Formations. Low $\delta^{65}Cu$ values of country rock-hosted massive sulfides below the Partridge River Intrusion can be explained by mixing with an isotopically light reservoir, although such a reservoir has yet to be observed.

Ni isotopes of massive sulfides and other samples from the Midcontinent Rift System

A systematic documentation of Ni isotopic compositions from banded iron formations has not been performed, but the IF-G reference material from the ~ 3.8 Ga banded iron formation of the Isua Greenstone Belt has a δ^{60}Ni value of 0.46 ‰ (Gueguen et al., 2013) and is consistent with the positive δ^{60}Ni value reported here for the Biwabik Iron Formation (Fig. 44). The average seawater value of 1.44 ‰ (Cameron and Vance, 2014) is similar to the value of 1.71 ‰ we report for disseminated sulfides in the Virginia Formation. Perhaps the most surprising Ni isotopic compositions we have found are the highly negative values of sedimentary sulfides from the Thompson Formation and the Bedded Pyrrhotite Unit in the Virginia Formation (Fig. 46). The negative δ^{60}Ni values we report for the Bedded Pyrrhotite Unit and the Thomson Formation are unexpected in sedimentary rocks. However, previously reported S isotopic measurements of these sulfides have δ^{34}S values from 0 to 30 ‰, confirming they are sedimentary sulfides (Ripley, 1981; Ripley and Al Jassar, 1987). A possible resolution is that Proterozoic oceans experienced ranges in terms of Ni isotope compositions, whereby lower δ^{60}Ni values may have resulted from increased weathering of mantle-derived sulfides. Another possibility is that ($\Delta^{60}Ni_{solution\text{-}solid}$) for Ni-bearing sulfidic sediments becomes larger as the fraction of Ni incorporated increases. For example, euxinic sediments from the Black Sea only have 20 to 70 ppm Ni (Vance et al., 2016), whereas the Bedded Pyrrhotite Unit in the Virginia Formation can contain up to 900 ppm Ni (Samalens et al., 2017a,b). Additionally, there may still be undocumented fractionations that could have caused the sediments to be exceptionally light in δ^{60}Ni. These options are necessarily speculative and require further low-temperature experimental work on Ni isotope fractionation. Regardless of the mechanism(s), sedimentary sulfides from this study clearly have a wide range in δ^{60}Ni from -3.12 to 1.71 ‰.

Near-zero and slightly negative δ^{60}Ni values from the massive sulfides near the Tamarack, Eagle, and Partridge River intrusions (Fig. 44) are suggestive of magmatic processes that preferentially incorporated ^{58}Ni into the sulfides, as has been documented for komatiites (Gueguen et al., 2013) and the Partridge River intrusion (Asp, 2016). δ^{60}Ni values in massive sulfides below the Partridge River intrusion are lighter than values from massive sulfides from Tamarack and Eagle, suggesting an additional mechanism beyond equilibrium silicate-sulfide fractionation must be controlling the δ^{60}Ni composition of the massive sulfides. To address this possibility, Figure 47 shows model results for sulfide δ^{60}Ni values as a function of silicate liquid:sulfide liquid mass ratios (R-factor of Campbess and Naldrett, 1979). The modeling assumed a δ^{60}Ni value of 0.23 ± 0.06 ‰, for a mantle-derived melt (Gall et al., 2017), and a $\Delta^{60}Ni_{silicate\text{-}sulfide}$ of 0.5 ‰ (Asp, 2016). Figure 47 illustrates how the Ni isotope composition of the sulfides in equilibrium with a silicate melt will vary systematically, depending on the R-factor at which they were produced. As higher R-factors are approached, the δ^{60}Ni values of the sulfides decrease, asymptotically approaching a value of -0.27 ‰, which is 0.5 ‰ lighter than the coexisting melt. Starting with an uncontaminated and sulfide-saturated mantle magma, R-factors from 100 to 1,000 can produce sulfides with δ^{60}Ni values from 0.15 to -0.1 ‰, which are similar to many of the δ^{60}Ni values reported here for Tamarack. δ^{60}Ni values at Eagle are slightly lower than this range and would require either higher R-factors or assimilation of Ni from an isotopically light source, similar to the Thomson Formation or Bedded Pyrrhotite Unit. Additionally, we have modeled the process of contamination of a silicate melt by sulfidic, Ni-bearing sediments with isotopically light δ^{60}Ni values, like those from the Thomson Formation or Bedded Pyrrhotite Unit. The mixing trend is shown by the red line in Fig. 47 and illustrates that as contamination from sulfidic sediments increases, both R-factors and δ^{60}Ni decrease.

Importantly, these models demonstrate two points: (1) δ^{60}Ni compositions of magmatic sulfides decrease as the R-factor increases, and; (2) S addition by contamination will yield lower R-factors. Lower R-factors produce higher δ^{60}Ni unless the contaminants have δ^{60}Ni values lower than the melt. The near-zero to slightly negative δ^{60}Ni values of country rock-hosted massive sulfides from Tamarack and Eagle could have been produced simply due to variable R-factors in conjunction with minor crustal contamination. Furthermore, the δ^{60}Ni values of Cu-poor massive sulfides from near the Partridge River intrusion range from -0.77 to -0.52 ‰ and cannot be explained by variable R-factors in a typical mantle-derived melt. Consistent with previous work, the modeling presented above suggests the sulfides related to the Partridge River intrusion experienced higher degrees of crustal contamination (relative to those at Eagle and Tamarack; Fig. 47) from sulfidic sediments with isotopically light Ni, such as the Bedded Pyrrhotite Unit. Mixing calculations, although highly dependent on the chosen endmembers, suggest that as much as 7 to 17 % of the Ni in the country rock-hosted massive sulfides below the Partridge River intrusion may have been provided by the Bedded Pyrrhotite Unit.

Silicate crystallization history in the magma chambers will also affect the Ni isotope composition of the melt. For example, the biggest Ni sink in igneous silicates is olivine. Gall et al. (2017) showed that olivine also incorporates isotopically light Ni and is commonly ~ 0.1 ‰ lighter than the coexisting silicate. Using a $\Delta^{60}Ni_{melt\text{-}olivine}$ of 0.1 ‰ and a simple model of olivine fractional crystallization (Fig. 48), it is shown that both the olivine and melt will become enriched in ^{60}Ni with progressive crystallization. Sulfides derived from any new silicate liquid would also become correspondingly heavier than typical mantle-derived sulfides and could not have produced the isotopically lighter compositions of the massive sulfides below the Partridge River Intrusion. Ripley et al. (2015) suggested differences in Cu isotope compositions between

the conduit- and sheet-style intrusions may also be due to different degrees of partial melting in the mantle or isotopic heterogeneities in the mantle source, as discussed previously. Because Ni is incorporated in olivine, sulfide, and other phases in the mantle, it is difficult to assess the impact of variable degrees of partial melting, or mantle heterogeneity without experimental data.

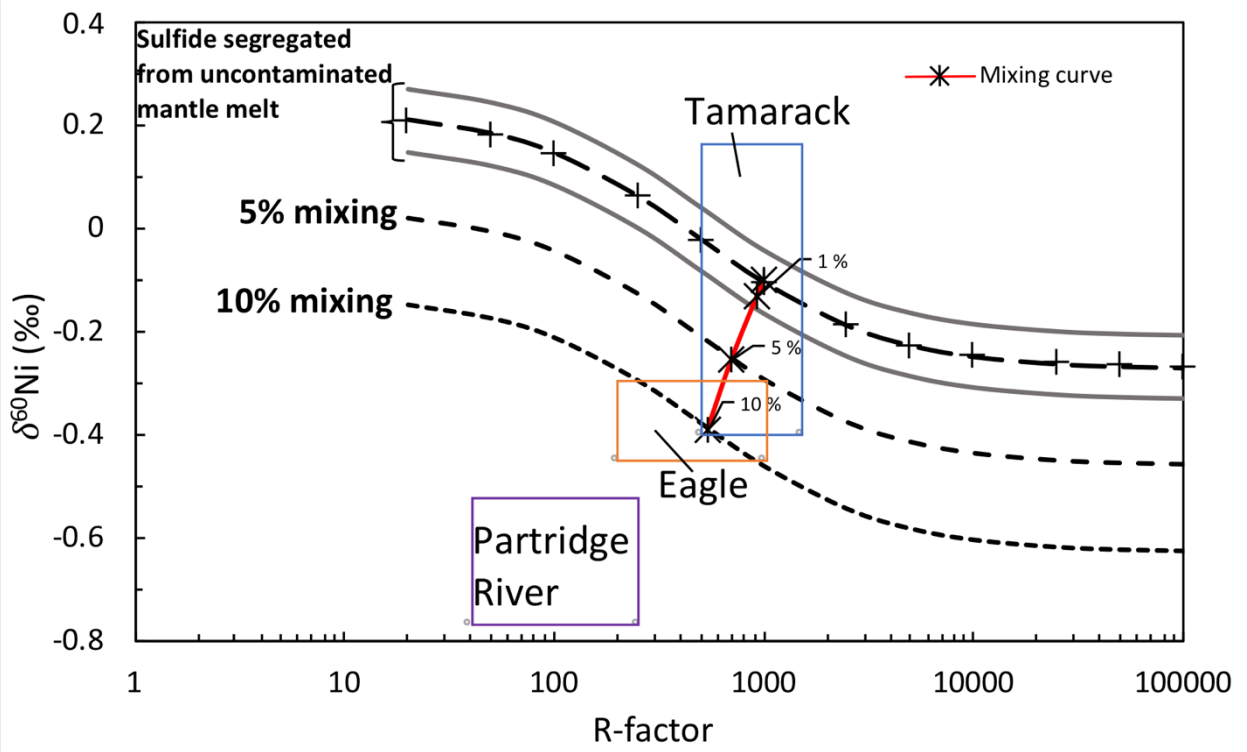

Figure 47: Model of δ^{60}Ni values vs R-factors in response to variable degrees of crustal contamination from sulfidic, Ni-bearing sediments. The uncontaminated system is initially assigned an R-factor of 1,000. See text for explanation.

An additional possibility is that the light δ^{60}Ni values below the PRI are a result of post-magmatic hydrothermal alteration. Ripley (1990) and Smith et al. (in press) show that the most reasonable explanation for decoupling of platinum group element (PGE) systematics of some sulfides associated with the Partridge River Intrusion is due to circulating hydrothermal fluids that preferentially solubilized PPGEs (Pt, Pd, and Au) but not IPGEs (Os, Ir, Ru, Rh). Spivak-

Birndorf et al., (2018) interpreted that fluids associated with Ni laterites preferentially incorporated ^{60}Ni, leaving the residues with lower $\delta^{60}Ni$ compositions. However, Gall et al. (2017) determined that serpentinization does little to affect the $\delta^{60}Ni$ composition of peridotites, but further work is needed to address how hydrothermal alteration affects the Ni isotope composition of sulfides.

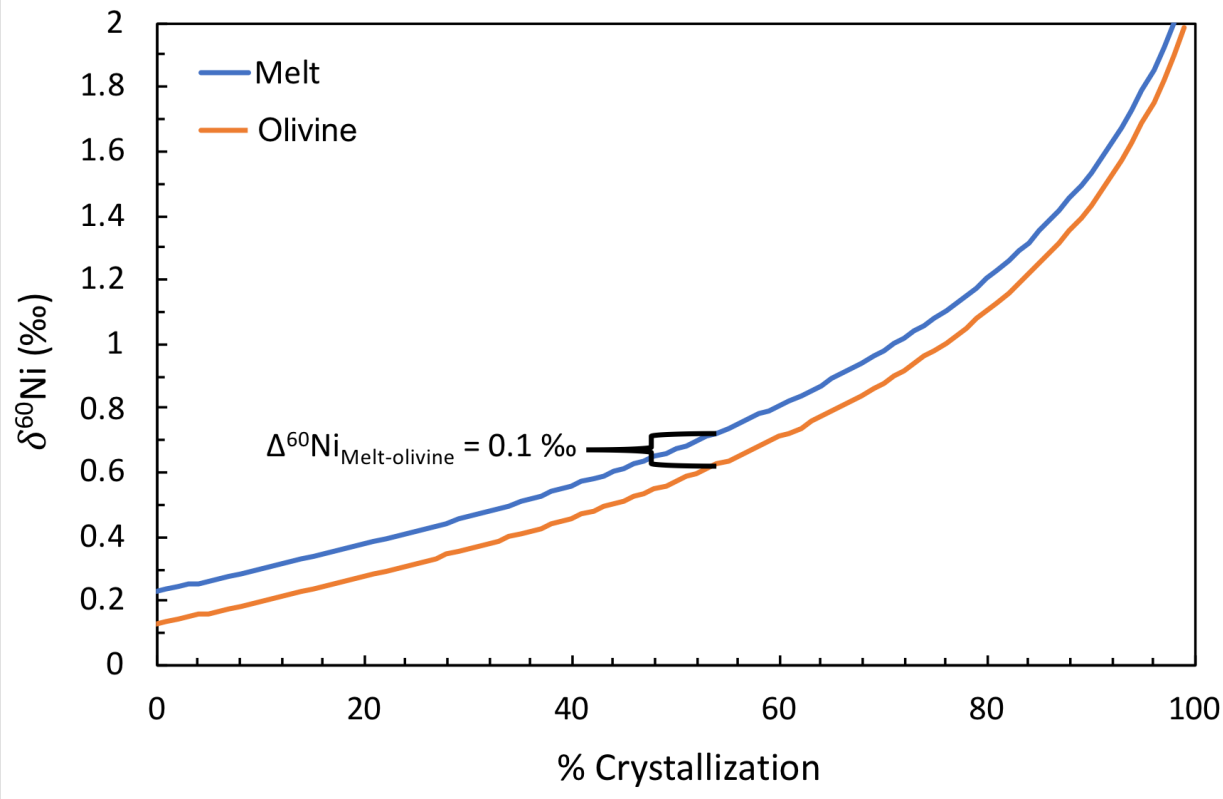

Figure 48: Modeling of $\delta^{60}Ni$ values during olivine fractional crystallization, showing the melt becomes progressively heavier as isotopically lighter olivine is removed. This model of fractional crystallization was performed using a mass balance approach to fractional crystallization, and the numerical solution approaches the analytical solution as the crystallization interval approaches 0.

Two high-Cu samples from below the Partridge River intrusion were also analyzed for $\delta^{60}Ni$ and have very high values of 1.64 and 3.01 ‰. These values are inconsistent with the assimilation of sulfidic sediments with light $\delta^{60}Ni$, as proposed for the low-Cu samples. Instead,

the positive δ^{60}Ni values in the high-Cu samples could be explained by assimilation of isotopically heavy sulfidic sediments, keeping in mind that the Biwabik Iron Formation and a sample of Virginia Formation have δ^{60}Ni values of 0.35 and 1.71 ‰. Alternatively, olivine fractional crystallization could have helped to drive the melt to heavier δ^{60}Ni values (as demonstrated in Fig. 48), which would have produced higher δ^{60}Ni values in the sulfide upon sulfide saturation. Other mechanisms may also play a role, most notably, sulfide liquid fractional crystallization. Although no experimental work exists regarding the isotopic fractionation of Ni between early crystallizing monosulfide solid solution (MSS) and the coexisting sulfide liquid, *ab initio* modeling from Liu et al. (2018) has suggested that the Ni isotope composition of MSS will be sensitive to both temperature and Fe/Ni ratios. Without additional experimental and analytical work, the controls on the δ^{60}Ni compositions of the high-Cu samples remain purely speculative. The discussion above underscores the importance of both R-factors and variable Ni isotope compositions of the contaminants.

Cu isotopes from the Stillwater Complex

Three samples of country rock-hosted massive sulfides below the Stillwater Complex have δ^{65}Cu values between -0.74 to -0.16 ‰, which are within the values reported by Larson et al. (2003) and Malitch et al. (2014) of -1.06 and -0.1 ‰ for the Stillwater Complex (Fig. 49). Smith et al. (in press) have suggested that the country rock-hosted massive sulfides(-oxides) below the Stillwater Complex were deposited prior to emplacement of the igneous rocks in the Complex, most likely as sedimentary sulfides. The negative δ^{65}Cu values reported here are lower than most known sediments, although Chi Fru et al. (2016) report sulfides from Archean black shales that were deposited before the Great Oxidation Event have δ^{65}Cu ratios as low as -0.55 ‰.

Future plans include analyses of igneous-hosted material from the JM Reef and Basal Series of the Stillwater Complex, but without other additional constraints on Cu isotopic composition of the igneous rocks, it is difficult to assess the Cu isotope systematics of the country rock-hosted massive sulfides beneath the Stillwater Complex.

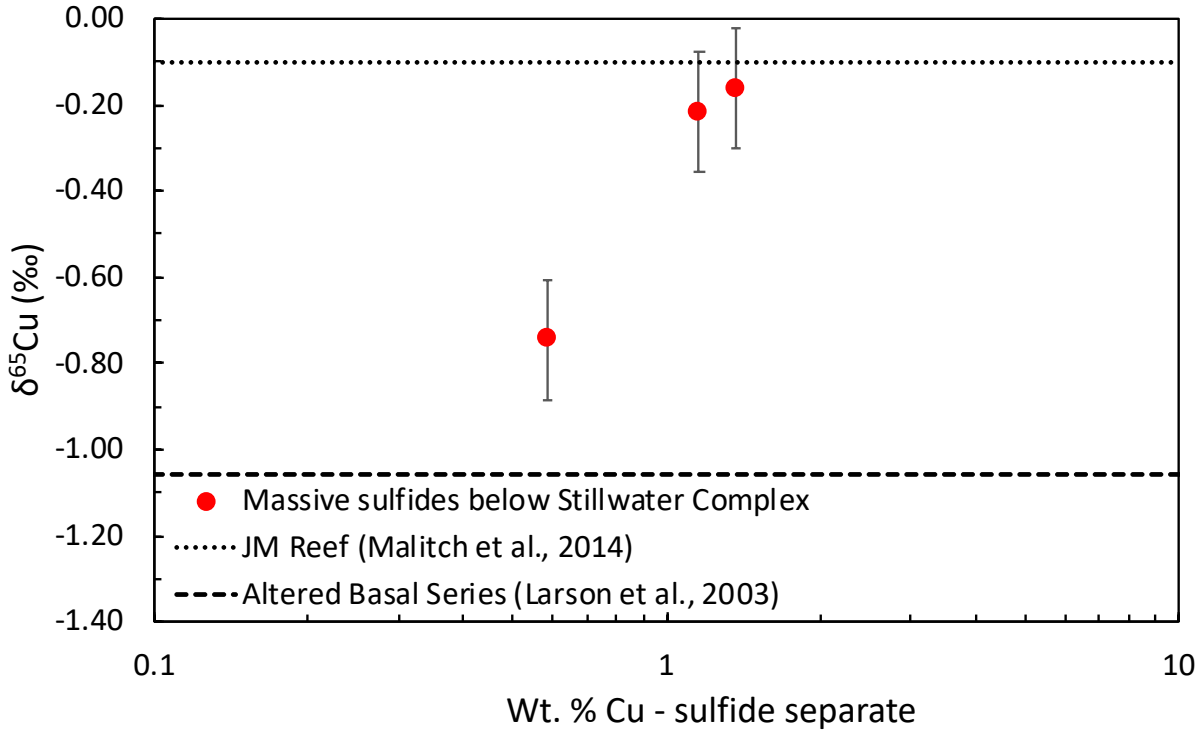

Figure 49: Cu isotope values of country rock-hosted massive sulfides below the Stillwater Complex in relation to two previously published values. Error bars are shown at the 2σ level.

Ni isotopes from the Stillwater Complex

The low δ^{60}Ni values of country rock-hosted massive sulfides below the Stillwater Complex are extremely consistent (Fig. 50), with all samples averaging -0.33 ± 0.16 ‰ (2σ; *n* = *9*). Smith et al. (in press) interpret the country rock-hosted massive sulfides to be the result of sedimentary (or possibly seafloor hydrothermal) processes, prior to emplacement of the Stillwater Complex. If the massive sulfides were chemically precipitated sediments, then it stands that the negative

δ^{60}Ni values may be the result of a lower temperature, fluid-sulfide fractionation. Mineral pairs from the hornfels hosting the massive sulfides have been used to determine that temperatures in the country rocks may have reached as high as ~ 800 ° C during contact metamorphism (Labotka and Kath, 2001; Thomson, 2008; Singha et al., 2011), and a Ni isotope fractionation associated with metamorphism cannot be discounted.

δ^{60}Ni values from the JM Reef are heavy (Fig. 50) in comparison to values of other magmatic sulfides, which are mostly negative or near zero (Gall et al., 2013; Asp, 2016). This suggests that some process(es) aside from an initial magmatic silicate-sulfide fractionation must have contributed to the Ni isotopic composition of the Reef. One possible explanation is that high values may be elevated in part by fractional crystallization of olivine (in addition to other silicates), as demonstrated in Figure 48. However, Jenkins and Mungall (2018) showed that the parental magma of the peridotite zone from the Ultramafic Series in the Stillwater Complex was likely a highly contaminated komatiitic magma. In Figure 51 we have modeled δ^{60}Ni values during fractional crystallization of a high Fe, high Mg siliceous basalt, using a fraction history derived from MELTS (Ghiorso and Sack, 1995). The starting composition is similar to the contaminated komatiite composition of Jenkins and Mungall (2018). Olivine crystallization only occurs in the first ~ 4 % of fractional crystallization (Fig. 51A) and ultimately has little effect on the δ^{60}Ni composition of the of silicate melt (Fig. 51B). However, orthopyroxene crystallization between the interval of 4 and 27 wt. % crystallization causes the δ^{60}Ni value in the melt to rise from 0.23 ‰ to a maximum of 0.39 ‰ at 27 % crystallization. If sulfides form at this point and are associated with high R-factors, they will have δ^{60}Ni values of ~ -0.11 ‰, which is unlike the positive δ^{60}Ni values we report for sulfides in the JM Reef. If sulfide is formed at this point at extremely low R-factors, however, the δ^{60}Ni value in the sulfide will approach the value of 0.39

‰ in the silicate melt, as nearly all the Ni is being partitioned into sulfide (analogous to the illustration in Figure 47). In magmatic models of the JM Reef, high PGE concentrations necessitate extremely high R-factors (Campbell et al., 1983; Keays et al., 2012; Ripley et al., 2017), which would have promoted lower δ^{60}Ni values in the JM Reef. Unless substantially more olivine crystallization occurred, the positive δ^{60}Ni values of high R-factor sulfides from the JM Reef cannot be the result of fractional crystallization of a starting composition like that of the Ultramafic Series.

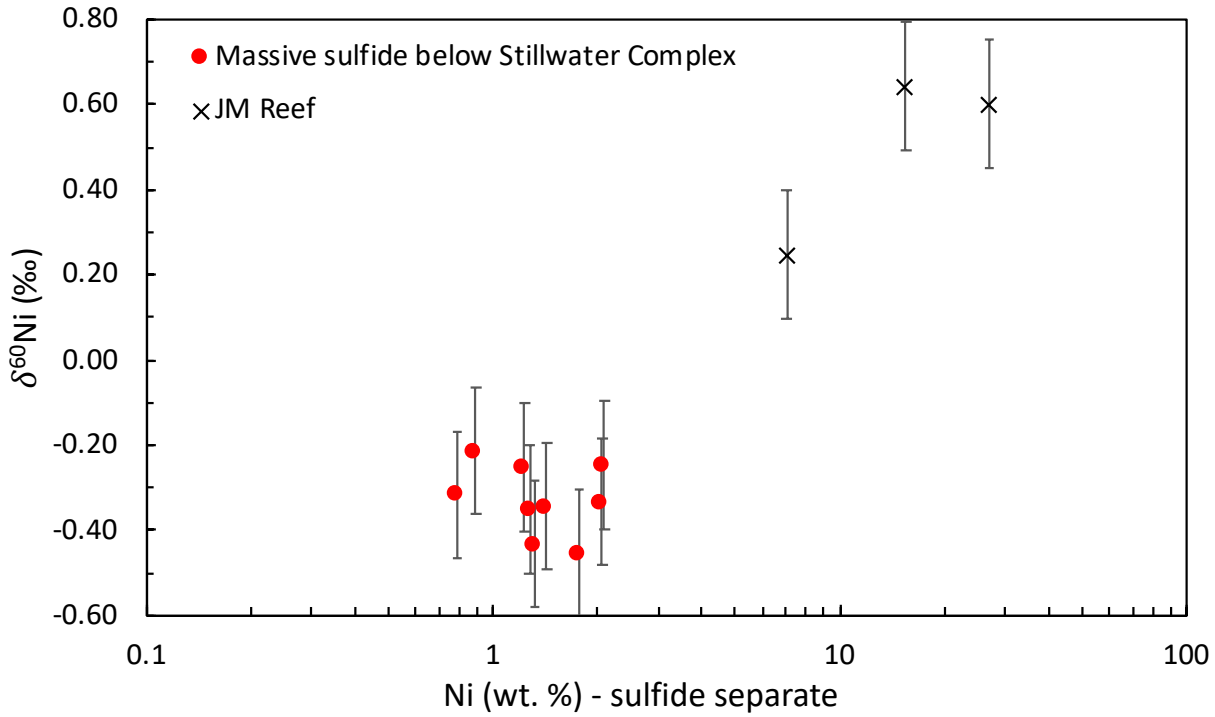

Figure 50: Ni isotope values of country rock-hosted massive sulfides below the Stillwater Complex in relation to Ni isotope values from the JM Reef. Error bars are shown at the 2σ level.

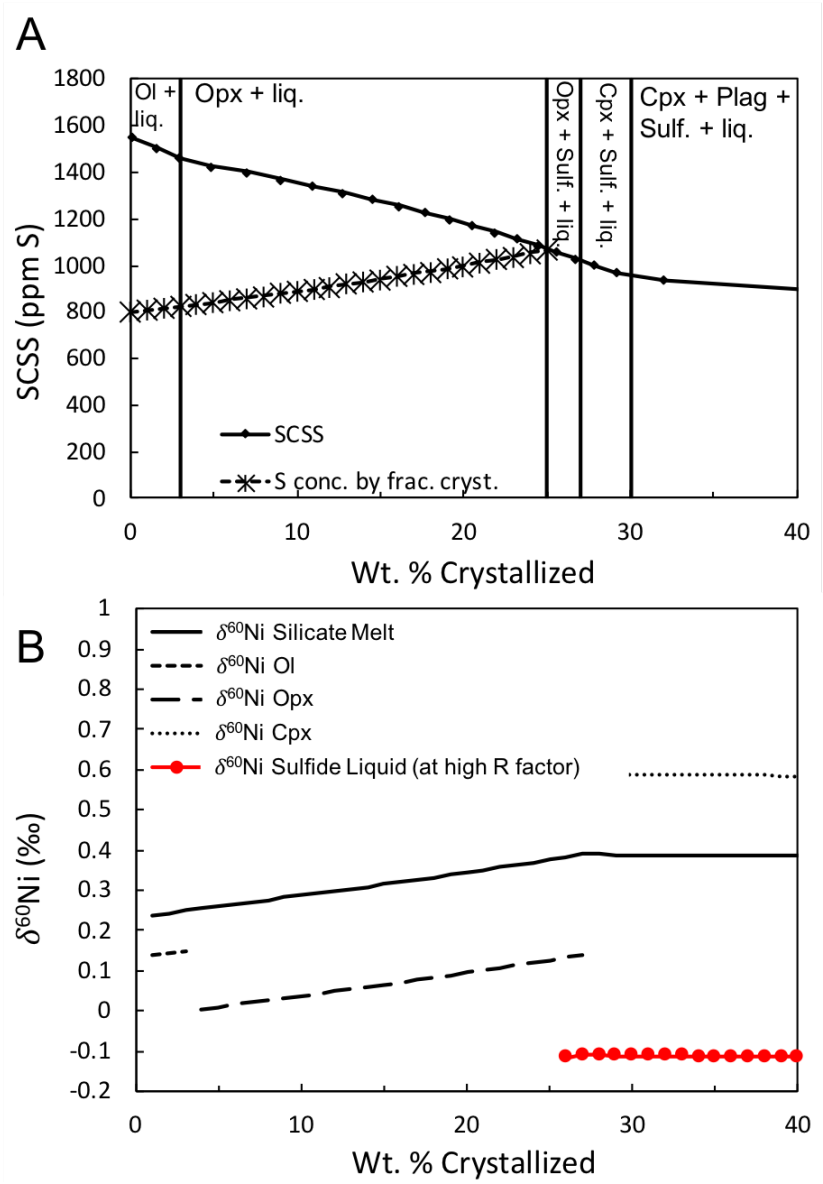

Figure 51: A. Crystallization sequence of a high Fe, high Mg siliceous basalt at QFM (Ghiorso and Sack, 1995). Also plotted is the Sulfur Content at Sulfide Saturation (SCSS) curve and the concentration of S in the silicate magma during crystallization. The SCSS curve was calculated using the equation of Li and Ripley (2009), and the initial magma is assumed to contain 800 ppm S. B. Modeling of δ^{60}Ni values during fractional crystallization of the high Fe, high Mg siliceous basalt. The melt acquires more positive δ^{60}Ni values by olivine and orthopyroxene crystallization and becomes slightly less positive by clinopyroxene crystallization. Sulfide in equilibrium with the silicates is relatively constant and has a maximum δ^{60}Ni of -0.11 ‰ at high R-factors and 0.39 ‰ at very low R-factors. Melt-mineral fractionation factors for silicates were estimated from Gall et al. (2017) and were taken to be 0.1, 0.2, and -0.2 for olivine, orthopyroxene, and clinopyroxene, respectively. The melt-sulfide fractionation factor was taken to be 0.5 (Asp, 2016). Partition coefficients for Ni were assumed to be 7, 2, 0.5, and 500 for olivine, orthopyroxe, clinopyroxene, and sulfide liquid, respectively.

We have also modeled the effects of fractional crystallization on Ni isotope composition, beginning with a more tholeiitic composition, representing the Banded Series from the Stillwater Complex (Fig. 52). Here we have modeled a high aluminum olivine tholeiite, which produces olivine over a longer crystallization interval than in the siliceous basalt (Fig. 52A). In the first 10 percent of crystallization, plagioclase is produced, with no effect on the Ni isotope composition of the magma (Fig. 52B). At 11 percent crystallization, olivine becomes a liquidus phase and begins to incorporate light Ni, driving the δ^{60}Ni of the silicate melt to higher values. However, because the mass ratio of plagioclase to olivine is high, very little of the total Ni is taken up by olivine and the δ^{60}Ni of the melt reaches a maximum of only 0.29 ‰ at 46 % fractional crystallization. Sulfides formed at this point by extremely high R-factors will have a δ^{60}Ni value of ~ -0.21 ‰, whereas sulfides formed at very low R-factors will have δ^{60}Ni values of ~ 0.29 ‰.

Formation of isotopically light sulfides during fractional crystallization would also drive the melt to higher δ^{60}Ni values, leaving later-formed sulfides with heavier δ^{60}Ni values; however, the first formed sulfides would be PGE-enriched and have lower δ^{60}Ni values, and later sulfides would have higher δ^{60}Ni values and low PGE contents. This is inconsistent with the JM Reef, which has both heavy δ^{60}Ni values and high PGE contents.

High R-factors, promoting effective scavenging of PGEs and other chalcophile elements, are typically used to explain the extreme PGE enrichments in the Reef (Campbell et al., 1983; Keays et al., 2012; Ripley et al., 2017); however, the high δ^{60}Ni values in the Reef cannot be explained by high R-factors alone, as high R-factors will drive the sulfides to lower δ^{60}Ni values (see above). The Ni isotope composition of the JM Reef could be explained by substantial crustal contamination from sedimentary rocks with heavy Ni compositions. The only substantially nickel-rich rocks near the Stillwater Complex are the country rock-hosted massive sulfide(-

oxides) (Smith et al., in press). However, the country rock-hosted massive sulfide(-oxides) have negative δ^{60}Ni values and could not have produced the compositions in the JM Reef by mixing with a mantle-derived melt. Additionally, most previous work generally proposes only minor amounts of crustal contamination were involved in production of the JM Reef (Martin, 1989; Lambert et al., 1994; Ripley et al., 2017).

Others have suggested that the JM Reef is a product of upward migrating magmatic-hydrothermal fluids that carried dissolved Pd and Pt as chloride or bisulfide complexes (Boudreau and McCallum, 1992), although Barnes and Liu (2012) have suggested the relative immobility of Pt and Pd in aqueous hydrothermal fluids is inconsistent with this model. In many cases, alteration of primary magmatic sulfides has apparently caused metal upgrading by residual enrichment (Holwell et al., 2017). Regardless, Ni isotopic compositions of weathering profiles have shown that isotopically depleted Ni is retained in weathered mineral phases, whereas the fluid is enriched in isotopically heavy Ni (Spivak-Birndorf et al., 2018). Provided that quantitative scavenging of Ni from the hydrothermal fluids occurred, the Ni isotope compositions of the sulfides precipitated from this solution may also be enriched in ^{60}Ni. Without additional analyses, the most reasonable interpretation based on Ni isotope data is that Ni in the JM Reef was added by isotopically heavy hydrothermal fluids. If this model is correct, then the measured Ni isotopic compositions are clearly not representative of the original composition of a mantle-derived melt. Additional work is aimed at documenting δ^{60}Ni compositions of sulfides from the Basal Series, which do show substantial S isotope evidence of crustal contamination, unlike the JM Reef (Zientek and Ripley, 1990; Ripley et al., 2017).

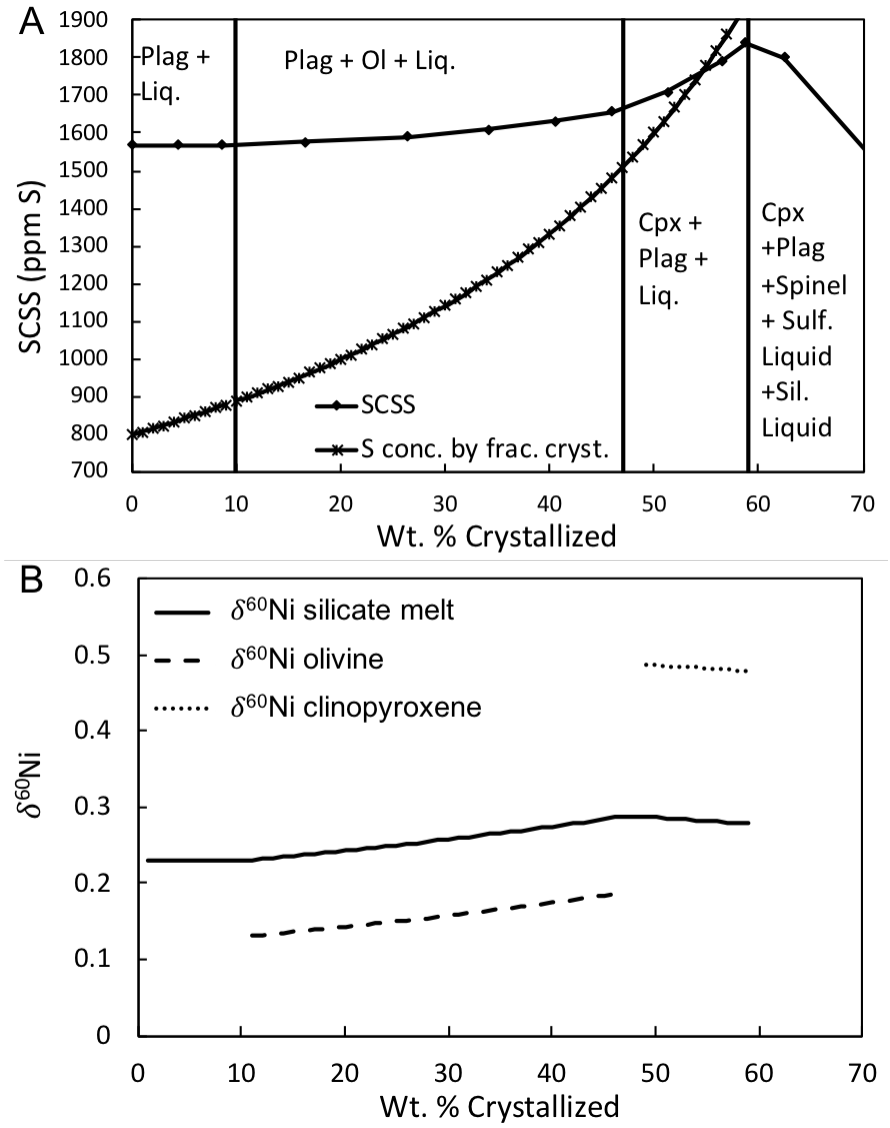

Figure 52: A. Crystallization sequence of a high aluminum olivine tholeiite at QFM (Ghiorso and Sack, 1995). Also plotted is the Sulfur Content at Sulfide Saturation (SCSS) curve and the concentration of S in the silicate magma during crystallization. The SCSS curve was calculated using the equation of Li and Ripley (2009), and the initial magma is assumed to contain 800 ppm S. B. Modeling of δ^{60}Ni values during fractional crystallization of the high aluminum olivine tholeiite. The melt δ^{60}Ni value is unaffected by early plagioclase crystallization. Olivine crystallization causes the melt to attain more positive δ^{60}Ni values, although the effect is subdued due to the preponderance of plagioclase crystallization. Sulfide in equilibrium with the silicates is relatively constant and has a maximum δ^{60}Ni of -0.21 ‰ at high R-factors and a maximum of 0.29 ‰ at low R-factors. Melt-mineral fractionation factors for silicates were estimated from Gall et al. (2017) and were taken to be 0.1, 0.2, and -0.2 for olivine, orthopyroxene, and clinopyroxene, respectively. The melt-sulfide fractionation factor was taken to be 0.5 (Asp, 2016). Partition coefficients for Ni were assumed to be 7, 2, 0.5, and 500 for olivine, orthopyroxe, clinopyroxene, and sulfide liquid, respectively.

Conclusions

Cu isotope values of country rock-hosted massive sulfides near conduit-style intrusions from the Midcontinent Rift have mantle-like δ^{65}Cu values that require little in the way of crustal contamination to explain their measured compositions. They are different from many of the heavy δ^{65}Cu values reported for igneous-rock hosted sulfides from Tamarack and Eagle (Ripley et al., 2015), but as noted in the discussion, because those samples are from different generations of mineralization, they may not serve as the best comparisons. Country rock-hosted massive sulfides below the sheet-style Partridge River intrusion have δ^{65}Cu that are in excellent agreement with the range of igneous-rock hosted sulfides from the intrusion (Ripley et al., 2015; Asp, 2016). Most samples cannot be explained by mixing with known crustal reservoirs, such as the Virginia and Thomson Formations, as those sedimentary rocks have heavier δ^{65}Cu values than both the mantle and the massive sulfides. Instead, we suggest an unknown reservoir of isotopically light Cu has yet to be identified (such as the Bedded Pyrrhotite Unit or Biwabik Iron Formation). Additionally, modeling from Huang et al. (2017) has shown that magmas produced by low degrees of partial mantle melting can be up to 0.3 ‰ lighter than residual mantle due to incomplete sulfide melting. Because the Partridge River intrusion is genetically related to high aluminum olivine tholeiites, which may be produced by low degrees of partial melting, we suggest this process may have partly contributed to the light δ^{65}Cu values of samples in and below the Partridge River intrusion. The negative δ^{65}Cu values from country rock-hosted massive sulfides below the Stillwater Complex are non-unique, as they fall in the range of two previous analyses of igneous rocks from the Complex (Larson et al., 2003; Malitch et al., 2014), and also have similar δ^{65}Cu values to Archean sedimentary sulfides (Chi Fru et al., 2016).

Ni isotope compositions of country rock-hosted massive sulfides near Tamarack and Eagle have slightly positive to slightly negative δ^{60}Ni values. These can be explained by small amounts of crustal contamination involving an isotopically depleted sedimentary source, such as the Bedded Pyrrhotite Unit or the Thomson Formation, assuming a $\Delta^{60}Ni_{silicate\text{-}sulfide}$ of 0.5 ‰ (Asp, 2016) and negligible olivine crystallization prior to sulfide saturation. δ^{60}Ni values from Eagle require slightly more contamination than samples from Tamarack, which is consistent with previous S, Pb, and Re-Os analyses (Smith et al., in press). Cu-poor massive sulfides from below the Partridge River intrusion have lighter δ^{60}Ni values than those at Tamarack and Eagle and require higher degrees of contamination from the isotopically light sedimentary source. We emphasize the effect crustal contamination has on magmas in terms of both R-factors and δ^{60}Ni compositions. Addition of sulfidic sedimentary rocks will decrease R-factors. Lower R-factors (like those proposed for these intrusions) will promote higher δ^{60}Ni values in the coexisting sulfide liquids, unless the δ^{60}Ni value in the contaminants are lower than the expected δ^{60}Ni value of the sulfide (based on the calculated R-factor). This appears to be the case for samples in and below the Partridge River intrusion, which have highly negative δ^{60}Ni values. The cause of extremely positive δ^{60}Ni values in two Cu-rich massive sulfides below the Partridge River intrusion remains unknown, but we speculate they may have resulted from mixing with isotopically heavier sources, such as the Virginia Formation, or there may be a Ni isotopic fractionation that accompanies sulfide liquid fractional crystallization. High temperature experiments are needed in order to determine if such fractionations exist. Samples of country rock-hosted massive sulfides below the Stillwater Complex have very consistent δ^{60}Ni values averaging -0.33 ‰, whereas the JM Reef has δ^{60}Ni values from 0.25 to 0.64 ‰. Smith et al. (in press) interpret the country rock-hosted massive sulfides to be sedimentary or seafloor

hydrothermal products, which likely contaminated the Basal Series. However, the δ^{60}Ni values from the JM Reef could not be produced by contamination involving the massive sulfides, as the Reef is heavier than mantle derived rocks and the massive sulfides. From our modeling, it also appears that without significantly more olivine or orthopyroxene crystallization, the positive δ^{60}Ni values of sulfides from the JM Reef could not have been the result of fractional crystallization. Instead, we suggest the positive δ^{60}Ni values in the Reef were the result of post-magmatic fluids that preferentially incorporated ^{60}Ni.

Conclusions

- Massive sulfides near the Tamarack Intrusive Complex are very similar to igneous-hosted mineralization, especially semi-massive sulfides from the CGO intrusion. As with the igneous-hosted sulfides, their S, Pb, and Os, isotopic compositions are consistent with mixing of mantle-derived magmas and crustal contaminants. Additionally, insights from Ni and Cu isotope compositions suggest the country rock-hosted massive sulfides are mainly controlled by the mantle Ni/Cu composition, whereas slight deviations from the mantle range may be due to crustal contamination. Crustal contamination may also play a role in minor heterogeneity of Ni isotope compositions due to R factor variations on the deposit scale. PGE analyses and fractional crystallization models suggest the massive sulfides were produced by fractional crystallization of semi-massive sulfides within the CGO intrusion. Because the country rock-hosted massive sulfides occupy a space between the FGO and the underlying CGO, it appears the massive sulfides were igneous sulfides filter-pressed from the CGO below. After emplacement, the sulfide fractionally crystallized from the bottom-up.

- Country rock-hosted massive sulfides proximal to the Eagle Intrusion are also very similar to igneous-hosted mineralization, especially igneous-hosted massive sulfides. None of the country rock-hosted massive sulfides appear to be related to the semi-massive sulfides. As with the igneous-hosted sulfides, S, Pb, and Os isotope results are consistent with mixing of mantle derived magmas and minor degrees of crustal contamination. Ni and Cu isotope compositions are mostly controlled by the mantle Ni/Cu composition, and like at Tamarack, minor deviation in the Ni isotope compositions may be due to contamination, although the Ni isotope compositions at Eagle are more tightly constrained than those at Tamarack. PGE analyses and fractional crystallization models also indicate the country rock-hosted massive sulfides are identical to massive sulfides within the igneous rocks. The country rock-hosted massive sulfides were, therefore, igneous sulfides that leaked from the igneous-hosted massive sulfides at variable times in their crystallization history
- Country rock-hosted massive sulfides below the Partridge River Intrusion are mostly similar to igneous-hosted mineralization, with exception of two main features: the country rock-hosted massive sulfides are all depleted in PPGEs, especially Pt, relative to igneous-hosted sulfides and the S, Pb, and Os isotope compositions of the country rock-hosted massive sulfides record higher degrees of crustal contamination than the igneous-hosted sulfides. Ni isotope compositions are also consistent with higher degrees of contamination in the country rock-hosted massive sulfides. It is expected that Cu isotope compositions will also be consistent with this if an appropriate crustal reservoir is found with negative δ^{65}Cu values. We suggest this may be the bedded pyrrhotite unit within the Virginia Formation. PPGE depletions were likely a result of hydrothermal alteration, whereas all other PGEs are explained by formation of low-R factor sulfides, similar to many disseminated sulfides within the Partridge River Intrusion. The country rock-hosted massive sulfides reflect primarily igneous processes as they formed when igneous sulfides leaked from the igneous-hosted sulfides. Ongoing devolatilization reactions, or direct

contamination, during metamorphism provided additional crustal input, which produced isotopic compositions in the massive sulfides consistent with higher degrees of bulk contamination than in the igneous rock-hosted sulfides.

- Massive sulfides below the Stillwater Complex have very different PGE compositions than igneous-hosted sulfides, and are instead more similar to disseminated sulfides from the hornfels. S, Pb, and Os isotopic compositions of the country rock-hosted massive sulfides display anomalous $\Delta^{33}S$ and very radiogenic Pb and Os compositions, which are consistent with a crustal source. Results of Ni and Cu isotope analyses are non-unique but are consistent with sedimentary origins. O isotope analyses of magnetite from massive sulfide(-oxides) have similar $\delta^{18}O$ values to the Stillwater Iron Formation. They are clearly unlike igneous magnetites associated with magmatic sulfides, which we have documented, in samples from the Voisey's Bay deposit, to be lighter than the igneous silicates. The country rock-hosted massive sulfides below the Stillwater Complex are non-magmatic and their original deposition was genetically unrelated to emplacement of the Stillwater Complex. They are either sedimentary or hydrothermal in origin. Any textural evidence to support either of these models has been destroyed by pyroxene hornfels facies metamorphism which is estimated to have reached up to 825 °C in the Stillwater Complex metamorphic aureole. However, elevated S/Se ratios and low Co/Ni ratios suggest a sedimentary model is appropriate.
- In general, Ni isotope compositions of igneous sulfides are controlled by modal mineralogy of the mantle, olivine crystallization, silicate liquid:sulfide liquid ratios (R-factors), and crustal contamination. Circulating postmagmatic hydrothermal fluids may also effect Ni isotopic compositions in the igneous rocks. Sulfide liquid fractional crystallization and variable degree of partial melting may also influence Ni isotope compositions of the sulfides, but experimental work is needed to properly evaluate this possibility. Ni isotope compositions of sedimentary sulfides,

possibly like those below the Stillwater Complex, are likely controlled by a primary fluid-sulfide fractionation.

- Cu isotope compositions of igneous sulfides are controlled by the degree of partial melting in the mantle and crustal contamination. Because the partition coefficient for Cu in sulfide is very high, little isotopic fractionation is thought to occur during silicate crystallization or as a result of variable R-factors. Sulfide liquid fractional crystallization may also influence Cu isotope composition of the sulfides, but again, experimental work is needed to thoroughly assess this possibility.

References:

Acholla, F.V. and Orr, W.L., 1993, Pyrite removal from kerogen without altering organic matter: the chromous chloride method: Energy and Fuels, v. 7, p. 406 – 410.

Albarède, F., 2004, The stable isotope geochemistry of copper and zinc: Reviews in Mineralogy & Geochemistry, v. 55, p. 409 – 427.

Andrews M. and Ripley E. M., 1989, Mass transfer and sulfur fixation in the contact aureole of the Duluth Complex, Dunka Road Cu-Ni deposit, Minnesota. Canadian Mineral. v. 27, p. 293-310.

Archer, C. and Vance, D. ,2006, Coupled Fe and S isotope evidence for Archean microbial Fe(III) and sulfate reduction: Geology, v. 34, p. 153 – 156.

Arcuri, T., Ripley, E.M., and Hauck, S.A., 1998, Sulfur and oxygen isotopic studies of the interaction between pelitic xenoliths and basaltic magma at the Babbitt and Serpentine Cu-Ni deposits, Duluth Complex, Minnesota: Economic Geology, v. 93, p. 1063–1075.

Asael, D., Matthews, A., Bar-Matthews, M., and Halicz, L., 2007, Copper isotope fractionation in sedimentary copper mineralization (Timna Valley, Israel): Chemical Geology, v. 243, p. 238 – 254.

Asp, K., 2016, An investigation of Ni and Cu isotopic fractionation in basal Duluth Complex Cu-Ni-PGE mineralization, Northeastern Minnesota: M.S. thesis, University of Minnesota, Duluth (176pp, https://conservancy.umn.edu/handle/11299/181811).

Bajwah, Z., Seccombe, P., and Offler, R., 1987, Trace element distribution, Co:Ni ratios and genesis of the Big Cadia iron-copper deposit, New South Wales, Australia: Mineralium Deposita, v. 22, p. 292 – 300.

Balistrieri, L.S., Borrok, D.M., Wanty, R.B., Ridley, W.I., 2008, Fractionation of Cu and Zn isotopes during adsorption onto amorphous Fe(III) oxyhydroxide: experimental mixing of acid rock drainage and ambient river water: Geochimica et Cosmochimica Acta, v. 72, p. 311 – 328.

Barker, R.W., 1975, Metamorphic mass transfer and sulfide genesis, Stillwater intrusion, Montana: Economic Geology, v. 70, p. 275 – 298.

Barnes, S.J. and Liu, W., 2012, Pt and Pd mobility in hydrothermal fluids: evidence from komatiites and from thermodynamic modelling: Ore Geology Reviews, v. 44, p. 49 – 58.

Barnes, S.J. and Naldrett, A.J., 1985, Geochemistry of the J-M (Howland) reef of the Stillwater Complex, Minneapolis adit area I. Sulfide chemistry and sulfide-olivine equilibrium: Economic Geology, v. 80, p. 627 – 645.

Barnes, S.J., Makovicky, E., Karup-Moller, S., Makovicky, M., Rose-Hansen, J., 1997, Partition coefficients for Ni, Cu, Pd, Pt, Rh, and Ir between monosulphide solid solution and sulphide liquid and the implications for the formation of compositionally zoned Ni-Cu sulphide bodies by fraction of sulfide liquid: Canadian Journal of Earth Sciences, v. 34, p. 366 – 374.

Barnes, S.J., Staude, S., Le Vaillant, M., Piña, R., and Lightfoot, P.C., 2018, Sulfide-silicate textures in magmatic Ni-Cu-PGE sulfide ore deposits: massive, semi-massive, and sulfide-matrix breccia ores: Ore Geology Reviews, v. 101, p. 629 – 651.

Barnes, S-J. and Lightfoot, P.C., 2005, Formation of magmatic nickel sulfide deposits and processes affecting their copper and platinum group element contents. *In*: Hedenquist, J.W., Thompson, J.F.H., Goldfarb, R.J., and Richards, J.P. (eds) Economic geology 100th anniversary volume. Society of Economic Geologists, Littleton, p. 179 – 213.

Barnes, S-J. and Naldrett, A.J., 1987, Fractionation of the platinum-group elements and gold in some komatiites of the Abitibi greenstone belt, northern Ontario: Economic Geology, v. 82, p. 165 – 183.

Barnes, S-J., Naldrett, A.J., and Gorton, M.P., 1985, The origin of the fractionation of platinum group elements in terrestrial magmas: Chemical Geology, v. 53, p. 303 – 323.

Barnes, S-J., Melezhik, V.A., and Sokolov, S.V., 2001, The composition and mode of formation of the Pechenga nickel deposits, Kola peninsula, Northwestern Russia: Canadian Mineralogist, v. 39, p. 447 – 471.

Barnes, S-J., Savard, D., Bédard, P., and Maier, W.D., 2009, Selenium and sulfur concentrations in the Bushveld Complex of South Africa and implications for formation of the platinum-group element deposits: Mineralium Deposita, v. 44, p. 647 – 663.

Barnes, S.-J., Maier, W.D., and Curl, E.A., 2010, Composition of the marginal rocks and sills of the Rustenburg Layered Suite, Bushveld Complex, South Africa: Implications for formation of the platinum group element deposits: Economic Geology, v. 105, p. 1491 – 1511.

Barnes, S-J., Pagé, P. Prichard, H.M., Zientek, M.L., and Fisher, P.C., 2016, Chalcophile and platinum-group element distribution in the ultramafic series of the Stillwater Complex, MT, USA – implications for processes enriching chromite layers in Os, Ir, Ru, and Rh: Miner. Deposita, v. 51, p. 25 – 47.

Bea, F., Pereira, M.D., and Stroh, A., 1994, Mineral/leucosome trace-element partitioning in a peraluminous migmatite (a laser ablation-ICP-MS study): Chemical Geology, v. 117, p. 291 – 312.

Ben Othman, D., Luck, J.M., Bodinier, J.L., Arndt, N.T., Albarede, F., 2006, Cu-Zn isotopic variations in the earth's mantle: Geochimica et Cosmochimica Acta, v. 70, p. 46 (abstract)

Bonnichsen, B., 1975, Geology of the Biwabik iron formation, Dunka River area, Minnesota: Economic Geology, v. 70, p. 319 – 340.

Boudreau, A.E., 2016, The Stillwater Complex, Montana – overview and the significance of volatiles: Mineralogical Magazine, v. 80, p. 585 – 637.

Boudreau, A.E., and McCallum, I.S., 1986, Halogen geochemistry of the Stillwater and Bushveld Complexes; evidence for transport of platinum group elements by Cl-rich fluids: Journal of Petrology, v. 27, p. 967 – 986.

Boudreau, A.E. and McCallum, I.S., 1992, Concentration of platinum group elements by magmatic fluids in layered intrusions: Economic Geology, v. 87, p. 1830 – 1848.

Bow, C., Wolfgram, D., Turner, A., Barnes, S., Evans, J., Zdepski, M., and Boudreau, A., 1982, Investigations of the Howland Reef of the Stillwater Complex, Minneapolis adit area: stratigraphy, structure, and mineralization: Economic Geology, v. 77, p. 1481 – 1492.

Braxton, D., and Mathur, R., 2011, Exploration applications of copper isotopes in the supergene environment: a case study of the Bayugo porphyry copper-gold deposit, southern Philippines: Economic Geology, v. 106, p. 1447 – 1463.

Brenan, J.M., Cherniak, D.J., and Rose, L.A., 2000, Diffusion of osmium in pyrrhotite and pyrite: implications for closure of the Re-Os isotopic system: Earth and Planetary Science Letters, v. 180, p.

Cameron, V., and Vance, D., 2014, Heavy nickel isotope compositions in rivers and the oceans: Geochimica et Cosmochimica Acta, v. 128, p. 195 – 211.

Cameron, V., Vance, D., Archer, C., House, C.H., 2009, A biomarker based on the stable isotopes of nickel: Proceedings of the National Academy of Sciences, v. 106, p. 10944 – 10948.

Campbell, I.H., 2001, Identification of ancient mantle plumes. *In* Ernst, R.E. and Buchan, K.L., eds., Mantle Plumes: their identification through time: Boulder, Colorado, Geological Society of America Special Paper 352, p. 5 – 21.

Campbell, I.H., and Murck, B.W., 1993, Petrology of the G and H chromitite zones in the Mountain View area of the Stillwater Complex, Montana: Journal of Petrology, v. 34, p. 291 – 316.

Campbell, I.H. and Naldrett, 1979, The influence of silicate:sulfide ratio on the geochemistry of magmatic sulfides: Economic Geology, v. 74, p. 1503 – 1505.

Campbell, I.H., Naldrett, A.J., and Barnes, S.J., 1983, A model for the origin of the platinum-rich sulfide horizons in the Bushveld ad Stillwater Complexes: Journal of Petrology, v. 24, p. 133 – 165.

Cannon, W.F., 1994, Closing of the Midcontinent rift – a far-field effect of Grenvillian compression: Geology, v. 22, p. 155 – 158.

Chapman, J.B., Mason, T.F.D., Weiss, D.J., Coles, B.J., Wilkinson, J.J., 2006, Chemical separation and isotopic variations of Cu and Zn from five geological reference materials: Geostandards and Geoanalytical Research, v. 359, p. 136 – 149.

Chi Fru, E., Rodriquez, N.P., Partin, C.A., Lalonde, S.V., Andersson, P., Weiss, D.J., El Albani, A., Rodushkin, I., and Konhauser, K.O., 2016, Cu isotopes in marine black shales record the Great Oxidation Event: Proceedings on the National Academy of Sciences, v. 113, p. 4941 – 4946.

Claire, M.W., Kastin, J.F., Domagal-Goldman, S.D., Stueken, E.E., Buick, R., and Meadows, V.S., 2014, Modeling the signature of sulfur mass-independent fractionation produced in the Archean atmosphere: Geochimica et Cosmochimica Acta, v. 141, p. 365 – 380.

Coffin, M.F., and Eldholm, O., 1994, Large igneous provinces: Crustal structure, dimension, and external consequences: Reviews of Geophysics, v. 32, p. 1 – 36.

Cooper, R.W., 1997, Magmatic unconformities and stratigraphic relations in the peridotite zone, Stillwater Complex, Montana: Canadian Journal of Earth Science, v. 34, p. 407 – 425.

Corson, S.R., Childs, J.F., Dahy, J.P., Keith, D.W., Koski, M.S., LeRoy, L.W., 2002, The reef package stratigraphy that contains the J-M platinum-palladium reef of the Stillwater Complex, Montana: 9th International Platinum Symposium, Billings, MT, 2002, Extended Abstracts 105.

Cox, K.G., Bell, J.D., and Pankhurst, R.J., 1979, The interpretation of igneous rocks: London, Boston, Allen, and Unwin, 450 p.

Czamanske, G.K., Force, E.R., Moore, W.J., 1981, Some geologic and potential resources aspects of rutile in porphyry copper deposits: Economic Geology, v. 76, p. 2240 – 2245.

Czamanske, G.K., Kunilov, V.E., Zientek, M.L., Cabri, L.J., Likhachev, A.P., Calk, L.C., and Oscarson, R.L., 1992, A proton-microprobe study of magmatic sulfide ores from the Noril'sk – Talnakh district, Siberia: The Canadian Mineralogist, v. 30, p. 249 – 287.

Czamanske, G., Zen'ko, T., Fedorenko, V., Calk, L, Budahn, J., Bullock, J., Fries, T., King, B, and Siems, D., 1995, Petrography and geochemical characterization of ore-bearing intrusion of the Noril'sk type, Siberia; with discussion of their origin: Resource Geology, special issue 18, p. 1 – 48.

Dahl, P.S., 1979, Comparative geothermometry based on major-element and oxygen isotope distributions in Precambrian metamorphic rocks from southwestern Montana: American Mineralogist, v. 64, p. 1280 – 1293.

Dare, S., Barnes, S-J., Prichard, H., and Fisher, P., 2014, Mineralogy and geochemistry of Cu-rich ores from the McCreedy East Ni-Cu-PGE deposit (Sudbury, Canada): implications for the behavior of platinum group and chalcophile elements at the end of crystallization of a sulfide liquid: Economic Geology, v. 109, p. 343 – 366.

Davis, D.W. and Paces, J.B., 1990, Time resolution of geologic events on the Keweenaw Peninsula and implications for development of the Midcontinent Rift system: Earth and Planetary Science Letters, v. 97, p. 54 – 64.

Dekov, V.M., Rouxel, O., Asael, D., Halenius, U., Munnik, F., 2013, Native Cu from the oceanic crust: isotopic insights into native metal origin: Chemical Geology, v. 359, p. 136 – 149.

DePaolo, D.J. and Wasserburg, G.J., 1979, Sm-Nd age of the Stillwater Complex and the mantle evolution curve for neodymium: Geochim. et Cosmochim. Acta, v. 43, p. 999 – 1008.

Ding, T., Valkiers, S., Kipphardt, H., De bi'evre, P., Taylor, P, Gonfiantini, R., and Krouse, R., 2001, Calibrated sulfur isotope abundance ratios of three IAEA sulfur isotope reference materials and V-CDT with a reassessment of the atomic weight of sulfur: Geochimica et Cosmochimica Acta, v.65, p. 2433-2437.

Ding, X., Li, C., Ripley, E.M., Rossell, D., and Kamo, S., 2010, The Eagle and East Eagle sulfide ore-bearing mafic-ultramafic intrusions in the Midcontinent Rift System, Upper Michigan: geochronology and petrologic evolution: Geochemistry, Geophysics, and Geosystems. http://dx.doi.org/10.1029/2009GC002546.

Ding, X., Ripley, E., and Li, C., 2012a, PGE geochemistry of the Eagle Ni-Cu-(PGE) deposit, Upper Michigan: constraints on ore genesis in a dynamic magma conduit: Mineralium Deposita, v. 47, p. 89-104.

Ding, X., Ripley, E., Shirey, S., and Li, C., 2012b, Os, Nd, O, and S isotope constraints on country rock contamination in the conduit-related Eagle Cu-Ni-(PGE) deposit, Midcontinent Rift System, Upper Michigan: Geochimica et Cosmochimica Acta, v. 89, p. 10-30.

Ebel, D.S. and Naldrett, A.J., 1997, Crystallization of sulfide liquids and the interpretation of ore composition: Canadian Jounal of Earth Science, v. 34, p. 352 – 365.

Eckstrand, O.R. and Hulbert, L.J., 1987, Selenium and the source of Sulphur in magmatic nickel and platinum deposits: Geological Association of Canada – Mineralogical Association of Canada Annual Meeting, Program with Abstracts, p. 40.

Ernst, R.E. and Buchan, K.L., 2001, Large mafic magmatic events through time and links to matnel-plume heads, *in* Ernst, R.E. and Buchan, K.L., eds., Mantle Plumes: Their identification through time: Boulder, Colorado, Geological Society of America Special Paper 352, p. 483 – 575.

Ewers, G.R., 1977, Experimental hot water-rock interactions and their significance to natural hydrothermal system in New Zealand: Geochimica et Cosmochimica Acta, v. 41, p. 143 – 150.

Farquhar, J. and Wing, B.A., 2003, Multiple sulfur isotopes and the evolution of the atmosphere: Earth and Planetary Science Letters, v. 213, p. 1 – 13.

Farquhar, J., Wu, N., Canfield, D., and Oduro, H., 2010, Connections between sulfur cycle evolution, sulfur isotopes, sediments, and base metal sulfide deposits: Economic Geology, v. 105, p. 509-533.

Ferry, J., 1981, Petrology of graphitic sulfide-rich schists from south-central Maine: an example of desulfidation during prograde regional metamorphism: American Mineralogist, v. 66, p. 908 – 930.

Fleet, ME., Chryssoulis, S.L., Stone, W.E., and Weisener, C.G., 1993, Partitioning of platinum-group elements and Au in the Fe-Ni-Cu-S system: experiments on the fractional crystallization of sulphide melt: Contributions to Mineralogy and Petrology, v. 115, p. 36 – 44.

Fonseca, R.O., Campbell, I.H., O'Neill, H.S.C., and Fitzgerald, J.D., 2008, Oxygen solubility and speciation in sulphide-rich mattes: Geochimica et Cosmochimica Acta, v. 72, p. 2619 – 2635.

French, B., 1968, Progressive contact metamorphism of the Biwabik iron-formation, Mesabi Range, Minnesota: Minnesota Geological Survey Bulletin 45, 126 p.

Gall, L., Williams, H.M., Siebert, C., Halliday, A.N., Herrington, R.J., and Hein, J.R., 2013, Nickel isotopic composition of ferromanganese crusts and the constancy of deep ocean inputs and continental weathering effects over the Cenozoic: Earth and Planetary Science Letters, v. 375, p. 148 – 155.

Gall, L., Williams, H.M., Halliday, A.N., and Kerr, A.C., 2017, Nickel isotopic composition of the mantle: Geochimica et Cosmochimica Acta, v. 199, p. 196 – 209.

Genkin, A.D. and Evstigneeva, T.L., 1986, Associations of platinum-group minerals of the Noril'sk copper-nickel sulfide ores: Economic Geology, v. 81, p. 1203 – 1212.

Geraghty, E., 2013, Geologic map of the Stillwater Complex within the Beartooth Mountains Front Laramide Triangle Zone south-central Montana: Montana Bureau of Mines and Geology Open-File Report 645, 22 p., 1 sheet, scale 1:48,000.

Ghiorso, M.S. and Sack, R.O., 1995, Chemical mass transfer in magmatic processes IV. A revised and internally consistent thermodynamic model for the interpolation and extrapolation

of liquid-solid equilibria in magmatic systems at elevated temperatures and pressures: Contributions to Mineralogy and Petrology, v. 119, p. 197 – 212.

Godel, B. and Barnes, S-J., 2008, Platinum-group elements in sulfide minerals and the whole rocks of the J-M Reef (Stillwater Complex): implication for the formation of the reef: Chemical Geology, v. 248, p. 272 – 294

Goldner, B.D., 2011, Igneous petrology of the Ni-Cu-PGE mineralized Tamarack intrusion, Aitkin and Carlton Counties: Unpublished M.S. thesis, Department of Geological Sciences, University of Minnesota-Duluth, Minnesota, 155p.

Grant, F., 1985, Aeromagnetic, geology and ore enviornments, I. magnetite in igneous, sedimentary and metamorphic rocks: an overview: Geoexploration, v. 23, p. 303 – 333.

Gregory, D.D., Large, R.R., Halpin, J.A., Baturina, E.L., Lyons, T.W., Wu, S., Danyushevsky, L, Sack, P.J., Chappaz, A., Maslennikov, V.V., and Bull, S.W., 2015, Trace element content of sedimentary pyrite in black shales: Economic Geology, v. 110, p. 1389 – 1410.

Gueguen, B., Rouxel, O., Ponzevera, E., Bekker, A., and Fouquet, Y., 2013, Nickel isotope variations in terrestrial silicate rocks and geological reference materials measured by MC-ICP-MS: Geostandards and Geoanalytical Research, v. 37, p. 297 – 317.

Guo, Q., Strauss, H., Kaufman, A., Schroder, S., Gutzmer, J., Wing, B., Baker, M., Bekker, A., Jin, Q., Kim, S-T., and Farquhar, J., 2009, Reconstructing Earth's surface oxidation across the Archean-Proterozoic transition: Geology, v. 37, p. 399 – 402.

Hanley, J., Mungall, J., Pettke, T., Spooner, E., and Bray, C., 2005, Ore metal redistribution by hydrocarbon – brine and hydrocarbon – halide melt phases, North Range footwall of the Sudbury igneous complex, Ontario, Canada: Mineralium Deposita, p. 237 – 256.

Hannah, J.L., Stein, H.J., Zimmerman, A., Yang, G., Markey, R.J., Melezhik, V.A., 2006, Precise 2004±9 Ma Re-Os age for Pechenga black shale: comparison of sulfides and organic material: Geochim. Cosmochim. Acta 70, A228.

Hattori, K.H., Arai, S., and Clarke, D.B., 2002, Selenium, tellurium, arsenic, and antimony contents of primary mantle sulfides: Canadian Mineralogist, v. 40, p. 637 – 650.

Hauck, S., Severson, M., Ripley, E., Goldberg, S., and Alapieti, T., 1997, Geology and Cr-PGE mineralization of the Birch Lake area, South Kawishiwi Intrusion, Duluth Complex: University of Minnesota, Duluth, Natural Resource Research Institute Technical Report NRRI/TR-97/13.

Heaman, L.M., Easton, R.M., Hart, T.R., Hollings, P., MacDonald, C.A., Smyk, M., 2007, Further refinement to the timing of Mesoproterozoic magmatism, Lake Nipigon region, Ontario: Canadian Journal of Earth Science, v. 44, p. 1055 – 1086.

Hemming, S., McLennan, S, and Hanson, G., 1995, Geochemical and Nd/Pb isotopic evidence for the provenance of the early Proterozoic Virginia Formation, Minnesota. Implications for the tectonic setting of the Animikie Basin: The Journal of Geology, v. 103, p. 147-168.

Holwell, D.A., Adeyemi, Z., Ward, L.A., Smith, D.J., Graham, S.D., McDonald, I., and Smith, J.W., 2017, Low temperature alteration of magmatic Ni-Cu-PGE sulfides as a source for hydrothermal Ni and PGE ores: a quantitative approach using automated mineralogy: Ore Geology Reviews, v. 91, p. 718 – 740.

Horan, M., Morgan, J., Walker, R., and Cooper, R., 2001, Re-Os isotopic constraints on magma mixing in the peridotite zone of the Stillwater Complex, Montana, USA: Contrib. Mineral. Petrol., v. 141, p. 446 – 457.

Huang, J., Huang, F., Wang, Z., Zhang, X., and Yu, H., 2017, Copper isotope fractionation during partial melting and melt percolation in the upper mantle: evidence from massif peridotites in Ivrea-Verbano Zone, Italian Alps: Goechimica et Cosmochimica Acta, v. 211, p. 48 – 63.

Huminicki, M.A.E., Sylvester, P.J., Lastra, R., Cabri, L.J., Evans-Lamswood, D., and Wilton, D.H.C., 2008, First report of platinum-group minerals from a hornblende gabbro dyke in the vicinity of the Southeast Extension Zone of the Voisey's Bay Ni-Cu-Co deposit, Labrador: Mineralogy and Petrology, v. 92, p. 129 – 164.

Hutchinson, D., White, R., Cannon, W., and Schulz, K., 1990, Keweenaw hot spot: geophysical evidence for a 1.1 Ga mantle plume beneath the Midcontinent rift system: Journal of Geophysical Research, v. 95, p. 10,869-10,884.

Irvine, T.N., Keith, D.W., and Todd, S.G., 1983, The J-M platinum-palladium reef of the Stillwater Complex, Montana II: Origin by double-diffusive convective magma mixing and implications for the Bushveld Complex: Economic Geology, v. 78, p. 1287 – 1334.

Jackson, E.D., 1961, Primary textures and mineral associations in the ultramafic zone of the Stillwater Complex, Montana: U.S. Geol. Survey Prof. Paper 358, 106 p.

Jaffe, L.A., Peucker-Ehrenbrink, B., and Petsch, S.T., 2002, Mobility of rhenium, platinum group elements and organic carbon during black shale weathering: Earth and Planetary Science Letters, v. 198, p. 339 – 353.

Jenkins, M.C. and Mungall, J.E., 2018, Genesis of the peridotite zone, Stillwater Complex, Montana, USA: Journal of Petrology, v. 59, p. 2157 – 2190.

Jones, W.R., Peoples, J.W., and Howland, A.L., 1960, Igneous and tectonic structures of the Stillwater Complex Montana: Geological Survey Bulletin 1071-H, p. 281 – 333.

Keays, R. and Lightfoot, P., 2004, Formation of Ni-Cu-platinum group element sulfide mineralization in the Sudbury impact melt sheet: Mineralogy and Petrology, v. 82, p. 217 – 258.

Keays, R.R., Lightfoor, P.C., and Hamlyn, P.R., 2012, Sulfide saturation history of the Stillwater Complex, Montana: chemostratigraphic variation in platinum group elements: Mineralium Deposita, v. 47, p. 171 – 173.

Kendall, B., Creaser, R.A., and Selby, D., 2006, Re-Os geochronology of postglacial black shales in Australia: constraints on the timing of "Sturtian" glaciation: Geology, v. 34, p. 729 – 732.

Kerr, A., and Leitch, A.M., 2005, Self-destructive sulfide segregation systems and the formation of high-grade magmatic ore deposits: Economic Geology, v. 100, p. 311 – 332.

Kullerud, G., 1986, Monoclinic pyrrhotite: Bull. Geol. Soc. Finland, v. 58, p. 293 – 305.

Kullerud, G. and Yoder, H.S., 1959, Pyrite stability relations in the Fe-S system: Economic Geology, v. 54, p. 533 – 572.

Kunilov, V.Y., 1994, Geology of the Noril'sk region: the history of the discovery, prospecting, exploration, and mining of the Noril'sk deposit: *in* Proceedings of the Sudbury – Noril'sk Symposium, Ontario Geological Surveyk, Special Volume 5, p. 203 – 216.

Labotka, T.C., 1985, Petrogenesis of the metamorphic rocks beneath the Stillwater Complex: Assemblages and conditions of metamorphism, *in* Czamanske, G.K., and Zientek, M.L., eds., The Stillwater Complex, Montana: Geology and guide: Butte, Montana Bureau of Mines and Geology, p. 70 – 76.

Labotka, T.C. and Kath, R.L., 2001, Petrogenesis of the contact-metamorphic rocks beneath the Stillwater Complex, Montana: Geol. Soc. Am. Bull. v. 113, p. 1312 – 1323.

Labotka, T.C., Vaniman, D.T., and Papike, J.J., 1982, Contact metamorphic effects of the Stillwater Complex, Montana; the concordant iron formation; a reply to the role of buffering in metamorphism of iron-formation: American Mineralogist, v. 67, p. 149 – 152.

Labotka, T.C., White, C.E., and Papike, J.J., 1984, The evolution of water in the contact-metamorphic aureole of the Duluth Complex, northeastern Minnesota: Geological Society of America Bulletin, v. 95, p. 788 – 804.

Lambert, D.D., Morgan, J.W., Walker, R.J., Shirey, S.B., Carlson, R.W., Zientek, M.L., and Koski, M.S., 1989, Rhenium-osmium and samarium-neodymium isotopic systematics of the Stillwater Complex: Science, v. 244, p. 1169 – 1174.

Lambert, D., Walker, R., Morgan, J., Shirey, S., Carlson, R., Zientek, M., Lipin, B., Koski, M., and Cooper, R., 1994, Re-Os and Sm-Nd isotope geochemistry of the Stillwater Complex, Montana: implications for the petrogenesis of the J-M Reef: Journal of Petrology, v. 35, p. 1717 – 1753.

Large, R.R., Halpin, J.A., Danyushevsky, L.V., Maslennikov, V.V., Bull, S.W., Long, J.A., Gregory, D.D., Lounejeva, E., Lyons, T.W., Sack, P.J., McGoldrick, P.J., and Calver, C.R., 2014, Trace element content of sedimentary pyrite as a new proxy for deep-time ocean-atmosphere evolution: Earth and Planetary Science Letters, v. 389, p. 209 – 220.

Larson, P.B., Maher, K., Ramos, F.C., Chang, Z., Gaspar, M., Meinert, L.D., 2003, Copper isotope ratios in magmatic and hydrothermal ore-forming environments: Chemical Geology, v. 201, p. 337 – 350.

Lazar, C., Young, E.D., and Manning, C.E., 2012, Experimental determination of equilibrium nickel isotope fractionation between metal and silicate from 500 °C to 950 °C: Geochimica et Cosmochimica Acta, v. 86, p. 276 – 295.

Leach, D.L., Marsh, E., Emsbo, P., Romback, C.S., Kelley, K.D., and Anthony, M., 2004, Nature of hydrothermal fluids at the shale-hosted Red Dog Zn-Pb-Ag deposits, Brooks Range, Alaska: Economic Geology, v. 90, p. 1449 – 1480.

Lee, I. and Ripley, E.M., 1996, Mineralogic and oxygen isotopic studies of open system magmatic processes in the South Kawishiwi intrusion, Spruce Road area, Duluth Complex, Minnesota: Journal of Petrology, v. 37, p. 1437 – 1461.

Lewan, M. and Maynard, J., 1982, Factors controlling enrichment of vanadium and nickel in the bitumen of organic sedimentary rocks: Geochimica et Cosmochimica Acta, v. 46, p. 2547 – 2560.

Li, C. and Naldrett, A.J., 1994, A numerical model for the compositional variations of Sudbury sulfide ores and its application to exploration: Economic Geology, v. 88, p. 1599 – 1607.

Li, C. and Ripley, E.M., 2009, Sulfur contents at sulfide-liquid or anhydrite saturation in silicate melts: empirical equations and example applications: Economic Geology, v. 104, p. 405 – 412.

Li, C., Naldrett, A., Coats, C., and Johannessen, P., 1992, Platinum, palladium, gold, copper-rich stringers at the Strathcona Mine, Sudbury: their enrichment by fracation of a sulfide liquid: Economic Geology, v. 87, p. 1584-1598.

Li, C., Barnes, S.J., Makovicky, E., Rose-Hansen, J., Makovicky, M., 1996, Partitioning of nickel, copper, iridium, rhenium, platinum, and palladium between monosulfide solid solution and sulfide liquid: effects of composition and temperature: Geochimica et Cosmochimica Acta, v. 60, p. 1231 – 1238.

Li, W., Jackson, S.E., Pearson, N.J., and Graham, S., 2010, Copper isotopic zonation in the Northparkes porphyry Cu-Au deposit, SE Australia: Geochimica et Cosmochimica Acta, v. 74, p. 4078 – 4096.

Lianxing, G. and Vokes, F.M., 1996, Intergrowths of hexagonal and monoclinic pyrrhotites in some sulphide ores from Norway: Mineralogical Magazine, v. 60, p. 303 – 316.

Lightfoot, P., 2007, Advances in Ni-Cu-PGE sulphide deposit models and implications for exploration technologies: Proceedings of Exploration 07: Fifth Decennial International Conference on Mineral Exploration, p. 629-646.

Little, S.H., Vance, D., Walker-Brown, C., and Landing, W.M., 2014, The oceanic mass balance of copper and zinc isotopes, investigated by analysis of their inputs and outputs to ferromanganese oxide sediments: Geochimica et Cosmochimica Acta, v. 125, p. 673 – 693.

Little, S.H., Vance, D., McManus, J., Severmann, S., and Lyons, T.W., 2017, Copper isotope signatures in modern marine sediments: Geochimica et Cosmochimica Acta, v. 212, p. 253 – 273.

Liu, S-A., Huang, J., Liu, J., Wörner, G., Yang, W., Tang, Y-J., Chen, Y., Tang, L., Zheng, J., and Li, S., 2015, Copper isotopic composition of the silicate Earth: Earth and Planetary Science Letters, v. 427, p. 95 – 103.

Liu, S., Li, Y., Ju, Y., Liu, J., Liu, J., and Shi, Y., 2018, Equilibrium nickel isotope fractionation in nickel sulfide minerals: Geochimica et Cosmochimica Acta, v. 222, p. 1 – 16.

Lorand, J.P., Alard, O., Luguet, A., and Keays, R.R., 2003, Sulfur and selenium systematics of the subcontinental lithospheric mantle: inferences from the Massif Central xenolith suite (France): Geochim. Cosmochim. Acta, v. 67, p. 4137 – 4151.

Lott, D.A., Coveney, Jr., R.M., Murowchick, J.B., and Grauch, R.I., 1999, Sedimentary exhalative nickel-molybdenum ores in south China: Economic Geology, v. 94, p. 1051 – 1066.

Luczaj, J. and Huang, H., 2018, Copper and sulfur isotope ratios in Paleozoic-hosted Mississippi Valley-type mineralization in Wisconsin, USA: Applied Geochemistry, v. 89, p. 173 – 179.

Maier, W. and Barnes, S-J., 2010, The Kabanga Ni sulfide deposits, Tanzania: II. Chalcophile and siderophile element geochemistry: Mineralium Deposita, v. 45, p. 443 – 460.

Malitch, K. and Latypov, R., 2011, Re-Os and S isotope constraints on timing and source heterogeneity of PGE-Cu-Ni sulfide ores: a case study at the Talnakh ore junction, Noril'sk province, Russia: The Canadian Mineralogist, v. 49, p. 1653 – 1677.

Malitch, K.N., Latypov, R.M., Badanina, I.Y., and Sluzhenikin, S.F., 2014, Insights into ore genesis of Ni-Cu-PGE sulfide deposits of the Noril'sk province (Russia): evidence from copper and sulfur isotopes: Lithos, v. 204, p. 172 – 187.

Malone, D.H., Stein, C.A., Craddock, J.P., Kley, J., Stein, S., and Malone, J.E., 2016, Maximum depositional age of the Neoproterozoic Jacobsville Sandstone, Michigan: implications for the evolution of the Midcontinent Rift: Geosphere, v. 12, 1271 – 1282, doi:10.1130/GES01302.1.

Manhes, G., Allegre, C., Dupre, B., and Hemelin, B., 1980, Lead isotope study of basic-ultrabasic layered complexes: speculations about the age of the earth and primitive mantle characteristics: Earth and Planetary Science Letters, v. 47, p. 370-382.

Mann, J., Vocke, R, and Kelly, W., 2009, Revised δ34S reference values for IAEA sulfur isotope reference materials S-2 and S-3: Rapid Communications in Mass Spectrometry, v. 23, p. 1116-1124.

Mao, J., Lehmann, B., Du, A., Zhang, G., Ma, Dongsheng, M., Wang, Y., Zeng, M., and Kerrick, R., 2002, Re-Os dating of polymetallic Ni-Mo-PGE-Au mineralization in lower Cambrian black shales of south China and its geologic significance: Economic Geology, v. 97, p. 1051 – 1061.

Marcantonio, F., Zindler, A., Reisberg, L., and Mathez, E.A., 1993, Re-Os isotopic systematics in chromitites from the Stillwater Complex, Montana, USA: Geochimica et Cosmochimica Acta, v. 57, p. 4029 – 4037.

Markl, G., Lahaye, Y., and Schwinn, G., 2006, Copper isotopes as monitors of redox processes in hydrothermal mineralization: Geochimica et Cosmochimica Acta, v. 70, p. 4215 – 4228.

Marsh, S.P., 1979, Rutile mineralization in the White Mountain andalusite deposit, California: U.S. Geological Survey Open-File Report 79-1622. 7 p.

Martin, C.E., 1989, Re-Os isotopic investigation of the Stillwater Complex, Montana: Earth and Planetary Science Letters, v. 93, p. 336 – 344.

Mason, T.F.D., Weiss, D.J., Chapman, J.B., Wilkinson, J.L., Tessalina, S.G., Spiro, B., Horswood, M.S.A., Spratt, J., Coles, B.J., 2005, Zn and Cu isotopic variability in the Alexandrinka volcanic-hosted massive sulphide (VHMS) ore deposit, Urals, Russia: Chemical Geology, v. 221, p. 170 – 187.

Mathur, R., Ruis, J., Titley, S., Liermann, L., Buss, H., Brantley, S., 2005, Cu isotopic fractionation in the supergene environment with and without bacteria: Geochimica et Cosmochimica Acta, v. 69, p. 5233 – 5246.

Mathur, R., Titley, S., Barra, F., Brantley, S., Wilson, M., Phillips, A., Munizaga, F., Maksaev, V., Vervoort, J., and Hart, G., 2009, Exploration potential of Cu isotope fractionation in porphyry copper deposits: Journal of Geochemical Exploration, v. 102, p. 1 – 6.

McCallum, I.S., Raedeke, L.D., and Mathez, E.A., 1980, Investigations of the Stillwater Complex: Part I. Stratigraphy and structure of the Banded zone: Am. Jour. Sci., v. 280-A, p. 59 – 87.

McCallum, I.S., Thurber, M.W., O'Brien, H.E., and Nelson, B.K., 1999, Lead isotopes in sulfides from the Stillwater Complex, Montana: evidence for subsolidus remobilization: Contrib. Mineral. Petrol., v. 137, p. 206 – 219.

McClay, K.R. and Ellis, P.G., 1984, Deformation of pyrite: Economic Geology, v. 79, p. 400 – 403.

McDonough, W. and Sun, S-S., 1995, The composition of the Earth: Chemical Geology, v. 120, p. 223 – 253.

Merino, M., Keller, G.R., Stein, S., and Stein, C., 2013, Variations in Mid-Continent Rift magma volumes consistent with microplate evolution: Geophysical Research Letters, v. 40, p. 1513 – 1516.

Miller, J.D., and Nicholson, S.W., 2013, The geology and mineral deposits of the 1.1 Ga Midcontinent rift in the Lake Superior region – an overview, *in* Miller, J.D., ed., Field guide to the copper-nickel-platinum group element deposits of the Lake Superior region: Precambrian Research Center Guidebook 13-01, p. 1 – 50.

Miller, J.D., Jr., and Ripley, E.M., 1996, Layered intrusions of the Duluth Complex, USA, *in* Cawthorn, R.G., ed., Layered intrusions: Amsterdam, Elsevier, p. 257–301.

Miller, J.D. and Vervoort, 1996, The latent magmatic stage of the Midcontinent rift: A period of magmatic underplating and melting of the lower crust: 42nd Annual Institute on Lake Superior Geology, Proceedings Volume, Part I – Program and Abstracts, p. 33 – 35.

Miller, J., Green, J., Severson, M., Chandler, V., Hauck, S., Peterson, D., and Wahl, T., 2002, Geology and mineral potential of the Duluth Complex and related rocks of northeastern Minnesota: Minnesota Geological Survey Report of Investigations, v. 58, 207 p.

Moucha, R., Rooney, T.O., Stein, S.A., Brown, E., 2013, Geodynamic modeling of the Mid-Continental Rift System: is a mantle plume required?: American Geophysical Union, Fall Meeting 2013, abstract.

Mountain, B.W. and Wood, S.A., 1988, Chemical controls on the solubility, transport, and deposition of platinum and palladium in hydrothermal solutions: a thermodynamic approach: Economic Geology, v. 83, p. 492 – 510.

Moynier, F., Vance, D., Fujii, T., and Savage, P., 2017, The isotope geochemistry of zinc and copper: Reviews in Mineralogy & Geochemistry, v. 82, p. 543 – 600.

Mudd, G., 2010, Global trends and environmental issues in nickel mining: sulfides versus laterites: Ore Geology Reviews, v. 38, p. 9-26.

Mudd, G., 2012, Key trends in the resource sustainability of platinum group elements: Ore Geology Reviews, v. 46, p. 106-117.

Mudd, G. and Jowitt, S., 2014, A detailed assessment of global nickel resource trends and endowments: Economic Geology, v. 109, p. 1813 – 1841.

Mueller, P.A., Mogk, D.W., Henry, D.J., Wooden, J.L, and Foster, D.A., 2008, Geologic evolution of the Beartooth Mountains: insights from petrology and geochemistry: Northwest Geology, v. 37, p. 5 – 20.

Mungall, J.E., 2007, Crystallization of magmatic sulfides: an empirical model and application to Sudbury ores: Geochimica et Cosmochimica Acta, v. 71, p. 2809 – 2819.

Mungall, J.E. and Brenan, J.M., 2014, Partitioning of platinum-group elements and Au between sulfide liquid and basalt and the origins of mantle-crust fractionation of the chalcophile elements: Geochimica et Cosmochimica Acta, v. 125, p. 265 – 289.

Mungall, J.E., Andrews, D.R.A., Cabri, L., Sylvester, P.L., and Tubrett, M., 2005, Partitioning of Cu, Ni, Au, and platinum-group elements between monosulfide solid solution and sulfide melt under controlled oxygen and sulfur fugacities: Geochimica et Cosmochimica Acta, v. 69, p. 4349 – 4360.

Naldrett, A.J., 1969, A portion of the system Fe-S-O between 900 and 1080 ° C and its application to sulfide ore magmas: Journal of Petrology, v. 10, p. 171 – 201.

Naldrett, A.J., 2011, Fundamentals of magmatic sulfide deposits: Reviews in Economic Geology, v. 17, p. 1 – 50.

Naldrett, A.J., Singh, J., Krstic, S., and Li, C., 2000, The mineralogy of the Voisey's Bay Ni-Cu-Co deposit, Northern Labrador, Canada: influence of oxidation state on textures and mineral compositions: Economic Geology, v. 95, p. 889 – 900.

Nunes P.D., 1981, The age of the Stillwater complex – comparison of U-Pb zircon and Sm-Nd isochron systematic: Geochimica et Cosmochimica Acta, v. 45, p. 1961 – 1963.

Nunes, P.D. and Tilton, G.R., 1971, Uranium-lead ages of minerals from the Stillwater igneous complex and associated rocks, Montana: Geol. Soc. America Bull, v. 82, p. 2231 – 2249.

Ohmoto, H., 1996, Formation of volcanogenic massive sulfide deposit: the Kuroko perspective: Ore Geology Reviews, v. 10, p. 135 – 177.

Ohmoto, H., Watanabe, Y, Ikemi, H., Poulson, S., and Taylor, B., 2006, Sulphur isotope evidence for an oxic Archaean atmosphere: Nature, v. 442, p. 908 – 911.

Paces, J.B. and Bell, K., 1989, Non-depleted subcontinental mantle beneath the Superior Province of the Canadian Shield: Nd-Sr isotopic and trace element evidence from Midcontinent Rift basalts: Geochimica et Cosmochimica Acta, v. 53, p. 2023 – 2035.

Paces, J.B., and Miller, J.D., 1993, Precise U-Pb ages of Duluth Complex and related mafic intrusions, northeastern Minnesota: Geochronological insights into physical, petrogenetic, paleomagnetic, and tectonomagnetic processes associated with the 1.1 Ga Midcontinent rift system: Journal of Geophysical Research, v. 98, p. 13,997–14,013.

Page, N.J., 1977, Stillwater Complex, Montana: rock succession, metamorphism, and structure of the complex and adjacent rocks: U.S. Geological Survey Professional Paper 999, 79 p.

Page, N.J., 1979, Stillwater Complex, Montana – structure, mineralogy, and petrology of the basal zone with emphasis on the occurrence of sulfides: U.S. Geol. Survey Prof. Paper 1038, 69 p.

Page, N.J. and Jackson, E.D., 1967, Preliminary report on sulfide and platinum-group minerals in the chromitites of the Stillwater Complex, Montana: Geological Survey Research 1967, Chapter D, p. 123 – 126.

Panoramic Resource, LTD, Savannah North Intrusion, 2017; http://panoramicresources.com/geology-and-mineralisation/.

Park, Y.-R., Ripley, E.M., Miller, J.D., Li, C., Mariga, J., and Shafer, P., 2004, Stable isotopic constraints on fluid-rock interaction and Cu-PGE-S redistribution in the Sonju Lake intrusion: Economic Geology, v. 99, p. 325–338.

Penniston-Dorland, S.C., Wing, B.A., Nex, P.A.M., Kinnaird, J.A., Farquhar, J., Brown, M. and Sharman, E.R., 2008, Multiple sulfur isotopes reveal a magmatic origin for the Platreef platinum group element deposit, Bushveld Complex, South Africa: Geology, v. 36, p. 979 – 982.

Peterson, D., 2013, The Maturi deposit, Duluth complex, Minnesota: University of Minnesota Duluth, copper-nickel-platinum group element deposits of the Lake Superior region, Duluth, Minnesota, Oct. 6 – 13, 2013, Short Course, p. 109 – 118.

Piersonn-Wickmann, A-C., Reisberg, L., and France-Lanord, C., 2002, Behavior of Re and Os during low-temperature alteration: results from Himalayan soils and altered black shales: Geochim. Cosmochim. Acta, v. 66, p. 1539 – 1548.

Pokrovsky, O.S., Viers, J., Emmova, E.E., Kompantseva, E.J., Freydier, R., 2008, Copper isotope fractionation during its interaction with soil and aquatic microorganisms and metal oxy(hydr)oxides: possible structural control: Geochimica et Cosmochimica Acta, v. 72, p. 1742 – 1757.

Porter, S.J., Selby, D., Cameron, V., 2014, Characterising the nickel isotopic composition of organic-rich marine sediments: Chemical Geology, v. 387, p. 12 – 21.

Powell, J.L., Skinner, W.R., and Walker, D., 1969, Whole-rock Rb-Sr age of the metasedimentary rocks below the Stillwater Complex, Montana: Geological Society of America Bulletin, v. 80, p. 1605 – 1612.

Premo, W.R., Helz, R.T. Zientek, M.L., and Langston, R.B., 1990, U-Pb and Sm-Nd ages for the Stillwater Complex and its associated sills and dikes, Beartooth Mountains, Montana: Identification of a parent magma?: Geology, v. 18, p. 1065 – 1068.

Prichard, H.M., Knight, R.D., Fisher, P.C., McDonald, I. Zhou, M-F., and Wang, C.Y., 2013, Distribution of platinum-group elements in magmatic and altered ores in the Jinchuan intrusion, China: an example of selenium remobilization by postmagmatic fluids: Mineralium Deposita, v. 48, p. 767 – 786.

Queffurus, M. and Barnes, S-J., 2015, A review of sulfur to selenium ratios in magmatic nickel-copper and platinum-group element deposits: Ore Geology Reviews, v. 69, p. 301 – 324.

Raedeke, L.D. and McCallum, I.S., 1984, Investigation in the Stillwater Complex: part II. Petrology and petrogenesis of the ultramafic series: Journal of Petrology, v. 25, p. 395 – 420.

Raedeke, L.D. and Vian, R.W., 1986, A three-dimensional view of mineralization in the Stillwater J-M reef: Economic Geology, v. 81, p. 1187 – 1195.

Rao, B.V. and Ripley, E.M., 1983, Petrochemical studies of the Dunka Road Cu-Ni deposit, Duluth Complex, Minnesota: Economic Geology, v. 78, p. 1222 – 1238.

Reinhard, C., Raiswell, R., Scott, C., Anbar, A., and Lyons, T., 2009, A late Archean sulfidic sea stimulated by early oxidative weathering of the continents: Science, v. 326, p. 713 – 716.

Ripley, E., 1981, Sulfur isotopic studies of the Dunka Road Cu-Ni deposit, Duluth Complex, Minnesota: Economic Geology, v. 76, p. 610–620.

Ripley, E., 1990a, Platinum-group element geochemistry of Cu-Ni mineralization in the basal zone of the Babbitt deposit, Duluth Complex, Minnesota: Economic Geology, v. 85, p. 830-841.

Ripley, E.M., 1990b, Se/S ratios of the Virginia formation and Cu-Ni sulfide mineralization in the Babbitt area, Duluth Complex, Minnesota: Economic Geology, v. 85, p. 1935 – 1940.

Ripley, E., 2014, Ni-Cu-PGE mineralization in the Partridge River, South Kawishiwi, and Eagle intrusions: a review of contrasting styles of sulfide-rich occurrences in the Midcontinent Rift System: Economic Geology, v. 109, p. 309-324.

Ripley, E., and Al-Jassar, T., 1987, Sulfur and oxygen isotope studies of melt-country rock interaction, Babbitt Cu-Ni deposit, Duluth Complex: Minnesota: Economic Geology, v. 82, p. 87–107.

Ripley, E., and Alawi, J., 1988, Petrogenesis of pelitic xenoliths at the Babbit Cu-Ni deposit, Duluth Complex, Minnesota, U.S.A.: Lithos, v. 21, p. 143-159.

Ripley, E., and Li, C., 2003, Sulfur isotope exchange and metal enrichment in the formation of magmatic Cu-Ni-(PGE) deposits: Economic Geology, v. 95, p. 635–641.

Ripley, E.M. and Nicol, D., 1981, Sulfur isotopic studies of Archean slate and graywacke from northern Minnesota: evidence for the existence of sulfate reducing bacteria: Geochimica et Cosmochimica Acta, v. 45, p. 839 – 846.

Ripley, E., Lambert, D., and Frick, L., 1999, Re-Os, Sm-Nd, and Pb isotopic constraints on mantle and crustal contributions to magmatic sulfide mineralization in the Duluth Complex: Geochimica et Cosmochimica Acta, v. 62, p. 3349-3365.

Ripley, E.M., Park, Y-R., Li, C., and Naldrett, A.J., 2000, Oxygen isotope studies of the Voisey's Bay Ni-Cu-Co deposit, Labrador, Canada: Economic Geology, v. 95, p. 831 – 844.

Ripley, E.M., Park, Y-R., Lambert, D.D., Frick, L.R., 2001, Re-Os isotopic composition and PGE contents of proterozoic carbonaceous argillites, Virginia Formation, northeastern Minnesota: Organic Geochemistry, v. 32, p. 857 – 866.

Ripley, E.M., Li, C., Shin, D., 2002, Paragneiss assimilation in the genesis of magmatic Ni-Cu-Co sulfide mineralization at Voisey's Bay, Labrador: $\delta^{34}S$, $\delta^{13}C$, and Se/S evidence: Economic Geology, v. 97, p. 1307 – 1318.

Ripley, E.M., Taib, N.I., Li, C., and Moore, C.H., 2007, Chemical and mineralogical heterogeneity in the basal zone of the Partridge River Intrusion: Implications for the origin of Cu-Ni mineralization in the Duluth Complex, Midcontinent rift system: Contributions to Mineralogy and Petrology, v. 154, p. 35–54.

Ripley, E.M., Shafer, P., Li, C., and Hauck, S.A., 2008, Re-Os and O isotopic variations in magnetite from the contact zone of the Duluth Complex and the Biwabik Iron Formation, northeastern Minnesota: Chemical Geology, v. 249, p. 213 – 226.

Ripley, E. and Li, C., 2013, Sulfide saturation in mafic magmas: Is external sulfur required for magmatic Ni-Cu-(PGE) ore genesis?: Economic Geology, v. 108, p. 45–58.

Ripley, E., Dong, S., Li, C., and Wasylenki, L., 2015, Cu isotope variations between conduit and sheet-style Ni-Cu-PGE sulfide mineralization in the Midcontinent Rift System, North America: Chemicaal Geology, v. 414, p. 59-68.

Ripley, E.M. Wernette, B., Ayre, A., Li, C., Smith, J., Underwood, B., and Keays, R., 2017, Multiple S isotope studies of the Stillwater Complex and country rocks: an assessment of the role of crustal S in the origin of PGE enrichment found in the J-M Reef and related rocks: Geochimica et Cosmochimica Acta, v. 214, p. 226 – 245.

Robertson, J., Ripley, E.M., Barnes, S.J., and Li, C., 2015, Sulfur liberation from country rocks and incorporation in mafic magmas: Economic Geology, v. 110, p. 111 – 1123.

Rouxel, O., Fouquet, Y., Ludden, J.N., 2004, Copper isotope systematics of the Lucky Strike, rainbow, and Logatchev sea-floor hydrothermal fields on the Mid-Atlantic ridge: Economic Geology, v. 99, p. 585 – 600.

Rudge, J.F., Reynolds, B.B.C., and Bourdon, B., 2009, The double spike toolbox: Chemical Geology, v. 265, p. 420 – 431.

Samalens, N., Barnes, S-J., Sawyer, E.W., 2017a, A laser ablation inductively couple plasma mass spectrometry study of the distribution of chalcophile elements amon sulfide phases in sedimentary and magmatic rocks of the Duluth Complex, Minnesota, USA: Ore Geology Reviews, v. 90, p. 352 – 370.

Samalens, N., Barnes, S-J., and Sawyer, E.W., 2017b, The role of black shales as a source of sulfur and semimetals in magmatic nickel-copper deposits: Example from the Partridge River Intrusion, Duluth Complex, Minnesota, USA: Ore Geology Reviews, v. 81, p. 173 – 187.

Saunders, J.A., Mathur, R., Kamenov, G.D., Shimizu, T., Brueseke, M.E., 2016, New isotopic evidence bearing on bonanza (Au-Ag) epithermal ore-forming processes: Mineralium Deposita, v. 51, p. 1 – 11.

Savage, P.S., Moynier, F., Chen, H., Shofner, G., Siebert, J., Badro, J., and Puchtel, I.S., 2015, Copper isotope evidence for large-scale sulphide fractionation during Earth's differentiation: Geochemical Perspectives Letters, v. 1, p. 53 – 64.

Savard, D., Barnes, S-J., and Meisel, T., 2010, Comparison between nickel-sulfur fire assay Te co-precipitation and isotope dilution with high-pressure asher acid digestion for the determination of platinum-group elements, rhenium, and gold: Geostandards and Geoanalytical Research, v. 34, p. 281 – 291.

Segerstrom, K. and Carlson, R., 1982, Geologic map of the banded upper zone of the Stillwater Complex and adjacent rocks, Stillwater, Sweet Grass, and Park counties, Montana: U.S. Geol. Survey Misc. Inv. Ser. Map I-1383, scale 1:24,000, 2 sheets.

Selby, D. and Creaser, R.A., 2005, Direct radiometric dating of the Devonian-Mississippian time-sclae boundary using the Re-Os black shale geochronometer: Geology, v. 33, p. 545 – 548.

Severson, M.J., 1994, Igneous stratigraphy of the South Kawishiwi intrusion, Duluth complex, northeastern Minnesota, Natural Resources Research Institute, University of Minnesota, Duluth, Technical Repost, NRRI/TR-93/34, 302 p.

Severson, M.J. and Hauck, S., 1990, Geology, geochemistry, and stratigraphy of a portion of the Partridge River intrusion: Natural Resources Research Institute, University of Minnesota, Duluth, Technical Report, NRRI/TR-89/11, 230 p.

Severson, M.J., and Hauck, S., 2008, Finish logging of Duluth Complex drill core (and a reinterpretation of the geology at the Mesaba (Babbitt) deposit): Natural Resources Research Institute, University of Minnesota, Duluth, Technical Report, NRRI/TR-2008/17, 68 p.

Sherman, D.M., 2013, Equilibrium isotopic fractionation of copper during oxidation/reduction, aqueous complexation, and ore-forming processes: predictions from hydrid density functional theory: Geochimica et Cosmochimica Acta, v. 118, p. 85 – 97.

Shirey, S.B., 1997, Re-Os isotopic compositions of Midcontinent rift system picrites: implications for plume-lithosphere interaction and enriched mantle sources: Canadian Journal of Earth Sciences, v. 34, p. 489–503.

Shirey, S.B. and Walker, R.J., 1995, Carius tube digestion for low-blank rhenium-osmium analysis: Analytic Chemistry, v. 67, p. 2136 – 2141.

Shirey, S.B. and Walker, R.J., 1998, The Re-Os isotope system in cosmochemistry and high-temperature geochemistry: Annual Rev. Earth Planet. Sci., v. 26, p. 423 – 500.

Shirey, S.B., Klewin, K.W., Berg, J.H., and Carlson, R.W., 1994, Temporal changes in the sources of flood basalts: Isotopic and trace element evidence from the 100 Ma old Keweenawan Mamainse Point Formation, Ontario, Canada: Geochimica et Cosmochimica Acta, v. 58, p. 4475–4490.

Sillitoe, R.H., 1983, Enargite-bearing massive sulfide deposits high in porphyry copper systems: Economic Geology, v. 78, p. 348 – 352.

Singha, M.K., 2011, Sulfur isotope studies of rocks from the basal series of the Stillwater Complex and associated metasedimentary country rocks, Mountain View area, Montana: Unpublished M.S. thesis, Indiana University.

Skinner, B.J., Luce, F.D., Dill, J.A., Ellis, D.E., Hagan, H.A., Lewis, D.M., Odell, D.A., Sverjensky, D.A., and Williams, N., 1976, Phase relations in ternary portions of the system Pt-Pd-Fe-As-S: Economic Geology, v. 71, p. 1469 – 1475.

Smith, J.W., Holwell, D.A., McDonald, I., and Boyce, A.J., 2016, The application of S isotopes and S/Se ratios in determining ore-forming processes of magmatic Ni-Cu-PGE sulfide deposits: a cautionary case study from the northern Bushveld Complex: Ore Geology Reviews, v. 73, p. 148 – 174.

Spandler, C., Mavrogenes, J., and Arculus, R., 2005, Origin of chromitites in layered intrusions: evidence from chromite-hosted melt inclusionsfrom the Stillwater Complex: Geology, v. 33, p. 893 – 896.

Spivak-Birndorf, L.J., Wang, S.J., Bish, D.L., and Wasylenki, L.E., 2018, Nickel isotope fractionation during continental weathering: Chemical Geology, v. 476, p. 316 – 326.

Stacey, J.S. and Kramers, J.D., 1975, Approximation of terrestrial lead isotope evolution by a two-stage model: Earth and Planetary Science Letters, v. 26, p. 207 – 221.

Stein, S., Stein, C., Kley, J., Keller, R., Merino, M., Wolin, E., Wiens, D., Wysession, M.E., Al-Equabi, G., Shen, W., Frederiksen, A., Darbyshire, F., Jurdy, D., Waite, G., Rose, W., Vye, E., Rooney, T., Moucha, R., and Brown, E., 2016, New insights into North America's Midcontinent Rift: EOS, v. 97, p. 10 – 15.

Studley, S.A., Ripley, E..M., Elswick, E.R., Dorais, M.J., Fong, J., Finkelstein, D., and Pratt, L., 2002, Analysis of sulfides in whole rock matrices by elemental analyzer-continuous flow isotope ratio mass spectrometry: Chemical Geology, v. 192, no. 1-2, p. 141 – 148.

Taib, N.I., 2001, Open system magmatism and the emplacement of the Partridge River intrusion, Duluth Complex, Minnesota (Ph.D. thesis), Indiana University, 187 p.

Takano, S., Tanimizu, M., Hirata, T., Sohrin, Y., 2013, Determination of isotopic composition of dissolved copper in seawater by multi-collector inductively coupled plasma mass spectrometry after pre-concentration using an ethylenediaminetriacetic acid chelating resin: Analytica Chimica Acta, v. 784, p. 33 – 41.

Taranovic, V., Ripley, E.M., Li, C., Rossell, D., 2015, Petrogenesis of the Ni-Cu-PGE sulfide-bearing Tamarack Intrusive Complex, Midcontinent rift System, Minnesota: Lithos, v. 212, p. 16 – 31.

Taranovic, V., Ripley, E., Li, C., and Rossell, D., 2016, Chalcophile element (Ni, Cu, PGE, and Au) variations in the Tamarack magmatic sulfide deposit in the Midcontinent Rift System: implications for dynamic ore-forming processes: Mineralium Deposita, v. 51, p. 937-951.

Taranovic, V., Ripley, E.M., Li, C., and Shirey, S.B., 2018, S, O, and Re-Os isotope studies of the Tamarack Igneous Complex: melt-rock interaction during the early stage of Midcontinent Rift development: Economic Geology, v. 113, p. 1161 – 1179.

Thacker, J.O., Lageson, D.R., and Mogk, D.W., 2016, Subsurface structural and mineralogical characterization of the Laramide South Prairie fault in the Stillwater Complex, Beartooth Mountains, Montana: Lithosphere, v. 9, p. 100 – 116.

Thériault, R.D., Barnes, S-J., and Severson, M.J., 1997, The influence of country-rock assimilation and silicate to sulfide ratios (R factor) on the genesis of the Dunka Road Cu-Ni-

platinum-group element deposit, Duluth Complex, Minnesota: Canadian Journal of Earth Science, v. 34, p. 375 – 389.

Thériault, R.D. and Barnes, S-J., 1998, Compositional variations in Cu-Ni-PGE sulfides of the Dunka Road deposit, Duluth Complex, Minnesota: the importance of combined assimilation and magmatic processes: Canadian Mineralogist, v. 36, p. 869 – 886.

Thompson, C.M., Ellwood, M.J., Wille, M., 2013, A solvent extraction techniquie for the isotopic measurement of dissolved copper in seawater: Analytica Chimica Acta, v. 775, p. 106 – 113.

Thomson, J., 2008, Beneath the Stillwater Complex: Petrology and geochemistry of quartz-plagioclase-cordierite (or garnet)-orthopyroxene-biotite±spinel hornfels, Mountain View area, Montana: American Mineralogist, v. 93, p. 438 – 450.

Todd, S.G., Keith, D.W., LeRoy, L.W., Schissel, D.J., Mann, E.L., and Irvine, T.N., 1982, The J-M platinum-palladium reef of the Stillwater Complex, Montana: 1. Stratigraphy and petrology: Economic Geology, v. 77, p. 1454 – 1480.

Toulmin, III, P., and Barton, Jr., P.B., 1964, A thermodynamic study of pyrite and pyrrhotite: Geochimica et Cosmochimica Acta, v. 28, p. 641 – 671.

Tuba, G., Molnar, F., Ames, D., Pentek, A, Watkinson, D., and Jones, P., 2014, Multi-stage hydrothermal processes involved in “low-sulfide” Cu(-Ni)-PGE mineralization in the footwall of the Sudbury igneous complex (Canada): Amy Lake PGE zone, East Range: Mineralium Deposita, v. 49, p. 7 – 47.

Vance, D., Archer, C., Bermin, J., Statham, P., Lohan, M., Ellwood, M., Mills, R., 2008, The copper isotope geochemistry of rivers and the oceans: Earth and Planetary Science Letters, v. 274, p. 204 – 213.

Vance, D., Little, S.H., Archer, C., Cameron, V., Andersen, M.B., Rijkenberg, M.J.A., and Lyons, T.W., 2016, The oceanic budgets of nickel and zinc isotopes: the importance of sulfidic environments as illustrated by the Black Sea: Phil. Trans. R. Soc. A 374: 20150294.

Vaniman, D., Papike, J., and Labotka, T., 1980, Contact-metamorphic effects of the Stillwater Complex, Montana: the concordant iron formation: American Mineralogist, v. 65, p. 1087 – 1102.

Vermeesch, P., 2018, IsoplotR: a free and open toolbox for geochronology: Geoscience Frontiers, doi: 10.1016:j.gsf.2018.04.001.

Wall, C.J. and Scoates, J.S., 2016, High-precision U-Pb zircon-baddeleyite dating of the J-M reef platinum group element deposit in the Stillwater Complex, Montana (USA): Economic Geology, v. 111, p. 771 – 782.

Wang, S-J. and Wasylenki, L.E., 2017, Experimental constraints on reconstruction of Archean seawater Ni isotopic composition from banded iron formations: Geochimica et Cosmochimica Acta, v. 206, p. 137 – 150.

Wang, P., Dong, G., Santosh, M., Liu, K., and Li, X., 2017, Copper isotopes trace the evolution of skarn ores: a case study from the Hongshan-Hongniu Cu deposit, southwest China: Ore Geology Reviews, v. 88, p. 822 – 831.

Wernette, B., 2017, An investigation into the 2.7 Ga Stillwater Complex, Montana, USA: platinum-group element and sulfur isotope geochemistry. M.S. thesis, Indiana University (83 pp, ProQuest Dissertation and Theses).

Wheeler, K.T., Walker, D., Fei, Y., Minarik, W.G., and McDonough, W.F., 2006, Experimental partitioning of uranium between liquid iron sulfide and liquid silicate: implications for radioactivity in the Earth's core: Geochimica et Cosmochimica Acta, v. 70, p. 1537 – 1547.

Williams, H.M. and Archer, C., 2011, Copper stable isotopes as tracers of metal-sulphide segregation and fractional crystallization processes on iron meteorite parent bodies: Geochimica et Cosmochimica Acta, v. 75, p. 2011.

Wooden, J.L., Czamanske, G.K, and Zientek, M.L., 1991, A lead isotopic study of the Stillwater Complex, Montana: constraints on crustal contamination and source regions: Contrib. Mineral. Petrol., v. 107, p. 80 – 93.

Yamamoto, M., 1976, Relationship between Se/S and sulfur isotope ratios of hydrothermal sulfide minerals: Mineralium Deposita, v. 11, p. 197 – 209.

Yang, G., Hannah, J.L., Zimmerman, A., Stein, H.J., and Bekker, A., 2009, Re-Os depositional age for Archean carbonaceous slates from the southwestern Superior Province: challenges and insights: Earth and Planetary Science Letters, v. 280, p. 83 – 92.

Zhao, Y., Xue, C., Liu, S-A., Symons, D.T.A., Zhao, X., Yang, Y., and Ke, J., 2017, Copper isotope fractionation during sulfide-magma differentiation in the Tulaergen magmatic Ni-Cu deposit, NW China: Lithos, v. 286 – 287, p. 206 – 215.

Zientek, M.L., 1993, Mineral resources appraisal for locatable minerals: the Stillwater Complex. *In* Mineral resource assessment of the Absaroka-Beartooth study area, Custer and Gallatin National Forests, Montana, (eds. J.M. Hamarstrom, M.L. Zientek, and J.E. Elliott). USGS Open-File Report 93 – 207, F1 – F83.

Zientek, M.L. and Ripley, E.M., 1990, Sulfur isotope studies of the Stillwater Complex and associated rocks, Montana. Economic Geology, v. 85, p. 376 – 391.

Zientek, M.L., Czamanske, G.K., and Irvine, T.N., 1985, Stratigraphy and nomenclature for the Stillwater Complex: Montana Bur. Mines Geology Spec. Pub. 92, p. 21 – 32.

Curriculum Vitae

Joshua M. Smith
E-mail: jms44@iu.edu

Education

Indiana University, Bloomington, Geological Sciences, Ph.D., Nov. 2019
University of Nevada, Reno, Geology, M.S., Dec. 2014
Eastern Illinois University, Geology, B.S., May 2012

Papers and Abstracts

Smith, J.M., Ripley, E.M., Li, C., and Shirey, S.B. (In prep.) Evidence of Igneous Controls on the Formation of Metasedimentary Rock-Hosted Massive Ni-Cu-PGE Sulfides Near Intrusions in the Midcontinent Rift: Preparing for submission to *Economic Geology*.

Smith, J.M., Ripley, E.M., Wasylenki, L.E., and Li, C. (In prep.) Ni and Cu Isotope Variations of Country Rock-Hosted Massive Sulfides located near Midcontinent Rift Intrusions: Preparing for submission to *Economic Geology*.

Smith, J.M., Ripley, E.M., Shirey, S.B., and Wernette, B.W. (In prep.) Non-magmatic origins of country rock-hosted massive sulfide(-oxides) beneath the Stillwater Complex, Montana: Preparing for submission to *Mineralium Deposita.*

Smith, J.M., Ripley, E.M., Li, C., and Shirey, S.B., 2019, S, Pb, and Os isotopic studies of massive Ni-Cu±PGE sulfides hosted in metasedimentary country rocks of the Midcontinent Rift System, USA: Crossroads Geology Conference, Bloomington, IN 2019, Program with Abstracts, p. 35.

Smith, J.M., Ripley, E.M., Li, C., and Shirey, S.B., 2018, Origins of country rock-hosted massive sulphides beneath the Stillwater complex, MT, USA: 13th International Platinum Symposium, Polokwane, South Africa, Abstracts with Programs, p. 172 – 173.

Smith, J.M., Ripley, E.M., Li, C., and Shirey, S.B., 2018, S, Pb, and Os isotopic studies of massive Ni-Cu±PGE sulfides hosted in metasedimentary country rocks of the midcontinent rift system, USA: Geological Society of America Abstracts with Programs. Vol. 50, No. 6, ISSN 0016-7592, doi: 10.1130/abs/2018AM-320745.

Smith, J.M., Ripley, E.M., Li, C., and Shirey, S.B., 2018, Genetic controls of country rock-hosted massive sulfides beneath the Stillwater complex, MT, USA: Crossroads Conference 2018, Bloomington, IN, USA, Abstracts with Programs, p. 17 – 18.

Ripley, E.M., Wernette, B.W., Ayre, A., Li, C., Smith, J.M., Underwood, B.S., and Keays, R.R., 2017, Multiple S isotope studies of the Stillwater Complex and country rocks: An assessment of

the role of crustal S in the origin of PGE enrichment found in the J-M Reef and related rocks: *Economic Geology*, v. 214, p. 226 – 245.

Smith, J.M., Ripley, E.M., and Li, C., 2017, Variable genetic models for the origin of country rock-hosted massive sulfides. In *Proceedings of the 14th Biennial SGA Meeting, Society of Geology Applied to Mineral Deposits*, Quebec City.

Smith, J., Ripley, E., Li, C., Wernette, B., and Taranovic, V., 2016, S, Os, and Cu isotope variations between sheet- and conduit-style Ni-Cu-PGE mineralization in the Midcontinent Rift System, USA; *2016 Annual GSA Abstracts with Programs.*

Wernette, B., Ripley, E., Li, C., Smith, J., and Zhou, Y., 2016, Variations in the distribution of Platinum-group elements associated with varying degrees of silicate alteration within the J-M Reef of the Stillwater Complex, Montana, USA; *2016 Annual GSA Abstracts with Programs.*

Smith, J., Ripley, E., and Li, C., 2016, Petrographic and isotopic studies of sediment-hosted Ni-Cu-PGE massive sulfides associated with layered intrusions of the Stillwater Complex and the Midcontinent Rift System, USA; 2016 *GSA Penrose Conference on Layered Mafic Intrusions and Associated Economic Deposits.*

Ripley, E., Wernette, B., Smith, J., Li, C., Underwood, B., and Ayre, A., 2016, Multiple sulfur isotope evidence for a lack of crustal sulfur in the J-M reef of the Stillwater Complex, Montana, USA; 2016 *GSA Penrose Conference on Layered Mafic Intrusions and Associated Economic Deposits.*

Smith, J., Prokopf, D., Ripley, E., Li, C., 2016, Sulfur isotope studies of Ni-Cu-PGE sulfide mineralization hosted in metasedimentary country rocks of the Midcontinent Rift System and the Stillwater Complex, USA; *13th International Ni-Cu-PGE Symposium*.

Wernette, B., Ripley, E., Li, C., Smith, J., Underwood, B., Ayre, A., 2016, Multiple S isotope studies of PGE enrichment in the J-M Reef, Stillwater Complex, Montana; *13th International Ni-Cu-PGE Symposium*.

Ripley, E., Li, C., Smith, J., Wernette, B., and Taranovic, V., 2016, S, Os and Cu isotope variations between sheet- and conduit-style Ni-Cu-PGE mineralization in the Midcontinent Rift System, USA; *13th International Ni-Cu-PGE Symposium*.

Smith, J., Ripley, E., Li, C., Dong, S., and Wasylenki, L., 2016, Cu isotope variations between Ni-Cu mineralized intrusions of picritic and high-Al olivine tholeiite descent in the Midcontinent Rift System, North America; *2016 North-Central GSA Abstracts with Programs.*

Prokopf, D., Smith, J., Ripley, E., and Li, C., 2016, Sulfur isotope studies of Ni-Cu-PGE sulfide mineralization hosted in metasedimentary country rocks of the Duluth Complex, Eagle Intrusion and Tamarack Igneous Complex, Midcontinent Rift; *2016 North-Central GSA Abstracts with Programs.*

Smith, J.M., Muntean, J.L., and Vikre, P.G., 2015, Controls on high grade Au-Ag mineralization within the Clementine vein system in the Hollister low-sulfidation epithermal deposit, NV; *GSN Symposium 2015, Poster Session/Abstracts with Programs.*

Smith, J.M., Muntean, J.L., and Vikre, P.G., 2014, Controls on high grades within the Clementine vein system at the Hollister low-sulfidation epithermal gold-silver deposit, Nevada; *SEG Keystone Conference 2014, Poster Session/Abstracts with Programs*.

Smith, J.M. and Chesner, C.A., 2012, The growth history of quartz crystals from the Youngest Toba Tuff, Sumatra, Indonesia; *GSA Abstracts with Programs,* v. 44, no. 5, p. 9

Funded Grants

Controls on high grades within the Clementine vein system at the Hollister low-sulfidation epithermal gold-silver deposit, Nevada. PI: Smith, UNR. SEG Foundation, Inc., Newmont Mining Corporation Fund, May 2013 – December, 2013: $2,500.00

The growth history of quartz crystals from the Youngest Toba Tuff, Sumatra, Indonesia. PI: Smith, EIU. EIU Honors College, Undergraduate Student Research Committee, August 2011 – May 2012: $500.00

Mining Company Support

Controls on High Grades within the Clementine Vein System at the Hollister Low-Sulfidation Epithermal Gold-Silver Deposit, Nevada. Great Basin Gold, Ltd., August 2012 – December 2014.

Associate Instructor (AI) and Teaching Assistant (TA) Experience

IU – Bloomington	
2018 – 2019	Earth Materials (AI)
	Oceanography (AI)
CSU – Sacramento	
2014	Geology Field Camp (TA)
EIU	
2010 – 2011	Mineralogy (TA)
	Petrology (TA)
2011 – 2012	Intro. to Earth Science (TA)

Related Coursework

IU	Economic Geology
	Mineral Deposit Seminar
	Geochemistry
	Igneous Geochemistry
	Isotope Geochemistry
	Linear Algebra
	Mathematical Modeling in Geoscience

UNR	Ore Deposits
	Hydrothermal Alteration and Vein Petrology
	Reflected Light Microscopy
	Anaconda Field Mapping of Ore Deposits
	Field Spectroscopy Apps. to Hydrothermal Alteration and Exploration
	Hydrothermal Mineral Deposits
	Hydrothermal Geochemistry
EIU	Metallic Ore Deposits
	GIS
	Volcanology
	Mineralogy
	Petrology

Professional Society Memberships

Geologic Society of Nevada, Member, 2013 – present
Society of Economic Geologists, Member, 2012 – present
Geologic Society of America, 2016 – present

Awards

2019 Outstanding associate instructor, IU, Dept. of Earth and Atmospheric Sciences
2018 Best Ph.D. student presentation, IU Crossroads Conference
2012 Errett and Mazie Warner Presidential Award, EIU, Geology/Geography Dept.